Université de Montréal

Variability in tree-water relations from tree-line to tree-line in Canada's western boreal forest

Par

Nia Sigrun Perron

Département de Géographie,
Faculté des arts et des sciences

Thèse présentée en vue de l'obtention du
grade de Philosophiæ Doctor (Ph.D.) en Géographie

août, 2023

Université de Montréal

Département de géographie, Faculté des arts and sciences

Cette thèse intitulée

Variability in tree-water relations from tree-line to tree-line in Canada's western boreal forest

Présentée par

Nia Sigrun Perron

A été évaluée par un jury composé des personnes suivantes

James King (Université de Montréal)
Président-rapporteur

Oliver Sonnentag (Université de Montréal)
Directeur de recherche

Jennifer Baltzer (Wilfrid Laurier University)
Codirecteur

Vincent Maire (Université du Québec à Trois-Rivières)
Membre du jury

Kathy Steppe (Ghent University)
Examinateur externe

Résumé

Dans la forêt boréale, les températures augmentent et les régimes de précipitations changent, ce qui entraîne une augmentation de l'intensité et de la fréquence des conditions de sécheresse. Ces changements devraient se poursuivre et avoir des effets complexes et variables sur la végétation de la forêt boréale, notamment la modification de la composition due à la sécheresse, la mortalité des arbres et la disparition des forêts. L'objectif de cette thèse était de fournir une meilleure compréhension fonctionnelle des relations arbre-eau pour deux espèces d'arbres boréales communes et co-occurrentes (l'épinette noire; *Picea mariana* et le mélèze laricin; *Larix laricina*) à travers la forêt boréale de l'ouest du Canada. Pour ce faire, j'ai étudié comment les différents éléments de l'hydraulique des arbres, y compris la transpiration, et le déficit hydrique, étaient affectés par les conditions locales (structure du peuplement, conditions édaphiques et type de couverture terrestre), les stratégies fonctionnelles des arbres (caractéristiques structurelles et foliaires) et/ou les conditions climatiques (déficit de pression de vapeur, rayonnement, température de l'air, pluie et évapotranspiration). J'ai déterminé que l'utilisation acquisitive des ressources se traduisait par une productivité plus élevée chez le mélèze laricin, lorsque la disponibilité en eau était élevée, que les nutriments n'étaient pas limités et que la concurrence pour la lumière était favorable. L'épinette noire, en revanche, avait une acquisition lente des ressources, privilégiant la conservation de l'eau par rapport à la croissance radiale. J'ai déterminé que la transpiration de l'épinette noire et du mélèze laricin était influencée par l'hétérogénéité du site dans un complexe de tourbières boréales boisées, entraînant une variabilité de la contribution de la transpiration à l'échelle de l'évapotranspiration de l'écosystème. J'ai associé des variables environnementales au déficit hydrique des arbres au niveau de l'espèce afin de déterminer les facteurs de stress hydrique chez l'épinette noire et le mélèze laricin sur cinq sites de la limite sud à la limite nord de la forêt boréale. J'ai determiné que le déficit hydrique quotidien des arbres était contrôlé par la transpiration, tandis que les périodes plus longues (jours à semaines) de stress dû à la sécheresse étaient contrôlées par le rayonnement solaire et la disponibilité de l'eau, et étaient coordonnées avec les flux d'évapotranspiration à l'échelle du peuplement. Il est important de comprendre les relations hydriques des espèces d'arbres dans le biome boréal occidental du Canada, car la disponibilité en eau devrait devenir de plus en plus limitée dans cette région. Malgré des stratégies

différentes selon les espèces pour faire face aux conditions actuelles de la forêt boréale, il existe des incertitudes quant à la résilience des arbres face aux changements environnementaux prévus. La poursuite des travaux visant à quantifier les réponses des espèces d'arbres communes et répandues à des conditions progressivement limitées en eau aidera à comprendre la résilience des forêts boréales face aux changements environnementaux rapides et à maintenir leurs services écosystémiques liés à la régulation du climat, à la séquestration du carbone, à l'habitat de la faune et de la flore, à la culture et à l'économie.

Mots-clés : déficit hydrique de l'arbre, épinette noire, évapotranspiration, forêt boréale, humidité du sol, mélèze, pergélisol, sécheresse, transpiration

Abstract

In the boreal forest, air temperatures are increasing, and precipitation regimes are changing, leading to amplified intensity and frequency of drought conditions. Changes are projected to continue, resulting in complex and variable effects on boreal forest vegetation including drought-induced forest compositional changes, tree mortality and, in some places, forest loss. The objective l of this work was to provide an improved functional understanding of tree-water relationships for two common and co-occurring boreal tree species (black spruce; *Picea mariana* and tamarack; *Larix laricina*) across Canada's western boreal forest. To achieve this objective, I explored how different elements of tree-water relations, including transpiration, and tree water deficit were affected by local conditions (stand structure, edaphic conditions, and land cover type), tree functional strategies (structural and foliar traits), and/or meteorological conditions (vapor pressure deficit, radiation, air temperature, rain, and evapotranspiration). In Chapter 2, I explored the coordination between resource-use strategies of tamarack and black spruce, and found that acquisitive resource-use resulted in higher productivity in tamarack, when water availability was high, nutrients were not limited and competition for light was favourable. Black spruce, by contrast, had slow resource acquisition, prioritizing water conservation over radial growth. Next, in Chapter 3, I determined that transpiration of black spruce and tamarack were influenced by site heterogeneity across a forested boreal peatland complex, leading to variability in the contribution of stand-level transpiration to ecosystem evapotranspiration. Finally, in Chapter 4, I paired environmental variables with species-level tree water deficit to determine the drivers of water-stress in black spruce and tamarack across five sites spanning the extent of the boreal biome in western North America from the southern to northern boreal tree-line. I determined that daily tree water deficit was controlled by transpiration, while longer periods (days to weeks) of drought stress were controlled by solar radiation and water availability. Both short and long periods of tree water deficit caused greater stand-level fluxes of evapotranspiration. Understanding water relations of tree species in Canada's western boreal biome is of utmost importance as water availability is projected to become increasingly limited in this region. Although tree species have different strategies to cope with current conditions in the boreal forest, there is uncertainty regarding the resilience of black spruce and tamarack to projected environmental changes. Continued work to quantify the

responses of common and widespread tree species to progressively water-limited conditions will help to understand the resilience of boreal forests in the face of rapid environmental change, and to maintain their ecosystem services related to climate regulation, carbon sequestration, wildlife habitat, culture and economy.

Keywords : boreal forest, drought, evapotranspiration, soil moisture, permafrost, black spruce, tamarack, transpiration, tree water deficit

Table of Contents

List of Tables

List of Figures

List of Appendices

List of Abbreviations

°C : Degrees Celsius

ΔSR : Stem radius change

A_G : Ground area

AIC : Akaike's information criterion

$A_{,max}$: Light-saturated photosynthetic rate

A_s : Sapwood area

BAC : Baker Creek

B_t : Bark thickness

CA : Crown area

CO_2 : Carbon dioxide

DBH : Diameter at breast height

E_{max} : Maximum transpiration rate

ET : Evapotranspiration

ForestGEO : Forest Global Earth Observatory

GRO : Growth

g_{sw} : Stomatal conductance to water vapor

H : Tree height

H_2O : Water

HPC: Havikpak Creek

HRM : Heat ratio method sap flow sensors

J_s : Sap flux density

k : Thermal diffusivity of fresh wood

LCR : Live crown ratio

MAAT : Mean annual air temperature

MAP : Mean annual precipitation

N_{mass} : Foliar nitrogen concentration

OBS : Old Black Spruce

PAR : Photosynthetically active radiation

PC1 : First principal component

PC2 : Second principal component

PCA : Principal component analysis

PERMANOVA : Permutational analysis of variance

SCC : Scotty Creek

S_d : Sapwood depth

SLA : Specific Leaf Area

SMC : Smith Creek

T : Transpiration

T_{adj_BA} : Transpiration adjusted for basal area

T_{adj_high} : Transpiration adjusted to high productivity areas

T_{adj_low} : Transpiration adjusted to low productivity areas

T_{adj_PC1} : Transpiration adjusted for the first principal component

T_{air} : Air temperature

T_{cell} : Grid cell level transpiration

TD : Thermal dissipation

T_{plot} : Plot-level transpiration

TWD : Tree water deficit

v_1 : Upstream temperature

v_2 : Downstream temperature

V_h : Heat pulse velocity

VPD : Vapor pressure deficit

WUE_i : Instantaneous water-use efficiency

x : Distance

$\delta^{13}C$: integrated water-use efficiency

Ψ : Water potential

Dedicated to Jonina and Richard,

Parents who fostered a deep love of learning and an even deeper love of the forest.

Acknowledgments

The Université de Montréal is located in Tiohtià:ke (Montréal), the non-ceded territory of the Kanien'kehá꞉ka (Mohawk), and is where I spent most of my time composing my thesis. My fieldwork took place on Treaties 6, 8, 11, and 1876 territory, which spans the lands of Indigenous peoples and Nations including the Akaitcho, Cree, Dehcho Dene, Dënéndeh (Dënësųłinḝ Nëné), Gwich'in Settlement Region, Inuit Nunangat ᐃᓄᐃᑦ ᓄᓇᖅᑐᑦ , Inuvialuit, Michif Piyii (Métis), and the Tłı̨chǫ Ndè.

A sincere thanks goes to my supervisors Oliver Sonnentag and Jennifer Baltzer who provided me with scientific, logistical, financial, and emotional support during this process. Their wisdom, guidance and patience was greatly appreciated. Thanks to the members of my jury and the external examiners including Julie Talbot, Vincent Maire, and Kathy Steppe, and to my committee chair, James King, for providing me with valuable critiques that have gone towards strengthening this dissertation.

Thank you to the Canada Foundation for Climate and Atmospheric Sciences, Canada Foundation for Innovation, Canada Research Chairs, Centre Étude de la Forêt, department de geography at the Université de Montreal, Fonds de recherche du Québec - Nature et technologies, Natural Sciences and Engineering Research Council of Canada, Northern Scientific Training Program, Northern Water Futures (Global Water Futures), POLAR Knowledge Canada, and the Smithsonian Forest Global Earth Observatory for various forms of financial support.

Thank you to my co-authors Bram Hadiwijaya, Christopher Spence, Colin Laroque, Gabriel Hould-Gosselin, Jennifer Baltzer, Katherine Standen, Magali Nehemy, Matteo Detto, and Oliver Sonnentag for their support and collaboration.

Thanks to the ATMOSBIOS group for being my research family in Montreal and to the long distance support from the Forest Ecology Research Group at Wilfrid Laurier University. I was

lucky to have a wide network of people willing to help me through this journey. A special thanks goes to:

Mariam, for your inspiring work ethic. You constantly pushed me out of my comfort zone to get involved and do more, my PhD wouldn't have been the same without you. Magali, for science talks, for shared field work, and for a great time together at conferences. You've become a real mentor to me. Jay for taking a risk and flying up to Yellowknife to help a complete stranger in the field for a week. Chris Spence, for your support, both in and out of the field. Your calm demeanor and knowledge of the Baker Creek watershed is an inspiration. Penelope, for sharing a summer of fieldwork that I will forever cherish. It felt powerful to be two young women doing science together. Haley, for our conversations on how we do science and what we need to change. Gabriel, for being the lubricant and the glue that kept the lab together. Thanks for keeping an eye out when I was on the verge of a breakdown. Rose and Camille for your hawk eye edits. Daniel, for all your support (and there was lots!), but especially during COVID. You were a solid rock, always at the office holding me accountable. I won't miss your humming but I will miss working alongside you. Katie, for joining our group at just the right time. You've become an important friend and hopefully a long lasting colleague. Sophie, for always being there to build me up. Your confidence in me was invaluable during low times when I all but lost all confidence in myself. Finally, Joce. Thanks for being a loving cheerleader, patient companion, and for helping me keep a (somewhat) level head. This was hard, but you kept things in perspective. And you're right, getting a cat really helped.

Chapter 1 – Introduction

Boreal forests and climate change

The boreal biome is the largest forested biogeoclimatic region, spanning North America and Eurasia, south of the Arctic biome, including ~552 million hectares in Canada (Brandt *et al*. 2013, Price *et al*. 2013). Boreal landscapes represent a diversity of ecosystems shaped by climatic and topographic variation, as well as episodic disturbance regimes, including fire, insect outbreaks, and permafrost thaw (McCullough *et al*. 1998, Bond-Lamberty *et al*. 2014, Bergeron *et al*. 2014, Helbig *et al*. 2017, Elliott-Fisk 2000). In Canada alone, the boreal biome provides valuable ecosystem services in the form of carbon and freshwater storage, wildlife habitat, economic resources, and recreation, and is of significant cultural and traditional value for many Indigenous communities (Brandt *et al*. 2013, Gauthier *et al*. 2015).

Climate gradients (e.g., temperature, precipitation, radiation), disturbance regimes (e.g., fire, insect outbreaks, and permafrost thaw), and variation in local conditions (e.g., topography, soil conditions, and vegetation) control the extent and heterogeneity of forests in the boreal biome (Bonan and Shugart 1989, Elliott-Fisk 2000). Forest successional stage, local disturbance history, and site productivity also contribute to boreal landscape heterogeneity by shaping forest structure, including stand age, size, and canopy architecture (Hämäläinen *et al*. 2023). Local water availability is crucially important for forests in the boreal biome. Soil moisture shapes east-to-west gradients in water availability and forest productivity, and influences the distribution of common boreal tree species including (but not limited to) black spruce (*Picea mariana* [Mill.] B.S.P) and tamarack (*Larix laricina* [Du Roi] K. Koch, Bonan and Shugart 1989, Bergeron *et al*. 2014, D'Orangeville *et al*. 2016).

In many regions of the boreal biome climate change is causing instability in local conditions, resulting in changes to forest communities (Price *et al.* 2013). Canada's climate has warmed at a pace that nearly doubles the global average rate, increasing by 1.7°C between 1940 and 2016 (Zhang *et al.* 2019). Warmer air temperatures have the potential to lengthen the growing season

and increase productivity in the boreal biome. In northern forests with wet, cold soils, warming has increased tree productivity and growth (D'Orangeville *et al.* 2018, Wang *et al.* 2023). Warmer, longer growing seasons will increase soil nutrient availability, and ultimately expand species ranges northward (D'Orangeville *et al.* 2023).

The positive effect of warming air temperature on boreal forest productivity has not been uniform across the biome (D'Orangeville *et al.* 2016, Sniderhan *et al.* 2021). Temperature increases have restricted growth in Canada's northwestern and western boreal forests (Mirabel *et al.* 2022), and increased evaporative demands associated with warming have driven decreases in boreal tree growth and productivity (Reich *et al.* 2018, Mirabel *et al.* 2023, Wang *et al.* 2023). Mean annual precipitation across Canada has increased over the last few decades but the change has been modest compared to that of temperature (Zhang *et al.* 2019). As a result, much of Canada's boreal forest are experiencing drying with measurable negative consequences for forest ecosystems (Figure 1.1, Wang *et al*. 2014). For example, drought-induced water stress has resulted in widespread tree mortality across Canada's southern (Peng *et al.* 2011, Mirabel *et al.* 2022), western (Hogg *et al.* 2008, Peng *et al.* 2011, Liu *et al.* 2023), and central (Silva *et al.* 2010, Liu *et al.* 2023) boreal forests. Longer and more frequent periods of low precipitation and high temperatures have caused drought induced declines in forest productivity and tree mortality (Buermann *et al.* 2014, Sánchez-Pinillos *et al.* 2022). Drought frequency has also led to higher mortality among conifer species in the Canadian boreal biome (Sánchez-Pinillo *et al.* 2022).

Disturbance regimes that shape the boreal forest are intensifying with warming air temperatures and climate change (Gauthier *et al.* 2015, Seidl *et al.* 2017). More frequent and severe fires have led to a decrease in the regeneration of black spruce, the most common boreal tree species in North America, while simultaneously causing an increase in the regeneration of broadleaf taxa (Wang *et al.* 2020, Baltzer *et al.* 2021). Declining black spruce recruitment and forest compositional change toward deciduous species has also been observed in regions where warming has induced the rapid thaw of permafrost (ground that remains below 0°C for at least two years, Grosse *et al.* 2011*,* Helbig *et al.* 2016a, Dearborn *et al.* 2021). The frequency, severity and extent of insect outbreaks, fire, permafrost thaw, and drought will increase over the next ~100 years with consequences for forested ecosystems (Gauthier *et al.* 2015).

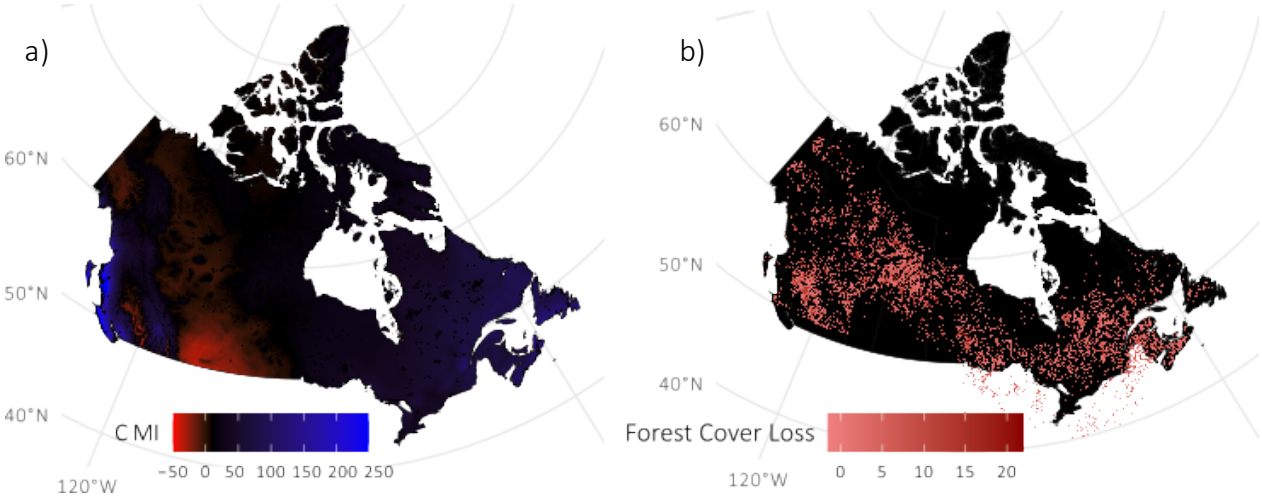

Figure 1.1 Maps representing the climate moisture index (CMI, a) and the forest cover loss (b) in Canada. The CMI is the difference between annual precipitation, and potential evapotranspiration determined from monthly temperature and precipitation records from climate stations in the 30-year period between 1981 and 2010. Positive CMI indicated wet or moist conditions that can support closed canopy forests, and negative values indicate dry conditions. Data from Hogg, 1997 and Wang *et al*. 2014, obtained through the Government of Canada. The change in forest cover (b) was determined between 2000 and 2022 using a time-series analysis of Landsat images and is presented at 5km resolution (Hansen *et al*. 2013). Forest cover loss is defined as a stand replacement disturbance or a change from a forested to a non-forested state and is represented as either no loss (0) or a value from 1 to 20, representing forest loss that occurred in 2000 – 2022, respectively. Data from (Hansen *et al*. 2013), obtained through the University of Maryland and the Global Forest Watch (Hansen/UMD/Google/USGS/NASA).

The rate of temperature change in Canada's boreal zone over the next century will be unprecedented (increases from 4-11 °C; Saxe *et al.* 2001, Gauthier *et al.* 2015, Zhang *et al.* 2019). Canadian boreal forests will be exposed to a climate substantially different from what has been experienced in the past (Sulla-Menashe *et al.* 2018). Warming and changing disturbance regimes will not only lead to shifts in community composition (Ameray *et al.* 2023), but will impact forest resilience to disturbance and ecosystem functions including carbon storage, water and energy fluxes, and wildlife habitat (Gautheir *et al.* 2015, D'Orangeville *et al.* 2023, Triviño *et al.* 2023). It is difficult to predict the degree of climate change across Canada's boreal forest, in part because it remains unclear how human populations will manage emissions of greenhouse gasses into the future. As such, the rate of change will likely be variable across Canada's boreal region with the north-west

continuing to experience the most rapid rate of warming (Gauthier *et al.* 2015, Sulla-Menashe *et al.* 2018, Zhang *et al.* 2019). The heterogeneity of conditions in the boreal biome also means that the response of vegetation to climate change will be variable, making it difficult to predict the future of Canada's boreal forests. However, the boreal biome is dominated by just a few species with broad geographic distributions, including black spruce and tamarack. Thus, investigating the effect of local conditions on the function and productivity of dominant species will help produce more accurate predictions of how boreal forests will respond to climate change.

Ecology of black spruce and tamarack

Black spruce is one of the most abundant and widespread conifers in North America's boreal forest (Burns and Honkala, 1990, Hermosilla *et al*. 2022). With a range that extends from the eastern coast to the northern treeline, black spruce can tolerate a variety of climatic and environmental conditions (mean annual temperature raging from 7 to -11 °C and mean annual precipitation between 1500 mm in the east to 150 mm in the northwest; Burns and Honkala, 1990). Black spruce is often associated with the presence of permafrost, as its shallow rooting habit (typically 10 – 20 cm and up to 60 cm) is suitable for the thin active layer above permafrost (Burns and Honkala, 1990). Growth of black spruce is dependent on climatic factors, nutrient availability, and soil moisture and is one of the slowest growing northern conifers (Lewis and Morton, 1921, Burns and Honkala, 1990).

In productive areas with well drained peat with highly decomposed organic material, black spruce average 12 – 20 m in height with an average diameter at breast height of 23 cm at maturity, and live up to 200 years (Burns and Honkala, 1990). Despite being shade tolerant, black spruce perform best on peatlands with limited competition. Lower productivity stands are located on poorly drained thick organic deposits of partially decomposed sphagnum (Burns and Honkala, 1990). Waterlogging in the rooting zone of black spruce can reduce hydraulic uptake, stomatal conductance, and carbon assimilation (Islam and MacDonald 2003), negatively affecting aboveground growth (Lieffers and Rothwell 1986, Baltzer *et al*. 2014) and leading to tree mortality (e.g., Dearborn *et al.* 2021). In the north, black spruce are common on well drained sites and are often found in a dwarfed or shrub stage (Lewis and Morton, 1921). Vegetative reproduction by

layering is common in open canopy stands of black spruce, including the north where conditions for seed development are less favorable and disturbance from fire is less frequent. With semi-serotinous cones, black spruce is an early colonizer post fire disturbance (Burns and Honkala, 1990). However, regeneration is dependent on an adequate seedbank, and black spruce demonstrate minimal recovery following severe burns (Baltzer *et al*. 2021) and following other disturbances including permafrost thaw, insect outbreaks, windthrow, and drought (Burns and Honkala, 1990).

Tamarack is also widespread across north America's boreal forest but is less abundant than black spruce. With a similar geographic range, tamarack lives under variable climatic regimes with average January temperatures ranging from - 30 to -1 °C, average July temperatures ranging from 13 to 25 °C, and mean annual precipitation between 1400 mm in the east and 180 mm in the northwest (Burns and Honkala, 1990). Tamarack's tall tapered stem contains small needles that grow in clusters of 12 – 20 and is the only conifer in North America's boreal forest to shed its needles each fall (Lewis and Morton, 1921, Gower *et al.* 1992). As one of the fastest growing northern conifers, tamarack growth outpaces that of other conifers in short rotations (Foweler 1992). However, nutrient availability, and soil moisture/aeration (including waterlogging and low soil water availability) limit tamarack growth (Burns and Honkala, 1990). At maturity, tamarack on average reach 15 to 23 m in height (up to 35 m) with a diameter at breast height between 36 – 51 cm (up to 102 cm), and a maximum age of 150 to 180 years (Burns and Honkala, 1990).

Tamarack is suitable to a range of conditions as it can withstand high moisture (but not waterlogging), high acidity and low temperatures (Burns and Honkala, 1990, Islam and MacDonald 2003). Compared to black spruce, tamarack has a greater ability for photosynthetic uptake and light capture in the canopy and requires greater annual nitrogen and water uptake (Gower *et al.* 1992, Kloeppel *et al.* 2000). It is most common in mesic sites such as peatlands with nutrient rich decomposed organic soils, but can be found growing in loamy sites with mineral soils and shallow organic matter, or on well-drained shallow soils over bedrock (Burns and Honkala, 1990). South in its range tamarack grows in association with black spruce mainly in peatlands, bogs and swamps (Lewis and Morton, 1921). In its northern range, tamarack is found in more well-drained areas (Lewis and Morton, 1921). Similar to black spruce, tamarack is a pioneer species, being amongst the first species to colonize filled lakes and bogs, and post burned landscapes (Burns and Honkala,

1990). However, tamarack is shade intolerant and competition for light severely reduces performance (Fry and Phillips 1977).

Plant resource-use strategies

To maximize performance, plants balance access to fundamental resources such as light, water, carbon dioxide, and nutrients, with growth, survival, and reproduction (Calow 1987, Díaz *et al.* 2016). Functional trait expressions define plant resource-use strategies, and allow plants to acquire and allocate limited resources, thus providing valuable information related to plant function within and between species, and across gradients in resource availability (Westoby *et al.* 2002). The plant economic spectrum uses functional trait expression to explain plant growth and survival strategies as an investment and reinvestment in carbon, nutrients, and water (Wright *et al.* 2004, Reich 2014). Plants categorized as fast (acquisitive) prioritize acquisition of resources to support rapid growth and reproduction, while plants categorized as slow (conservative) favor survival and protection over growth (Figure 1.2; Westoby *et al.* 2002, Wright *et al.* 2004, Reich 2014, Díaz *et al.* 2016).

Plant functional traits are highly constrained on a global scale, with few key traits representing a significant amount of variability in plant form and function (Díaz *et al.* 2016). Traits related to plant size (e.g., tall versus short plants), the leaf economic spectrum (e.g., high specific leaf area and leaf nitrogen, versus low specific leaf area and leaf nitrogen concentration), and in woody species, competition for light (e.g., crown height and diameter), explain the majority of variation in resource-use strategies among tree species (Figure 1.2). Therefore, the measurement of key foliar and structural traits can be used to accurately assess the resource-use strategies of boreal tree species (Díaz *et al.* 2016, Maynard *et al.* 2022).

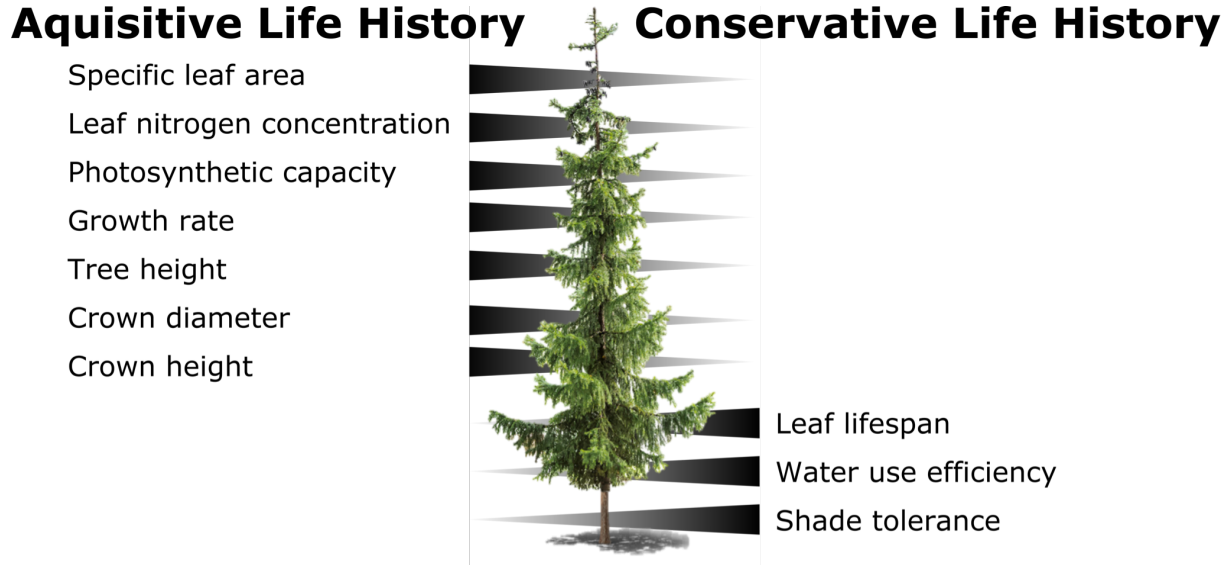

Figure 1.2 Key foliar traits to determine the resource-use strategies of boreal trees. Arrows signify the trait expressions of plants with acquisitive vs. conservative traits. Darker shading indicated high values (e.g., greater specific leaf area (SLA) is characteristic of acquisitive species, while conservative species have lower SLA). Adapted from Weemstra *et al*. 2016.

Throughout the boreal biome, trees demonstrate a range of conservative to acquisitive resource-use strategies (Osnas *et al.* 2018, Wright *et al.* 2004, Reich 2014). The availability of essential resources, including nutrients, light, and water can shape the resource-use strategies expressed both within and among species. For example, nitrogen is an important part of the enzyme ribulose-1,5-bisphosphate carboxylase/oxygenase and plays a key role in plant photosynthesis (Taiz and Zeiger, 2002). Species with acquisitive resource-use strategies require more nitrogen to support greater photosynthesis rates and faster growth, while species with conservative resource-use strategies can tolerate nitrogen limited environments (Chapin *et al.* 1980, Reich *et al*. 1995, Reich 2014). Similarly, access to, and competition for light will influence tree structure and architecture between individuals with different resource-use strategies (Maynard *et al.* 2022). Fast growing acquisitive species tend to dominate the canopy, with taller trees and a canopy architecture that is better suited to capture light resources (Hagemeier and Leuschner, 2019). By contrast, conservative species are often found in the shade below the canopy because their slow growth requires lower photosynthetic rates and thus, lower light interception (Maynard *et al.* 2022). Trees with a conservative strategy have canopy architectures that promotes longevity over access to light. Local water availability will also influence resource-use strategies and performance of boreal species. Acquisitive species

require more water to support rapid growth, while conservative species generally have lower requirements and can tolerate more water limited environments (Reich 2014). Variation in water availability, including drought frequency and severity, atmospheric water vapor concentration, precipitation and soil moisture, can drive functional strategies associated with water acquisition, transport, storage and flux in tree species (Sack and Holbrook 2006, Anderegg 2015, Rosas *et al.* 2019, Anderegg *et al.* 2019). Thus, water availability shapes the success of tree species across different environments and is one of the many important constraint on tree growth.

Tree-water relations

Trees use water for structural support through maintenance of cell turgor (the pressure of water inside a cell), and for biological and physiological processes including nutrient transport, photosynthesis and growth (Taiz and Zeiger 2002, Hirons and Thomas 2017). Tree growth is reliant on water because cell division and elongation requires well-hydrated cells with positive cell turgor (Deslauriers *et al.* 2014, Steppe *et al.* 2015, Hirons and Thomas 2017). Water potential gradients between the soil, plant and air allow trees to uptake and transport water through the vascular system, and release water into the atmosphere (the soil-plant-air continuum; Taiz and Zeiger 2002, Bernacchi and VanLoocke 2015, Venturas *et al*. 2017). Lower water potentials in the roots versus the soil draws water into the tree through uptake; lower water potentials in the leaves versus the stem draws water towards the canopy through sap flow, and lower water potential in surrounding air versus the leaves draws water into the atmosphere through transpiration (the evaporation of water from the leaf surface, Figure 1.3, Tyree and Ewers 1991). Greater tension (negative potential) is created through transpiration, which in turn pulls water molecules (held together by cohesion) into the leaves from the vascular tissue and into the roots from the soil (Dixon and Joly, 1894).

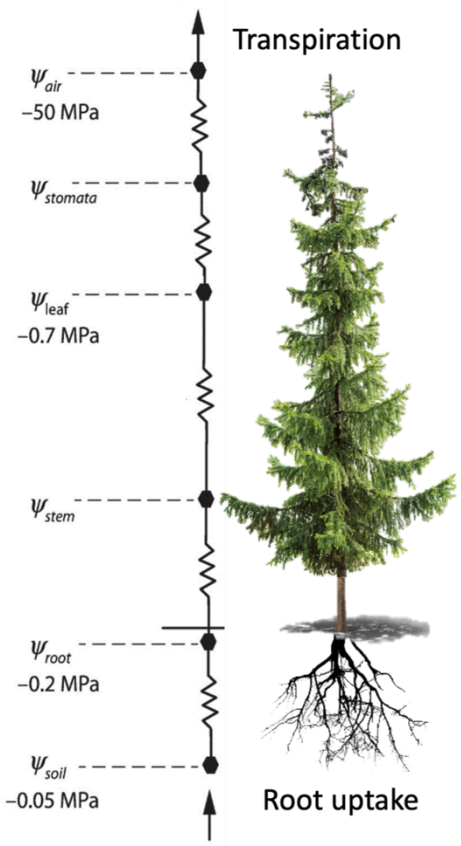

Figure 1.3 The soil-plant-atmosphere continuum. Flow of water and water potentials from soil (ψsoil), root (ψroot), stem (ψstem), leaf (ψleaf), stomata (ψstomata), to air (ψair). Adapted from (Tyree and Ewers 1991).

Water moves up the stem via highly specialized xylem cells (sapwood), down the stem via the phloem, and laterally between both the xylem and phloem (Figure 1.4). Only a small fraction of water used by trees is incorporated into biomass, the remaining 95 – 99% of water taken up by the roots is temporarily stored in stem tissue before being moved through the vascular system and released to the atmosphere via transpiration (Lambers 1998, Steppe *et al.* 2015, Hirons and Thomas 2017). To support transpiration trees first access water stored in the stem tissue, causing the stem to shrink and water potentials to drop. Between 5 – 22 % of the stored water in the stem is used daily for transpiration (Köcher *et al*. 2013, Steppe *et al*. 2015), making the changing stem radius an important indicator of tree hydration (Schulze *et al*. 1985, Zweifel and Hasler 2001, Fatichi *et al.* 2016, Landsberg and Waring 2016). Lower stem water potentials initiate root water uptake to support transpiration. However uptake is typically slower then transpiration, causing water to flow

from living cells into the xylem to support transpiration (Schulze *et al.* 1985, Steppe *et al.* 2015). Root water uptake continues after transpiration declines into the evening, refilling the depleted storage tissues in the tree, and initiating a stem swelling (Schulze *et al.* 1985, Steppe *et al.* 2015). Tree-water balance is often restored overnight through uptake and stem refilling while the stomates are closed. When water loss exceeds uptake and stem refilling, the water balance of the tree may not entirely recover overnight, leading to an accumulation of tree water deficit and a greater daily stem shrinking (Steppe *et al*. 2015, Hirons and Thomas 2017). If the supply of water continues to fall behind the transpirational demand for several days, trees become vulnerable to stress damage associated with water deficit (Hirons and Thomas 2017).

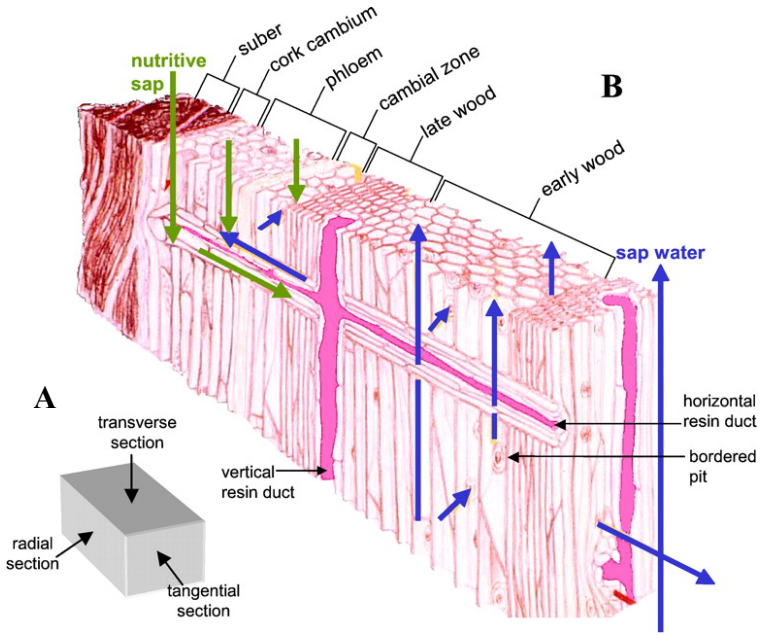

Figure 1.4 A schema of the transverse, radial, and tangential (A) sections of conifer wood (B). Sap water ascends via the xylem (late wood and early wood) and nutritive sap descends via the phloem. Sap can also be transported radially via the ray cells and tangentially by bordered pits. Adapted from Plomion *et al*. 2001. Copyright © 2001 American Society of Plant Physiologists.

Trees possess many strategies to prevent water loss through transpiration, the most important being stomatal regulation. Stomata offer a pathway of low resistance for water loss via transpiration (i.e., water movement through a plant and its loss to the atmosphere through evaporation), while simultaneously acting as a pathway for leaf carbon dioxide uptake necessary to sustain photosynthesis (Sack and Holbrook 2006). Thus, trees regulate the opening and closing of stomata

to balance the needs for carbon gains, against the costs of water loss (McDowell *et al.* 2008). Stomatal regulation is dynamic, changing in response to atmospheric conditions (i.e., light, temperature, CO_2 concentrations, and VPD), biological conditions within the plant (i.e., xylem conductance and internal water storage), and edaphic conditions (i.e., soil water availability and soil droughts, Taiz and Zeiger 2002, Matheny *et al.* 2017).

The efficiency by which plants withstand water loss is variables across species and environments, and can be categorized along a spectrum from anisohydric to isohydric (McDowell *et al*. 2008, Hochberg *et al*. 2018). Anisohydric plants apply a resistance strategy; stomata are kept open to maintain photosynthesis while the leaf water potential decreases with reduced soil water availability (McDowell *et al.* 2008, Fatichi and Pappas 2017). Anisohydric plants have traits that support an acquisitive life strategy, including xylem capable of withstanding negative water potentials, root systems that facilitate water movement and storage, and higher growth/carbon flux rates (McDowell *et al.* 2008, Reich 2014, Aubin *et al.* 2016). The investment into costly xylem with a higher safety margin is paid-off during drought conditions when plants keep stomata open longer, supporting more photosynthetic uptake of CO_2 (Reich 2014). These adaptations make anisohydric plants more able to withstand prolonged drought conditions of lower intensity (McDowell *et al.* 2008). Isohydric plants maintain near-constant leaf water potential through the regulation of stomata, regardless of soil moisture and atmospheric demands (McDowell *et al.* 2008). The rapid closure of stomata at the onset of water stress prevents high tensile pressure from accumulating in the vascular tissues of isohydric plants, reducing the likelihood of xylem embolism and hydraulic desiccation (Brodribb *et al.* 2014). Thus, isohydric plants can withstand short but intense droughts. The isohydric strategy is a trade-off, where plants forego carbon assimilated through photosynthesis in order to minimize xylem cavitation (Brodribb *et al*. 2014). Isohydric plants thus adopt a drought avoidance strategy associated with a conservative resource-use strategy with slower rates of water/carbon flux rates, and total growth (McDowell *et al.* 2008, Reich 2014).

Main objectives

The primary objective of my dissertation is to provide an improved functional understanding of tree-water relations for two common and co-occurring boreal tree species (black spruce and

tamarack) across Canada's western boreal forest. Plant physiology, environmental conditions and local meteorology all play important roles in tree-water relations, and their individual influences can be challenging to disentangle. Thus, in this dissertation, I evaluate the effect of plant physiology, environmental conditions and local meteorology on different aspects of tree-water relations in three distinct chapters (Figure 1.5). The chapter goals are :

- To determine the resource-use strategies of black spruce and tamarack, and the influence of these strategies on tree productivity and tree water deficit at three different sites (*Chapter two*).

- To determine how spatio-temporal variation in local environmental conditions influence black spruce and tamarack transpiration, and the implications of this variability on upscaling tree-level measurements to the forest stand (*Chapter three*).

- To determine the meteorological drivers of tree water deficit in black spruce and tamarack at different time scales in Canada's western boreal forest (*Chapter four*).

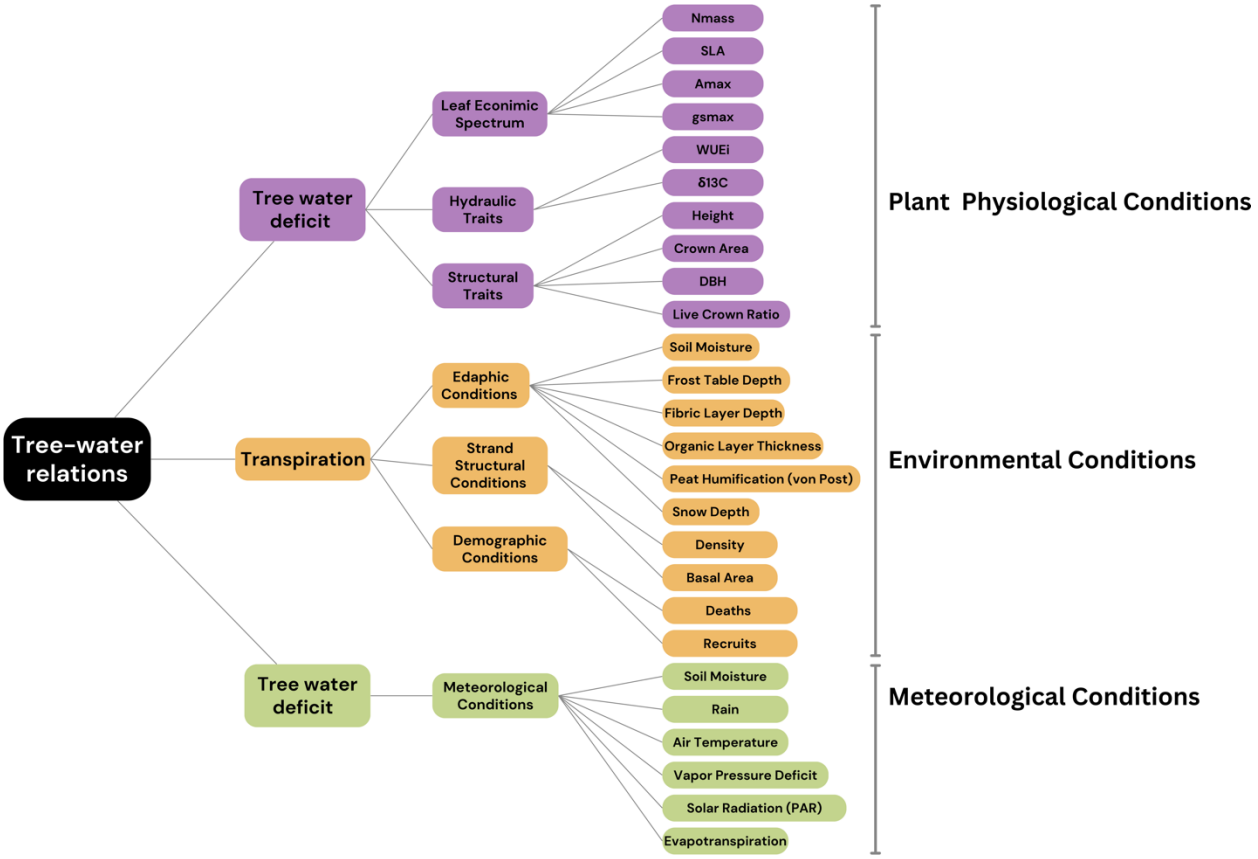

Figure 1.5 The plant physiological, environmental and local meteorological conditions that were included in my analysis of boreal tree-water relations. The different colors represent different chapters; chapter two in purple examines plant physiology alongside growth and tree water deficit, chapter three in orange examines environmental conditions, and chapter four in green examines meteorological conditions.

Methodological approaches to characterize tree-water relations

The boreal forest in western Canada is characterized by a heterogeneous landscape. Tree species that are widespread across the boreal biome must contend with vastly different conditions from one region to the next. Thus, Canada's boreal forest provides a unique opportunity for studying how species' tree-water relations vary across a range of local conditions. My work took place at five sites in Canada's western boreal forest from its southern limit in Saskatchewan (SK) to the forest-tundra ecotone in the Northwest Territories (NT, Figure 1.6). The sites cover a portion of Canada's western boreal forest that is facing great risks from warming and drying (Wang *et al.* 2014). The sites cross three ecozones (Boreal Plains, Taiga Plains and Taiga Shield), four permafrost classes

(permafrost-free, extensive discontinuous, sporadic discontinuous, and continuous; (Brown *et al.* 1997, Obu *et al.* 2019), and include forests with differing densities and species compositions. While the five sites have unique local characteristics, they share an important attribute; each forest stand is dominated by black spruce and at the three most southern sites, tamarack is present in the forest stand. The occurrence of these two common boreal tree species allows me to investigate the inter- and intra-specific variability in tree-water relations across sites.

The southernmost site is Old Black Spruce (OBS), ~100 km northeast of Prince Albert, SK, located at the edge of the southern delimitation of the boreal forest within the Boreal Plains ecozone (Figure 1.6). Old Black Spruce is the only permafrost-free site. Scotty Creek (SCC) is a subarctic boreal peatland complex characterized by sporadic discontinuous permafrost, located ~50 km south of Fort Simpson, NT in the Taiga Plains ecozone (Figure 1.6, Quinton *et al.* 2009; Natural Resources Canada, 2016). SCC has permafrost plateaus dominated by black spruce that are separated by bogs and fens that are largely treeless apart from infrequent tamarack (Dearborn *et al.* 2021). Baker Creek (BAC) is located ~15 km from Yellowknife, NT in the Taiga Shield ecozone (Figure 1.6). Permafrost in this region is extensive discontinuous, located in the forested areas and peatlands between bedrock outcrops (Morse *et al.* 2016). In this high-density mixed forest, overstory vegetation is dominated by black spruce with sporadic individuals of tamarack, birch and jack pine (Spence and Hedstrom 2018). Smith Creek (SMC) is a low-density spruce woodland with extensive discontinuous permafrost located in the Taiga Plains ecozone, near the town of Wrigley, NT (Figure 1.6, Natural Resources Canada, 2016). The northernmost site, Havikpak Creek (HPC), is located at the northern boundary of the boreal forest (i.e., the forest-tundra ecotone), ~10 km south of Inuvik, NT (Figure 1.6). In this region, permafrost is continuous and the land cover consists of low-density evergreen forests, dominated by black spruce in low-lying areas (Krogh *et al*. 2017).

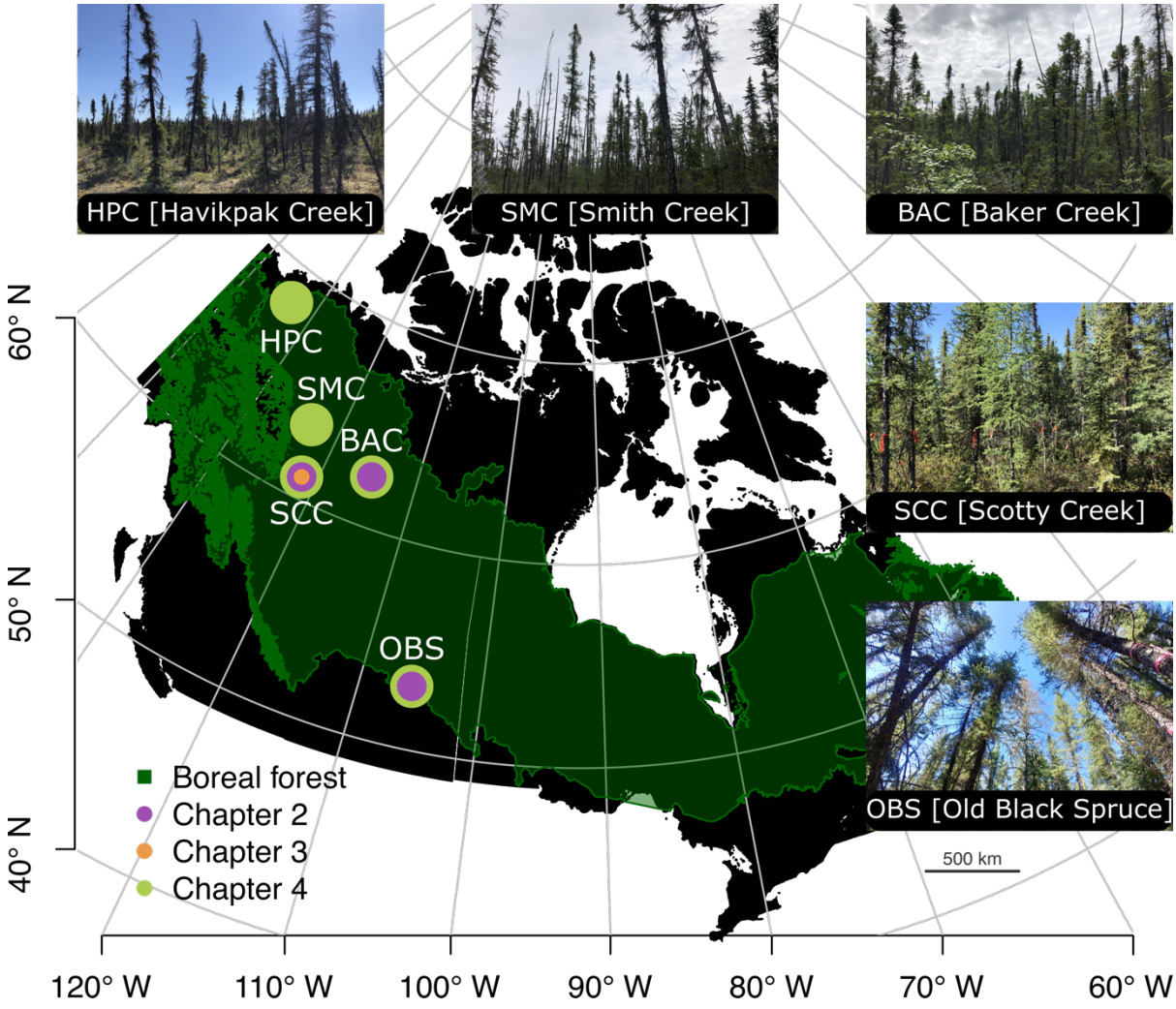

Figure 1.6 The location of the five study sites within the Canadian boreal forest. Sites include Old Black Spruce (OBS), Scotty Creek (SCC), Baker Creek (BAC), Smith Creek (SMC) and Havikpak Creek (HPC). The color circles represent which sites contribute to each chapter of the manuscript.

In chapter two, I explore how plant resource-use strategies relate to tree water deficit and growth at OBS, SCC and BAC, the three southern sites where black spruce and tamarack co-occur. I examine how resource-use strategies change across sites from three ecozones (Boreal Plains for OBS, Taiga Plains for SCC and Taiga Shield for BAC, Figure 1.6) and how this variability relates to productivity and tree water deficit.

In the third chapter, I focused on the influence of local site heterogeneity on tree transpiration at the forest dynamics plot located at SCC (Figure 1.6). The forest dynamics plot is one of 61 sites

part of the Smithsonian Forest Global Earth Observatory (ForestGEO) network (Anderson-Teixeira *et al.* 2015). Spanning 9.6-ha (800 m east-west by 120 m north-south) divided into 240 grid cells, the forest dynamics plot covers diverse features of a forested boreal peat landscape at the headwater of the SCC boreal peatland complex (Quinton *et al.* 2019, Dearborn *et al.* 2021). I use information on forest mortality, recruitment, growth, composition and structure, as well as local (20 m by 20 m) edaphic conditions available for the plot to investigate drivers of transpiration across the diverse landscape.

In the fourth chapter I perform a cross-site analysis of tree water deficit traversing Canada's western boreal forest using the three sites mentioned previously as well as Smith Creek (SMC), and Havikpak Creek (HPC, Figure 1.6). With sites spanning from southern to northern tree-lines, I focus the fourth chapter on investigating the dominant drivers of tree water deficit across the extent of Canada's western boreal forest.

Dendrometers to monitor tree water deficit and growth

An important component of tree-water relations is the water stored internally in tree stems. Water in stems fluctuates diurnally as water flows into the xylem from the phloem, and from root water uptake. Stems shrink in the day as water is transported to the canopy and used for transpiration, and then swell at night when internally stored water is resupplied by root uptake (Steppe *et al*. 2015). Diurnal fluctuations in stem radial swelling and shrinking, or stem radius change (ΔSR), are tightly linked to plant transpiration and soil water availability (Čermák *et al*. 2007). Thus, monitoring diurnal and seasonal stem hydraulics through ΔSR have been used to determine the dynamic nature of tree hydraulics and its intrinsic link to environmental conditions (e.g., Cermák *et al.* 2007, Steppe *et al.* 2010, De Swaef *et al.* 2015, Salomón *et al.* 2022).

Automatic circumference dendrometers are instruments used to acquire near-continuous high resolution measurements ΔSR (Figure 1.7). Each dendrometer possesses a thermally stable invar cable that is wrapped around the stem of a tree and attached to a spring-loaded plunger. As the tree stem shrinks and swells, the plunger activates a high precision linear potentiometer that measures the distance moved by the plunger (μm). Dendrometers of this type operate with low power

requirements and demand minimal maintenance, making them ideal for monitoring stem hydraulics in remote field sites. I was able to instrument between 8 to 16 trees at each site to obtain near-continuous dendrometer measurements throughout the summer months.

Figure 1.7 A dendrometer installed on a black spruce at Smith Creek. Photo: Nia Perron.

Values of ΔSR measured with dendrometers represent both reversible stem shrinkage/swelling (tree water deficit; TWD) and irreversible radial stem growth (Zweifel *et al.* 2001, 2005, Steppe *et al.* 2006, Zweifel 2016). Greater TWD in trees (smallest stem diameter) is reached mid-day during peak transpiration when stem water storage is lowest (Herzog *et al.* 1995, King *et al.* 2013, Köcher *et al.* 2013). Continuous measurements of TWD in black spruce and tamarack were used in chapter 4 to monitor stem hydration throughout the summer months. To obtain a physiologically realistic measure of changing water potential in the tree stems, it is necessary to partition total ΔSR into growth and tree water deficit (Zweifel 2016). Proposed by Zweifel (2016), the Zero Growth Method assumes that growth cannot take place during periods of water deficit, as turgor pressure of cells is insufficient to support cell expansion. In this approach, TWD is identified as periods when the measurement of ΔSR falls *below* a previous maximum ΔSR, while growth can be attributed to any measurement falling *above* the previous maximum ΔSR (Zweifel 2016). In chapters two and four, I used dendrometers to derive tree water deficit and growth of black spruce and tamarack to better understand plant physiological processes and drivers of water stress in trees.

The Zero Growth method makes assumptions about tree growth that may constrain the partitioning of ΔSR. The first assumption is that any decrease in stem radius is a result of decreasing water potential in the stem (i.e. increasing TWD, Zweifel *et al*. 2016). This assumption can be erroneous as bark degradation and thermal contraction can also cause decreases in stem radius. In the winter, fall and spring, stem radius change can be influenced greatly by freeze-thaw cycles when sub-zero temperatures cause the bark tissue to contract with freezing and degradation (Zweifel and Häsler, 2000, Zweifel *et al*. 2021). Stem thawing when temperatures increase can cause stem swelling that can be (but is not always) associated with water uptake (Zweifel *et al*. 2021). To limit the influence of freezing temperatures on the partitioning of TWD and growth from ΔSR, I isolated the study period to the warmest summer months (June, July and August) when freezing is minimal.

The second important assumption of the Zero Growth method is that growth occurs when the stem radius exceeds the previous maximum measured value (Zweifel *et al*. 2016). With this assumption, growth can only take place when the stem is saturated, or near saturated. However, there is evidence that growth also occurs during periods of TWD when stems are not fully saturated (Zweifel *et al.* 2016). Additionally, growth partitioned from ΔSR accounts for cell division and elongation, but is unable to account for growth associated with cell wall thinking (Zweifel *et al*. 2021). Thus, the Zero Growth method may underestimate the growth occurring during the study period.

With dendrometers located over the bark, growth includes bark development, which can account for a significant portion of growth in trees with a small annual increment (Gričar & Čufar, 2008, Zweifel *et al*. 2021). Dendrometers that include changes in bark swelling are also susceptible to hygroscopic swelling, where rain water flowing along the stem is absorbed by the bark tissue (Oberhuber *et al*. 2020, Zweifel *et al*. 2021). Bark swelling could potentially increase the measure of stem radius above the previous maximum, resulting in a TWD equal to zero and an erroneous attribution to growth. To mitigate this influence we removed dead bark, which is susceptible to water absorption, before installing the dendrometers. A validation of the Zero Growth method with independent growth measurements would require destructive sampling that was not undertaken as part of this project. However, validation would have increased our ability to determine growth and TWD from the two species in this study.

Sap flux density to monitor transpiration

Another important component of tree-water relations is the transpirational water loss. Transpiration dictates plant growth and productivity by affecting turgor pressure, links plants to the atmosphere in the soil-plant-air-continuum, and contributes to forest hydrological and weather regimes through water and energy fluxes (Steppe *et al*. 2015, Tyree and Ewers 1991). Transpiration can be estimated using field based empirical data including upscaled measurements of sap flow from trees (e.g., Tang *et al.* 2006, Oishi *et al.* 2008, Matheny *et al.* 2014). While several techniques exist to measure sap flow in trees, the heat-ratio method (HRM) is a reliable method that has proved effective for measuring sap flow in small trees, like the ones we found across our northern study sites (Figure 1.8). The HRM sap flow sensors consist of three needles; a central heater probe and two temperature probes equipped with two thermistors (at 12.5 mm and 27.5 mm). The three needles are inserted perpendicular into the xylem of the tree, forming a vertical line spaced equidistant (0.6 cm) apart (Burgess *et al*. 2001). The spacing of the needles is crucial for HRM measurements, and is determined with the assistance of a spacing guide when the needles are installed. The central heater probe releases a heat pulse, warming the surrounding sap and transferring heat towards the downstream and upstream temperature probes. Convection through the warmed sap transfers the heat towards the downstream and upstream temperature. The temperature differences between the downstream/upstream temperature probes are used to derive the magnitude and direction of sap flux density (J_s: $cm^3\ cm^{-2}\ hr^{-1}$). This method takes into account the thermal properties of wood, the wound correction factor (1.7853 based on measurements in the field and a wound diameter of 0.18 mm), wood density, the specific heat capacity of wood (1200J $kg^{-1}\ °C^{-1}$ at 20°C), specific heat capacity of sap (4182J $kg^{-1}\ °C^{-1}$ at 20°C), the density of water (1,000 $kg \cdot m^{-3}$), and the water content of sapwood. For this work, sensors were not calibrated for the site/species, and were not corrected for needle distance or temperature gradients within the stem. Only measurements from the thermistor at 12.5 mm are used when the thermistor at 27.5 mm in located in the heartwood tissues. The Sap Flow Tool software (ICT International Armidale, New South Wales, Australia) is used to calculate J_s and visually correct the time series to ensure that the lowest points on the time series corresponded with near zero flow rate conditions.

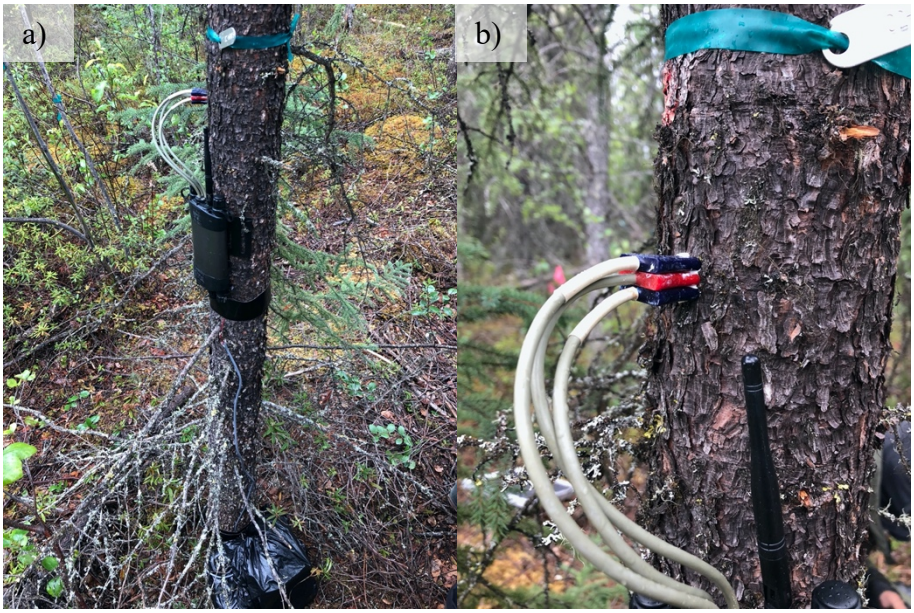

Figure 1.8 A heat ratio method sap flow sensor installed on the trunk of a black spruce tree at Scotty Creek in 2018. The sensors and the logger are visible in a), while the installation of the upstream, central, and downstream probes into the tree stem are visible in b). Photo by Nia Perron.

Measures of sap flow can then be used to derive transpiration estimates at the tree to stand-level using measures of sapwood area and species-specific allometric relationships with diameter at breast height (e.g., Warren *et al*. 2018, see Chapter 3). Ground-based estimates of transpiration can be collected at a small spatial scale (tree to stand level) but with high temporal resolution over multiple years, making them an important source of transpiration estimation for understanding forest productivity, partitioning evapotranspiration and validating land surface models, among other purposes (Stoy *et al.* 2019). In chapter three, I used HRM sensors to estimate transpiration of black spruce and tamarack across the ForestGEO plot. To assess how local heterogeneity influences stand transpiration, I also used measurements of environmental conditions from across the ForestGEO plot (Figure 1.5).

Micrometeorology to monitor local meteorological conditions

Micrometeorological approaches are effective for monitoring local environmental and meteorological conditions, as well as fluxes of water, heat, carbon dioxide, and methane (Figure 1.9, e.g., Helbig *et al*. 2016b, Baldocchi 2014). Micrometeorological towers can be operated from

off the grid power supply systems (e.g., solar, wind), making them suitable for remote field locations. To meet the goals of chapters two and four, I use pre-existing micrometeorological towers equipped with eddy covariance instrumentation, and instrumentation to measure supporting environmental variables such as net radiation, air temperature and humidity (Figure 1.9).

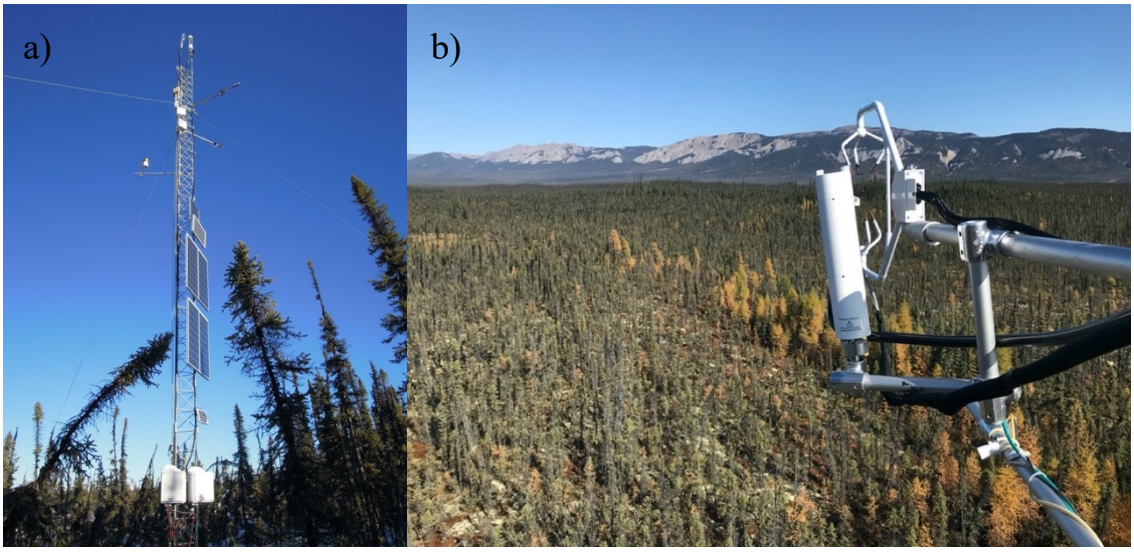

Figure 1.9 An example of a micrometeorological tower located at Scotty Creek a) and a close- up of an enclosed-path gas analyser and 3-D sonic anemometer for eddy covariance measurements on a micrometeorological tower at Smith Creek near Wrigley, NT (b). Photos by Gabriel Hould-Gosselin.

As airflow moves vertically and horizontally across a landscape it transports energy and matter (e.g., water) from the land surface to the atmosphere (Fisher *et al.* 2011, Wang and Dickinson 2012). The vertical movement, or fluxes of air, energy and matter can be measured from micrometeorological towers using eddy covariance techniques (Baldocchi *et al.* 1996, Baldocchi 2014). Eddy covariance techniques use a 3D sonic anemometer with an open- or enclosed-path infrared CO_2/H_2O gas analyzers (e.g., Helbig *et al.* 2016b), or a krypton hygrometer (e.g., Spence *et al.* 2020) to quasi-continuously measure water and heat fluxes. Evapotranspiration is the flux of water and energy from the land surface (evaporation) and from vegetation (transpiration) and is an important metric that can be used to determine ecosystem energy supply, water balance, and productivity (Fisher *et al.* 2011, Wang and Dickinson 2012). Tree-water relations are coupled with

evapotranspiration as vegetation controls transpiration through root uptake, transport and stomatal conductance and evapotranspiration regulates the water available for plants through surface evaporation (Novák 2012).

Additional meteorological variables known to influence tree-water relations including photosynthetically active radiation (PAR), vapor pressure deficit (VPD), air temperature, and rainfall can also be measured using instruments on micrometeorological towers. A quantum sensor is commonly used to determine PAR by measuring the amount of photons that reach the sensor's photodiode within a certain period of time (i.e., the photon flux density, μmol m^{-2} s^{-1}). Vapor pressure deficit is derived from air temperature and relative humidity measurements taken from temperature and relative humidity probes, and rainfall can be measured using a tipping bucket. Micrometeorological stations are also often equipped with instruments to continuously measure soil moisture (measured as volumetric water content using a Water Content Reflectometer) and to determine the level of soil water availability at various soil profiles. In chapter four, I used instrumentation on micrometeorological towers to evaluate the controls (referred to as environmental controls in Chapter 4) of black spruce and tamarack tree water deficit at various time scales.

Additional measurements can be taken from near micrometeorological towers to determine the site characteristics. These measurements can include edaphic conditions (e.g., soil material, and soil moisture), stand structure, density and composition, and information on permafrost (e.g., presence/absence, active layer thickness). For my work, I used measurements of the organic layer thickness (measures with a 1.5 m auger), fibric layer thickness (the upper layer of less humified organic soil) and the level of peat humification (with the Von Post scale) to characterize soil material (Chapter 3). I used continuous measurements of soil moisture to determine the level of water availability throughout the growing season (Chapter 4) and measures of volumetric soil water content from the top 5 cm of soil (using time domain reflectometry) to identify areas that were relatively wet and dry (Chapter 3). Frost table depth was used to determine the active layer thickness and the presence of permafrost within 2m of the surface (Chapter 3). Measurements of snow depth (measured in March using an automatic snow depth probe, Snow-Hydro LLC) were used to determine the amount of snow cover during the winter (Chapter 3). Surveys of tree and

stand structure (species dominance, tree height, crown area and live crown ratio), stand density, and species composition were used to understand the spatial variability of trees within and among forest stands (Chapters 3 and 4).

Thesis components

My thesis consists of five chapters; a general introduction (this current chapter), three chapters presented in article form, and a fifth chapter with general conclusions. I co-authored the article chapters with support from collaborators. Below, I provide details about co-author involvement and the publication status of each chapter.

Chapter 2

Perron N, Sonnentag O, Nehemy M, Standen K, Spence C, Laroque CP, and Baltzer JL. (*Reject and resubmit*). Exploring relationships between tree life-history and water-use strategies in Canada's Western Boreal Forest. *Tree Physiology.*

In Chapter two, I examine how resource-use strategies of black spruce and tamarack related to growth and tree water deficit. I collected and processed the dendrometer and tree structural trait data, performed the statistical analysis, wrote the manuscript, and created all the visualizations. Magali Nehemy provided assistance with data processing, interpretation and manuscript preparation. Katherine Standen collected the foliar trait data and provided assistance with manuscript preparation. Colin P. Laroque and Chris Spence provided assistance with the manuscript preparation. Jennifer Baltzer and Oliver Sonnentag helped develop the study design, and provided guidance on the analysis, interpretation and manuscript preparation. The manuscript resulting from chapter two has been submitted to the journal Tree Physiology where it was rejected with encouragement to resubmit pending revisions. At the time this thesis was submitted, chapter two was undergoing revisions. Thus, the resulting manuscript will deviate from the chapters' current form.

Chapter 3

Perron N, Baltzer J L and Sonnentag O 2023 Spatial and temporal variation in forest transpiration across a forested boreal peatland complex *Hydrological Processes* **37** Online: https://onlinelibrary.wiley.com/doi/10.1002/hyp.14815

Chapter three examines how variation in environmental conditions in a heterogenous boreal peatland complex influences black spruce and tamarack transpiration. I collected and processed the dendrometer data for 2018, processed the data for 2017, and incorporated processed datasets from earlier years. I performed the analysis, created the visualizations and prepared the manuscript. Jennifer Baltzer and Oliver Sonnentag helped develop the study design, and provided guidance on the analysis and manuscript preparation. A version of chapter three has been published in Hydrological Processes.

Chapter 4

Perron N, Baltzer J, Detto M, Nehemy M, Spence C, Hould-Gosselin G, Hadiwijaya B and Sonnentag O (*in preparation for Geophysical Research Letters*) Radiation, air temperature and soil water availability drive tree water deficit across temporal scales in Canada's western boreal forest.

Chapter four determines the environmental controls of tree water deficit in black spruce and tamarack across various temporal scales. I processed the dendrometer data, performed the analysis, created the visualizations and prepared the manuscript for chapter four. Matteo Detto assisted with the analysis. Magali Nehemy, Gabriel Hould-Gosselin, Christopher Spence and Bram Hadiwijaya provided assistance processing the dendrometer, evapotranspiration, meteorological, and sap flow data. Jennifer Baltzer and Oliver Sonnentag helped to design the study, guide the analysis, and prepare the manuscript. At the time of my thesis submission, a version of chapter four is being prepared for submission to Geophysical Research Letters. Thus, the resulting manuscript may deviate from the chapters' current form.

Together, findings from these chapters will help improve our understanding of boreal tree-water relations, improve how transpiration is estimated in heterogeneous environments, and strengthen our ability to predict forest responses to environmental and meteorological change. Together with climate and land surface modeling, this work could help forest managers, conservationists, and Indigenous communities, identify, and mitigate risks posed to the boreal forest over the upcoming decades.

Chapter 2 – Exploring relationships between tree resource-use strategies, tree water deficit and growth in Canada's western boreal forest

Nia Perron[1,2], Oliver Sonnentag [1,2], Magali Nehemy [3,4], Katherine Standen [5], Christopher Spence[6], Colin P. Laroque [4,] and Jennifer Baltzer [7].

[1] Département de géographie, Université de Montréal, Montréal, Québec, Canada, [2] Centre d'étude de la forêt, Université du Québec à Montréal, Montréal, Québec, Canada, [3] Trent School of the Environment, Trent University, Peterborough, Ontario, Canada, [4] Mistik Askiwin Dendrochronology Laboratory (MAD Lab), University of Saskatchewan, Saskatoon, Canada, [5] Department of Plant Science, University of Saskatchewan, Saskatchewan, Canada, [6] Environment and Climate Change Canada, Saskatoon, Saskatchewan, Canada, [7] Biology Department, Wilfrid Laurier University, Waterloo, Ontario, Canada

Perron N, Sonnentag O, Nehemy M, Standen K, Spence C, Laroque CP, and Baltzer JL. (*Reject and resubmit*) Exploring relationships between tree life-history and water-use strategies in Canada's Western Boreal Forest. *Tree Physiology.*

Abstract

Boreal tree species possess resource-use strategies that balance productivity and safety under variable environmental conditions. The coordination of these strategies and their combined influence on tree growth and tree water deficit is understudied across boreal environments. We used foliar and structural traits to determine the resource-use strategies and high-resolution measurements from dendrometers to determine the growth and tree water deficit of two widespread boreal tree species (black spruce; *Picea mariana* and tamarack; *Larix laricina*). We evaluated the influence of resource-use strategies on species performance using cumulative annual growth as an indicator of productivity and on species tree water deficit. We found consistent trait separation between species representing foliar productivity, but site specific differences in species structural traits representing competition for light. Tamarack engaged in an acquisitive resource-use strategy supported by greater tree water deficit and higher growth at two of the three sites, while black spruce engaged primarily a conservative strategy coordinated with low growth and lower tree water

deficit. This work provides a comprehensive evaluation of the relationship between the resource-use strategies and tree water deficit of two common boreal tree species in northwestern Canada, and how these strategies influence species performance in changing environments.

Introduction

Across the globe, air temperature has been increasing, and precipitation regimes changing, leading to amplified intensity and frequency of heat waves and drought (Wang *et al*. 2014; Daì 2018; Robinson *et al*. 2021). Arctic-boreal regions are warming two to four times faster than the global average, with complex and variable impacts on local vegetation (Sulla-Menashe *et al*. 2018; Rantanen *et al*. 2022). Where water is limited, warming and drying could lead to decreased boreal ecosystem productivity and health (Gauthier *et al*. 2015; Girardin *et al*. 2016a; Wang *et al*. 2020). In areas of the boreal biome with ice-rich permafrost (i.e., ground that remains frozen for a minimum of two years) thaw is leading to surface subsidence and either improved drainage or soil waterlogging, triggering tree mortality and forest loss (Osterkamp *et al*. 2000; Baltzer *et al*. 2014; Patankar *et al*. 2015; Helbig *et al*. 2016a). However, local to regional increases in vegetation growth and boreal ecosystem productivity have been observed in wetter portions of the boreal biome (Wang *et al*. 2023). To better understand how the boreal biome may be affected by changing conditions, we must first understand how boreal species respond to local conditions.

To maintain growth, reproduction, and/or survival under spatially or temporally variable environmental conditions, plants have developed different resource-use strategies (Díaz *et al*. 2004, 2016; Wright *et al*. 2004; Reich, 2014). The plant economics spectrum uses coordinated functional traits to categorise plant resource-use strategies. An acquisitive resource-use strategy has traits that support rapid growth, and high resource-use; while a conservative resource-use strategy has traits that promote high survival, resource conservation, and protection mechanisms from herbivores and pathogens (Niinemets, 2001; Wright *et al*. 2004; Reich, 2014; Díaz *et al*. 2016). Two distinct axes have been identified to describe the ecological trade-offs and global variation in tree traits, capturing different aspects of the acquisitive and conservative resource-use strategies (Maynard *et al.* 2022). A first axis includes key aspects of the leaf-economic spectrum (Wright *et al*. 2004) and represents a foliar productivity gradient (i.e., specific leaf area, foliar nitrogen). A second axis

includes plant structural traits and represents a gradient of plant size and competition for light (i.e., tree height and crown size, Maynard *et al*. 2022). The first axis demonstrates a tree's photosynthetic compatibles versus a risk of desiccation at the leaf-level, while the second axis demonstrates a tree's ability to intercept light versus their vulnerability to mechanical damage (Maynard *et al.* 2022). Our understanding of how the resource-use strategies of boreal trees corresponds to the two axes remains incomplete, highlighting the need for further research on tree resource-use strategies (Díaz *et al*. 2016; Reich *et al*. 2014; Martínez-Vilalta & Garcia-Forner, 2017).

Plant resource-use strategies regulated by functional traits represent trade-offs linked to the acquisition and allocation of limited resources and provide important information on the potential resilience of ecosystem functioning to changing resource availability (Wright *et al*. 2004; Reich, 2014; Osnas *et al*. 2018). Tree resource-use strategies can be characterized by measuring foliar traits associated with photosynthesis, tree hydraulics, nutrient use, and light interception (Wright *et al*. 2004; Reich, 2014; Díaz *et al*. 2016; Maynard *et al*. 2022). Functional traits along the plant economics spectrum are sensitive to local environmental conditions, such as air temperature, soil nutrient and water availability, leading to inter- and intraspecific variation in trait expression (Maire *et al*. 2015; Wright *et al*. 2017; Rosas *et al*. 2019; Maynard *et al*. 2022). Thus, an improved understanding of inter- and intraspecific trait variation and resource-use strategies will enhance the ability to discern species' capacity for adapting to anticipated environmental changes through trait plasticity, or whether vegetation response is more likely through species turnover and vegetation change (Kichenin *et al*. 2013; Anderegg, 2015; Standen & Baltzer, 2021).

An important aspect of resources-use strategies, is tree-water relations. Water is crucial for plant growth and survival, and the capacity to move and lose water influences a species resource-use strategy (Reich 2014). Continuous information on tree-water relations can be obtained with measurements of stem radius change (ΔSR) (Garnier & Berger, 1986; Čermák *et al*. 2007). To support transpiration, trees rely on root water uptake and water stored in bark tissue, cambium, and immature xylem (Meinzer *et al*. 2004; Scholz *et al*. 2008; Zweifel *et al*. 2016; Salomón *et al*. 2022). As transpiration draws on stored water, stems dehydrate and shrink. However, when transpiration decreases at night, trees refill depleted tissues, causing stems to swell with rehydration (Garnier & Berger, 1986; Zweifel *et al*. 2010, Steppe *et al.* 2015). When transpiration-induced water loss

cannot be recovered through water uptake at night, the stem stays dehydrated (Hinckley & Bruckerhoff, 1975; Zweifel *et al*. 2016; Dietrich *et al*. 2018). The state of dehydration and resulting stem shrinkage can be expressed through tree water deficit (TWD) (Zweifel *et al*. 2016). During the growing season, ΔSR can be partitioned into TWD and cumulative annual growth, thus providing key information related to plant water status and productivity, which can improve our understanding of tree resource-use strategies and overall species performance.

With a relatively small number of tree species across the boreal biome, examinations of inter- and intraspecific variation in tree functional traits and tree-water relations of two dominant species are tractable. Black spruce (*Picea mariana* [Mill.] B.S.P) is the most common and widespread tree species throughout boreal Canada (Hermosilla *et al*. 2022) and often co-occurs with tamarack (*Larix laricina* [Du Roi] K. Koch). However, our understanding of the resource-use strategies of *Picea* and *Larix* species has been largely developed through site-level studies. Black spruce and tamarack may be expected to demonstrate variable functional traits across the diversity of environmental conditions that characterize boreal North America, with consequences for forest productivity.

With this work, we aimed to examine the resource-use, growth and tree water deficit of two dominant boreal tree species in three ecozones, covering a range of environmental conditions in Canada's northwestern boreal biome. Specifically, we asked (i) what are the resource-use strategies of black spruce and tamarack and how do these strategies vary across sites?, (ii) how do resource-use strategies influence species productivity?, and (iii) are the resource-use strategies associated with species tree water deficit? We hypothesized that tamarack would demonstrate an acquisitive resource-use strategy across sites, coordinated with higher growth rates and higher tree water deficit. Additionally, we hypothesized that black spruce would demonstrate conservative trait expression and lower growth with minimal water requirements thus more hydrated trees and lower tree water deficit. By the end of the 21st century, high-latitude regions, including the boreal biome, will be exposed to substantially warmer conditions. An increase in air temperature, changes in precipitation regimes, and accelerated permafrost thaw are projected to continue across the boreal biome with consequences to tree species (Gauthier *et al*. 2015). This work will help us to better

understand how resource-use strategies influence species tolerance and vulnerability to resource limitation (water deficit) in rapidly changing environments.

Materials and methods

Study sites

Our work took place at three mature black spruce-dominated forest sites in northwestern Canada, each located in a different ecozone (Wiken *et al*. 2011; Figure 2.1, Table 2.1). Old Black Spruce (OBS; 53.98 °N, -105.12 °W, within the Boreal Ecosystem Research and Monitoring Sites program) is a black spruce-dominated forest with sporadic tamarack and jack pine (*Pinus banksiana* [Lamb.]) (Gower *et al*. 1997; Jarvis *et al*. 1997). Located in the Boreal Plains ecozone, OBS is permafrost-free and the warmest of the three sites, with the greatest projected drying for the 21st century (Ireson *et al*. 2015).

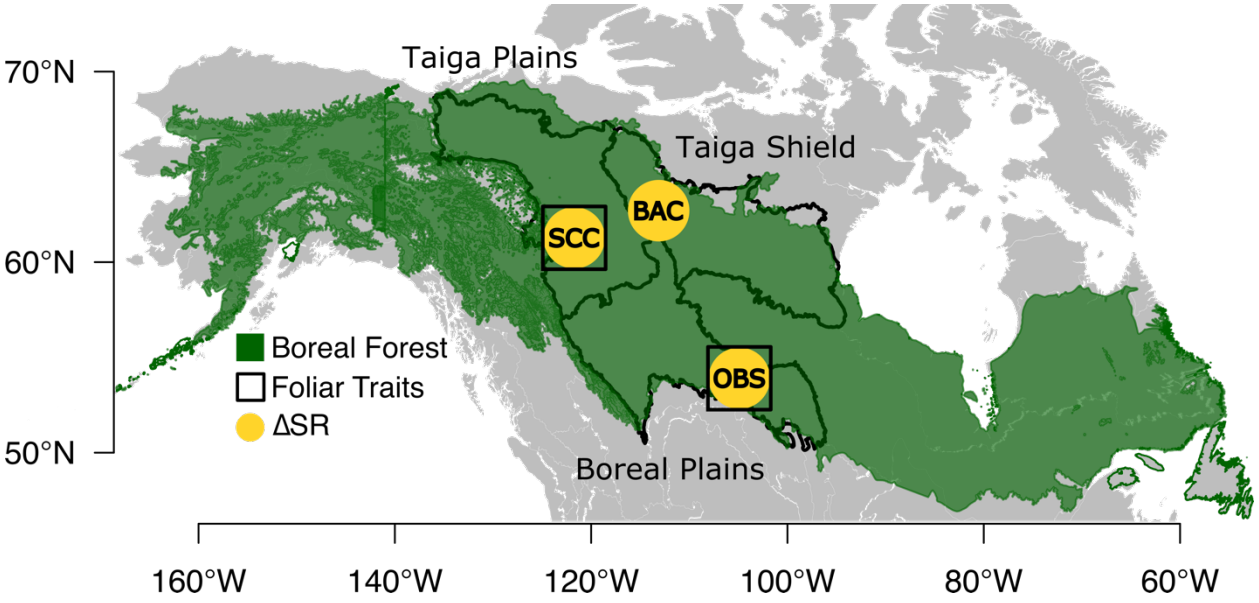

Figure 2.1 The location of Old Black Spruce (OBS), Scotty Creek (SCC) and Baker Creek (BAC) within North America's boreal biome (shaded green). Stem radius change (ΔSR) of tamarack and black spruce were sampled from all three sites, foliar traits sampling was limited to OBS and SCC.

Scotty Creek (SCC; 61.18 °N, -121.18 °W) is a boreal peatland complex located in the Taiga Plains ecozone, composed of forested permafrost peat plateaus and largely treeless permafrost-free

wetlands (Quinton *et al*. 2019). In more productive areas of SCC, black spruce and tamarack co-occur (Dearborn *et al*. 2021). Like much of the southern portion of the Taiga Plains, permafrost at SCC is sporadic and is strongly associated with raised dry peat plateaus (Ecosystem Classification Group, 2009; Quinton *et al*. 2019; Gibson *et al*. 2021; Wright *et al*. 2022). Permafrost at SCC is experiencing rapid thaw that is likely to continue over the next century. Permafrost thaw below the center of raised peat plateaus occurs laterally, causing the water table to drop and surface layers to dry. By contrast, permafrost thaw at peat plateau edges occurs laterally, causing the water table to rise relative to the subsiding surface, often until inundation (Baltzer *et al.* 2014, Patankar *et al.* 2015).

Table 2.1 Site information for Old Black Spruce (OBS), Scotty Creek (SCC) and Baker Creek (BAC). The mean annual air temperature (MAAT) and mean annual precipitation (MAP) of each site represent the 30-year climate normals (1981 to 2010; ECCC, 2021). Forest composition was determined from three density plots of at least 90 trees at each site. Black spruce refers to *Picea mariana* and tamarack is *Larix laricina*. A more detailed site description can be found in the main references for each site.

Site	OBS	SCC	BAC
MAAT (°C)	1.4	-2.8	-4.3
MAP (mm)	427.7	390	289
Location	53.98 °N, -105.12 °W	61.18 °N, -121.18 °W	62.55 °N, -114.43 °W
Ecozone	Boreal Plains	Taiga Plains	Taiga Shield
Permafrost	Absent	Sporadic (>10 % – 15 % in areal extent)	Discontinuous (>50 % – 90 % in areal extent)
Forest Composition	Black spruce 90 % Tamarack 10 %	Black spruce 80 % Tamarack 11 % Birch species complex (*Betula spp*.; 7 %)	Black spruce 75 % Jack pine (*Pinus banksiana* 14 %) Paper birch (*Betula papyrifera* 6 %) Tamarack 3 %
Soil Type	Poorly drained peat (20 – 30 cm) over coarse-texture mineral soil	Thick poorly drained Organic Soils (wetlands) and well-drained Organic Cryosols (plateaus) atop mineral soils	Thick organic soil layer atop fine-grained mineral sediment and bedrock
References	Gower *et al*. 1997; Jarvis *et al*. 1997	Dearborn *et al*. 2021; Standen & Baltzer, 2021	Spence & Hedstrom, 2018

Baker Creek (BAC; 62.55 °N, -114.43 °W) is an open-canopy mixed forest located in the Taiga Shield ecozone, and dominated by black spruce (Ecosystem Classification Group, 2008). Mosaic landscapes are typical of the Taiga Shield with Precambrian bedrock ridges dispersed between forested hillslopes, peat-filled bedrock depressions, wetlands, and lakes (Spence & Woo, 2002; Ecosystem Classification Group, 2008). The locally diverse topography gives rise to distinct and often isolated vegetation types, including forests, and peatlands with discontinuous permafrost (Morse *et al*. 2016). Tamarack at BAC can be found mainly in bedrock depressions, and black spruce are dispersed throughout forest hillslopes below the bedrock ridges and the depressions (Spence & Hedstrom, 2018).

Stem radius change

We installed circumference dendrometers (DC3, Ecomatik GmbH, Munich, Germany) on four to eight black spruce and five to eight tamarack at each site for accurate (± 0.1 % of the measured value) and high-resolution (5-30 minutes) measurements of ΔSR (mm) (Table 2.2). At each site, the trees were located in the same forest stand, in an area with a radius of 30 m. Each dendrometer was installed on a branch-free section of the main stem near breast height (1.3 m; Figure SI.1). Up to four dendrometers were recorded on a single HOBO data logger (UX120-006M, Onset, Bourne, MA), and averaged at 30-minute intervals for near continuous time series of ΔSR starting April 1st, 2018 (2019 for two sites, SCC and BAC) and ending October 1st, 2020. Gaps in the data (≦ 3 h) were filled using linear interpolation. Longer periods with missing data (>3 hours) due to data logger failure and/or animal damage to instruments were not gap-filled (Nehemy *et al*. 2022).

To examine the ΔSR related to tree hydraulics and growth, we focused on ΔSR during the peak summer months, June, July and August, herein referred to as the study period. These months were all part of the transpiration period for each species, defined as the time of year when trees were actively transpiring and could initiate growth. The transpiration periods were delineated from the individual ΔSR time series each year (2018 – 2020) using the daily mean ΔSR approach (King *et al*. 2013). Briefly, daily mean ΔSR was subtracted from the half-hour measurement of ΔSR to detrend each ΔSR time series (King *et al*. 2013). The transpiration period of each tree began with transpiration onset; the first day of a consecutive series of days (>5 excluding days with rain), in

which the sinusoidal pattern of detrended ΔSR switched from being air temperature-driven (negative sinusoidal) to transpiration-driven cycle (positive sinusoidal), reaching a maximum in the night/early morning and a minimum mid-day (Zweifel *et al*. 2001; Pierrat *et al*. 2021; Nehemy *et al*. 2023; Figure SI.2). The end of the transpiration period was identified as the day when the temperature-driven sinusoidal pattern returned, with maximum ΔSR during the day and minimum ΔSR at night.

Cumulative annual growth of the stem radius (herein referred to as growth; mm) and tree water deficit (TWD; μm) of each tree were partitioned from ΔSR using the 'Zero Growth' method during the study period (Zweifel *et al*. 2016). The 'Zero Growth' method assumes no growth occurs during periods of stem shrinkage because turgor pressure is insufficient to facilitate cell division and enlargement (Lockhart, 1965; Hinckley & Bruckerhoff, 1975; Zweifel *et al*. 2016; Dietrich *et al*. 2018). Growth was measured as the difference between the given measure of stem radius change (ΔSR_t) and the previous maximum (ΔSR_{max}) when $\Delta SR_t > \Delta SR_{max}$ (Zweifel, 2016; Zweifel *et al*. 2021). This created a stepwise increase in growth where ΔSR_{max} was reset to a new higher level when the current ΔSR_t exceeded the previous ΔSR_{max}.

Growth was subtracted from the ΔSR time series to obtain TWD (Zweifel *et al*. 2016). The value of TWD represents the volume of water required for a stem to fully re-hydrate. Bark degradation in the winter, and temperature fluctuations, including freeze-thaw events can also influence ΔSR and TWD (Zweifel *et al.* 2021). Thus, our study period was isolated to the summer months (June, July August) when temperatures are above freezing to limit the influence of bark degradation and thermal expansion. During heavy rainfall, the ΔSR may increase as a result of bark absorbing water flowing along the stem, resulting in TWD of zero that does not fully reflect tree growth. We were unable to distinguish between periods of TWD coordinating with bark absorption versus growth. We assumed that a TWD equal to zero represented fully hydrated stem tissue, and a positive TWD (> 0) represented dehydrated stem tissue. The number of days trees reach full hydration (TWD = 0) thus provides key information related to re-hydration and drought stress (Hinckley & Lassoie, 1981; Zweifel *et al*. 2005; Drew *et al*. 2011; Köcher *et al*. 2013; Dietrich *et al*. 2018). At all three sites, ΔSR was synchronous among black spruce and tamarack, but the amplitude of stem shrinkage

and swelling varied. Species-averaged ΔSR, TWD and growth were calculated for each site (e.g., Zweifel *et al*. 2016; Maillet *et al*. 2022) and used for demonstrative purposes in figures.

Tree structural traits and foliar traits

Structural traits, including tree height (m), diameter at breast height (1.3 m; DBH; cm), crown area (measured as the elliptical crown area occupied by the foliage which considers the widest length of the plant canopy through its center and the perpendicular canopy width; CA; m^2), and the live crown ratio (percentage of the stem supporting live foliage from crown base to top relative to the tree height; LCR %), were measured for each tree instrumented with a dendrometer (Table 2.2).

Table 2.2 Mean (standard deviation) for measured tree structural traits, including diameter at breast height (DBH, cm), height (m), crown area (CA, m^2) and live crown ratio (LCR; %) of the tamarack and black spruce individuals (n) instrumented with dendrometers to measure stem radius change at Old Black Spruce (OBS), Scotty Creek (SCC) and Baker Creek (BAC). Tree species include black spruce (*Picea mariana*) and tamarack (*Larix laricina*), n indicates the number of trees instrumented with dendrometers for which structural traits were measured and interval indicated the measurement interval period (in minutes).

Site	Species	n	Interval	DBH [cm]	Height [m]	CA [m^2]	LCR [%]
OBS	Tamarack	7	30 min	15 (± 4)	13.5 (± 2.7)	10.8 (± 2.9)	62 (± 3)
	Black spruce	4	30 min	10 (± 1)	9.1 (± 2.1)	3.9 (± 0.8)	62 (± 9)
SCC	Tamarack	8	5 min	10 (± 2)	8.2 (± 1.4)	4.5 (± 1.9)	59 (± 11)
	Black spruce	8	5 min	16 (± 5)	10.6 (± 2.6)	5.4 (± 1.3)	85 (± 9)
BAC	Tamarack	5	5 min	14 (± 5)	8.9 (± 2.6)	9.7 (± 3.8)	84 (± 18)
	Black spruce	5	5 min	8 (± 1)	7.1 (± 0.8)	3.7 (± 1.1)	81 (± 5)

Foliar traits were measured from five black spruce (n = 5) and three tamarack trees (n = 3) on July 19th (OBS) and June 28th (SCC), 2017, respectively. Foliar traits included specific leaf area (SLA; $cm^2\ g^{-1}$), foliar nitrogen concentration (N_{mass}; mg N g^{-1} leaf), area-based light-saturated photosynthetic rate (A_{max}; µmol $CO_2\ m^{-2}\ s^{-1}$), stomatal conductance to water vapor (g_{sw}; mol $H_2O\ m^{-1}\ s^{-1}$), integrated (measured in the needles; ‰) and instantaneous water-use efficiency (WUE_i; µmol CO_2 $mmol^{-1}$ H_2O). WUE_i was determined by dividing A_{max} by the maximum rate of

transpiration (E_{max}). Foliar traits, including SLA, N_{mass}, A_{max} and $g_{sw,}$ inform potential productivity, while water-use efficiency can be derived from measures of WUE_i and $\delta^{13}C$ (Wright *et al*. 2004; Seibt *et al*. 2008).

Simultaneous measurements of A_{max}, E_{max} and g_{sw} were performed on branchlets with healthy needles using a portable photosynthesis system (LI-6400XT; LI-COR Biosciences Inc., Lincoln, NE) equipped with the opaque conifer chamber (LI6400-22) and the RGB light source (LI-6400-18A; LI-COR Biosciences). For each measurement, the sample chamber CO_2 concentration was maintained at 400 μmol CO_2 mol^{-1} with chamber humidity ranging from 30 % to 60 % (Pérez-Harguindeguy *et al.* 2013). To conserve battery power while operating in the field without immediate power sources, we used ambient air temperature and took all measurements before solar noon (no later than 13:00 to avoid peak heat of the day). Gas exchange measurements were made under saturating light (photon flux density = 1500 μmol m^{-2} s^{-1}) with equal intensities of each color light in the RGB light source. Each gas exchange measurement is an average of five point measures taken within a 30 second interval after stabilization of gas exchange within the chamber and corrected for leaf area. After measurement, all needles were removed from the branchlet and digitized to determine needle area (see below). Needle area was used to correct A_{max}, E_{max} and g_{sw} measurements returned by the LI640XT system.

To determine SLA, $N_{mass,}$ and $\delta^{13}C$, needles measured for gas exchange were collected and immediately put in sealed plastic bags to maintain hydration. Within 2-3 hours of sampling, the fresh needles were scanned to determine leaf area using ImageJ (Schneider *et al*. 2012). To calculate SLA (the ratio between fresh area and dry mass), needles were oven-dried at 50 ºC for five days and weighed (scale accuracy of 0.001 g). These samples were then ground using a ball mill for the determination of N_{mass} and foliar $\delta^{13}C$. During photosynthesis, ribulose-1,5-bisphosphate carboxylase oxygenase discriminates against ^{13}C over the lighter ^{12}C (Farquhar *et al*. 1989), as stomata close, the concentration, and uptake, of ^{13}C increases. Therefore, $\delta^{13}C$ can be used as a proxy for stomatal control and WUE over an integrated period (i.e., carbon gained vs. water lost). Samples were processed for $\delta^{13}C$ by the University of California Davis Stable Isotope Facility using a PDZ Europa ANCA-GSL elemental analyser interfaced with a PDZ Europa 20-20 isotope ratio mass spectrometer (Sercon Ltd., Cheshire, UK). To obtain N_{mass}, ground samples were

analyzed using a 2,400 Series II CHNS/O Elemental Analyzer (Perkin Elmer, Waltham, MA) with an acetanilide standard and an accuracy of <0.3 %.

Foliar traits were collected from OBS and SCC as part of a separate project aimed at understanding plant trait variability across the Northwest Territories and were not paired with structural trait, TWD, and growth data at the tree-level (Standen, 2022). Measurements of foliar traits were not obtained for BAC.

Meteorological conditions

Regional climate normals (1981 - 2010) were obtained from air temperature and precipitation measurements made at the nearest Environment and Climate Change Canada meteorological station (OBS: Prince Albert, SK, ca. 90 km; SCC: Fort Simpson, NT, ca. 50 km; BAC: Yellowknife, NT, ca. 10 km). The daily data from the meteorological stations were also used to determine mean air temperature and total rainfall during the summer (May to September 2018, 2019 and 2020). Additionally, local mean air temperature and total rainfall for the three summers were computed from half-hourly measurements made at micrometeorological stations located at the sites themselves. There, air temperature and relative humidity were measured using temperature and relative humidity probes (HPM45C, Campbell Scientific Inc., Logan, UT). Rainfall was measured using precipitation gauges outfitted with altar shields (OBS and SCC: T-200B, GENOR Inc., Augusta, NJ) and a tipping bucket rain gauge (BAC: TE525, Texas Instruments, Dallas, TX).

Statistical analysis

To determine the resource-use strategies of black spruce and tamarack we performed a principal component analysis (PCA) using the *PCA* function from the R package *FactoMineR* (Lê *et al*. 2008). The PCA was used to assess co-variation among structural and foliar traits within and between black spruce and tamarack individuals. Trait data was scaled (standardized) to accommodate different measurement scales. We extracted the eigenvalues using the *get_eigenvalue* function from the R package *factoextra* to determine the number of principal components to keep in the analysis (Kaiser, 1961). Only principal components with eigenvalues >1 were kept (Girden & Kabacoff, 2011). The first three principal components, represented by the

first three axes, were kept. Individuals were grouped using 95 % concentration ellipsoids to visualize the clustering within a species, overlap between species, and species' relative locations in trait space. We used the *adonis2* and the *betadisper* functions in the *vegan* package (Oksanen *et al*. 2018) to assess the statistical differences in foliar and structural traits among- and within sites. We performed a permutational analysis of variance (PERMANOVA) and a beta dispersion test to determine whether the PERMANOVA results were due to differences among centroids or due to differences in dispersion around the centroid of each site (i.e., beta dispersion). We used the Student's t-test and the Wilcoxon rank sum test for comparisons of normally and non-normally distributed foliar and structural trait data, respectively.

To determine how resource-use strategies influenced species productivity, we compared radial growth between black spruce and tamarack among- and within sites. We determined the growth for individual trees at OBS, SCC, and BAC from June to August 2018 – 2020. We used a Wilcoxon rank sum test to compare growth between tamarack and black spruce at the site level and species level (all sites combined). We also compared the values associated with the first and second principal component for tamarack and black spruce at the site level and species level (all sites combined), however the sample size was too small for meaningful statistical comparisons.

Finally, to determine if the resource-use strategies were associated with species TWD, we used a Wilcoxon rank sum test to compare TWD between tamarack and black spruce at the site level. Data processing and statistical analyses were performed in R (version 3.6.3, R Core Team, 2020) with a significance level set to $\alpha = 0.05$. Figures were created with *ggplot2* (Wickham, 2016) and *ggpubr* (Kassambara, 2023).

Results

Resource-use strategies of black spruce and tamarack

The first three axes of the PCA analysis, performed with foliar and structural traits, explained a combined 85.4 % of the total variance and revealed site and species-specific resource-use strategies of tamarack and black spruce (Figure 2.2a and b). The first principal component (PC1) explained 46.6 % of the total variance and represented a productivity gradient with positive PC1 values reflecting higher values of A_{max}, g_{sw}, N_{mass}, and SLA, key aspects of the leaf-economic spectrum (Wright *et al*. 2004, Figure 2.2a). Black spruce and tamarack separated along the first axis, with tamarack having a more productive suite of traits compared to black spruce. Tamarack had significantly greater SLA ($p < 0.05$), N_{mass} ($p < 0.005$), A_{max} ($p < 0.005$), and g_{sw} ($p = 0.001$) compared to black spruce at both OBS and SCC (Figure 2.3a-d). The second principal component (PC2) explained 26.4 % of the total variance and represented a gradient of tree size and competition for light with positive PC2 values representing larger-diameter individuals that were generally taller with a fuller canopy (higher CA, DBH, and H; positive PC2 values; Figure 2.2a and b). Black spruce and tamarack were separated along PC2, but the separation was site specific. The crown area of tamarack was significantly larger then black spruce across all three sites ($p < 0.05$) but tree height and LCR varied across sites (Figure 2.3g-i). The third principle component (PC3) explained 12.5 % of the variance and represented a gradient of water-use efficiency ($\delta^{13}C$ and WUE_i) with positive PC3 values representing lower water-use efficiency (Figure 2.2b). Sites separated along the third axis, with black spruce and tamarack showing higher water-use efficiency at OBS compared to SCC. Black spruce and tamarack were not well separated along PC3 and there was no significant differences in the WUE_i or $\delta^{13}C$ values between species (Figure 2.3e & f).

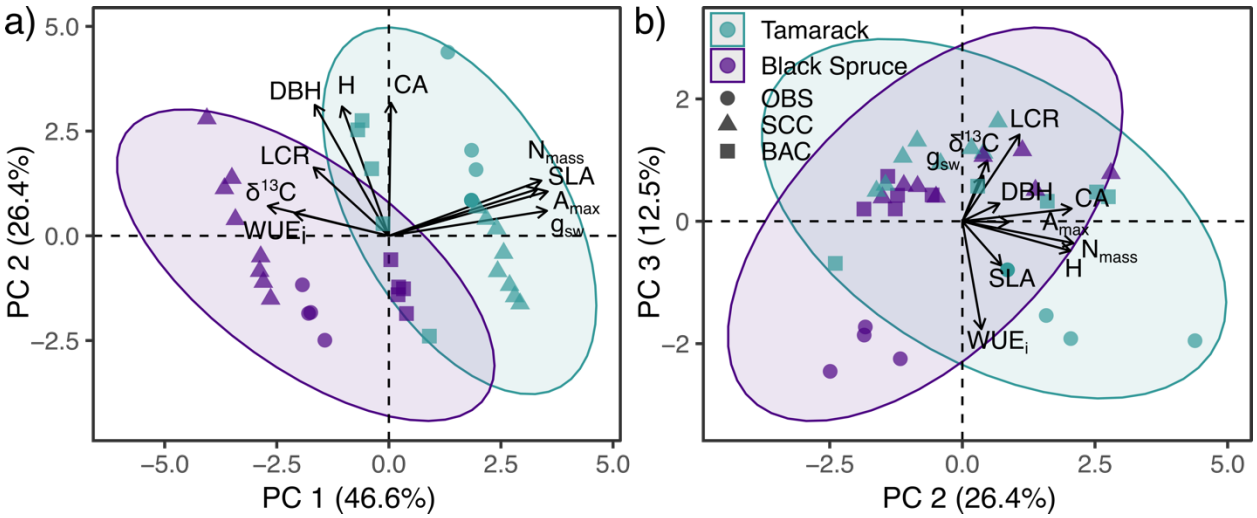

Figure 2.2 Principal component analysis summarizing tree foliar functional traits and structural traits. The first three principal components are displayed with principal component one (PC1) representing productivity gradient of functional foliar traits (a), principal component two (PC2) representing a gradient of tree size and competition for light (a and b), and principal three (PC3) representing a gradient of water-use efficiency (b). Individual trees at Old Black Spruce (OBS), Scotty Creek (SCC) and Baker Creek (BAC) are represented by symbols. The teal and purple shaded areas are concentration ellipsoids representing regions containing 95 % of the tamarack and black spruce samples, respectively. Variance explained by each principal component is indicated in parentheses. Structural traits included tree height (H; m), diameter at breast height (DBH; cm), live crown ratio (LCR; unitless ratio) and crown area (CA; m2). Foliar traits include specific leaf area (SLA; $cm^2\ g^{-1}$), foliar nitrogen concentration (N_{mass}; mg N g^{-1} leaf), maximum photosynthetic rate (A_{max}; µmol CO_2 m^{-2} s-1), integrated water-use efficiency ($\delta^{13}C$; ‰), instantaneous water-use efficiency (WUE_i; µmol CO_2 $mmol^{-1}$ H_2O) and stomatal conductance to water vapor (g_{sw}; mol H_2O m^{-1} s^{-1}). Variables were scaled and centred before analysis.

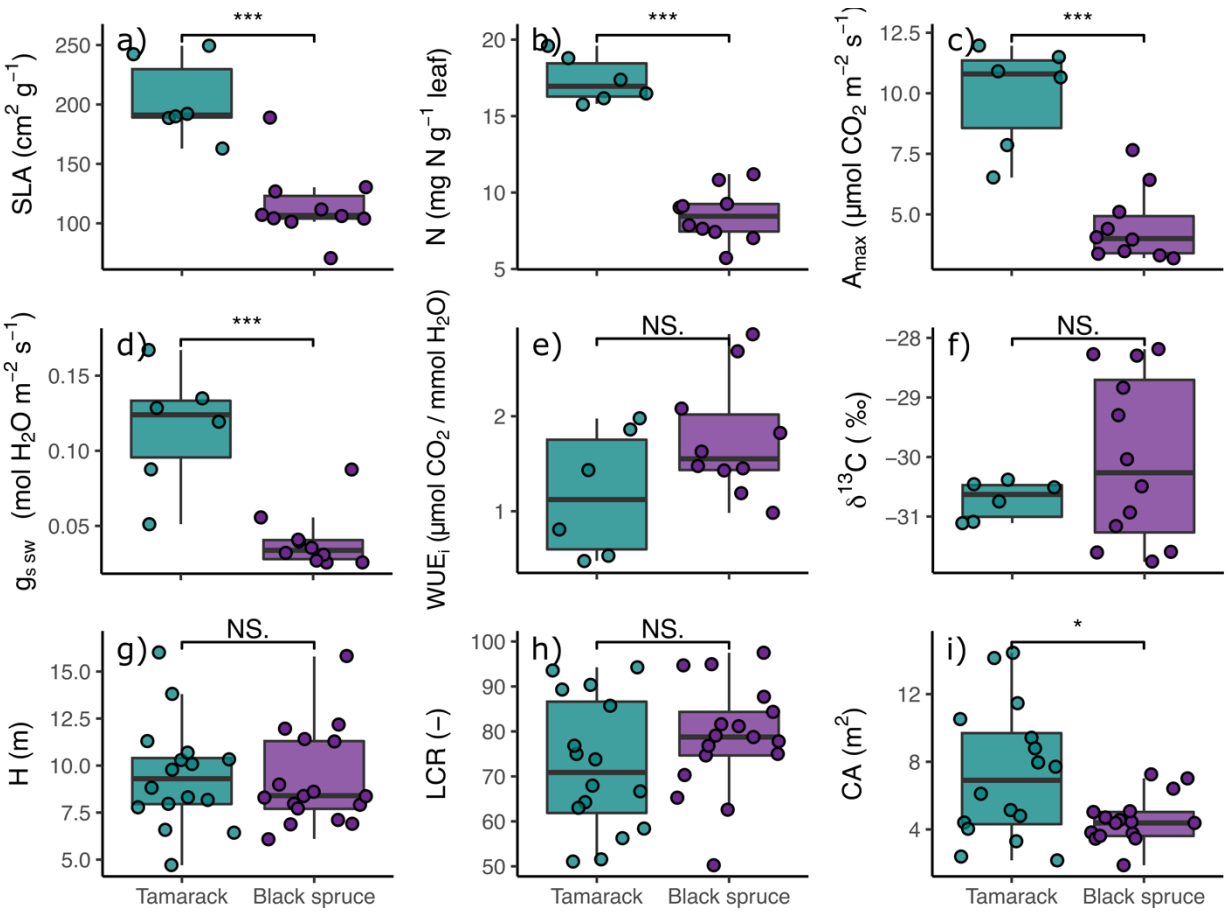

Figure 2.3 Plant foliar and structural traits associated with black spruce and tamarack. Foliar traits (a – f) include specific leaf area (SLA; $cm^2\ g^{-1}$), foliar nitrogen concentration (N_{mass}; mg N g^{-1} leaf), maximum photosynthetic rate (A_{max}, µmol CO_2 m^{-2} s^{-1}), stomatal conductance to water vapor (g_{sw}; mol H_2O m^{-1} s^{-1}), instantaneous water-use efficiency (WUE_i; µmol CO_2 $mmol^{-1}$ H_2O), and integrated water-use efficiency ($\delta^{13}C$; ‰). Structural traits (g – i) included tree height (H; m), live crown ratio (LCR; unitless ratio) and crown area (CA; m^2). The difference between species was compared using a Wilcoxon rank sum test (NS. = not significant,* p = 0.05, ** p = 0.01, *** p < 0.001).

Results from the PERMANOVA analysis revealed a significant difference between the structural traits within- (p = 0.004) and among sites (p = 0.012). The variation between species (F = 10.3, R^2 = 0.17) was similar to the variation between sites (F = 5.4, R^2 = 0.17). Both black spruce and tamarack were fairly evenly spread across the two axes, and the beta dispersion test revealed no significant difference in the distribution of variance between species (F = 2.6, p = 0.11) or among sites (F = 2.8, p = 0.07).

Growth of black spruce and tamarack

Black spruce and tamarack productivity (i.e., growth) were assessed across sites. Growth primarily occurred in early summer (June), followed by a plateau in the mid-to-late summer (July – August; Figure SI.3). Growth averaged across years and sites, was almost two times greater in tamarack (0.612 mm ± 0.46 mm) compared to black spruce (0.313 mm ± 0.26 mm; $p = 0.001$, Figure 2.4). At OBS and BAC, tamarack growth was significantly greater than black spruce ($p < 0.001$ and $p = 0.04$, respectively), but at SCC, growth did not differ between the two species (Figure 2.4b). Tamarack and black spruce growth was greatest at OBS, and significantly higher compared to SCC and BAC (Figure 2.4c).

The two main principal components were also assessed across sites. The PC1, representing a foliar productivity gradient was higher for tamarack compared to black spruce at OBS and SCC (Figure 2.4d and e). Foliar traits were not measured at BAC. The foliar productivity gradient was similar among sites for each species (Figure 2.4f). The PC2, representing a gradient of tree size and competition for light, was similar between species (Figure 2.4g). At OBS tamarack had higher PC2 values and larger, and taller trees with a wider canopy, while at SCC black spruce had larger PC2 values (Figure 2.3a, b and Figure 2.4g). Baker Creek also had lager PC2 values for black spruce, however, only DBH was larger. Tamarack height, CA and LCR were all greater than black spruce at BAC (Table 2.2).

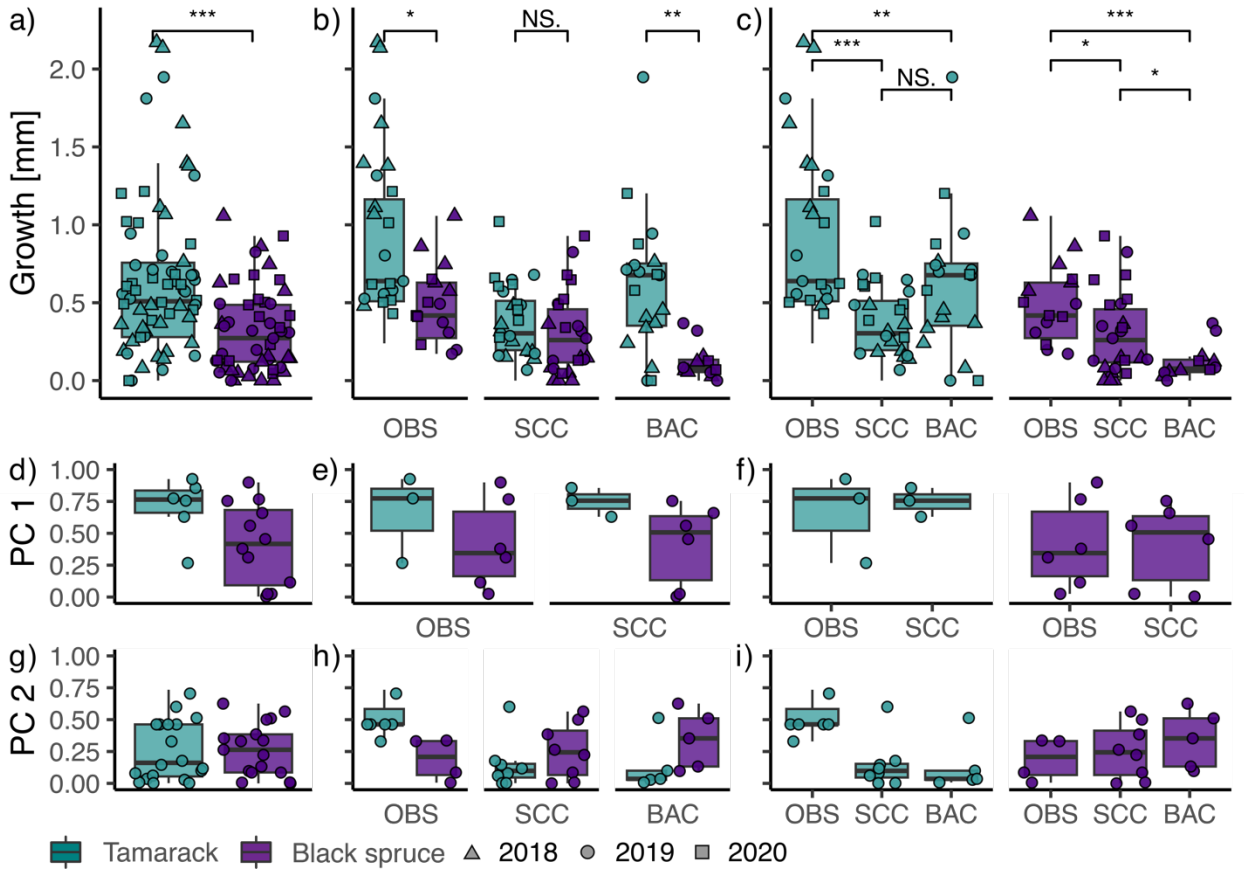

Figure 2.4 Cumulative annual radial growth (Growth; mm) of tamarack and black spruce across all sites (a), at each site (b) and between sites for each species (c). Each point represents the total growth of an individual tree in 2018, 2019 or 2020 at Old Black Spruce (OBS), Scotty Creek (SCC) and Baker Creek (BAC). The lower panels compare the principal component values between species across all sites (d, g and j), at each site (e, h, and k) and between sites for each species (f, i, l). Each point represents the principal component value assigned to each measured individual. Principal component one (PC1) represents a gradient in productivity associated with functional foliar traits and principal component two (PC2) represents a gradient in tree size and competition for light associated with tree structural traits. The difference were compared using a Wilcoxon rank sum test (NS. = no significance,* p = 0.05, ** p =0.01, *** p < 0.001).

Species tree water deficit

Regional meteorological conditions were generally wetter and cooler than normal during the study period. As indicated by the local meteorological observations, the summers of 2018, 2019 and 2020 had more rain and cooler air temperatures compared to the 1981-2010 normals (Figure SI.4). The

only summer with drier conditions than average was BAC in 2019, and the only summer with temperatures warmer than average was SCC in 2018.

Tree water deficit was determined from the ΔSR of each tree measured at OBS, SCC and BAC (Figure 2.5 a - f; Figure SI.3). The daily pattern of TWD, averaged by species, were similar between black spruce and tamarack, with differences in amplitude and the number of days in which trees were fully hydrated (Figure 2.5 a, c and e; Table 2.3). At OBS, tamarack TWD was significantly higher ($p < 0.05$) than that of black spruce, indicating a greater water deficit (Figure 2.5b, Table SI.1). However, tamarack was more responsive to rain events at OBS and rehydrated quickly, spending 13 days (± 5 days) fully hydrated, representing 14 % of the study period compared to 11 days (± 3 days) for black spruce (12 % of the study period; Figure 2.5a, Table 2.3). At SCC, black spruce had higher TWD than tamarack (not significant, $p = 0.1$; Figure 2.5d, Table SI.1), and spent only 7 days (± 5 days), or 5 % of the study period fully hydrated, compared to 12 % for tamarack (Table 2.3). At BAC, tamarack was better at rehydrating than black spruce and spent nearly five times as many days fully hydrated (15 days ± 6 days vs. 3 ± 1 day for black spruce), representing 17 % and 3 % of the study period, respectively (Table 2.3). However, there was no statistically significant difference between the TWD of black spruce and tamarack at BAC (Figure 2.5e and f).

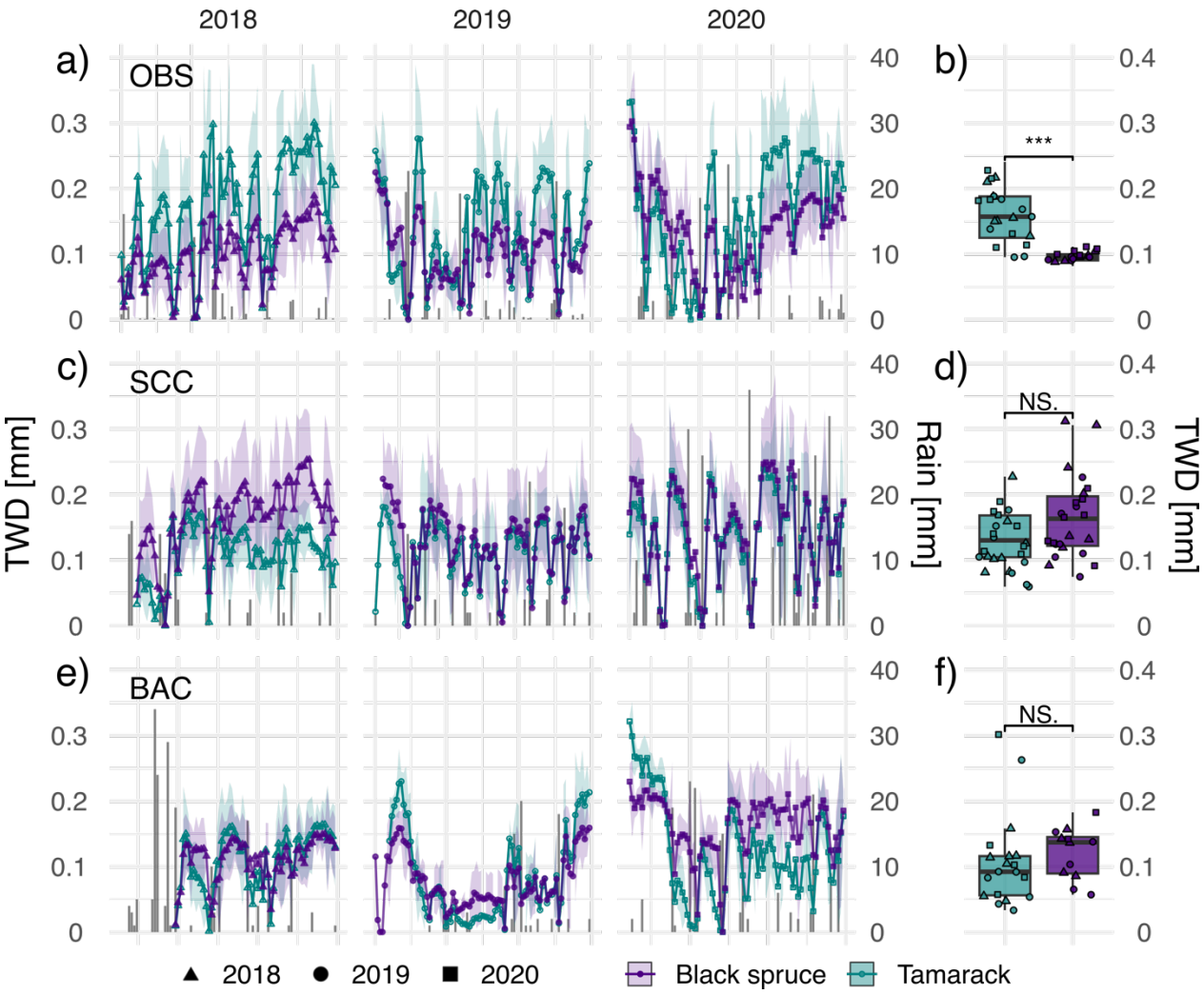

Figure 2.5 Averaged daily tree water deficit (TWD) of black spruce and tamarack at Old Black Spruce (OBS; a – b), Scotty Creek (SCC; c - d), and Baker Creek (BAC; e - f). Points denote the average daily TWD for each species, while the shaded areas represent the standard deviation among individuals. The panels on the right demonstrate the average annual TWD for each individual of black spruce and tamarack at OBS (b), SCC (d) and BAC (f). The difference between species average annual TWD was compared using a Wilcoxon rank sum test (NS. = no significance,* p = 0.05, ** p =0.01, *** p < 0.001).

Table 2.3 Average days (and standard deviation) with full hydration (i.e. days the tree water deficit returning to zero within a 24 -hour period) for of black spruce and tamarack at Old Black Spruce (OBS), Scotty Creek (SCC) and Baker Creek (BAC) in in 2018, 2019 and 2020. The portion hydrated (%) represents the number of day with full hydration, compared to the study period length. The study period is variable as not all trees recorded continuous measurements from June 1st 2018 to August 30th 2020 due to variable installation times, animal damage and power supply challenges.

	Tamarack	Black spruce	Tamarack	Black spruce
	Days with full hydration (days)		**Portion hydrated (%)**	
BAC	15 (± 6)	3 (± 1)	17.5 (± 9.9)	2.4 (± 2.4)
SCC	9 (± 4)	7 (± 5)	11.9 (± 7.0)	4.6 (± 4.2)
OBS	13 (± 6)	11 (± 3)	14.0 (± 6.4)	11.7 (± 3.2)

Discussion

Species' resource-use strategies

Our work found that that tamarack and black spruce traits partitioned into the same primary axes that describe global trait variation in trees, with one axis representing the leaf economic spectrum, and a second representing tree size and competition for light (Maynard *et al*. 2022). A species separation was found along the first axis of foliar productivity, indicating a distinction between acquisitive and conservative resource-use strategies for tamarack and black spruce that was consistent across sites (Burns and Honkala, 1990, Fleming *et al.* 1994, Wright *et al.* 2004). Tamarack had more positive values along the first axis (Figure 2.2a and Figure 2.4d) with traits indicative of an acquisitive resource-use strategy, as previously reported for the species (Gower and Richards, 1990). Higher foliar N_{mass} was found in tamarack, corresponding to a greater potential for photosynthetic CO_2 uptake and a greater demand for nitrogen acquisition (Evans, 1989; Wright *et al*. 2004). In correspondence with higher foliar N_{mass}, tamarack had leaves with higher SLA and faster CO_2 uptake (A_{max}, and g_{sw}; Figure 2.3a-d; Wright *et al*. 2004; Lambers *et al*. 2008). As a deciduous species, tamarack requires greater investment in photosynthetic CO_2 uptake and fixation to support annual needle loss and shorter periods of growth (Reich *et al*. 1992; Wright *et al*. 2004). Black spruce was on the other side of the foliar productivity gradient, with

traits associated with structural resistance at the cost of photosynthetic potential, indicating a conservative resource-use strategy (Figure 2.2a; Wright *et al*. 2004). The thick, long-lived needles of black spruce (with lower SLA) offer protection against frost damage, nutrient limitation, and desiccation (Figure 2.2a and Figure 2.4a; Onoda *et al*. 2011). However, the lower N_{mass} and A_{max} of black spruce likely limited photosynthetic CO_2 uptake (Reich *et al*. 1992; Wright *et al*. 2004). Tree resource-use strategies cannot be determined based on their foliar productivity alone, as tree structure contributes to the function diversity of tree species (Maynard *et al.* 2022).

The resource-use strategies of black spruce and tamarack were dependent, to some extent, on local environmental conditions that affected the structural traits of trees at each site. The separation of black spruce and tamarack along the second axis (PC2), representing tree size and competition for light, was dependent on site (Figure 2.2a and b). Trees compete for light by investing resources into growing taller, expanding their canopy area and depth (i.e. LCR, Maynard *et al*. 2022). However, structural traits, including crown diameter, crown height, and stem diameter are sensitive to local environmental conditions (Maynard *et al*. 2022). Tree height and crown size of both black spruce and tamarack are positively affected by precipitation (Maynard *et al*. 2022), temperature (Dufour-Tremblay *et al.* 2012, Joyce *et al.* 2017, Oboite *et al*. 2019) and soil nutrient concentrations (Tilton 1978). At one of the three sites (OBS), tamarack demonstrated acquisitive traits along PC2, characterized by larger and taller trees with a wider CA (Figure 2.2a). OBS is the warmest of the three sites, and has sandy loam soils that provides better access to soil nutrients (CASCC, 1998, Qu *et al.* 2023). Thus, tamarack likely had access to the nutrient resources needed to support taller trees with a wider crown area (Tilton 1978, Reich 2014). By contrast, tamarack at SCC had shorter trees with smaller CA, LCR, and DBH (Figure 2.2a, Table 2.2). Scotty Creek is nutrient-poor peatland complex where thick organic soils limit plant access to underlying mineral material (Braverman & Quinton, 2016; Dearborn *et al*. 2021). As an acquisitive species, tamarack has higher nutrient demands than black spruce, thus, the shorter and smaller tamarack at SCC likely resulted from nutrient, not water, limitation (Islam & Macdonald, 2005).

Variation in productivity associated with species' foliar and structural traits

The coordination of growth with foliar productivity aligned with our hypothesis; the acquisitive resource-use strategy of tamarack contributed to greater radial growth compared to black spruce at two of our three sites (OBS and BAC) and across the three sites combined (Figure 2.4a,c and d). Indeed, foliar traits supporting greater resource acquisition and use such as high A_{max} and N_{mass} have been associated with higher growth (Poorter *et al*. 2008; Martínez-Vilalta *et al*. 2010; Gibert *et al*. 2016). At OBS and BAC, tamarack maximised photosynthetic CO_2 assimilation with trees that were better at intercepting light (taller with higher CA and LCR) and had higher foliar productivity, resulting in significantly higher growth compared to black spruce (Dusenge *et al*. 2020; Figure 2.4b).

We expected total radial growth of tamarack to exceed that of black spruce at SCC, mirroring observations at OBS and BAC because the species separation along the first principle component of foliar productivity was consistent across sites (Figure 2.2a). Additionally, black spruce productivity at SCC is reportedly low (e.g., Sniderhan *et al*. 2021) because permafrost thaw-induced drying of the hydrologically and biogeochemically active layer reduces transpiration, causes decreased growth, and mortality in black spruce but not tamarack at the site (Baltzer *et al*. 2014; Patankar *et al*. 2015; Sniderhan & Baltzer, 2016; Dearborn *et al*. 2021). However, we found no difference in growth between black spruce and tamarack at SCC. For this study, the two species co-occurred in a low-lying stand bordering a fen, where soil nutrient concentrations were are high, relative to the rest of the peatland complex (Dearborn *et al*. 2021). We surmise that our sampled black spruce had adequate water and nutrient resource availability to maintained with its conservative foliar productivity strategy (Tilton 1978, Islam & Macdonald, 2005). By contrast, tamarack growth is positively correlated with nutrient supply, but with acquisitive foliar productivity nutrient demands are much higher (Burns & Honkala, 1990, Dearborn *et al*. 2021). Thus, nutrient availability at SCC was likely inadequate for tamarack, restricting the species' ability to dominate the canopy and compete with black spruce for light (as reflected by tamarack's position along PC2), resulting in low growth (0.394 ± 0.27 mm) relative to OBS and BAC (Figure 2.4b; Table SI.1) (Burns *et al*. 1990, Dearborn *et al*. 2021).

Competition for light and local conditions drove tree water deficit

We expected an acquisitive resource-use strategy for tamarack to be coordinated with higher TWD. To support photosynthetic CO_2 assimilation water is lost via transpiration (McDowell *et al*. 2008; Warren *et al*. 2021). Thus, an acquisitive resource-use strategy with higher growth and higher photosynthetic rates are often associated with greater transpiration and water loss (Gower *et al.* 1991, Reich 2014). We observed that, although TWD exhibited a degree of coordination with tree growth, it was also influenced by the gradient reflecting tree size and competition for light. As a result, species differences in TWD varied between sites.

At OBS, tamarack's acquisitive foliar productivity and enhanced competition for light allowed for more growth but resulted in TWD that was significantly higher than black spruce at OBS, and higher than tamarack at the other sites (although not significantly). Tamarack TWD increased sharply following periods of full hydration and radial growth suggesting tamarack maintained open stomata to maximise CO_2 assimilation at the expense of increased tree stem dehydration (Oberhuber *et al*. 2015; Warren *et al*. 2021; Figure 2.5a). These results could be explained by tamaracks reportedly anisohydric stomatal regulation (Oberhuber *et al*. 2015b; Sullivan *et al*. 2017; Dusenge *et al*. 2021; Warren *et al.* 2021). With stomatal conductance that allows for continued water loss during periods of high atmospheric demand and low soil water availability (Dusenge *et al*. 2020; Dusenge *et al*. 2021), tamarack are more likely to experience greater TWD. Lower water potential, which occur with greater TWD, has been associated with greater soil water uptake in *Larix spp*. (Oberhuber *et al*. 2015). Thus, higher TWD in tamarack likely contributed to greater water uptake which supported higher growth in tamarack compared to black spruce at OBS (Oberhuber *et al*. 2015; Figure 2.2b and Figure 2.5a).

With conservative foliar productivity and reduced competition for light black spruce at OBS had lower growth but maintained a lower and more constant TWD (Figure 2.5a). Black spruce TWD increased more gradually following periods of full hydration and growth (Figure 2.5a), suggesting stomates closed to minimize water loss during dry periods (McDowell *et al*. 2008; Sullivan *et al*. 2017; Dusenge *et al*. 2021). Tight stomatal regulation has been reported for *Picea* sp. in response to natural and experimental drying and warming (Macdonald & Lieffers, 1990; Pepin *et al*. 2002;

Oberhuber *et al*. 2015; Warren *et al*. 2021; Dusenge *et al*. 2021). The conservative resource-use strategy of black spruce comes as trade-offs (Salomón *et al.* 2022). By closing stomata earlier, the stem water potentials remain higher and can restrict root water uptake. As a result, stem refilling in black spruce was more limited after periods of full hydration, leading to fewer days with fully hydrated trees (12% of the study period, as opposed to 14% for tamarack, Figure 2.5a). While we did not measure the response of stomatal conductance to changing water availability, the low g_{sw} of black spruce indicates stomatal regulation that could limit growth (Figure 2.3d).

At SCC, TWD was more coordinated with species growth and ability to compete for light then with foliar productivity. Black spruce, with conservative foliar traits, but taller trees and had greater TWD than tamarack (not significant). In boreal species, tree architecture that enhances access to light impacts tree hydraulic functioning by increasing sap flow and transpiration rates (Pappas *et al.* 2018). The taller black spruce with larger crowns, likely had higher water demands then tamarack. To maintain stem water potentials when demands are high, black spruce are known to downregulate stomatal conductance (isohydric regulation), favouring protection from water stress over foliar productivity and growth (Pepin *et al*. 2002; Sullivan *et al*. 2017; Warren *et al*. 2021; Dusenge *et al*. 2021). However, the strategy to limit water loss reduces the capacity for stem refilling and does not fully prevent stem dehydration (Salomón *et al.* 2022). Lower stem refilling was apparent at SCC, with black spruce only able to fully rehydrate for 4.6 % of the study period (compared to 11.9 % for tamarack). Additionally, black spruce had higher $\delta^{13}C$ (used as a proxy for integrated water-use efficiency; Farquhar *et al*. 1989), indicating greater water stress compared to tamarack at SCC, and compared to black spruce at OBS (Warren *et al*. 2001; Martínez-Vilalta *et al*. 2004; Figure 2.3f and Figure 2.4b; Figure SI.5). Thus, the higher water demands in the larger trees and the reduced ability for water uptake likely contributed to a TWD that was higher for black spruce compared to tamarack at SCC.

At BAC, the TWD was similar between species despite tamarack growth being significantly greater than that of black spruce (Figure 2.4b and Figure **2.5**c). Black spruce had higher values along PC2, however, only DBH was greater for black spruce. Thus, structural traits including height, CA and LCR did not offer black spruce a competitive advantage for light (**Figure 2.2**a). Instead, environmental conditions likely played a pivotal role in driving TWD (and growth) at BAC. Like

much of the Taiga Shield, BAC is a mosaic landscape with soil moisture content ranging from < 10 % on the ridges to > 85 % in the depressions (Wolfe *et al*. 2011). Forests are clustered between bedrock outcrops where water flows into the depressed patches from upland outcrops and accumulates in the active (seasonally thawed) layer (40 – 130 cm thick) (Spence & Woo, 2002; Wolfe *et al*. 2011; Morse *et al*. 2016). Black spruce and tamarack co-occur at BAC but occupy different parts of the landscape (Evans *et al*. 2016). Black spruce grow on drier, elevated portions of the site, while tamarack occupies the deeper wetter depressions. However, the summer of 2018 witnessed the highest recorded rainfall in the past 50 year (Spence *et al.* in prep), leading to high water availability across the site during the three years in the study period (Spence *et al*. in prep). Thus, black spruce and tamarack at BAC were unconstrained by water limitations, resulting in very similar TWD between species. With an acquisitive strategy, tamarack was better at accessing water and nutrients compared to black spruce, resulting in more days of full hydration for tamarack, and over twice as much growth than black spruce (Tilton 1978; Figure 2.4f and Figure 2.5b).

There are limitations to inferring stomatal regulation and iso/anisohydric classification without explicit measures of plant water potential, xylem vulnerability, or stomatal conductance at each site (Martínez-Vilalta & Garcia-Forner, 2017; Hochberg *et al*. 2018). Stomatal regulation, and thus iso/anisohydric strategies vary with environmental conditions (Martínez-Vilalta & Garcia-Forner, 2017; Hochberg *et al*. 2018). From high to low soil water availability, plants of the same species will exhibit a range of stomatal regulation from anisohydric, to isohydric, respectively (Hochberg *et al*. 2018). While work at other boreal site have used needle and branch water potentials, and stomatal conductance to observe anisohydric and isohydric regulation for tamarack and black spruce, respectively, previous work using sap flux density and stem radius change measurements at OBS have described more isohydric regulation for tamarack (Pappas *et al*. 2018, Dusenge *et al*. 2021; Warren *et al.* 2021). Thus, more work is needed to confirm that higher growth and TWD in tamarack can be associated with anisohydric stomatal regulation at OBS, and that isohydric regulation constrained growth and TWD in black spruce at OBS and SCC.

Conclusions

With this work, we determined that resource-use strategies of black spruce and tamarack varied across sites when both foliar and structural traits were considered. Greater competition for light and enhanced foliar productivity at OBS led to more dehydration in tamarack (higher TWD) compared to black spruce, but increased tamarack's ability to rehydrate frequently throughout the study period, resulting in higher growth. However, in nutrient-poor conditions, tamarack exhibited reduced height and competitiveness for light, resulting in constrained growth, despite possessing acquisitive foliar traits. Thus, despite the importance of foliar productivity, structural traits and site conditions, including nutrient availability, contributed greatly to species productivity and tree water deficit, emphasizing the need for a more complete trait spectrum to understand tree functional diversity (Maynard *et al*. 2022). Although tree species have strategies to cope with current conditions in the boreal forest (Gauthier *et al*. 2015), there is uncertainty regarding how resource-use strategies will influence the resilience of black spruce and tamarack to projected environmental changes. Continued work to quantify the responses of common and widespread tree species to progressively water-limited conditions will help to understand the capability of boreal forests to manage changing environmental conditions, and to maintain their ecosystem services related to climate regulation, carbon sequestration, wildlife habitat, culture and economy (Gauthier *et al*. 2015).

Chapter 3 – Spatial and temporal variation in forest transpiration across a forested boreal peatland complex

Nia Perron [1,2], Jennifer L. Baltzer [3], and Oliver Sonnentag [1,2]

[1] Département de géographie, Université de Montréal, Montréal, Québec, Canada, [2] Centre d'étude de la forêt, Université du Québec à Montréal, Montréal, Québec, Canada, [3] Department of Biology, Wilfrid Laurier University, Waterloo, Ontario, Canada

Perron N, Baltzer J L and Sonnentag O 2023 Spatial and temporal variation in forest transpiration across a forested boreal peatland complex *Hydrological Processes* **37** Online: https://onlinelibrary.wiley.com/doi/10.1002/hyp.14815

Abstract

Transpiration is a globally important component of evapotranspiration. Careful upscaling of transpiration from point measurements are thus crucial for quantifying water and energy fluxes. In spatially heterogeneous landscapes common across the boreal biome, upscaled transpiration estimates are difficult to determine due to variation in local environmental conditions (e.g., basal area, soil moisture, permafrost). Here, we sought to determine stand-level attributes that influence transpiration scalars for a forested boreal peat landscape consisting of sparsely-treed wetlands and densely-treed permafrost plateaus as land cover types. The objectives were to quantify spatial and temporal variability in stand-level transpiration, and to identify sources of uncertainty when scaling point measurements to the stand-level. Using heat ratio method sap flow sensors, we determined sap flux density for black spruce and tamarack for two-week periods in 2013, 2017 and 2018. We found greater basal area, well drained soils, and the presence of permafrost increased daily sap flux density in individual trees, suggesting that local environmental conditions are important in sap flux density. When sap flux density was scaled to stand-level transpiration using gridded 20 m × 20 m resolution data across a ~10 ha plot, we observed significant differences in daily plot transpiration between years (0.17 to 0.30 mm day^{-1}), and across land cover types. Daily transpiration was lowest

in grid-cells with sparsely-treed wetlands compared to grid-cells with well-drained and densely-treed permafrost plateaus, where daily transpiration reached 0.80 mm, or 30 % of the daily evapotranspiration. When transpiration scalars (i.e., sap flux density) did not represent the different land cover types (i.e., permafrost plateaus and wetlands), scaled stand-level transpiration was overestimated by 42 %. To quantify the relative contribution of trees to evapotranspiration, we recommend sampling designs stratify local environmental conditions to accurately represent variation associated with land cover types, especially with different hydrological functioning as encountered in rapidly thawing boreal peat landscapes.

Introduction

Transpiration is the evaporative loss of water from plants to the atmosphere (Taiz and Zeiger, 2002). This process involves a phase change from liquid to gas which absorbs energy, cooling the surrounding area (Wang and Dickenson *et al*. 2012). Thus, transpiration is a key functional process that affects how vascular plants contribute to regional water cycling, the land surface energy balance and regional and global climate through its contribution to evapotranspiration (Bonan 2008, Price *et al*. 2013, Schlesinger and Jasechko 2014). Controls of transpiration include abiotic conditions (e.g., atmospheric water vapour and carbon dioxide concentrations, air temperature, net radiation, and soil water availability; Jarvis and McNaughton, 1986; Schulze 1986) and plant physiological function (e.g., leaf/stomatal conductance, root water uptake and transport; Taiz and Zeiger 2002, Fisher *et al*. 2011). In boreal forests, transpiration can contribute an estimated 65 % (± 18 %) to evapotranspiration (Schlesinger and Jasechko 2014) and thus, a better understanding of its drivers is needed to constrain estimates of forest ecosystem responses to global change (Poyatos *et al*. 2020).

Transpiration can be estimated using sap-flow methods comprising point measurements (e.g., sap flux density) of water fluxes through plant stems that are scaled to tree- or stand-level transpiration using species- or stand-specific characteristics (e.g., sapwood or leaf area per unit ground area; Granier 1987; Čermák and Nadezhdina 1998, Wullschleger *et al*. 1998, Oren *et al*. 1998; Poyatos *et al*. 2016). One challenge inherent in scaling sap flow from point measurements to stand-level transpiration is the variability in transpiration scalars (i.e., sap flux density and sapwood area)

within and among individual trees and forest stands (Ford *et al*. 2007; Angstmann *et al*. 2012; Poyatos *et al*. 2020). Heterogeneous landscapes are characterized by spatial variation in stand structural attributes (e.g., tree age and diameter, and canopy architecture and density) that cause variation in transpiration scalars (Zimmermann *et al*. 2000; Köstner 2001; Ewers *et al*. 2005; Moore *et al*. 2004; Forrester *et al*. 2015). Local environmental conditions, including edaphic characteristics, can also influence transpiration scalars (Traver *et al*. 2010; Mackay *et al*. 2010).

Variation in transpiration has been associated with soil moisture (Oren and Pataki, 2001; Angstmann *et al*. 2012; Looker *et al*. 2018), nutrient availability (Ewers *et al*. 2000; Cramer *et al*. 2008), topography (Looker *et al*. 2018; Gutierrez Lopez *et al*. 2021), and permafrost thaw (Cable *et al*. 2014; Patankar *et al*. 2015; Kropp *et al*. 2017). In forest stands in North America, transpiration rates were highest where environmental conditions did not limit growth (Traver *et al*. 2010; Mackay *et al*. 2010; Angstmann *et al*. 2013). While some work has been done to identify stand structural attributes (e.g., tree size distributions) required for accurate transpiration estimates (e.g., Kume *et al*. 2010, Berry *et al*. 2018), we lack detailed information on how structural, edaphic, and demographic attributes influence stand-level transpiration in northern boreal forest stands (Angstmann *et al*. 2012).

Understanding the temporal and spatial variability of stand-level transpiration, and the drivers of this variation, is especially important for boreal forests because they are one of the fastest warming systems on the planet. With rising air temperatures, the atmospheric demand for vapor pressure has increased, resulting in increased boreal biome evapotranspiration (Helbig *et al*. 2020). To understand the mechanisms behind forest evapotranspiration, and how it may change under future climate conditions, our goal was to better understand what is affecting stand-level transpiration. To achieve this goal, we deployed sap flow sensors in a forested boreal peat landscape with spatial variation in stand structure, edaphic, and demographic conditions in the southern Taiga Plains ecozone of the Northwest Territories, Canada. Our objectives were to (i) determine the temporal and spatial variability in transpiration, (ii) to identify key stand structural, edaphic, and demographic attributes affecting individual tree sap flux density and, in consequence, transpiration, and (iii) to demonstrate the potential sources of uncertainty associated with transpiration upscaling in a heterogeneous boreal peat landscape.

Data and methods

Study site

Our work was undertaken in the headwater portion of Scotty Creek, a 152 km^2 drainage basin located ~50 km south of Fort Simpson, NT (61° 180 N, 121° 180 W) (Quinton *et al*. 2019). This portion of Scotty Creek is characterized by forested permafrost plateaus underlain with discontinuous permafrost and surrounded by largely treeless, permafrost-free thermokarst wetlands (Quinton *et al*. 2009, 2019). The permafrost plateaus are composed primarily of Organic Cryosols, while the permafrost free thermokarst features have Organic Soils (Dearborn *et al*. 2021). Mean annual air temperature at Fort Simpson between 1981 and 2010 was -2.8 °C with a mean July temperature of 17.4 °C and a mean January temperature of -24.2 °C (Quinton *et al*. 2019). The mean annual precipitation for the same period was 390 mm, with only 38 % as snowfall (Quinton *et al*. 2019).

A 10-ha forest dynamics plot was established within Scotty Creek as part of the Smithsonian Institute's Forest Global Earth Observatory network (ForestGEO) (Anderson-Teixeira *et al*. 2015, Davies *et al*. 2021, Dearborn *et al*. 2021). The Scotty Creek ForestGEO plot (herein referred to as "the plot") is 800 m (east-west) by 120 m (north-south), divided into 240 20 m × 20 m grid-cells that encompass a gradient of edaphic and forest conditions (Dearborn *et al*. 2021; Figure 3.1). The forest is dominated by black spruce (*Picea mariana* [Mill] B.S.P, 80 % of all stems), followed by tamarack (*Larix laricina* (Du Roi) K. Koch, 11 % of stems), birch species, which form a species complex (*Betula spp*., 7 % of stems), and other common boreal tree and large shrub species (2 %) (Dearborn *et al*. 2021).

The establishment and re-census of the plot is detailed in Dearborn *et al*. (2020). Briefly, between 2012 and 2014 each live stem within the plot with a diameter at breast height (DBH, measured 1.3 m above the ground surface) greater than or equal to 1 cm was tagged, mapped, measured, and identified to species (or species complex in the case of birch, total of 40,584 stems). In 2018, a partial re-census was performed to identify the status of each tree (alive vs. dead) and to tag, measure and map any new stems with a DBH ≥1 cm (Anderson Teixeira *et al*. 2015; Dearborn *et*

al. 2021). DBH re-measurements were not performed during the second census due to the slow growth at the site (Sniderhan & Baltzer, 2016).

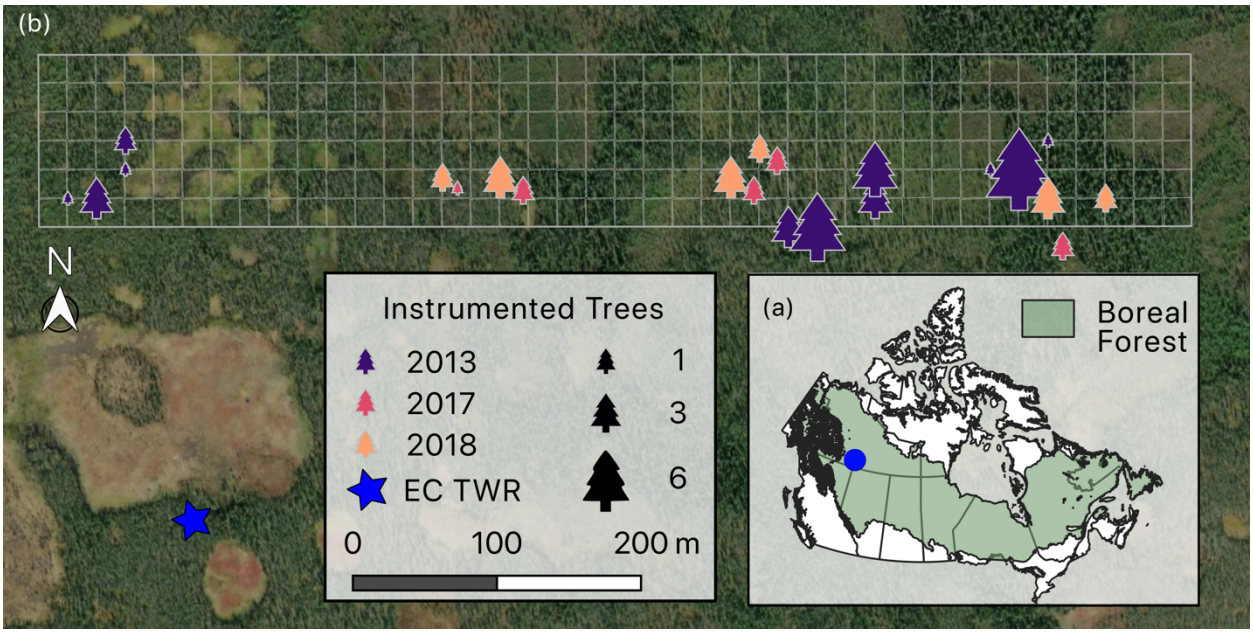

Figure 3.1 Location of Scotty Creek within the Canadian boreal biome (a); and the Scotty Creek ForestGEO plot subdivided into 20 m × 20 m grid-cells overlain on land cover imagery (b), (source: ESRI World Imagery). Coloured trees represent trees sampled for sap flow with the different colours reflecting sampling years and the size of the tree representing the sample size at each location. The blue star represents the location of the forest eddy covariance tower (EC TWR).

Sap flow measurements and conversion to sap flux density (J_s)

We used heat ratio method (HRM) sap flow sensors (SFM1 Sap Flow Meters; ICT International, Armidale, NSW, Australia) to obtain sap flux density (J_s; $mm^3\ mm^{-2}\ s^{-1}$) of black spruce and tamarack trees in 2013 (n = 21), 2017 (n = 6), and 2018 (n = 12). To ensure a consistent measurement period across years, the measurement start and end dates were 27 June to 11 July for each year (hereafter referred to as the "sampling period"). Outside of this period, data availability was limited. The instrumented trees spanned 15 grid-cells in the plot (Figure 3.1b). To minimize permanent damage to trees in the plot, only trees with a DBH > 6.0 cm were instrumented following the procedures outlined in Burgess *et al*. (2001) and Vandegehuchte *et al*. (2015).

The HRM uses a central heater probe in the conducting xylem (sapwood) of a tree stem, positioned equidistant between an upstream and downstream temperature probe (Burgess *et al*. 2001). Each temperature probe has two thermistors, the first located at 12.5 mm and second at 27.5 mm into the stem. For our analysis, only the first thermistor (12.5 mm) was used as the second thermistor (27.5 mm) was located in the non-conducting wood tissues (heartwood) of the sampled trees. The central heater probe released a heat pulse of 10 Joules which warms the surrounding sap and transfers heat towards the downstream and upstream probes. The temperature differential between the upstream and downstream probes, recorded at 10 (2017 and 2018) and 30 (2013) -minute intervals, was used to derive 30-minute heat pulse velocity (V_h; cm s^{-1}), calculated following Burgess *et al*. (2001) and Marshall (1958):

$$V_h = \frac{k}{x} ln\left(\frac{v_1}{v_2}\right) \qquad \text{Equation 1}$$

where k is the thermal diffusivity of fresh wood (2.5×10^{-3} cm^2 s^{-1}), x is the distance between the heat pulse probe and the temperature probes (0.6 cm); v_1 and v_2 are temperature (˚C) in the upstream and downstream temperature probes. Corrections for wounding and probe misalignment were applied according to Burgess *et al*. (2001). Using the Sap Flow Tool software package (ICT International), the corrected V_h were converted to J_s (mm^3 mm^{-2} s^{-1}) based on sapwood density and water content constants (Burgess *et al*. 2001). The 30-minute J_s time-series were manually adjusted using a linear transformation to coordinate zero-flow conditions with periods of no biophysical drivers of sap movement (i.e., night-time periods when vapour pressure deficit was near zero, or during or immediately following a precipitation event; Eliades *et al*. 2018). Small gaps in the data set (< 3 hours) were filled using linear interpolation, representing up to 4 % of each time series. If days had gaps longer than three hours, data from that day was removed from the analysis. We determined the total daily J_s for each tree over the two-week period before taking average daily value across all trees for each year (2013, 2017, and 2018) separately.

Scaling tree-level sap flux density to stand-level transpiration

Field surveys were conducted in 2016 and 2019 at Scotty Creek to measure sapwood area (A_s) for black spruce (n = 58) and tamarack (n = 31). This data was combined with samples from

northwestern Canada (Figure 3.2, Bond-Lamberty 2002) to develop species-specific allometric relationships between A_s and DBH for black spruce (n= 201, DBH range = 0.34 - 21.8 cm) and tamarack (n= 64, DBH range = 5.3 – 28.6 cm). To derive A_s, the equation ($A_s = a \times DBH^b$) was used, where a and b are species-specific coefficients.

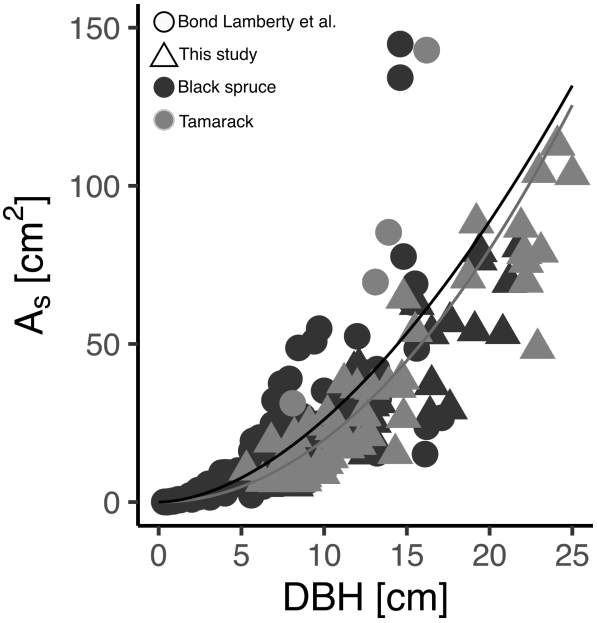

Figure 3.2 Allometric relationship between tree diameter at breast height (DBH; cm) and sapwood area (As; cm2) for black spruce (n = 201) and tamarack (n = 64). Samples were taken from trees at Scotty Creek and other boreal forest stands in northwestern Canada (Bond-Lamberty 2002).

At Scotty Creek, A_s was not measured directly from trees instrumented with HRM sensors to reduce damage that may influence the J_s measurements. A core (5.1 mm) was extracted from the main stem of nearby trees and held against the sunlight to identify the wet and translucent sapwood from the drier heartwood section, and to measure sapwood depth (S_d) and bark thickness (B_t; i.e., Warren *et al*. 2018). The S_d and B_t were used alongside stem DBH to derive A_s for each tree (Quiñonez-Piñón and Valeo 2017).

$$A_s = \pi \left(\frac{DBH}{2} - B_t\right)^2 - \left(\frac{DBH}{2} - B_t - S_d\right)^2 \qquad \text{Equation 2}$$

The relationship between DBH and A_s could be best described by the formula $A_s = 10^{-0.408} \times DBH^{1.766}$ for black spruce and $A_s = 10^{-0.767} \times DBH^{2.021}$ for tamarack (Figure 3.2, Figure SII.1). The allometric relationships were used to determine the A_s of each tree instrumented with HRM sap flow sensors, and each black spruce and tamarack with a DBH > 1 cm in the plot.

Daily transpiration for each grid-cell (T_{cell}, mm) in the plot was determined by upscaling daily J_s using the total A_s of all the trees in the plot (A_{s_total}) and the grid-cell area (A_G; 400 m^2).

$$T_{cell} = J_s \frac{A_{s\_total}}{A_G} \qquad \text{Equation 3}$$

The daily transpiration across the whole plot (T_{plot}) was determined by taking the average T_{cell} from the 240 grid-cells in the plot.

Stand structural, demographic, and edaphic attributes

Stand structural attributes were determined for each 20m × 20 m grid-cell using data collected during the 2012 – 2014 census (Dearborn *et al*. 2021). These included stem density (number of trees per grid-cell) and basal area (m^2 per grid-cell). To characterize the demographic attributes of each grid-cell, we tallied the total number of black spruce and tamarack deaths and recruits in each grid-cell between 2012 and 2018 (Dearborn *et al*.2020). Demographic data for other taxa were not included because the other taxa are rare in the plot and they had more consistent populations (Dearborn *et al*. 2021). However, these other taxa were included in grid-cell stem density and basal area estimates.

The edaphic attributes of the plot were determined between 2012 and 2018 for each grid-cell, as outlined in Dearborn *et al*. (2020). Briefly, spatial patterns of soil moisture for the top 5 cm of soil were determined based on volumetric soil water content (g cm^{-3}) measurements collected on July 19, 2012 using time domain reflectometry probes (ThetaProbe, Delta-T Devices, Cambridge, UK, and Stevens Hydra Probe, Stevens Water Monitoring Systems Inc., Portland, OR) and corrected using site-specific calibrations (Warren, 2015; Dearborn *et al*. 2021). The July 19, 2012 measurements correlated strongly with measurements taken from subsections of the plot for two

days in 2012, four days in 2013 and one day (at multiple depths) in 2017, confirming that the initial measurements represented spatial patterns of soil moisture across the plot. Snow depth was measured in 2013 using a GPS automatic snow depth probe (Snow-Hydro LLC) and re-measured with the same instrument in 2015 to assess the representativeness of the measurements through time in terms of snow depth rankings across grid-cells. In August 2018, the fibric layer depth (m), organic layer thickness (m), and peat humification (using the von Post scale; von Post, 1922) were determined for each grid-cell. Frost table depth (cm) as a depth to refusal was measured on July 19, 2012 using a 2 m steel rod. Since over 50 % of the frost table depth measurements were beyond the length of the probe (i.e., > 2 m), the values were categorized into three groups (< 50 cm, 50 - 200 cm, and > 200 cm). A full description of the edaphic sampling efforts and variables can be found in Dearborn, *et al*. (2020).

Dearborn *et al*. (2020) found that the edaphic variables (soil moisture, organic layer thickness, fibric layer depth, peat humification, frost table depth, and snow depth) covaried strongly. To account for the covariation, they used principal components analysis (PCA) to identify the major environmental gradients across the plot. The edaphic variables were both categorical (organic layer thickness, peat humification, and frost table depth), and continuous (soil moisture, fibric layer depth and snow depth), so a mixed PCA was used. This technique performs a multiple correspondence analysis on the categorical data, and a PCA on the continuous variables, before combining the two analyses into one ordination (Chavent *et al*. 2014). The first two principal components were retained for this analysis. The first principal component (PC1) explained 21.4 % of the variance in edaphic variables across grid-cells and represented a gradient of soil moisture and permafrost presence with high values of PC1 corresponding with dry soils and the presence of permafrost. The second principal component (PC2) explained 13.3 % of the variance in edaphic variables and reflected a gradient of organic layer thickness, peat humification and snow depth with high PC2 values corresponding with mineral soils nearer to the surface, more highly humified peat and a larger snow depth. Here, we use grid-cell PC1 and PC2 scores from Dearborn *et al*. (2020) as continuous variables reflecting edaphic conditions in the plot (Baltzer *et al*. 2020).

Evapotranspiration and meteorological conditions

Meteorological conditions and evapotranspiration (ET; mm) were estimated from measurements made on a micrometeorological tower installed in 2013 (Helbig *et al*. 2016b). The 15 m tower was located on a forested peat plateau ~200 m southwest of the plot. Photosynthetically active radiation (PAR) measured as photosynthetic photon flux density (μm m^{-2} s^{-1}; PQS1, Kipp and Zonen, Delft, The Netherlands), air temperature (T_{air}; °C), and relative humidity (HC2-S3, Rotronic AG, Bassersdorf, Switzerland) were measured at 30 min intervals. Vapour pressure deficit (VPD, hPa) was derived from the measurements of T_{air} and relative humidity. Precipitation (mm) was measured at 30 min intervals using a tipping bucket rain gauge (TR-5251, Texas Electronics Inc., Dallas, TX) located near the tower. Estimates of ET were obtained with the eddy covariance technique comprising sonic anemometer (CSAT3A; Campbell Scientific Inc., Logan, UT) and CO_2/H_2O open-path infrared gas analyser measurements (EC150; Campbell Scientific Inc.), both collected at 10-Hz frequencies. A detailed description of the Scotty Creek eddy covariance set-up and data processing can be found in Helbig *et al*. (2016b).

Statistical analysis

All statistical analyses were carried out in R (version 3.6.3, R Core Team, 2020). To determine the drivers of J_s in the plot, we fitted linear mixed models (lme4 package, Bates *et al*. 2015) with the grid-cell stand structural (basal area and stem density), edaphic (PC1 and PC2) and demographic (black spruce and tamarack deaths and recruits) attributes as fixed effects and year as a random effect. We compared the difference in Akaike's information criterion (AIC) between full and reduced models where $\Delta AIC = AIC_i - AIC_{min}$ to determine which attributes best describe the dependence of daily J_s. Values of $\Delta AIC < 2$ reflect little difference in the appropriateness of the models (Burnham & Anderson 2002), therefore the most parsimonious model with an $\Delta AIC < 2$ was used. For all models, we examined residuals plotted against predictors to confirm no patterns that indicate autocorrelation. For all statistical tests, the significance was set to $\alpha = 0.05$.

Four different adjustments were made to T_{cell} to demonstrate the sensitivity associated with upscaled transpiration (Table 3.1). First, we adjusted T_{cell} to account for stand structural, edaphic,

and demographic attributes with the strongest relationship to daily J_s. To account for the effect of stand structural attributes, T_{cell} was adjusted for basal area (T_{adj_BA}; see section 3.2), reflecting the potential neighbourhood effects of the surrounding trees located in the same grid-cell. To account for edaphic attributes, T_{cell} was adjusted for PC1 (T_{adj_PC1}), reflecting the impact of local (grid-cell) growth conditions on transpiration. We did not develop an adjustment for demographic attributes as they were not significantly related to daily J_s. We used the predict() function from the lme4() package to obtain adjusted daily J_s values for each grid-cell. These values were then used to scale grid-cell daily J_s to grid-cell daily adjusted transpiration (T_{adj_BA} and T_{adj_PC1}).

Table 3.1 Acronyms used to describe the adjustments made during transpiration upscaling.

Adjustment		Description
Unadjusted	T_{cell}	The daily grid-cell transpiration.
Unadjusted	T_{plot}	The daily plot transpiration averaged across grid-cells (n = 240).
Stand structural attributes	T_{adj_BA}	The daily grid-cell transpiration, adjusted for stand structure; basal area.
Edaphic attributes	T_{adj_PC1}	The daily grid-cell transpiration, adjusted for the first principle component of edaphic attributes (PC1), a gradient with higher values representing drier soils and permafrost presence.
High productivity	T_{adj_high}	The daily grid-cell transpiration, adjusted to represent high- productivity (average across the 10 % of cells with the highest daily transpiration).
Low productivity	T_{adj_low}	The daily grid-cell transpiration, adjusted to represent low- productivity (average across the 10% of cells with the lowest daily transpiration).

We then adjusted T_{cell} to reflect a spatially clustered sampling effort where only one part of the landscape was sampled, including permafrost plateaus (high productivity areas) or wetlands (low productivity areas). The high productivity areas were identified as the 24 grid-cells (ten percent of the plot) with the highest daily T_{cell}. The low productivity areas were identified as the 24 grid-cells with the lowest daily T_{cell}. We used the average predicted daily J_s across the high and low productivity areas for estimating upper estimates of daily grid-cell transpiration (T_{adj_high}) and lower estimates of daily grid-cell transpiration (T_{adj_low}), respectively. We compared the four T_{cell} adjustments to the unadjusted estimates of T_{cell} to evaluate the level of uncertainty that is introduced during transpiration upscaling in spatial heterogeneous landscapes.

Results

Temporal variation of plot measurements

During the sampling period (27 June to 11 July), J_s followed a diurnal pattern with peaks occurring mid-day (Figure 3.3a). In 2018, the J_s reached greater daily maximums than in 2013 and 2017. For all three years, daily J_s was affected by meteorological conditions (Figure SII.2). The T_{air} for the sampling period was 19.7 °C in 2013 (± 5.3 °C), 18.6 ºC in 2017 (± 4.5 ºC) and 17.12 ºC in 2018 (± 5.7 ºC; Figure 3.3b), all of which were close to the 30-year climate normals (1981-2010) for July (17.4 ºC). The mean annual temperature for 2013 (-2.5 ºC) was also close to the 30-year climate normal (-2.8 ºC) but 2017 and 2018 were both warmer (-0.9 and -1.0 ºC, respectively). The mean VPD and PAR during the sample period were both lowest in 2017 (0.8 kPa ± 0.5 kPa and 386.8 µmol m^{-2} s^{-1} ± 175.8 µmol m^{-2} s^{-1}), followed by 2018 (1.0 kPa ± 0.6 kPa and 417.6 µmol m^{-2} s^{-1} ± 107.3 µmol m^{-2} s^{-1}) and then 2013 (1.0 kPa ± 0.5 kPa and 419.3 µmol m^{-2} s^{-1} ± 152.1 µmol m^{-2} s^{-1}; Figure 3.3c, d). Rainfall was greatest in 2017 with 49.0 mm falling during the sampling period (Figure 3.3e). Rainfall for the same period was 14.2 mm in 2013 and 11.5 mm in 2018. Precipitation as rain for the snow-free period (May to October) for the three years was slightly higher than the 30-year climate normals (241 mm) with 255 mm falling in 2013, 287 mm in 2017, and 246 mm in 2018.

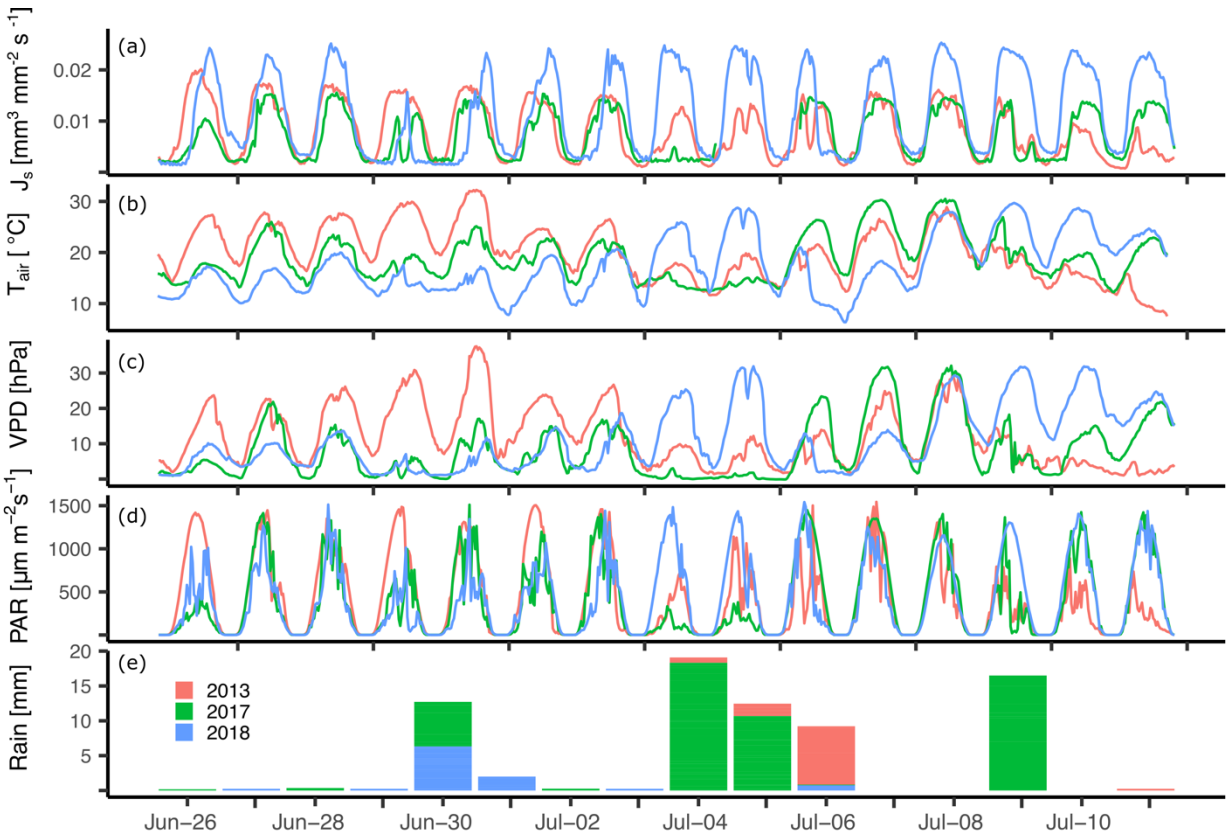

Figure 3.3 The half hourly sap flux density (J_s, mm s^{-1}, a) and meteorological conditions, including air temperature (T_{air}; °C, b), vapor pressure deficit (VPD; hPa, c), photosynthetically active radiation (µm m^{-2} s^{-1}, d) and total daily rainfall (mm, e), for the sampling period (27 June to 11 July) in 2013, 2017 and 2018.

Daily J_s was scaled to daily T_{cell} and T_{plot} for the three years in the study (Figure SII.3). The highest rate of daily T_{plot} occurred in 2018 (0.30 ± 0.22 mm, Table 3.2). The daily T_{cell} varied significantly between 2018 and 2013 (0.17 ± 0.13 mm; $p < 0.001$) and 2017 (0.16 ± 0.12 mm; $p < 0.001$). The average daily T_{cell} for 2018 was also significantly different than the average daily T_{cell} across the three-year period (0.21 ± 0.16 mm; $p < 0.001$). Mean daily stand-level ET per square meter during the sampling period was highest in 2017 (2.83 ± 1.13 mm) and lowest in 2013 (2.52 ± 0.89 mm; Table 3.2). Transpiration from black spruce and tamarack in the plot accounted for 6 to 12 % of the total ET (T:ET).

Table 3.2 The daily plot transpiration (T_{plot}; mm), mean daily evapotranspiration (ET; mm) and the contribution of T_{plot} to total ET (T:ET ratio) for 2013, 2017 and 2018. Tplot was determined by upscaling the daily J_s with the total sapwood area of black spruce and tamarack in each grid-cell, and then taking the averaged across the 240 grid-cells. The mean values represent the average across all three years.

Year	T_{plot} (mm)	ET (mm)	T:ET ratio
2013	0.17 (± 0.13)	2.52 (± 0.89)	7 %
2017	0.16 (± 0.12)	2.83 (± 1.13)	6 %
2018	0.30 (± 0.22)	2.59 (± 0.77)	12 %
Mean	**0.22 (± 0.16)**	**2.65 (± 0.93)**	**8 %**

Spatial variation in grid-cell transpiration across the plot

Daily T_{cell}, averaged across the three years, varied spatially (Figure 3.4). In the western third (0 – 240 m on the x axis), T_{cell} was lowest, with an average of 0.12 mm (± 0.09 mm). In the central (240 – 520 m) and eastern thirds (520 – 800 m) of the plot, T_{cell} was twice as high as in the western third but relatively comparable one another at 0.26 mm (± 0.16 mm) and 0.24 mm (± 0.16 mm), respectively. The contribution of black spruce and tamarack transpiration to evapotranspiration also varied across the plot. In the western third, daily T_{cell} represented less than 1 % of the total ET (T:ET as low as 0.4 %). Grid-cells located in the central and eastern thirds with daily T_{cell} measuring as high as 0.5 mm represent close to 19 % of the total ET.

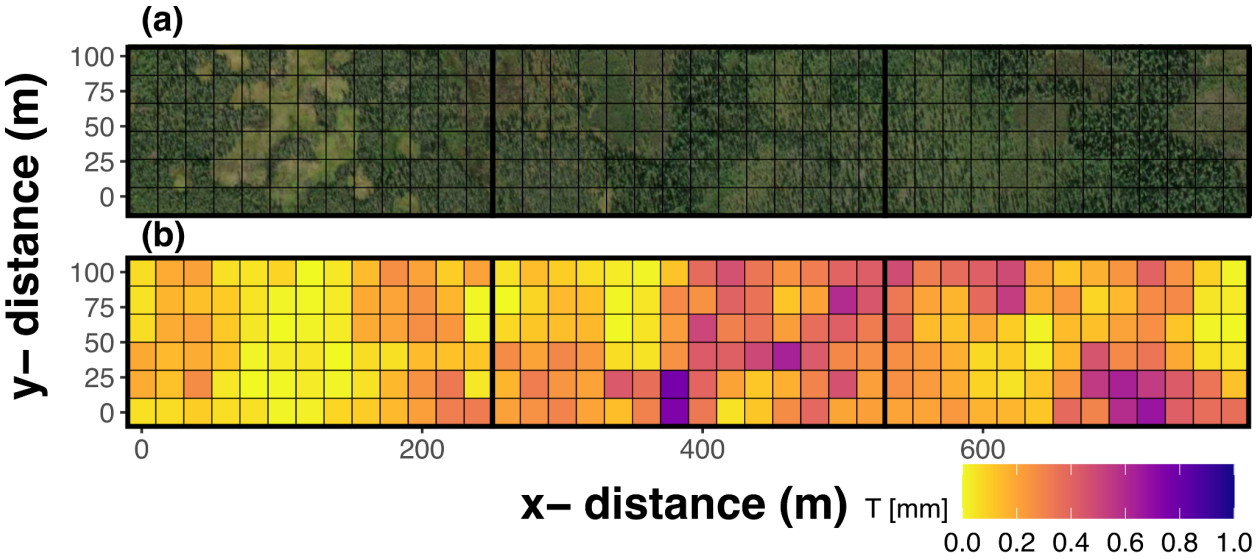

Figure 3.4 Scotty Creek ForestGEO plot (a; ESRI World Imagery) subdivided into 20 m × 20 m grid-cells. Daily grid-cell transpiration (b; T; mm) averaged between 2013, 2017, and 2018 for the sampling period (27 June to 11 July). Transpiration was determined using diameter at breast height (DBH) measurements of black spruce and tamarack measured in the plot between 2012 and 2014.

We determined the stand attributes driving tree-water fluxes using linear mixed effect models. The stand structural attribute (i.e., basal area and density) with the strongest positive relationship with daily J_s was basal area ($p < 0.001$ and conditional $R^2 = 0.26$; Figure 3.5; Table 3.3). For edaphic attributes, PC1 had a significantly positive effect ($p = 0.004$) on daily J_s. The best model for edaphic attributes included PC1 and PC2 (Table 3.3), however the model with just PC1 was equally effective at predicting daily J_s ($\Delta AIC = 1.08$) but was simpler and was therefore selected as the best fit model for the edaphic attributes (conditional $R^2 = 0.20$). There was no significant relationship between the demographic attributes and daily J_s.

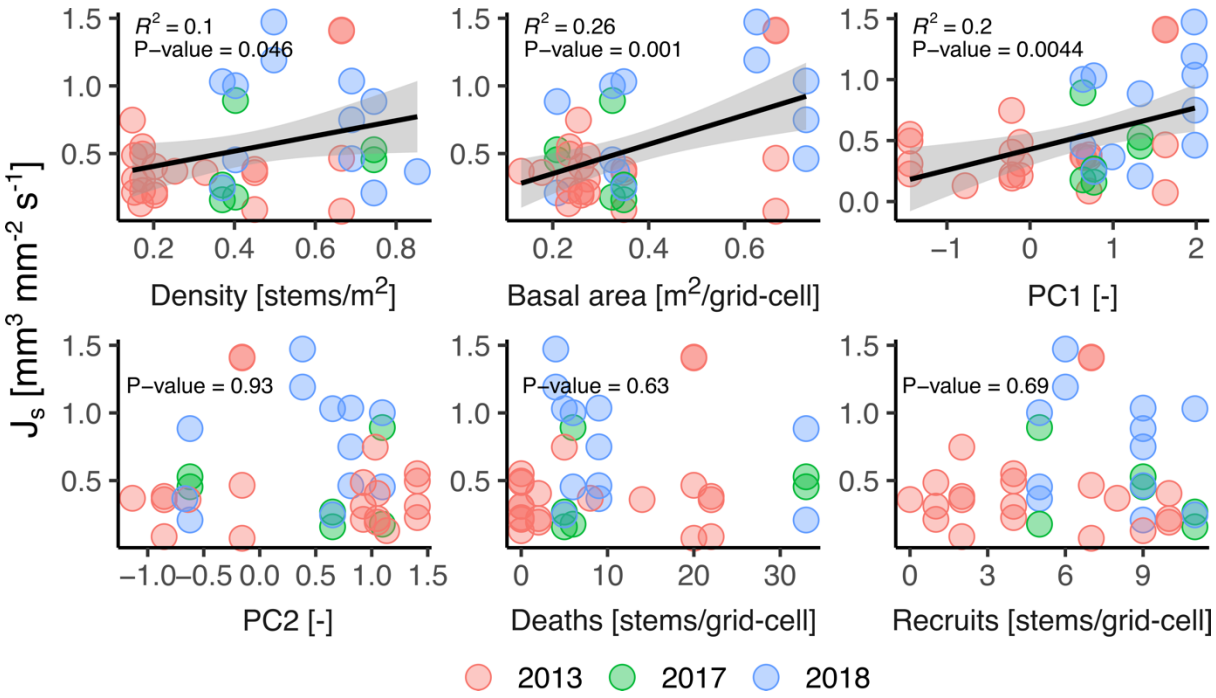

Figure 3.5 The direct effect of stand structural (density and basal area), edaphic (PC1, a gradient with higher values representing drier soils and permafrost presence, and PC2, a gradient with higher values representing the presence of mineral soil, decomposed peat and a deep snowpack) and demographic (deaths and recruits) attributes on mean daily sap flux density (J_s; mm^3 mm^{-2} s^{-1}). Each point represents an individual tree that was measured in 2013, 2017, or 2018 and the attributes for the grid-cell in which that tree was located. Linear fits were only drawn when the relationship was significant ($p < 0.05$).

Table 3.3 Akaike's information criterion (AIC), the difference in AIC between the best fit model and that model where $\Delta AIC = AIC_i - AIC_{min}$, the Akaike's weights ($w_i$), and the R^2 for the linear mixed effect models of the relationship between structural attributes (basal area and stem density), edaphic attributes (PC1, a gradient of soil moisture and permafrost presence and PC2, a gradient of organic layer thickness, peat humification and snow depth), demographic attributes (black spruce and tamarack deaths and recruits), and daily sap flux density in 2013, 2017 and 2018. The best fit model for each set of attributes is in bold. Each model was fitted with year as random effect (formula: ~1 | Year).

Model	AIC	ΔAIC	w_i	R^2
Structural attributes				
Basal area	**618.03**	**0.00**	**0.74**	**0.26**
Basal area + density	620.46	2.43	0.22	0.29
Density	625.28	7.24	0.02	0.10
Null	625.90	7.87	0.01	-
Edaphic attributes				
PC1 + PC2	**619.80**	**0.00**	**0.61**	**0.27**
PC1	**620.88**	**1.08**	**0.35**	**0.20**
Null	625.90	6.10	0.03	-
PC2	628.38	8.58	0.01	0.11
Demographic attributes				
Null	**625.90**	**0**	**0.59**	**-**
Deaths	628.20	2.30	0.19	0.10
Recruits	628.39	2.49	0.17	0.11
Deaths + Recruits	630.84	4.94	0.05	0.11

Uncertainties associated with transpiration upscaling

We used the stand attributes with a significant relationship to daily J_s to determine how daily T_{cell} differs when grid-cell variation is accounted for in upscaling. First, we adjusted daily transpiration to account for stand structure (basal area; T_{adj_BA}) and edaphic attributes (PC1; T_{adj_PC1}). The spatial patterns and magnitude of difference between the unadjusted transpiration estimates, T_{cell}, and T_{adj_BA} and T_{adj_PC1} showed strong congruence but slight variations existed between adjustments (Figure 3.6). Specifically, there were several grid-cells in the western third of the plot that increased for T_{adj_PC1} but decreased for T_{adj_BA}. Maximum adjusted grid-cell values reached as high as 1.66 mm for T_{adj_BA} and 1.37 mm for T_{adj_PC1}, with grid-cells contributing as much as 59 % of the total ET when stand structure (T_{adj_BA}) was accounted for.

The averaged plot T_{adj_BA} and T_{adj_PC1} were both not significantly different from the unadjusted estimate of T_{plot} (0.22 ± 0.16 mm), and their contribution to ecosystem ET fluxes was similar to that of the unadjusted T_{plot} (T:ET ratio of ~ 8 % ; Table 3.4). However, T_{cell} was higher than the adjusted values, T_{adj_BA} and T_{adj_PC1}, in 78 and 76 % of the grid-cells, respectively (Figure 3.6). In these grid-cells, the unadjusted T_{cell} overestimated daily transpiration by an average of 0.04 mm (± 0.02 mm) and 0.06 mm (± 0.05 mm) compared to T_{adj_BA} and T_{adj_PC1}, respectively. The difference between the unadjusted T_{cell} and the adjusted transpiration estimates were never greater than 0.08 mm for T_{adj_BA} and 0.3 mm for T_{adj_PC1}. In 22 and 24 % of the grid-cells, the unadjusted estimate of daily T_{cell} was lower than the adjusted values with a mean underestimation of 0.16 mm (± 0.19 mm) and 0.12 mm (± 0.14 mm) compared to T_{adj_BA} and T_{adj_PC1}, respectively.

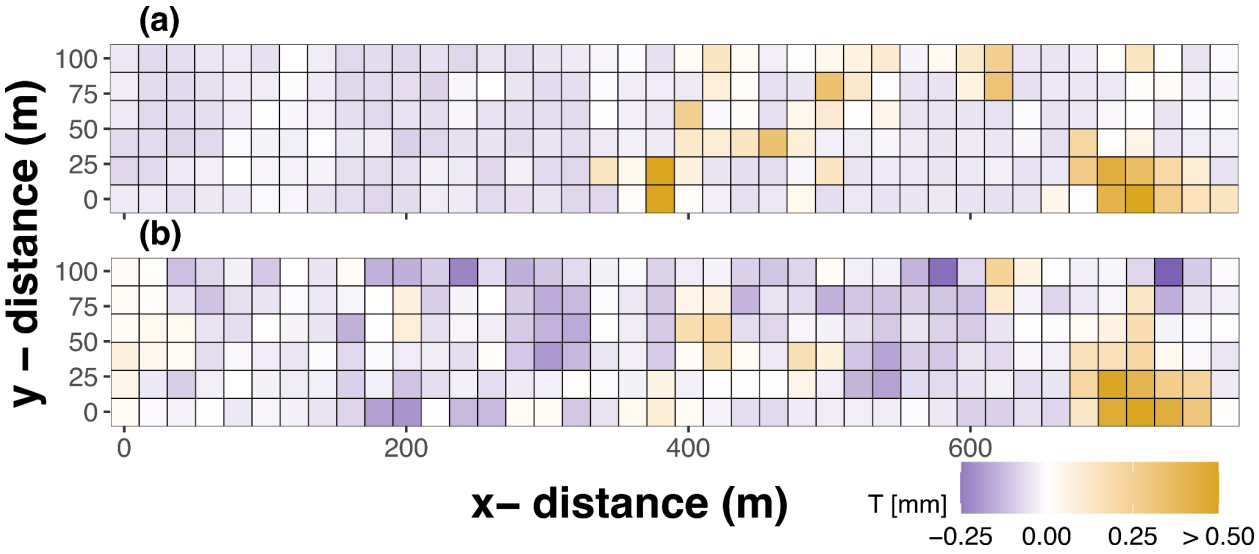

Figure 3.6 The difference in transpiration (T; mm) between the unadjusted estimates of daily grid-cell transpiration (T_{cell}; mm) and the daily grid-cell transpiration adjusted for basal area (a; T_{adj_BA}) and PC1 (a gradient with high values indicating drier soils and permafrost presence; b; T_{adj_PC1}). Grid-cells in purple indicate higher values of T_{cell} versus T_{adj_BA} and T_{adj_PC1} (overestimation of T_{cell}) and grid-cells in yellow represent lower values of T_{cell} versus T_{adj_BA} and T_{adj_PC1} (underestimation of T_{cell}).

Table 3.4 The mean and maximum daily grid-cell transpiration estimate (T_{cell}; mm) and adjusted daily grid-cell transpiration. T_{cell} was adjusted to better represent stand structural attributes (i.e., grid-cell basal area; T_{adj_BA}), grid-cell edaphic attributes (PC1, a gradient with high values representing drier soils and permafrost presence; T_{adj_PC1}), and spatially clustered sampling efforts where only certain parts of the landscape were sampled, including low productivity wetland areas (T_{adj_low}) and high productivity permafrost plateau areas (T_{adj_high}). The transpiration to evapotranspiration ratio (T:ET) was calculated for the daily mean and daily max T_{cell} and each adjustment. ET and T_{cell} was determined as the mean ET between June 27th and July 11th for 2013, 2017 and 2018.

	T_{cell}	T_{adj_BA}	T_{adj_PC1}	T_{adj_low}	T_{adj_high}
Mean	0.22 (± 0.16)	0.20 (± 0.25)	0.19 (± 0.19)	0.19 (± 0.14)	0.38 (± 0.28)
Max	0.80	1.53	1.00	0.68	1.38
T:ET	0.083	0.077	0.073	0.072	0.15
$T:ET_{max}$	0.30	0.59	0.39	0.26	0.53

Adjustments to T_{cell} were also made to represent scalars (i.e., daily J_s) from areas with low productivity (T_{adj_low}) versus areas with high productivity (T_{adj_high}; Figure 3.7). Daily T_{adj_low} averaged across the plot was 0.21 mm (range from 0.0 to 0.76 mm) and daily T_{adj_high} averaged across the plot was 0.41 mm (0.0 to 1.49 mm). There was a significant difference between unadjusted T_{cell} and both T_{adj_low} ($p = 0.019$) and T_{adj_high} ($p < .001$). With $T_{adj\_high,}$ the mean contribution of tree transpiration to total ET fluxes nearly doubled (~15 %) compared to contribution of the unadjusted T_{cell} (Table 3.2).

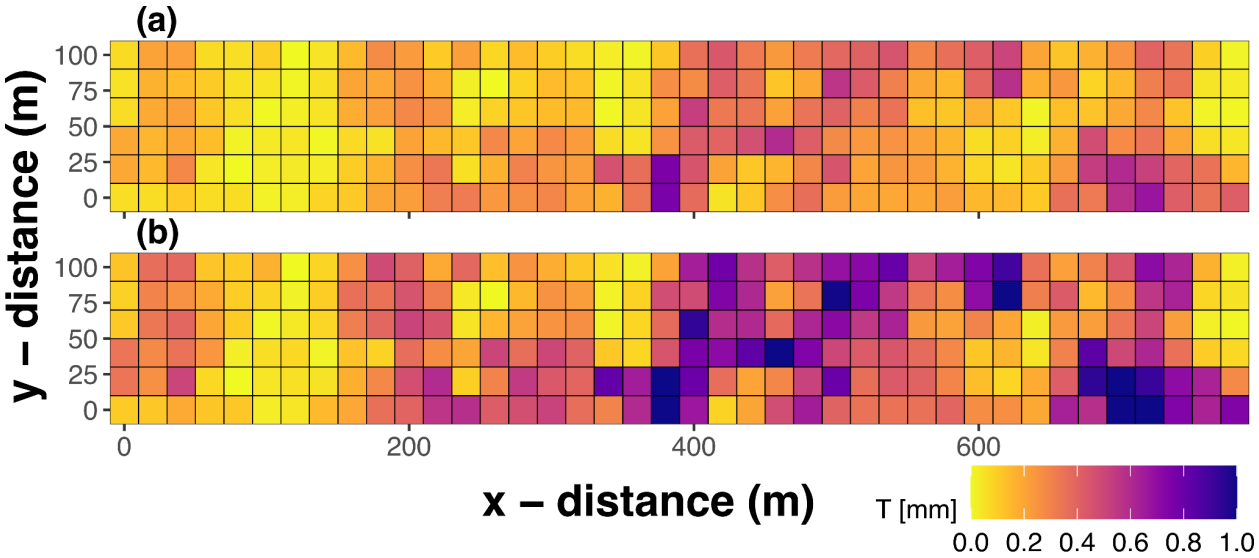

Figure 3.7 A comparison of the strategies depicting daily grid-cell transpiration across the plot determined based on the average daily sap flux density from low flux areas (i.e., the wetlands; a) versus those from high flux areas (i.e., the permafrost plateaus; b). Low flux areas were identified as the 24 grid-cells with the lowest daily transpiration and high flux areas were identified as the 24 grid-cells (ten percent of the plot) with the highest daily transpiration.

Discussion

Between-year variability in plot transpiration

The daily T_{plot} at Scotty Creek varied across years by a factor of ~2, with highest values observed in 2018. Reported values of daily T_{plot} over the three years were between 0.17 and 0.30 mm day^{-1}, within the range of those reported for black spruce- and tamarack-dominated stands in boreal North America (0.13 to 3 mm) (Ewers *et al*. 2005, Van Herk *et al*. 2011, Angstmann *et al*. 2012), but higher than daily rates previously reported for Scotty Creek (0.02 mm) (Warren *et al*. 2018). The daily T_{plot} compared to other sites was expected given the low productivity and slow growth at Scotty Creek (Sniderhan & Baltzer, 2016). Low daily T_{plot} is likely a result of low nutrient concentrations (Iijima *et al.* 2014; Dearborn *et al.* 2021), the permafrost dynamics (Patankar *et al.* 2015), and tree structure (smaller and shorter trees) at Scotty Creek compared to other boreal sites (Ewers *et al*. 2005, Angstmann *et al*. 2012). Former work at Scotty Creek used lidar-derived canopy height models and species-specific allometry to determine tree DBH across the landscape. Lidar is

less successful at identifying small versus large trees on the landscape (Krůček, *et al*. 2020). Our direct DBH measurements of all trees with a DBH > 1 cm therefore more accurately represented sapwood area on the landscape and accounting for some discrepancies between estimates. When scaling to stand-level transpiration, we recommend that the sapwood area of even the small individuals be included, when possible, to prevent underestimations.

In this study, the variation in daily J_s between years is unlikely a result of variation in meteorological conditions. Growing season meteorological conditions are strong drivers of diurnal and seasonal sap flow patterns in black spruce (e.g., Waring and Running 1998, Van Herk *et al*. 2011, Patankar *et al*. 2015), but are less associated with between-year variability (Zhang *et al*. 2015). If the meteorological conditions were a strong driver of between-year daily J_s (and daily T_{plot}), we would expect consistently higher values of J_s for all trees in one year compared to the other (i.e., consistently higher values in 2018 where conditions were more amenable to greater J_s). When daily J_s was examined for the same trees instrumented in 2017 and 2018 there was no systematic difference in J_s between years (Figure SII.4). We would also expect years with high daily T_{plot} to have high ET, if meteorological conditions were responsible for the between-year variation in daily J_s (and daily T_{plot}). However, the highest ET occurred in 2013, when the daily T_{plot} was comparable to the mean across years, and the lowest ET occurred in 2018 when daily T_{plot} was highest. At Scotty Creek, evaporation contributes more to ET than transpiration (Helbig *et al*. 2016, Warren *et al.* 2018). High evaporation rates can limit the water available for plant water uptake and reduce transpiration rates, especially for black spruce and tamarack with rooting primarily limited the top 10 cm of soil (Lieffers and Rothwell, 1987, Yang *et al.* 2023). When ET was low in 2018, evaporation from the soil surface was likely lower, reducing the constrains on water uptake by trees, resulting in higher transpiration rates in that year.

The differences in daily T_{plot} and daily J_s between years may instead be explained by tree- and stand-level variability (Wullschleger and King, 2000; Ford *et al*. 2007). At the tree-level J_s can vary with radial (Oren *et al*. 1998, Fiora and Cescatti 2006) and circumferential flow (Čermák *et al*. 2004), and at the stand level J_s can vary with differences in sapwood area, leaf area index, and tree size between individuals (Ford *et al*. 2007, Kume *et al*. 2010, Berry *et al*. 2018). The higher daily J_s in 2018 compared to either 2013 or 2017 may therefore be a product of variation within

and between trees sampled across years. We did not have enough tree-specific data (i.e., paired sapwood area, leaf area index) from our sampled trees to examine the impact of the sampled individuals in more detail.

Stand structural and edaphic variation mediates transpiration across a heterogeneous boreal peatland

Our results revealed considerable variation in daily T_{cell} between neighbouring grid-cells that was explained by variation in local environmental conditions (Figure 3.4). These pronounced changes from one grid-cell to the next were associated with forest structural and edaphic variability. Basal area was the strongest positive predictor of daily J_s, followed by PC1 (where drier soils and the presence of permafrost led to higher daily J_s). The demographic attributes of the plot (i.e., tree deaths and recruits) were not significant predictors of tree-level J_s or, as a consequence, T_{cell}.

Scotty Creek has distinct land cover types, including forested peat plateaus underlain by permafrost, and permafrost-free wetlands (Quinton *et al*. 2019), that are well characterized by the stand structural and edaphic attributes with the strongest relationship to daily J_s. The edaphic attributes represented by higher values of PC1 (dry soils and the presence of permafrost) are indicative of relatively well-drained permafrost plateaus, while low values are indicative of permafrost-free wetlands (Dearborn *et al*. 2021). The edaphic attributes represented by PC2 are a gradient of organic layer thickness, peat humification and snow depth. High values of both PC1 and PC2 corresponded to well-drained permafrost plateaus with higher nutrient availability (mineral soils nearer to the surface and more highly humified peat) and greater insulation in the winter (a larger snow depth). Conditions which lead to greater forest productivity. As a result, forest structure is also used as a proxy for discerning permafrost plateaus from permafrost-free wetlands as the former has a distinctly higher basal area, stem density and species richness and the two have distinctive plant communities (Dearborn *et al*. 2021; Standen and Baltzer 2021). When T_{plot} was adjusted to account for the effect of these predictors (basal area and PC1), both daily T_{adj_BA} and T_{adj_PC1} revealed major underestimations of daily T_{cell} from the productive permafrost plateaus and minor overestimations of daily T_{cell} from wetlands and sparsely-treed grid-cells. We

can infer from our results that trees from permafrost plateaus have higher rates of daily J_s compared to trees located in wetlands.

Stand structural attributes: accounting for basal area

When adjusted to account for basal area at the grid-cell level, daily T_{adj_BA} ranged from 0.0 to 1.53 mm, almost twice the range for the original, unadjusted T_{cell} (0.0 to 0.80 mm). Basal area has previously been identified as a stand characteristic that effectively explains the variability in stand transpiration across heterogeneous boreal landscapes (e.g., Angstmann *et al*. 2013). Our results corroborate these findings. By adjusting for basal area, we found a large increase in the maximum contribution of daily T_{adj_BA} to ET, with a T:ET reaching 59 % (almost double the upper limit of the unadjusted T:ET of 30%). This contribution is well above previous estimates for Scotty Creek (1 %), but within the range reported for boreal and subarctic forests in Canada, Sweden, and China (14 – 84 %; Kozii *et al*. 2020, Hadiwijaya *et al*. 2020, Sabater *et al*. 2020, Liu *et al*. 2020).

Basal area can represent both tree size, and the density of stems in a stand. While the permafrost plateaus at Scotty Creek have denser forest cover than the surrounding wetlands (Quinton *et al*. 2019; Dearborn *et al*. 2021), stem density was not included in the best-fit models that predicted daily J_s (Table 3.3). This suggests instead that the relationship between daily J_s and basal area is more representative of a correlation with tree-size (trees in grid-cells with higher basal area had higher average DBH; data not shown). This finding is supported by previous work that found positive relationships between tree size (DBH) and tree-water fluxes (Čermák *et al*. 2004; Menzier *et al*. 2005; Berry *et al*. 2018). In many ecosystems, a small number of large individuals contribute disproportionately to total stand transpiration (Köstner *et al*. 1992, Arneth *et al*. 1996, Martin *et al*. 2001, Čermák *et al*. 2004). When tree level J_s was scaled up to T_{cell} across the plot, we observed a similar tendency. A small number of cells that represent permafrost plateaus with high basal area and large trees have high daily T_{cell} and contribute a disproportionate amount to the total T_{plot}. Twenty percent of the grid-cells (n = 48) represented almost half (43 %) of the total daily T_{plot}, while over 100 grid-cells combined contributed 15 % of total T_{plot}.

Edaphic attributes: accounting for soil moisture and permafrost presence

When grid-cell transpiration was adjusted to reflect the edaphic attributes across the plot, the maximum contribution of T_{adj_PC1} to ET was 39 %, an increase of almost 10 % from the unadjusted T_{cell} contribution of 30 %. The largest positive difference between T_{cell} and T_{adj_PC1} occurred on the permafrost plateaus, suggesting that drier soils and the presence of permafrost leads to higher transpiration rates. Permafrost plateaus are elevated 1-2 m above the surrounding wetlands, allowing water to drain during the growing season, leading to drier soils compared to the surrounding wetlands (Quinton *et al*. 2009; 2019; Patankar *et al*. 2015). Previous work at Scotty Creek has also reported higher tree-water fluxes atop permafrost plateaus compared to wetlands (Baltzer *et al*. 2014, Patankar *et al*. 2015). Well-drained forest stands are known to have higher productivity, higher tree biomass (Van Cleve *et al*. 1981), and higher stand level transpiration due to nutrient availability and lower likelihood of waterlogging stress (Angstmann *et al*. 2013). Trees growing where permafrost is absent or degrading (i.e., in permafrost-free wetlands or at permafrost plateau-wetland margins) have lower daily J_s because they experience waterlogging throughout the growing season (Iijima *et al*. 2014, Patankar *et al*. 2015, Baltzer *et al*. 2014). Our results showed considerable overestimation of the unadjusted T_{cell} from the wetland areas, when compared to T_{adj_PC1}, supporting the claims that excess water and the absence of permafrost leads to lower transpiration.

Black spruce, the most abundant species in the plot, (Dearborn *et al*. 2021) and to a lesser extent tamarack, are intolerant to high soil water content (Islam *et al*. 2003). Waterlogging inhibits transpiration through diminished root function (Drew 1997; Baltzer *et al*. 2013; Iijima *et al*. 2014) and lower soil nutrient availability (Van Cleve *et al*. 1981, Lieffers and Rothwell 1987, Wolken *et al*. 2011, Göbel *et al*. 2019). When soil pores fill with water, oxygen required for root respiration is excluded (Pan *et al.* 2021). Most root water and nutrient uptake is an active process that is coupled with root respiration. Thus, when root respiration is limited, water and nutrient uptake is restricted, resulting in reduced energy production, stomates that close, lower photosynthetic activity, and lower transpiration (Pan *et al.* 2021). Soil waterlogging has been linked to stunted growth, including but not limited to, reduced sapwood area, an important covariate of tree level transpiration (Bond-Lamberty *et al*. 2004, Angstmann *et al*. 2013). At Scotty Creek, waterlogging

has led to reduced J_s by up to 65 % in black spruce (Patankar *et al*. 2015), and wetland expansion (in the presence of mineral soil), has been associated with an increase in tamarack recruitment (Dearborn *et al.* 2021). Therefore, deciduous species with a higher tolerance for wet conditions, may be less affected by high soil water content at Scotty Creek. However, there has been a net decrease in the recruitment and the radial growth of other deciduous species at Scotty Creek (e.g., *Betula* spp.), likely due to the nutrient poor conditions across the plot (Dearborn *et al.* 2021, Dearborn and Baltzer 2021).

When examining grid-cells that represent wetlands with higher soil moisture content (i.e., 20 % of grid-cells in the plot with the lowest daily water fluxes), the average daily T_{adj_BA} was 0.034 mm, a value far greater than what we would expect from wetlands (<0.01 mm; Warren *et al*. 2018). This could be due to the relatively large tamarack found in many of the wetland sections of the plot. The averaged T_{adj_PC1} across the same cells was lower (0.001mm) and more comparable to values previously found for wetlands at Scotty Creek (Warren *et al*. 2018). This provides evidence that by failing to account for soil moisture and permafrost, wetland transpiration in the plot will be overestimated. However, even by accounting for the differences in soil moisture between wetlands and permafrost plateaus, this work may fail to fully capture the drought effect that occurs on permafrost plateaus throughout the growing season.

As the active layer thickens in permafrost plateaus, the water table can drop below the shallow rooting zone (10 – 20 cm; Lieffers and Rothwell 1987) of black spruce (Patankar *et al*. 2015, Sniderhan and Baltzer 2016). Lower surface soil moisture can lead to drought induced stress and a decrease in stand transpiration, but often not until it drops below a certain threshold (Bovard *et al*. 2005, Van Herk *et al*. 2011). At Scotty Creek, drought-induced stress on permafrost plateaus mainly occurs towards the end of the growing season when the active layer is thickest (Patankar *et al*. 2015) and there is evidence of increasing drought stress in trees at Scotty Creek over the last several decades (Sniderhan *et al*. 2021). It is unlikely that our daily J_s measurements over relatively short sampling periods captured this seasonal phenomenon, and the fact that we did not follow the same trees through time negates the possibility of detecting a vertical thaw signature.

Importance of integrating landscape heterogeneity into transpiration upscaling

A major challenge in scaling point-measurements of sap flow to stand-level transpiration is ensuring that samples are representative of, and therefore reduce the uncertainty associated with, structural and environmental heterogeneity (Adelman *et al*. 2008; Angstmann *et al*. 2013). Tree-water fluxes can vary with tree size (Čermák *et al*. 2004), therefore, it has become common practice for sap flow studies to sample across a range of tree size (DBH) classes to establish a representative plot that is then used to scale up to stand-level T (Granier *et al*. 1996; Oren *et al*. 1998, 1999). This methodology can prove problematic in a heterogeneous landscape like Scotty Creek where the complete range of tree size classes can be found in a single land cover type. For example, a single grid-cell on the permafrost plateau has trees ranging from 1 cm DBH (smallest trees in the plot) to 24 cm DBH (largest tree in the plot). It would be possible to obtain a subsample of trees with individuals from each size class on a single permafrost plateau. While this subsample would adequately represent the size distribution of the plot, it would fail to accurately represent the water fluxes from trees growing in wetland or sparsely-treed areas.

We demonstrated how daily T_{cell} and T_{plot} would change if sap flow measurements were typical of just a single land cover type (permafrost plateaus vs. wetlands). Restricting sampling to just productive areas, T_{adj_high} averaged across the plot was 0.41mm, nearly double the unadjusted T_{plot} (0.22 mm). This indicates that scaled estimates of plot transpiration could be overestimated by up to 42 % if trees were only sampled from productive permafrost plateaus where basal area is high, permafrost is present, and the soil is dry. Across the southern Northwest Territories (Helbig *et al*. 2016a, Wang *et al*. 2020), including at Scotty Creek (Baltzer *et al*. 2014, Dearborn *et al*. 2021), permafrost thaw is leading to wetland expansion at the expense of forested permafrost plateaus (Quinton *et al*. 2019), reducing tree-water fluxes (Patankar *et al*. 2015), growth (Baltzer *et al*. 2014), and increasing mortality of the dominant tree species (Dearborn *et al*. 2021). Scaled estimates of plot transpiration based on trees from permafrost plateaus alone are unlikely to capture the full effect of permafrost thaw and could therefore lead to large-scale misrepresentations of transpiration fluxes.

The daily T_{adj_low}, representing spatially clustered sampling from wetlands, was just 5 % lower than the unadjusted daily T_{plot} but had a range of grid-cell T_{adj_low} that was smaller than any other estimate (T_{cell}, T_{adj_BA}, T_{adj_PC1} and T_{adj_high}). In their work in northern Manitoba, Angstmann *et al*. (2013) found that trees growing in close proximity had more similar transpiration rates compared to more distal trees (suggesting spatial autocorrelation of hydraulic function). They argued that the homogeneity at a smaller scale (i.e., 25m × 25m) needs to be evaluated cautiously, as it may mask the heterogeneity that exists at a larger scale after upscaling (e.g., stand-level; Angstmann *et al*. 2013). Our findings support those of Angstmann *et al*. (2013), demonstrating that sampling from just one land cover type could result in a failure to capture the variation of transpiration at the plot-level and to an over- or underestimation of scaled fluxes.

In our work, we have examined the consequences of variation in the J_s scalar (Equation 2). A limitation to this study is that we did not account for the variability in the A_s scalar. Across the plot, A_s was determined using species-specific allometric relationships with DBH. However, we are likely missing information on the intraspecific variability in A_s that has been reported to vary with edaphic conditions including soil water availability (Ewers *et al*. 2000; McDowell *et al*. 2002). Unfortunately, we do not have spatially explicit measurements of A_s across the plot, but this should be a consideration in future upscaling studies.

Conclusions

The goal of this work was to better understand the environmental attributes affecting stand-level transpiration. We examined the between-year differences in plot transpiration, identified the stand structural, edaphic, and demographic attributes that drove spatial variation of transpiration across the plot, and demonstrated potential sources of uncertainty associated with transpiration upscaling. We determined that between-year differences in mean daily T_{plot} were not well explained by annual meteorological conditions. Instead, the multi-year data served to better capture variation in T_{cell} attributed to within-tree and between-stand variation in transpiration scalars, including daily J_s. The pronounced spatial variation in daily T_{cell} are explained by differences in the stand structural and edaphic attributes that describe the distinct land cover types across the plot. Permafrost plateaus, with their presence of permafrost, drier soils, and high basal areas, represent the grid-cells with the

highest daily T_{cell} compared to the permafrost free wetlands. When upscaling to transpiration in heterogeneous boreal peatlands, we must account for the effect of stand attributes on daily J_s, and ensure sampling procedures adequately represent land cover types. A failure to do so will lead to overestimated T_{cell} in wetlands and a marked underestimation of T_{cell} from permafrost plateaus. More rigorous scaling methods of transpiration that integrate structural and edaphic gradients across spatially diverse boreal landscapes could help to constrain the partitioning of water and energy fluxes, and alter our understanding of forest water loss and latent energy exchanges in the boreal region.

Chapter 4 – Radiation, air temperature and soil water availability drive tree water deficit across temporal scales in Canada's western boreal forest

Nia Perron [1,2], Jennifer L. Baltzer [3], Matteo Detto [4], Magali Nehemy [5,6,7], Christopher Spence [8], Gabriel Hould-Gosselin [1,9], Bram Hadiwijaya[1] and Oliver Sonnentag [1,2]

[1] Département de géographie, Université de Montréal, Montréal, QC, Canada, [2] Centre d'étude de la forêt, Université du Québec à Montréal, Montréal, QC, Canada, [3] Department of Biology, Wilfrid Laurier University, Waterloo, ON, Canada, [4] Department of Ecology and Evolutionary Biology, Princeton University, Princeton, NJ, USA, [5] Trent School of the Environment, Trent University, Peterborough, ON, Canada, [6] Mistik Askiwin Dendrochronology Laboratory (MAD Lab), University of Saskatchewan, Saskatoon, SK, Canada, [7] Global Institute for Water Security, University of Saskatchewan, Saskatoon, SK, Canada, [8] Environment and Climate Change Canada, Saskatoon, SK, Canada, [9] Department of Geography, Wilfrid Laurier University, Waterloo, ON, Canada

Perron N, Baltzer J, Detto M, Nehemy M, Spence C, Hould-Gosselin G, Hadiwijaya B and Sonnentag O (*Accepted by Geophysical Research Letters*) Radiation, air temperature and soil water availability drive tree water deficit across temporal scales in Canada's western boreal forest. Geophysical Research Letters

Abstract

Changes are projected for the boreal biome with complex and variable effects on forest vegetation including drought-induced compositional changes, tree mortality and forest loss. With both soil and atmospheric conditions governing drought intensity, the specific drivers of tree water stress can be difficult to disentangle across temporal scales. We used wavelet analysis and causality detection to identify the potential environmental controls (evapotranspiration, soil moisture, rainfall, vapour pressure deficit, air temperature and photosynthetically active radiation) on daily tree water deficit, and on longer periods of tree dehydration in black spruce and tamarack. Daily tree water deficit was controlled by photosynthetically active radiation, vapour pressure deficit and air temperature causing greater stand evapotranspiration. Prolonged periods of tree water deficit (>

day) were regulated by photosynthetically active radiation and soil moisture. We provide empirical evidence that continued warming and drying will cause short-term increases in black spruce and tamarack transpiration, but greater drought stress with reduced soil water availability.

Introduction

Water, carbon and energy fluxes regulated by the boreal biome are important components of the global water and energy budgets and climate regimes (Bonan 2008, Price *et al.* 2013). By 2100, climate change is expected to warm the boreal biome by 3 to 8 °C leading to increased water limitation and stress (Berner *et al.* 2005, Gauthier *et al.* 2015). Water stress is a complex yet critically important condition influencing boreal forest health (Allen *et al.* 2010, Peng *et al.* 2011) and resilience to disturbance (Baltzer *et al.* 2021, Whitman *et al.* 2019, Yi and Jackson 2021, Yang *et al.* 2022). Without an increase in precipitation, forests in the boreal biome will experience more frequent and severe droughts over the next century (Wang *et al.* 2014, Zhang *et al.* 2019).

Drought (i.e., water stress) refers to the duration and frequency of water limitation, and the intensity of water deficit (Cook *et al.* 2014, McDowell *et al.* 2008, Seidl *et al.* 2017). In boreal forests, like other systems, there are various controls that contribute to drought stress in trees, including air temperature (Barber *et al.* 2000, Reich *et al.* 2022, Ruiz-Pérez and Vico 2020), reduced rainfall, soil water content (Hogg *et al.* 2005, Peng *et al.* 2011) and atmospheric water demand (Babst *et al.* 2019, Beck *et al.* 2011, Mirabel *et al.* 2022). These same controls contribute to increased evapotranspiration (ET) which in turn reduces water available for plant uptake, exacerbating drought stress in trees (Zhao *et al.* 2022).

Traditionally, the environmental controls on boreal tree species have been explored with dendrochronology by examining annual growth increments. These studies have determined that tree growth is stimulated by greater water availability combined with warmer temperatures (D'Orangeville *et al.* 2016, Wang *et al.* 2023, Zhang *et al.* 2019), but limited by high atmospheric water demand, low water availability (Lloyd and Bunn 2007, Babst *et al.* 2019, Sniderhan *et al.* 2021, Mirabel *et al.* 2023) and/or the timing and severity of drought stress (Mood *et al.* 2021). However, few studies have assessed the impact of environmental controls on water stress in boreal

trees at higher temporal resolution (from hours to multiple days) (e.g., Balducci *et al.* 2019, Dulamsuren *et al.* 2023, Maillet *et al.* 2022, Salomón *et al.* 2022). Thus, it remains unclear if the environmental controls of annual growth increment are also controlling water stress in boreal trees at smaller temporal scales.

By measuring variation in tree radius, automatic stem dendrometers are suitable for quantifying temporal dynamics of water stress in trees (De Swaef *et al.* 2015, Drew and Downes 2009, Zweifel *et al.* 2000, Zweifel and Hasler 2001). Changing water content (i.e., radial water potentials) in the stem tissue causes reversible shrinkage when transpiration is high, and swelling when stems refill. The amplitude of the reversible shrinking/swelling is a reliable measure of tree water deficit (TWD; Zweifel 2016, Zweifel *et al.* 2005, Dietrich *et al.* 2018). Environmental controls that limit stem refilling can lead to prolonged periods (days to weeks) of stem shrinkage, stem dehydration and potential drought stress in trees (Oberhuber *et al.* 2015b, Salomón *et al.* 2022, Schäfer *et al.* 2019, Zweifel *et al.* 2005). Previous studies using automatic stem dendrometers have focused on the relationship between stem radial change (growth) and environmental controls (Dulamsuren *et al.* 2023, Maillet *et al.* 2022), with few investigating the drivers of TWD across multiple sites and temporal scales (but see Salomón *et al.* 2022). To our knowledge, this is the first study to investigate the drivers of TWD in two widespread boreal species along a large latitudinal range in Canada's western boreal forest.

Our goal is to quantify environmental controls of tree water deficit in black spruce (*Picea mariana, (Mill.) B.S.P.*) and tamarack (*Larix laricina* (Du Roi) K. Koch), from southern to northern treeline in Canada's western boreal forest during peak growing season (June to August). Specifically, we asked: Are the environmental controls of tree water deficit consistent across temporal scales in black spruce and tamarack? We predict atmospheric water demand to be the strongest driver of daily tree water deficit, given its influence on tree-level transpiration, and we anticipate the environmental conditions influencing water availability, including soil water content and rainfall, will determine the tree water deficit of each species over multiple days during the growing season. Identifying the controls of seasonal water stress in trees provides a more holistic understanding of tree health, resilience, and ecosystem dynamics. This knowledge is essential for making informed decisions about forest management and conservation in the face of rapid environmental changes.

Methods

Site descriptions

Our work took place at five black spruce dominated forest stands spanning ~2000 km in Canada's western boreal biome (Figure SIII.1). From south to north, Old Black Spruce (OBS) is located ~100 km northeast of Prince Albert, SK at the southern edge of the boreal treeline and was the only permafrost-free site. Scotty Creek (SCC) is a subarctic boreal peatland complex characterised by sporadic discontinuous permafrost with forested permafrost plateaus interspersed with sparsely treed permafrost-free wetlands, located ~50 km south of Fort Simpson, NT (Dearborn *et al.* 2021; Quinton *et al.* 2019). Baker Creek (BAC) is ~15 km north of Yellowknife, NT with extensive discontinuous permafrost and forests located between bedrock outcrops (Morse *et al.* 2016). Similar to SCC, Smith Creek (SMC) is a subarctic boreal peatland complex characterised by extensive discontinuous permafrost (Natural Resources Canada, 2016; Schulze *et al. in prep*), ~15 km from Wrigley, NT. Havikpak Creek (HPC), is a woodland located in the forest-tundra ecotone ~10 km south of Inuvik, NT where permafrost is continuous (Krogh *et al.* 2017, Table SIII.1)

Stem radius change measurements

Mature, healthy black spruce and tamarack were instrumented with automatic circumference band dendrometers (model DC-2 and 3, Ecomatik, Munich, Germany) to obtain measurements of stem radius change (ΔSR). Black spruce ΔSR was measured at OBS (n= 8), SCC (n = 8), BAC (n = 5), SMC (n = 12) and HPC (n = 8) and tamarack ΔSR was measured at OBS (n= 9), SCC (n = 8) and BAC (n = 5). Data from up to four dendrometers were recorded on a single HOBO data logger (UX120-006M, Bourne, MA), and averaged at half-hourly intervals during the peak growing season (June 1st to August 31st) in 2018, 2019 and 2020. Measurements began between June 6 - 15, 2018 at SCC, BAC SMC, and HPC. Data gaps ≤ 3 hours from data logger failure and/or animal damage were gap-filled using linear interpolation. Gaps longer than 3 hours were not filled (Pierrat *et al*. 2021). The amplitude of ΔSR among individuals of black spruce and tamarack varied, but were synchronous; therefore, we derived species-averaged ΔSR at each site (e.g., Zweifel *et al*. 2016, Maillet *et al*. 2022).

Measurements of ΔSR represent reversible stem shrinkage/swelling related to water status (i.e., TWD) and irreversible radial stem growth (Steppe *et al.* 2015, Zweifel *et al.* 2016, 2005). Irreversible growth trends were removed from the species-averaged ΔSR time series to derive species-averaged TWD using the 'Zero Growth Concept', which assumes growth cannot occur during periods of stem shrinkage because turgor pressure is insufficient to facilitate cell division and enlargement (Figure SIII.2, Dietrich *et al.* 2018, Hinckley and Bruckerhoff 1975, Lockhart 1965, Zweifel *et al.* 2016). A positive TWD represents a departure from full hydration where larger values signify greater water deficit, and TWD of zero represents fully hydrated stem tissue (Drew *et al.* 2011, Köcher *et al.* 2013, Zweifel *et al.* 2005). We assumed trees were at full saturation (TWD = 0) at the start of the measurement period in June of each year given the large hydrological inputs of snowmelt in April-May across the sites. Stems refill within a 24 hour cycle with TWD refill zero, except during water deficit. Tree water deficit above zero for multiple consecutive days represents stem dehydration causing drought stress and growth suppression (e.g., Nehemy *et al.* 2021, Zweifel *et al*. 2021).

Eddy covariance and micrometeorological measurements

Stand-level evapotranspiration (ET) and potential environmental controls of TWD including photosynthetically active radiation (PAR; measured as photosynthetic photon flux density; μmol m^{-2} s^{-1}), air temperature (T_{air}; °C), vapour pressure deficit (VPD, derived from T_{air} and relative humidity; kPa), and rain (mm) were measured continuously on micrometeorological towers located near the instrumented trees (OBS: Barr *et al.* 2012, Nehemy *et al.* 2023, SCC and HPC: Helbig *et al.* 2016b, 2016b, BAC: Spence *et al.* 2018, SMC: Schulze *et al. in prep*). Only peak growing season (June, July and August) measurements from 2018, 2019, and 2020 were used. Rain data at HPC were obtained from the Environment and Climate Change Canada station located at the Inuvik airport (<1 km from the site, ECCC 2023). Near-surface soil moisture (θ; %), was measured from the top 5 - 10 cm of the ground surface at each site and calibrated using site-specific coefficients, or coefficients specific to the organic matter at the soil surface (e.g., Warren 2015, Spence *et al.* 2020).

Stand-level ET was estimated using gas analyser-based eddy covariance measurements of H_2O (mmol m^{-2} s^{-1}) flux at OBS, SCC, SMC and HPC (Barr *et al*. 2012, Helbig *et al*. 2016b, 2016b, Nehemy *et al*. 2023, Schulze *et al.* in prep), and hygrometer-based eddy covariance measurements at BAC (Spence *et al*. in prep). The eddy covariance instrumental set-up varied across sites (Table SIII.2) and was updated at OBS in 2018, resulting in a large data gap that was not filled (25 August 2018 to 22 July 2019). The half-hourly fluxes from SCC, BAC, SMC, HPC, and OBS were processed using in-house MATLAB codes (version: 9.13.0 (R2022b), MATLAB, Natick, Massachusetts) following standardised methodologies and the EddyPro software (version 6.1, LI-COR Biosciences, Lincoln, NE, see Helbig *et al.* 2016b for details), or downloaded from the Wiski web server using the R package WISKIr (Shook 2015).

Analysis

We used wavelet coherence analysis with the Morlet wavelet to identify the correlation and temporal structures between paired time series of environmental drivers (ET, PAR, VPD, T_{air}, rain and θ) and the species-averaged TWD (Torrence and Compo 1998, Hatala *et al*. 2012, Harmon *et al.* 2021, Leštianska *et al.* 2020). Hereafter, the predictor terms are denoted as X and TWD as Y. The wavelet coherence is computed by normalizing the continuous cross-wavelet power spectrum (the product of the wavelet transform of X and Y) by the individual continuous wavelet power spectra (Torrence and Compo 1998), producing a measure of correlation from 0 to 1 (Yu and Lin 2015). The wavelet coherence best identifies oscillations with a period larger than the data collection time step, and shorter than the data collection period, thus, we isolated our frequencies of interest between three hours to biweekly (Torrence and Compo 1998, Harmon *et al.* 2021). Statistical significance of the wavelet coherence was estimated using Monte Carlo simulations (n = 1000) with a significance level of $\alpha = 0.05$ (Grinsted *et al.* 2004, Torrence and Compo 1998). Analysis of species-specific wavelet coherence was done for each site in 2018, 2019 and 2020 (depending on data availability) using the Morlet wavelet implemented in the 'WaveletComp' R package (Rosch and Schmidbauer 2018). An ensemble was created for each species and site by time-averaging the continuous wavelet coherence and averaging across years.

Granger causality (or G-causality) analysis (Granger 1969) was used to determine if the coherence identified in the analysis described above can represent causal relationships. G-causality, originally developed for economics and now used in many disciplines including geosciences (e.g., Salvucci *et al.* 2002, Detto *et al.* 2012, Hatala *et al.* 2012, Wu *et al.* 2020, Li *et al.* 2022, Zhang *et al.* 2022), exploits the temporal order of events and statistical prediction to infer cause and effect (Granger 1988, Barraquand *et al.* 2021). A causal relationship exists between variables if time series X is better predicted when including the past values of time series Y than using the past values of X alone (or vice-versa; Granger 1969; Detto *et al.* 2012). We applied the unconditional bivariate G-causality to the spectrally transformed series to identify causal relationships as a function of periods ranging from 0.5 to 1.3 days and ≥ 1.3 to 14 days, herein referred to as *daily* and > *daily*, respectively (e.g., Detto *et al.* 2012). The daily period ranges from 0.5 to 1.3 to account for a variable daylength across sites and to capture any lag between variables on the daily scale. Initial observations of the TWD time series indicated that periods of TWD typically ranged from one day to two weeks. Thus, the >1.3 to 14 day period captures relationships that occur during these time scales. The analysis was performed for each species, at each site in 2018, 2019 and 2020, where data were available. Confidence intervals were evaluated using a bootstrap threshold of $\alpha = 0.05$ with the "Granger.inference.unconditional" function in the "grangers" R package (Farnè and Montanari 2018). Data processing, statistical analysis and graphics were performed in R (version 3.6.3, R Core Team 2020).

Results

Tree water deficit, and environmental conditions during the study period

The study period experienced weather that was generally cooler and wetter than climate normals between 1980 and 2010. For June, July and August, only SCC and BAC had warmer than average temperatures (in 2018 and 2020, respectively). As an example, Figure 4.1 shows the time series of tree water deficit and associated environmental variables for OBS in 2020. Mid-day there was greater stem shrinkage (i.e., larger TWD), and at night swelling increased (i.e., reduced TWD, closet to zero) a diel pattern typical for boreal trees during peak growing season (Figure 4.1a - c). The diel pattern of TWD was more pronounced during periods of water deficit (consecutive days

without TWD returning to zero), compared to periods with no water deficit (periods with TWD returning to zero at night; Figure 4.1a-c, and g-i). Rainfall was associated with an increase in θ and decreased TWD, T_{air}, VPD, PAR and ET (Figure 4.1d - i). The time series for other sites are presented in Figure SIII.3 - Figure SIII.7.

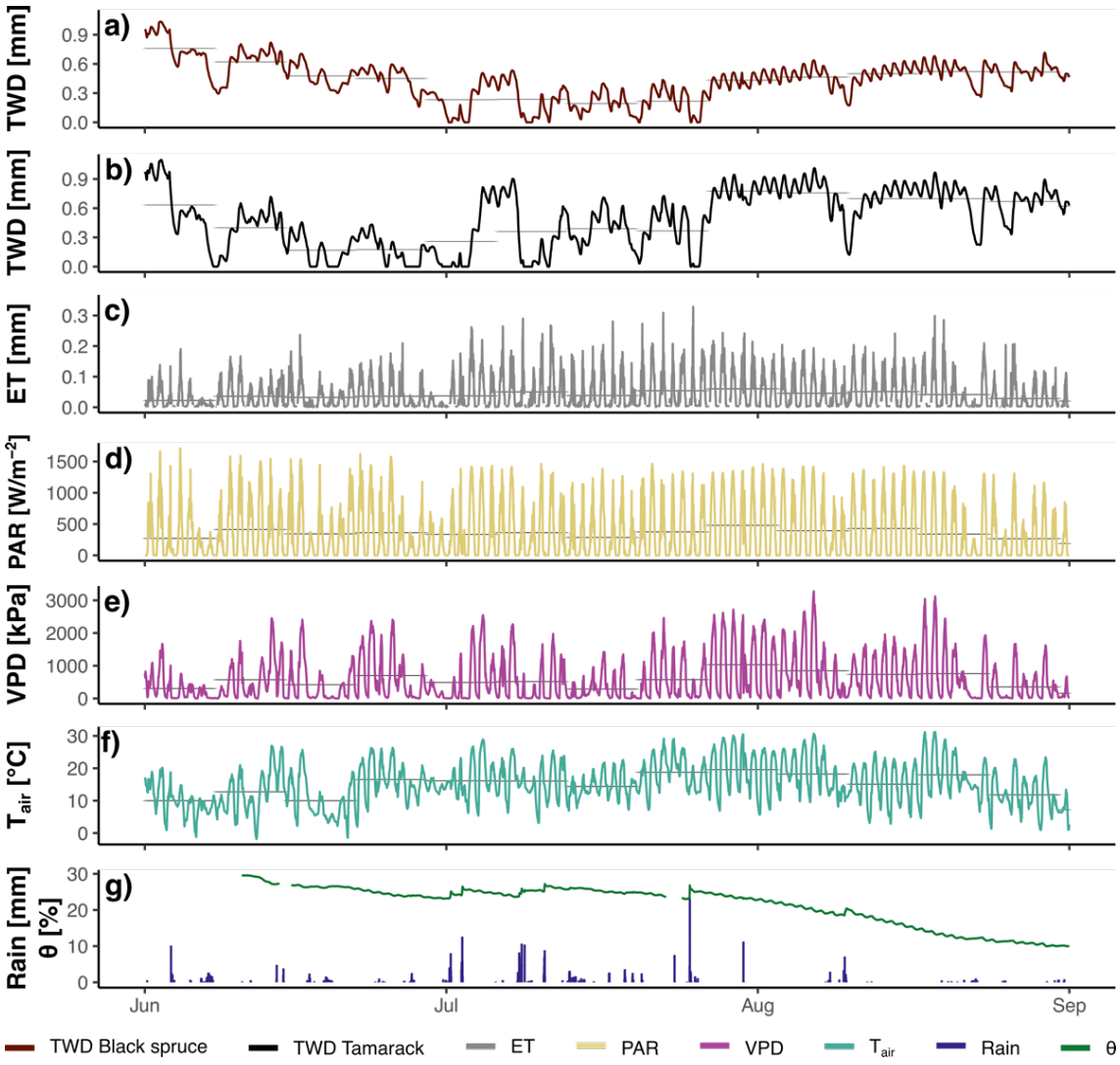

Figure 4.1 Half-hourly measurements of species-averaged tree water deficit (TWD) in black spruce (a) and tamarack (b), and potential environmental controls at Old Black Spruce in 2020. Environmental controls include evapotranspiration (ET, c), photosynthetically active radiation (PAR, d), vapour pressure deficit (VPD, e), air temperature (T_{air}, f), rain (g), and soil moisture (θ, g). Weekly average TWD, ET, PAR VPD and T_{air} are represented with grey lines (a-f).

Periodicity in tree water deficit and coherence with environmental controls

The wavelet analysis revealed common and significant periodicities in tamarack and black spruce TWD that were consistent across sites and between years. Wavelet power spectra of TWD were high for the daily and > daily (Figures SIII.6 and SIII.7), which is typical for environmental and eco-physiological series (Stoy *et al.* 2009). Wavelet coherence evaluated between TWD and the potential environmental controls was high at the same periodicity; coherence was highest daily and at > daily periods (Figure 4.2). Wavelet coherence was also observed at higher frequencies (< 0.5 day), but the wavelet power of TWD was not statistically significant at these frequencies and were therefore deemed unimportant (Figure 4.2 and Figure SIII.8 - Figure SIII.14).

For daily periods TWD had the highest coherence with PAR (not measured at BAC) followed by VPD, ET, and T_{air} (Figure 4.2a - h). Higher daily PAR, VPD, ET and T_{air} were correlated with higher TWD at the sites OBS, SCC, BAC and SMC. At HPC, greater TWD was also correlated with higher VPD, ET and T_{air} but with lower PAR (Figure SIII.15). High daily θ at SCC, BAC, SMC, and HPC was correlated with higher TWD however, the coherence at these sites was low (Figure 4.2a - d, f and g). By contrast, OBS had the lowest θ of all five sites but high coherence with daily θ TWD (Figure 4.2e and h). Rain had a weak coherence with daily TWD across all sites (Table SIII.3, Figure SIII.15).

At > daily, wavelet coherence was strongest for PAR, followed by VPD, θ (not significant at HPC), rain (not significant at SCC and BAC), and ET (not significant at HPC or BAC; Figure 4.2a - h). Higher PAR, VPD and ET were correlated with greater TWD while high θ and rainfall was correlated with a decrease in TWD. Air temperature had the lowest coherence with > daily TWD, and was only significant at SCC (Figure 4.2a - h, Table SIII.3, Figure SIII.15).

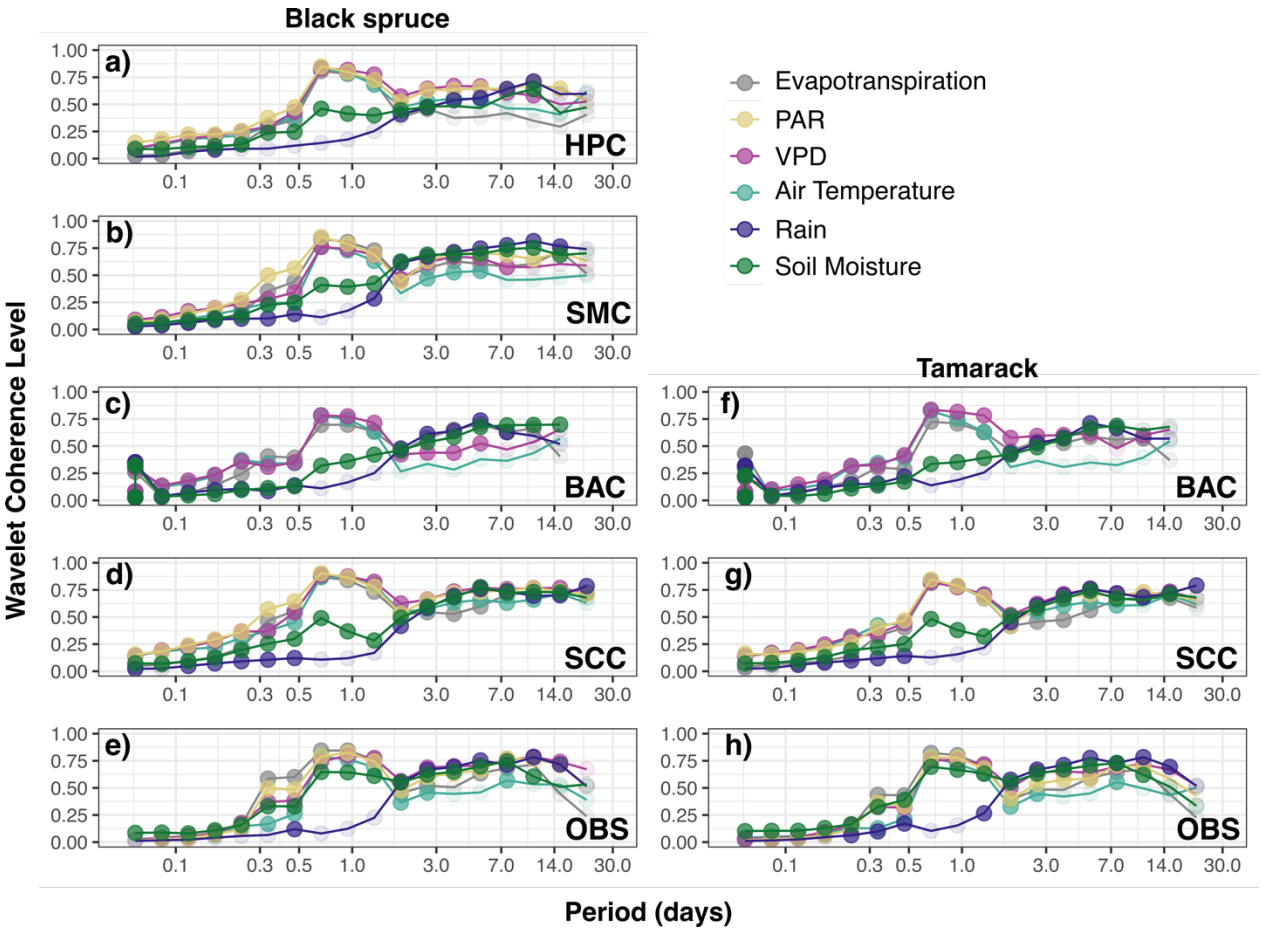

Figure 4.2 Wavelet coherence levels (0 - 1) between potential environmental controls and tree water deficit of black spruce and tamarack at Old Black Spruce (OBS), Scotty Creek (SCC), and Baker Creek (BAC), and black spruce at OBS, SCC, BAC, Smith Creek (SMC) and Havikpak Creek (HPC). Sites are listed from south (bottom) to north (top). Potential environmental controls include evapotranspiration, photosynthetically active radiation (PAR), vapour pressure deficit (VPD), air temperature, rain and soil moisture. Circles with dark shading indicate significant (a = 0.05) coherence between tree water deficit and environmental condition.

From the G-causality analysis we found differences in the interactions among the potential environmental controls at the daily and > daily periods. Daily, T_{air} and PAR controlled TWD (Figure 4.3b and d). Higher T_{air} and PAR caused greater TWD in both species. At > daily periods, PAR and T_{air} remained important controls of TWD (above the significance threshold in Figure 4.3h and j), however the causal effect was diminished compared to the daily period. The causal relationship between TWD and VPD varied between time periods. Daily, VPD had a strong causal

effect on TWD, but during longer periods the causal effect of TWD on VPD was stronger for both species (Figure 4.3c and i). Tree water deficit also has a strong causal effect on ET, a relationship that was consistent across time scales (Figure 4.3a and g). Increasing TWD in both species, but especially tamarack, led to greater ET during daily and longer periods. Soil moisture had a consistent causal effect on TWD daily and during > daily periods (Figure 4.3f and l), however, the coherence was low at the daily timescale (Figure 4.2a – h). There was little indication that rain had a direct causal effect on TWD at either timescale (Figure 4.3e and k), despite rain having high coherence with TWD during > daily periods (Figure 4.2a – h).

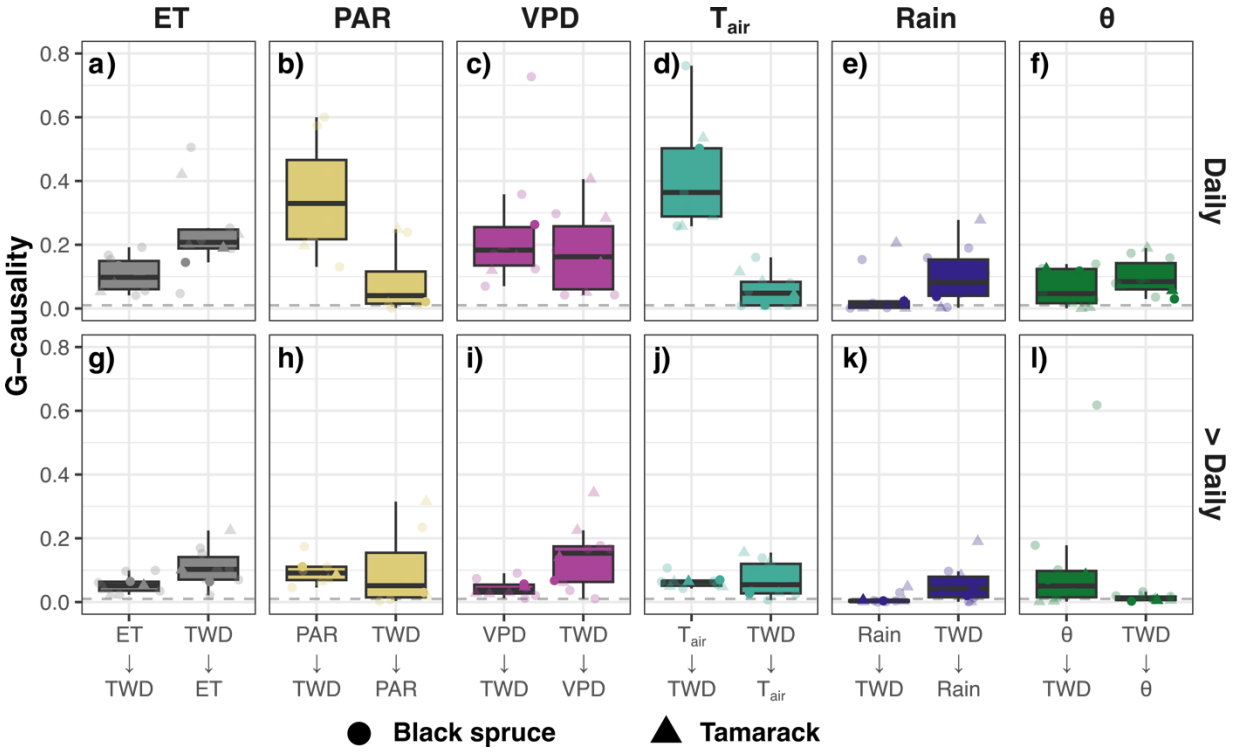

Figure 4.3 Across-site Granger-causality (G-causality) between black spruce and tamarack tree water deficit (TWD) and evapotranspiration (ET; a and g), photosynthetically active radiation (PAR; b and h), vapour pressure deficit (VPD; c and i), air temperature (T_{air}; d and j), rain (e and k) and soil moisture (θ, f and l) at the daily and > day periods (1.3 to 14 days). Individual points represent the causal effect of environmental controls on black spruce (circles) and tamarack (triangle) tree water deficit (TWD) at each site. Dark symbols represent the species-averaged granger-causality across sites, while the semi-transparent symbols represent site-specific values. Dashed lines indicate the significance threshold ($\alpha = 0.05$). Environmental controls have a causal

effect when the G-causality of the environmental control on tree water deficit is higher than the G-causality of tree water deficit on the environmental control (and vice versa).

Discussion

Our goal was to quantify the environmental controls that shape tree-water stress in Canada's western boreal forests. Central to our investigation was to determine if daily TWD, and extended periods of stem dehydration were determined by the same environmental controls across a large latitudinal range and between two of the most common tree species. Our analysis revealed that the environmental controls of TWD in black spruce and tamarack varied across temporal scales. At the daily timescale PAR, T_{air}, and VPD, exhibited the highest coherence and strongest causal influence on TWD. However, during > daily periods, PAR and θ emerged with the highest coherence and strongest causal effect on TWD (Figure 4.2a - h and Figure 4.3b - d, h and 1).

Photosynthetically active radiation, T_{air}, and VPD are known to affect transpiration in boreal (e.g., Oogathoo *et al*. 2020, Pappas *et al*. 2018, Patankar *et al*. 2015, Van Herk *et al*. 2011), temperate (e.g., Harrison *et al.* 2020) and tropical tree species (e.g., Brum *et al*. 2018, Ghimire *et al*. 2022). A high correlation between PAR and stem water storage, measured with dendrometers and electrical resistivity imaging, has been reported for ponderosa pine (*Pinus ponderosa*) in the temperate forest (Harmon *et al.* 2021), but has not been reported for boreal tree species. Photosynthetically active radiation promotes greater stem shrinking by increasing water loss via transpiration when incoming PAR is high and days are longer (i.e., larger window for photosynthetic uptake; Ahedor *et al.* 2018). Being higher in latitude, HPC had a lower potential for PAR, thus, the relationship between TWD and PAR was weaker at this site. Air temperature and VPD both increase alongside PAR, further driving transpiration and stem shrinking (Sack and Holbrook 2006, Taiz and Zeiger 2002, Zweifel and Hasler 2001). We found that daily TWD peaked after evapotranspiration and transpiration (derived from sap flow measurements at OBS, SCC, SMC and HPC between 2018 and 2021, Figure SIII.17), further confirming that transpiration, and the environmental controls of transpiration were the dominant causes of daily TWD. Increasing TWD with higher PAR, T_{air} and VPD had repercussions at the whole forest stand scale, driving an increase in ET at the daily period (Figure 4.3a).

With an expected increase in T_{air} and VPD during the peak growing season throughout the western boreal biome (Gauthier *et al.* 2015, Mirabel *et al*. 2023), there will likely be increased daily TWD, and thus greater daily transpiration (Van Herk *et al.* 2011). Greater daily transpiration could lead to increased forest productivity, consistent with observations of forest growth stimulated by increased temperatures in areas of the boreal biome (D'Orangeville *et al.* 2016, Reich *et al.* 2018, Babst *et al.* 2019, Wang *et al.* 2023). However, soil water content strongly affects boreal tree productivity by constraining water available for uptake, to refill stem water storages, sustain transpiration and support growth. Water supply and availability (i.e., rainfall and θ) were high during the study period compared to the climate normals between 1980 and 2010, and likely did not reach below the wilting point for either species at the daily timescale. Additionally, rainfall and θ had minimal, often negligible daily cycles. Thus, the observed impact of rainfall and θ on TWD was limited at the daily time scale (Figure 4.2a - h, Figure 4.3e - f).

While soil moisture was not the primary driver of daily TWD, it was a significant environmental control during > daily periods of TWD. Lower θ was strongly correlated with TWD, causing greater stem dehydration in both black spruce and tamarack (Figure 4.2a - h and Figure 4.3l). These findings were consistent with Maillet *et al.* (2022) who found that stem radius change of three boreal conifers was most strongly correlated with water availability (rainfall) at the weekly timescale. To support normal functioning, including transpiration, trees rely on internal water in stem reserves and water uptake (Čermák *et al.* 2007, Mészáros *et al.* 2011, Nehemy *et al.* 2021, Steppe *et al.* 2006, Zweifel and Hasler 2001). However, as TWD intensifies between rainfall events, trees increasingly rely on θ to support transpiration and stem refilling. Trees operate at narrow safety margins with respect to drought tolerance (Choat *et al.* 2012). Thus, with summer precipitation in western Canada projected to decrease (or stay stable) by the end of the 21st century while temperatures continue to rise (Zhang *et al*. 2019), boreal trees could experience greater TWD, drought stress and growth reductions during dry periods. The relationship between > daily TWD and θ was strongest in the south at OBS where θ was lowest of the five sites. Thus implying that the southern boreal forest may experience higher occurrences of water deficit before northern locations. However, with increased soil drying associated permafrost thaw (Helbig *et al.* 2016, Sniderhan *et al.* 2021, Foster *et al.* 2022), areas of the boreal forest with discontinuous permafrost may be susceptible to drying as well.

In the face of a warmer and drier climate projected for western Canada, intermittent wet and warm periods may promote increased growth in black spruce and tamarack, leading to enhanced productivity (D'Orangeville *et al*. 2018, Wang *et al*. 2022). Additionally, certain species, such as black spruce, have demonstrated low sensitivity of basal area increment to summer θ (Girardin *et al.* 2021), and prolonged stem dehydration has not consistently resulted in stress induced growth reduction (Belien *et al.* 2014). Consequently, boreal trees could exhibit resilience to anticipated drier and warmer conditions in the near future.

Species resilience may be attributed to specific physiological strategies that allow trees to maintain physiological function and growth during water deficit. Although the contribution of black spruce and tamarack transpiration is only a minor component of ET (Warren *et al*. 2018, Perron *et al*. 2023), we found that increasing TWD caused greater ET during > daily periods (Figure 4.3g). This suggests that black spruce and tamarack maintain transpiration despite reduced access to available soil water and increased TWD. Greater decoupling of ET to water deficit has been previously reported in moist sites where plants either regulate their stomata and hydraulic conductance, or access water deep in the soil column to maintain transpirational activity during dry periods (Giardina *et al.* 2023). Black spruce and tamarack have shallow rooting zones, thus were likely not able to access deeper soil water after top 10 - 20 cm were depleted. Thus, stomatal regulation to limit water loss during transpiration in the short term likely facilitated continued transpiration in both species, allowing for sustained ET during > daily periods with higher TWD (Dusenge *et al.* 2021, Giardina *et al.* 2023).

We expected VPD to drive tree dehydration in black spruce and tamarack during > daily periods of TWD. Vapour pressure deficit is known to influence tree-water stress by driving transpiration (Harmon *et al.* 2021, Nehemy *et al.* 2021, Salomón *et al.* 2022, Xue *et al.* 2022), and has been negatively correlated with weekly TWD in larch species (Tian *et al.* 2018) and growth in spruce species (Mirabel *et al.* 2023). However, we found that while TWD and VPD were coherent during > daily periods, TWD caused (i.e., led the relationship with) VPD, not the other way around. The effect of TWD on VPD was greatest at OBS, the denser southern forest with lower θ and higher $T_{air,}$ ET, and transpiration compared to the sparsely forested sites further north (Figure SIII.18 and Figure SIII.19). In response to high atmospheric water demands, boreal species have demonstrated

greater coupling between stem water content and VPD, as well as sensitive stomatal control (Ewers *et al.* 2005, Dusenge *et al.* 2021). Thus, black spruce and tamarack likely responded to atmospheric demands at OBS and across sites, by closing stomata before VPD peaked. Root water uptake continues after the stomates close, allowing storage tissue to refill and stems to swell, resulting in changes to TWD that occurred before VPD decreased in the evening. Air temperature, which drove TWD during > daily periods (Figure 4.3j), is also known to drive VPD. Warmer air has a greater atmospheric holding capacity for water, thus, the causal effect of TWD on VPD over longer periods may have been, in part, the effect of increasing T_{air}.

Limitations in the methodology to determine TWD could have also contributed to the causal influence of > daily TWD on VPD (Zweifel *et al*. 2021). The dendrometers used have a high thermal sensitivity, but have the potential for sensor drift with changing temperature (< 0.2 µm/°C). Cooler air temperatures over several days may have prompted thermal contraction of the sensors, resulting in higher TWD that preceded changes in VPD. Additionally, any method to partition TWD from ΔSR makes assumption about growth during periods of stem shrinkage (Zweifel *et al.* 2016). In the Zero Growth concept applied here, we assumed no growth took place during periods with TWD > 0 (i.e., during stem shrinking when current ΔSR was less than the previous maximum ΔSR, Zweifel *et al.* 2016). With TWD at a consistent zero during growth, we cannot fully detect the influence of VPD during these periods. Moreover, growth in the form of cell division and elongation, could have taken place during periods of stem shrinkage. During > daily periods of stem shrinkage, growth could have accumulated sufficiently over several days (ranging from 1.3 to 14 days), to reduce the measured values of TWD, and decouple from the influence VPD.

Conclusions

This work determined that the environmental controls on tree water deficit (TWD) in black spruce and tamarack vary across temporal scales. Photosynthetically active radiation (PAR), T_{air}, and VPD emerged as crucial controls of TWD at the daily scale, contributing to transpiration-driven stem shrinking. In contrast, PAR and soil water availability (θ) controlled TWD at daily to biweekly, where tree dehydration and potential drought stress became pronounced. With warming and drying

predicted for Canada's western boreal biome, trees will see greater daily TWD with benefits to productivity through increased transpiration and ET. However, with a decrease in the frequency and intensity of rainfall events throughout the peak growing season, soil water availability may be limited. Tree species will experience more numerous, longer, and more extreme periods of stem dehydration during dry periods, with potential consequences to boreal tree growth and forest vulnerability. This research underscores the challenges posed by warming and drying trends in boreal forests, highlighting the delicate balance between soil water availability, air temperature, and tree dehydration.

Chapter 5 – Conclusions

The three article chapters that make up my thesis provide an improved functional understanding of tree-water relations in Canada's western boreal forest. In the second chapter I found that resource-use strategies affected species growth and tree water deficit throughout the growing season. In the third chapter, I examined the effect of site heterogeneity on transpiration and determined that transpiration was highly sensitive to local environmental conditions. In the fourth chapter, I examined the drivers of tree water deficit across five sites in Canada's western boreal biome and determined that solar radiation, air temperature, and soil moisture were the strongest and most consistent drivers of water deficit in black spruce and tamarack across temporal scales (Figure 5.1).

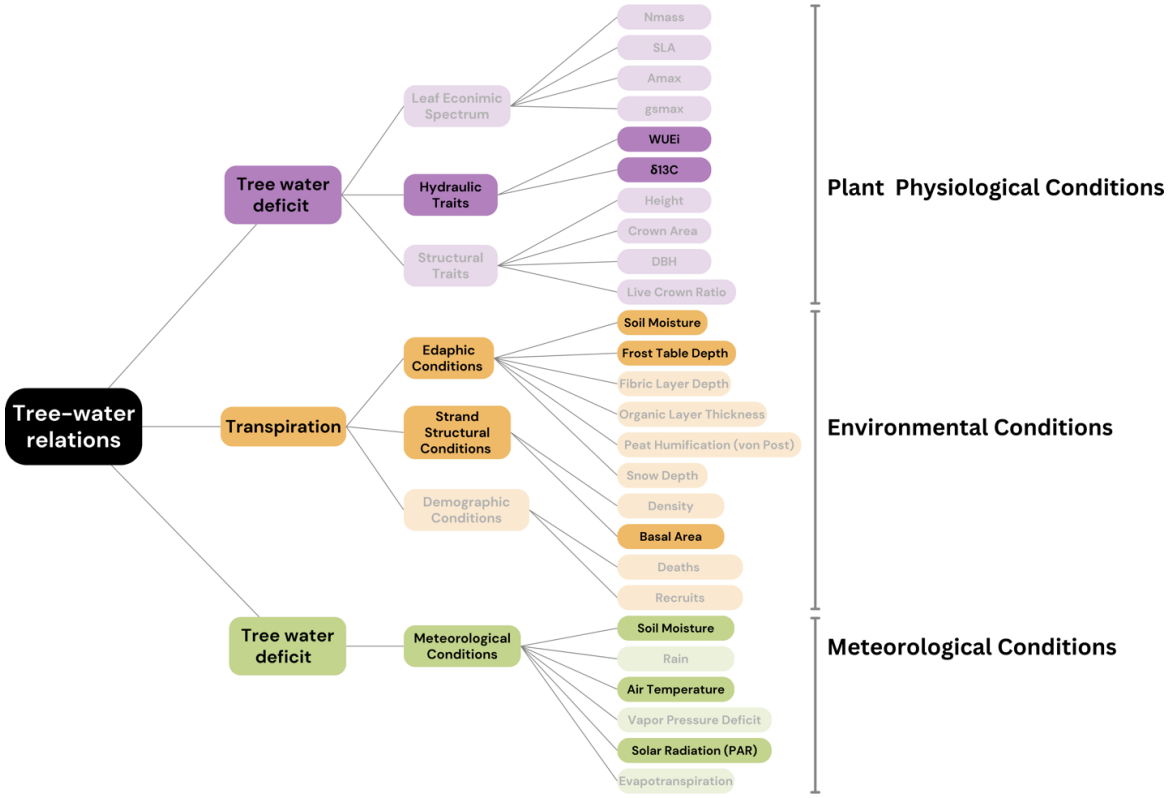

Figure 5.1 The physiological (purple, Chapter 2), environmental (orange, Chapter 3) and meteorological (green, Chapter 4) conditions that had the greatest influence on different aspects of tree-water relations. The dark boxes represent variables that we found had the greatest effect on tree water deficit and transpiration for each chapter.

Summary of results

In chapter two, I show that black spruce and tamarack employed contrasting resource-use strategies (acquisitive versus conservative) associated with the leaf economic spectrum, resulting in high growth rates for the acquisitive tamarack, and lower growth for the conservative black spruce across sites in Canada's western boreal forest (Chapter 2). However, there was species overlap in traits associated with tree height and competition for light. In nutrient poor conditions, tamarack was unable to maintain a competitive advantage for light, resulting in low growth but also lower tree water deficit. When water was abundant, tree water deficit was similar between species, and the conservative black spruce demonstrated slow growth compared to the fast growing acquisitive tamarack. These findings suggest that resource-use strategies of black spruce and tamarack offer complementary strategies for growth and survival when other resources are not limited. Tamarack was able to maintain higher growth rates by accessing water more consistently throughout the growing season. In contrast, black spruce resisted water stress by constraining growth thereby limiting excess water loss.

In chapter three, I found that transpiration rates were influenced by land cover type. Local environmental conditions characteristic of peat plateaus, including higher basal area, drier soils, and the presence of permafrost resulted in higher transpiration rates. This was in contrast to the wetlands which were wet, permafrost-free and had trees with lower transpiration rates. As in chapter two, there was no difference in tree water deficit between tamarack and black spruce; both species exhibited similar tree-level transpiration. This study emphasizes the importance of sampling trees across various land cover types to ensure accurate transpiration estimates in heterogeneous landscapes.

In chapter four, I took a broader perspective by investigating the meteorological conditions, referred to as potential environmental controls in the chapter, that contributed to water deficit in trees. The study revealed that patterns of tree water deficit could be divided into two periods: daily tree water deficit driven by transpiration, and multi-day periods indicative of drought stress. Solar radiation and air temperature drove the daily cycling of stem water, while drought stress was primarily regulated by solar radiation and soil moisture. Surprisingly, vapor pressure deficit, known

to strongly affect transpiration and growth limitations in boreal trees (Mirabel *et al.* 2023), was not a primary factor influencing water status in trees.

Implications

The outcomes of my three chapters have implications for ecological and atmospheric sciences, by enhancing our understanding of boreal forest function. Collectively, this work advances scientific knowledge of boreal tree species which is crucial for refining predictions of how boreal forests will respond to ongoing environmental changes. To highlight the cumulative implications of the three chapters, I present two syntheses that illustrate the current conditions for black spruce at Scotty Creek and tamarack at Old Black Spruce. I chose to examine black spruce at Scotty Creek because the species is on the decline at this site. Black spruce at Scotty Creek is undergoing reduced productivity (Patankar *et al*. 2015, Sniderhan and Baltzer, 2016), and a mortality rate that exceeds recruitment (Dearborn *et al*. 2021). I chose to examine tamarack at Old Black Spruce because this site is at the southern edge of the boreal biome and recent work indicates that *Larix* species, including tamarack, are more vulnerable to climate change at the southern margins of its range (Mamet *et al*. 2018). Each synthesis also offers a predictive insight into the potential changes each species may experience at these sites.

Synthesis one

At Scotty Creek, black spruce trees predominantly grow atop peat plateaus with dry soils underlain by permafrost. The peat plateaus exhibit higher stand basal area and transpiration rates compared to surrounding wetlands . The high soil drainage and greater organic matter decomposition on peat plateaus has a positive effect on transpiration rates (Chapter 3). These suitable growing conditions have allowed black spruce to dominated the canopy at Scotty Creek, with individuals were generally taller, and lager with a more expansive crown compared to tamarack. However, with a larger canopy comes a greater need for water to support photosynthesis and thus, black spruce demonstrated higher tree water deficit (Chapter 2). Daily fluctuations in black spruce water deficit at Scotty Creek are primarily controlled by air temperature, vapor pressure deficit, and soil moisture (Chapter 4, Patankar *et al.* 2015), with higher daily transpiration occurring on warm, dry days when

soil water availability is high. As the active layer (the seasonally thawed ground layer above the permafrost) thickens during the growing season, peat plateaus gradually dry out, reducing water availability in the rooting zone of black spruce. The decrease in soil moisture throughout the growing season, resulted in an increase in tree water deficit for black spruce(Chapters 2 and 4).

Permafrost thaw at Scotty Creek will further degrade peat plateaus through the deepening and drying of the active layer due to vertical permafrost thaw. Drought stress in black spruce at Scotty Creek, characterized as a multi-day tree water deficit, is controlled by solar radiation, rain, and soil moisture (Chapter 4). Thus, black spruce located on permafrost plateaus experiencing vertical thaw and surface drying are likely to encounter more frequent and prolonged periods of tree water deficit. As trees become more reliant on rainfall to recharge the soil moisture in the rooting zone, the conservative black spruce will likely reduce growth to prevent water loss, further decreasing its productivity (Chapter 2) with consequences for growth, water, and energy fluxes across the forest stands (Patankar *et al.* 2015, Warren *et al.* 2018, Sniderhan and Baltzer 2016). Given the projected increase in air temperature for Scotty Creek (Zhang *et al.* 2019), black spruce may be susceptible to severe drought stress, resulting in forest mortality and changes in community composition in drier and warmer conditions (Dearborn *et al.* 2021, Sánchez-Pinillos *et al.* 2022, Balducci *et al.* 2015, Whitman *et al.* 2019). Scotty Creek could also see a decrease in black spruce productivity as lateral permafrost thaw triggers plateau collapse into wetlands (Quinton and Baltzer 2013), where surface flooding limit root function, and thereby further limiting productivity of black spruce (Chapter 3, Patankar *et al.* 2015, Baltzer *et al.* 2014, Perron *et al.* 2023).

Synthesis two

At Old Black Spruce, soil moisture had a more pronounced impact on the daily tree water deficit of tamarack compared to any other site for both species (Chapter 4). As a consequence of its acquisitive resource-use , tamarack relies greatly on water availability to support growth (Chapter 2). Even after rain events, tamarack rapidly use stored stem reserves, leading to faster dehydration (and higher tree water deficit) compared to black spruce (Chapters 2 and 4). During extended water deficit periods when tamarack draws on soil water reserves to prevent dehydration, resulting in the depletion of water from the top ~10 cm of soil (Chapter 4).

Tamarack's high water resource requirements proved to be a successful strategy in conditions of abundant water availability. For example, our study period consisted of summers that were cooler and wetter than average for Old Black Spruce, and tamarack growth appeared to be uninhibited by water availability (Chapter 2). However, as warming and drying decrease water availability in the southern boreal forest (Zhang *et al.* 2019, Wang *et al.* 2014), and changing precipitation patterns alter the timing of rainfall through the summer (Zhang *et al.* 2019), tamarack may not have access to enough water to sustain such high growth rates. Potentially resulting in reduced productivity and even mortality at Old Black Spruce, as reported elsewhere throughout the southern range limit of the *Larix* sp. (Mamet *et al.* 2019).

Future research

My thesis presents empirical evidence that enhances our understanding of how plant physiology, environmental factors, and meteorological conditions influence tree-water relations. As temperatures rise and precipitation patterns shift, drought-induced stress will become a growing concern for boreal forests. To anticipate the effects of drought on forest composition, tree mortality, and overall forest health, it will be crucial to understand tree hydraulics in greater depth.

Through the creation of a dataset that combines high-resolution dendrometer measurements with supporting environmental and meteorological data for an underexplored region within North America's boreal biome, my thesis makes an important contribution towards better understanding tree water relations. This dataset has a wide range of potential applications including to improve our understanding of drought stress, plant functioning, growth, carbon relations, phenology, and dendroclimatology (De Swaef *et al.* 2015, Zweifel 2016, Salomón *et al.* 2022).

Seasonal tree water deficit and annual growth

An exciting research avenue would be to integrate seasonal tree water deficit information with interannual tree growth variability. While my work identified key controls of tree water deficit in black spruce and tamarack (Chapter 4), it did not explore how periods of water deficit affect the annual growth of either species. Future research opportunities include addressing questions such

as: ‘Does seasonal tree water deficit reduce growth in black spruce and tamarack?’ and ‘Do meteorological drivers of tree water deficit in boreal trees also limit growth?’. For instance, I found that vapor pressure deficit was not a strong driver of tree water deficit in black spruce and tamarack, but recent research has revealed interannual declines in tree growth linked to increasing vapor pressure deficit (Mirabel *et al.* 2023). Growth information can be obtained from dendrometer measurements (Chapter 2); nevertheless, the interpretation of absolute growth rates poses methodological challenges (Zweifel *et al.* 2016). To partition growth, assumptions must be made about when growth occurs (during water deficit or not) which can result in under or overestimations of radial growth. Therefore, integrating dendrometer data, site environmental and meteorological data and dendrochronological measurements, including microcores to determine intra-annual variation of growth, would provide a more reliable approach to addressing these questions (e.g., Deslauriers *et al.* 2014, Kannenberg *et al.* 2019).

Improving our knowledge of plant hydraulic strategies

For a deeper understanding of how resource acquisition strategies coordinate with tree hydraulics, future research should include more functional trait data. In this thesis, I focused on foliar traits associated with the leaf economic spectrum and overlooked several traits related to tree hydraulics that could have provided important insights. For instance, traits measuring stem wood density, Huber values, the ratio of cross sectional sapwood area to leaf area, (Tyree and Ewers, 1991), sapwood-specific and leaf-specific stem hydraulic conductivity, vulnerability to xylem embolism and turgor loss point are all important hydraulic, leaf, and stem traits (Rosas *et al.* 2019, Rosas *et al.* 2021). Many traits related to the leaf economic spectrum and tree hydraulics exhibit temporal variability (e.g., Ma *et al.* 2010, Anderegg 2015, Yang *et al.* 2016). However, specific traits are often quantified from campaign-based measurements that fail to capture important temporal variation in plant responses to changing environmental conditions, including water availability, throughout a growing season. Incorporating additional hydraulic and stem traits into future research, and increasing the sampling rate of these traits to multiple times during a single growing season, and over the course of several years, would provide a more comprehensive understanding of the resource-use strategies employed by boreal trees (e.g., Rosas *et al.* 2021).

Integrating dendrometer and sap flow data

One of the initial objectives of my PhD research was to combine dendrometer data with sap flow measurements. Trees at all research sites (Old Black Spruce, Scotty Creek, Baker Creek, Smith Creek and Havikpak Creek) were instrumented with paired dendrometers and custom-made Granier-style thermal dissipation sap flow sensors. Unfortunately, technical challenges during the measurement period and limitations imposed by the COVID-19 pandemic prevented me from using most of the sap flow data. However, some of the sap flow data was used to support the analysis in Chapter 4. Thus, an unrealized opportunity with this dendrometer data lies in its pairing with sap flow measurements to enhance our interpretation of tree hydraulics. Paired data would not only instill greater confidence when assessing drought stress in trees but would also enable a deeper understanding of plant physiological behavior (e.g., Ježík *et al.* 2015, Sánchez-Costa *et al.* 2015). Additional sap flow measurements would offer opportunities to estimate transpiration from more forest stands, and allow us to determine the contribution of tree-level transpiration to stand-level evapotranspiration across research sites beyond Scotty Creek.

Benchmark for evaluating change in the boreal forest

Forest dynamics plots serve as invaluable research tools used to untangle complex forest ecosystem processes (Davies *et al.* 2021, Anderson-Teixeira *et al.* 2015). However, within the Smithsonian's ForestGEO network, the majority of plots are concentrated in temperate and tropical regions. The scarcity of forest dynamics plots situated in the boreal biome make Scotty Creek ForestGEO valuable for observing forest processes beyond tropical and temperate forest biomes. My study (Chapter 3), which assessed transpiration across the plot, not only expanded upon the existing datasets within the ForestGEO network but also provided new information on forest processes specific to this location. Now that a forest fire has eradicated a substantial portion of the ForestGEO plot at Scotty Creek, this work, in combination with previous research (Dearborn *et al*. 2021, Standen and Baltzer 2021), has the potential to serve as a foundation for characterizing the pre-fire state of the boreal peatland complex and for assessing post-fire recovery.

Chapter 6 – Reflections

Through this thesis, I have presented the research outcomes of my PhD, but this left little room to delve into some of the most significant aspects of my doctoral journey. Therefore, I would like to take a moment to share some reflections I had during this experience.

First reflection: navigating obstacles in science

Originally, I had intended for my thesis to center on sap flow, with my main objective being to partition transpiration (T) from stand level fluxes of evapotranspiration (ET). As mentioned earlier, this objective could not be achieved. I believe that transpiration partitioning to determine T:ET across boreal forest sites could have made a more substantial contribution to the scientific community compared to the current results of my thesis. Transpiration estimates from trees would have held significant value in reducing uncertainties in climate, earth system and hydrological modeling (Coenders-Gerrits *et al.* 2014, Fatichi and Pappas 2017). Moreover, transpiration partitioning could have been used to determine the relative importance of trees in the water and energy balance in the western boreal forest. Failing to achieve this objective has taught me a great deal about loss, disappointment and significant setbacks often experienced but rarely discussed in academia. While I appreciate the valuable lessons learned, when I reflect upon my thesis and its value, I cannot help but feel a tinge of disappointment. However, similar to black spruce and tamarack thriving amid challenging and rapidly changing conditions, I persevered through these unforeseen challenges, managing to sustain only minor disruptions to my productivity.

Second reflection: western science on traditional lands

One of the most impactful experiences during my PhD was my participation in the Dehcho Youth Ecology and Traditional Knowledge Camp, held on the banks of the Mackenzie River in the Northwest Territories. I would be remiss not to share my insights from this experience, as my involvement in the camp has profoundly influenced how I envision my future as a researcher in Canada. The Dehcho camp introduced me to Traditional Ecological Knowledge, Indigenous partnerships, and the co-creation of knowledge. My time at the Dehcho camp, along with

subsequent contemplation, opened my eyes to the extractive nature of Western science in Canada, particularly in Canada's North. As Western scientists, we venture onto Indigenous territories to collect data for our projects, extracting knowledge from lands that are not inherently ours.

I've since questioned if my research genuinely aligns with what holds importance in these regions and whether I am the most suitable person to be conducting this research. I have asked myself: "Is it ethically sound for me to conduct research with little direct values to local communities?" and "Is it appropriate for me, a white woman with colonial heritage from southern Canada, to conduct research on the homelands of Indigenous Peoples?". Contemplating the ethical implications of my thesis, I have found comfort in collaborating with research groups and alongside colleagues who share a commitment to sincerely exploring these concerns and dedicating time to address these questions with care; however, these questions remain largely unanswered.

Third reflection: additional outcomes

Despite the challenges that arose during my PhD, the overall experience has positive. In addition to the studies presented as part of my thesis, I was able to contribute to other scientific and non-scientific projects. I received a POLAR scholarship that allowed me to conduct research in Iceland, and Cambridge Bay. Samples collected during this expedition contributed to two published manuscripts (Stimmler, P., M. Göckede, S. M. Natali, O. Sonnentag, B. S. Gilfedder, N. Perron, and J. Schaller. 2022. The importance of calcium and amorphous silica for arctic soil CO_2 production. Frontiers in Environmental Science 10:1019610. and Stimmler, P., M. Goeckede, B. Elberling, S. Natali, P. Kuhry, N. Perron, F. Lacroix, G. Hugelius, O. Sonnentag, J. Strauss, C. Minions, M. Sommer, and J. Schaller. 2023. Pan-Arctic soil element bioavailability estimations. Earth System Science Data 15:1059–1075.) The scholarship also led to the curation of data sets that will be used in the future. My work with dendrometers and sap flow sensors at Old Black Spruce was founded on collaboration that contributed to one published manuscript outside of my thesis (Nehemy, M. F., J. Maillet, N. Perron, C. Pappas, O. Sonnentag, J. L. Baltzer, C. P. Laroque, and J. J. McDonnell. 2022. Snowmelt Water Use at Transpiration Onset: Phenology, Isotope Tracing, and Tree Water Transit Time. Water Resources Research 58.). I shared my experiences at the Dehcho camp by contributing an article to the departmental journal (El-Amine, Mariam and

Perron, Nia 2022. Sur les rives du Deh Cho : à la confluence entre l'écologie et les savoirs traditionnels. GéoLibre, second edition), I shared my experience in the field through photo competitions, and shared my overall experience in academia in a museum exhibition dedicated to women in science. I also had the opportunity to participate in several conferences and speaker series, including the Canadian Geophysical Union in 2023, where I was invited to present my work.

Concluding remarks

If I were granted the opportunity to start my thesis over, there are a few things I would approach differently. To ensure success from the onset, I would be more self-assured in my role as a student with valuable experience. I would resist being swayed by the overconfidence of others, and approach collaborative work with greater prudence. I would actively seek to develop a greater knowledge of the Indigenous communities in the Northwest Territories before starting field work. I would strive to develop thesis topics through the co-creation of knowledge, addressing questions directly relevant to local communities. I might spend less time doing data processing, and more time fostering community engagement and building relationships with those who generously allowed their land to be part of this research. I would ensure that any and all knowledge generated through my thesis was shared directly with communities through non-traditional methods of communicating science. Lastly, I would invest in some Arduino circuit boards to get those sap flow sensors working properly.

Bibliography

Adelman, J. D., Ewers, B. E., & MacKay, D. S. (2008). Use of temporal patterns in vapor pressure deficit to explain spatial autocorrelation dynamics in tree transpiration. Journal of Ecology, 96(3), 647–658.

Ahedor, A., B. Spitz, M. Cowana, J. Miller, and M. Kamar. (2018). Comparative Transpiration Studies on the Invasive Eastern Redcedar (*Juniperus virginiana* L.) and Adjacent Woody Trees. Oklahoma Native Plant Record 18, 24–37.

Allen, C. D., A. K. Macalady, H. Chenchouni, D. Bachelet, N. McDowell, M. Vennetier, T. Kitzberger, A. Rigling, D. D. Breshears, E. H. (Ted) Hogg, P. Gonzalez, R. Fensham, Z. Zhang, J. Castro, N. Demidova, J.-H. Lim, G. Allard, S. W. Running, A. Semerci, and N. Cobb. (2010). A global overview of drought and heat-induced tree mortality reveals emerging climate change risks for forests. Forest Ecology and Management 259, 660–684.

Ameray, A., Cavard, X., & Bergeron, Y. (2023). Climate change may increase Quebec boreal forest productivity in high latitudes by shifting its current composition. Frontiers in Forests and Global Change, 6, 1020305.

Anderegg, W. R. L. (2015). Spatial and temporal variation in plant hydraulic traits and their relevance for climate change impacts on vegetation. New Phytologist, 205, 1008–1014.

Anderegg, W. R. L., Berry, J. A., Smith, D. D., Sperry, J. S., Anderegg, L. D. L., & Field, C. B. (2012). The roles of hydraulic and carbon stress in a widespread climate-induced forest die-off. Proceedings of the National Academy of Sciences, 109, 233–237.

Anderegg, W. R. L., Trugman, A. T., Bowling, D. R., Salvucci, G., & Tuttle, S. E. (2019). Plant functional traits and climate influence drought intensification and land–atmosphere feedbacks. Proceedings of the National Academy of Sciences, 116, 14071–14076.

Anderson-Teixeira, K. J., S. J. Davies, A. C. Bennett, E. B. Gonzalez-Akre, H. C. Muller-Landau, S. J. Wright, K. A. Salim, A. M. A. Zambrano, A. Alonso, J. L. Baltzer, Y. Basset, N. A. Bourg, E. N. Broadbent, W. Y. Brockelman, S. Bunyavejchewin, D. F. R. P. Burslem, N. Butt, M. Cao, D. Cardenas, G. B. Chuyong, K. Clay, S. Cordell, H. S. Dattaraja, X. Deng, M. Detto, X. Du, A. Duque, D. L. Erikson, C. E. N. Ewango, G. A. Fischer, C. Fletcher, R. B. Foster, C. P. Giardina, G. S. Gilbert, N. Gunatilleke, S. Gunatilleke, Z. Hao, W. W. Hargrove, T. B. Hart, B. C. H. Hau, F. He, F. M. Hoffman, R. W. Howe, S. P. Hubbell, F. M. Inman-Narahari, P. A. Jansen, M. Jiang, D. J. Johnson, M. Kanzaki, A. R. Kassim, D. Kenfack, S. Kibet, M. F. Kinnaird, L. Korte, K. Kral, J. Kumar, A. J. Larson, Y. Li, X. Li, S. Liu, S. K. Y. Lum, J. A. Lutz, K. Ma, D. M. Maddalena, J.-R. Makana, Y. Malhi, T. Marthews, R. M. Serudin, S. M. McMahon, W. J. McShea, H. R. Memiaghe, X. Mi, T. Mizuno, M. Morecroft, J. A. Myers, V. Novotny, A. A. de Oliveira, P. S. Ong, D. A. Orwig, R. Ostertag, J. den Ouden, G. G. Parker, R. P. Phillips, L. Sack, M. N. Sainge, W. Sang, K. Sri-ngernyuang, R. Sukumar, I.-F. Sun, W. Sungpalee, H. S. Suresh, S. Tan, S. C. Thomas, D. W. Thomas, J. Thompson, B. L. Turner, M. Uriarte, R. Valencia, M. I. Vallejo, A. Vicentini, T. Vrška, X. Wang, X. Wang, G. Weiblen, A. Wolf, H. Xu, S. Yap, and J. Zimmerman. (2015). CTFS-ForestGEO: a worldwide network monitoring forests in an era of global change. Global Change Biology 21, 528–549.

Angstmann, J. L., Ewers, B. E., & Kwon, H. (2012). Size-mediated tree transpiration along soil drainage gradients in a boreal black spruce forest wildfire chronosequence. Tree Physiology, 32, 599–611.

Angstmann, J. L., Ewers, B. E., Barber, J., & Kwon, H. (2013). Testing transpiration controls by quantifying spatial variability along a boreal black spruce forest drainage gradient. JEcohydrology, 6, 783–793.

Arneth, A., F. M. Kelliher, G. Bauer, D. Y. Hollinger, J. N. Byers, J. E. Hunt, T. M. McSeveny, W. Ziegler, N. N. Vygodskaya, I. Milukova, A. Sogachov, A. Varlagin, and E.-D. Schulze. (1996). Environmental regulation of xylem sap flow and total conductance of *Larix gmelinii* trees in eastern Siberia. Tree Physiology 16, 247–255.

Babst, F., O. Bouriaud, B. Poulter, V. Trouet, M. P. Girardin, and D. C. Frank. (2019). Twentieth century redistribution in climatic drivers of global tree growth. Science Advances 5, 4313.

Baldocchi, D. (2014). Measuring fluxes of trace gases and energy between ecosystems and the atmosphere - the state and future of the eddy covariance method. Global Change Biology, 20, 3600–3609.

Balducci, L., A. Deslauriers, S. Rossi, and A. Giovannelli. (2019). Stem cycle analyses help decipher the nonlinear response of trees to concurrent warming and drought. Annals of Forest Science 76:88.

Balducci, L., Deslauriers, A., Giovannelli, A., Beaulieu, M., Delzon, S., Rossi, S., & Rathgeber, C. B. K. (2015). How do drought and warming influence survival and wood traits of *Picea mariana* saplings? Journal of Experimental Botany, 66, 377–389.

Baltzer, J. L., N. J. Day, X. J. Walker, D. Greene, M. C. Mack, H. D. Alexander, D. Arseneault, J. Barnes, Y. Bergeron, Y. Boucher, L. Bourgeau-Chavez, C. D. Brown, S. Carrière, B. K. Howard, S. Gauthier, M.-A. Parisien, K. A. Reid, B. M. Rogers, C. Roland, L. Sirois, S. Stehn, D. K. Thompson, M. R. Turetsky, S. Veraverbeke, E. Whitman, J. Yang, and J. F. Johnstone. (2021). Increasing fire and the decline of fire adapted black spruce in the boreal forest. Proceedings of the National Academy of Sciences 118, e2024872118.

Baltzer, J. L., R. Patankar, K. Dearborn, and C. A. Wallace. 2020. Permafrost thaw in boreal peatlands is rapidly altering forest community composition. Dryad.

Baltzer, J. L., Veness, T., Chasmer, L. E., Sniderhan, A. E., & Quinton, W. L. (2014). Forests on thawing permafrost: fragmentation, edge effects, and net forest loss. Global Change Biology, 20, 824–834.

Baltzer, J., Patankar, R., Downey, A., & Quinton, W. (2013). Impacts of Seasonal Thaw and Permafrost Degradation on *Picea mariana* Root Function in a Subarctic Boreal Peatland. Acta Horticulturae, 141–148.

Barber, V. A., G. P. Juday, and B. P. Finney. (2000). Reduced growth of Alaskan white spruce in the twentieth century from temperature-induced drought stress. Nature 405, 668–673.

Barr, A. G., G. Van Der Kamp, T. A. Black, J. H. McCaughey, and Z. Nesic. (2012). Energy balance closure at the BERMS flux towers in relation to the water balance of the White Gull Creek watershed 1999–2009. Agricultural and Forest Meteorology 153, 3–13.

Barraquand, F., C. Picoche, M. Detto, and F. Hartig. (2021). Inferring species interactions using Granger causality and convergent cross mapping. Theoretical Ecology 14, 87–105.

Bates, D., Mächler, M., Bolker, B., & Walker, S. (2015). Fitting Linear Mixed-Effects Models Using lme4. Journal of Statistical Software, 67, 1–48.

Beck, P. S. A., G. P. Juday, C. Alix, V. A. Barber, S. E. Winslow, E. E. Sousa, P. Heiser, J. D. Herriges, and S. J. Goetz. (2011). Changes in forest productivity across Alaska consistent with biome shift: Changes in forest productivity across Alaska. Ecology Letters 14, 373–379.

Belien, E., S. Rossi, H. Morin, and A. Deslauriers. (2014). High-resolution analysis of stem radius variations in black spruce [Picea mariana (Mill.) BSP] subjected to rain exclusion for three summers. Trees 28, 1257–1265.

Bergeron, Y., Chen, H. Y. H., Kenkel, N. C., Leduc, A. L., & Macdonald, S. E. (2014). Boreal mixedwood stand dynamics: ecological processes underlying multiple pathways. The Forestry Chronicle, 90, 202–213.

Bernacchi, C. J., & VanLoocke, A. (2015). Terrestrial Ecosystems in a Changing Environment: A Dominant Role for Water. Annual Review of Plant Biology, 66, 599–622.

Berner, J., C. Symon, L. Arris, O. W. Heal, Arctic Climate Impact Assessment, National Science Foundation (U.S.), and United States, editors. (2005). Arctic climate impact assessment. Cambridge University Press, Cambridge ; New York, N.Y.

Berry, Z. C., Looker, N., Holwerda, F., Gómez Aguilar, L. R., Ortiz Colin, P., González Martínez, T., & Asbjornsen, H. (2018). Why size matters: the interactive influences of tree diameter distribution and sap flow parameters on upscaled transpiration. Tree Physiology, 38, 263–275.

Bonan, G. B. (2008). Forests and Climate Change: Forcings, Feedbacks, and the Climate Benefits of Forests. Science, 320, 1444–1449.

Bonan, G. B., & Shugart, H. H. (1989). Environmental Factors and Ecological Processes in Boreal Forests. Annual Review of Ecology and Systematics, 20, 1–28.

Bond-Lamberty, B., Rocha, A. V., Calvin, K., Holmes, B., Wang, C., & Goulden, M. L. (2014). Disturbance legacies and climate jointly drive tree growth and mortality in an intensively studied boreal forest. Global Change Biology, 20, 216–227.

Bond-Lamberty, B., Wang, C., & Gower, S. T. (2002). Aboveground and belowground biomass and sapwood area allometric equations for six boreal tree species of northern Manitoba. Canadian Journal of Forest Research, 32, 1441–1450.

Bond-Lamberty, B., Wang, C., & Gower, S. T. (2004). Net primary production and net ecosystem production of a boreal black spruce wildfire chronosequence. Global Change Biology, 10, 473–487.

Bovard, B. D., Curtis, P. S., Vogel, C. S., Su, H. B., & Schmid, H. P. (2005). Environmental controls on sap flow in a northern hardwood forest. Tree Physiology, 25, 31–38.

Brandt, J. P., Flannigan, M. D., Maynard, D. G., Thompson, I. D., & Volney, W. J. A. (2013). An introduction to Canada's boreal zone: ecosystem processes, health, sustainability, and environmental issues. Environmental Reviews, 21, 207–226.

Braverman, M., & Quinton, W. L. (2016). Hydrological impacts of seismic lines in the wetland-dominated zone of thawing, discontinuous permafrost, Northwest Territories, Canada: Hydrology of Seismic Lines in Discontinuous Permafrost. Hydrological Processes, 30, 2617–2627.

Brinkmann, N., Eugster, W., Zweifel, R., Buchmann, N., & Kahmen, A. (2016). Temperate tree species show identical response in tree water deficit but different sensitivities in sap flow to summer soil drying. Tree Physiology, 36, 1508–1519.

Brown, J., O. J. Ferrians Jr., J. A. Heginbottom, and E. S. Melnikov. (1997). Circum-Arctic map of permafrost and ground-ice conditions. USGS Numbered Series.

Brum, M., J. Gutiérrez López, H. Asbjornsen, J. Licata, T. Pypker, G. Sanchez, and R. S. Oiveira. (2018). ENSO effects on the transpiration of eastern Amazon trees. Philosophical Transactions of the Royal Society B: Biological Sciences 373, 20180085.

Buermann, W., Parida, B., Jung, M., MacDonald, G. M., Tucker, C. J., & Reichstein, M. (2014). Recent shift in Eurasian boreal forest greening response may be associated with warmer and drier summers. Geophysical Research Letters, 41, 1995–2002.

Burgess, S. S., Adams, M. A., Turner, N. C., Beverly, C. R., Ong, C. K., Khan, A. A., & Bleby, T. M. (2001). An improved heat pulse method to measure low and reverse rates of sap flow in woody plants. Tree Physiology, 21, 589–598.

Burnham, K. P., and D. R. Anderson. 2010. Model selection and multimodel inference: a practical information-theoretic approach. 2. ed. Springer, New York, NY.

Burns, R. M., and B. H. Honkala. (1990). Silvics of North America. U.S. Dept. of Agriculture, Forest Service : For sale by the Supt. of Docs., U.S. G.P.O, Washington.

Burns, R. M., Honkala, B. H., & Coordinators T. (1990). Silvics of North America: Volume 1. Conifers. United States Department of Agriculture (USDA), Forest Service, Agriculture Handbook 654. [Online].

Cable, J. M., K. Ogle, W. R. Bolton, L. P. Bentley, V. Romanovsky, H. Iwata, Y. Harazono, and J. Welker. (2014). Permafrost thaw affects boreal deciduous plant transpiration through increased soil water, deeper thaw, and warmer soils. Ecohydrology 7, 982–997.

Callañaupa Gutierrez, S., Segura Cajachagua, H., Saavedra Huanca, M., Flores Rojas, J., Silva Vidal, Y., & Cuxart, J. (2021). Seasonal variability of daily evapotranspiration and energy fluxes in the Central Andes of Peru using eddy covariance techniques and empirical methods. Atmospheric Research, 261, 105760.

Calow, P. (1987). Towards a Definition of Functional Ecology. Functional Ecology, 1, 57–61.

Canadian Agricultural Services Coordinating Committee (CASCC), National Research Council Canada, & Canada (Eds.). (1998). *The Canadian system of soil classification* (3rd ed). Ottawa: NRC Research Press.

Čermák, J., & Nadezhdina, N. (1998). Sapwood as the scaling parameter- defining according to xylem water content or radial pattern of sap flow? Annals of Forest Science, 55, 509–521.

Čermák, J., Kučera, J., & Nadezhdina, N. (2004). Sap flow measurements with some thermodynamic methods, flow integration within trees and scaling up from sample trees to entire forest stands. Trees, 18, 529–546.

Čermák, J., Kucera, J., Bauerle, W. L., Phillips, N., & Hinckley, T. M. (2007). Tree water storage and its diurnal dynamics related to sap flow and changes in stem volume in old-growth Douglas-fir trees. Tree Physiology 27, 181–198.

Chapin, F. S. (1980). The mineral nutrition of wild plants. Annual Review of Ecology and Systematics, 11(1), 233–260.

Chavent, M., Kuentz-Simonet, V., Labenne, A., & Saracco, J. (2014). Multivariate Analysis of Mixed Data: The R Package PCAmixdata.

Choat, B., S. Jansen, T. J. Brodribb, H. Cochard, S. Delzon, R. Bhaskar, S. J. Bucci, T. S. Feild, S. M. Gleason, U. G. Hacke, A. L. Jacobsen, F. Lens, H. Maherali, J. Martínez-Vilalta, S. Mayr, M. Mencuccini, P. J. Mitchell, A. Nardini, J. Pittermann, R. B. Pratt, J. S. Sperry, M. Westoby, I. J. Wright, and A. E. Zanne. (2012). Global convergence in the vulnerability of forests to drought. Nature 491,752–755.

Coenders-Gerrits, A. M. J., van der Ent, R. J., Bogaard, T. A., Wang-Erlandsson, L., Hrachowitz, M., & Savenije, H. H. G. (2014). Uncertainties in transpiration estimates. Nature, 506, E1–E2.

Cook, B. I., J. E. Smerdon, R. Seager, and S. Coats. (2014). Global warming and 21st century drying. Climate Dynamics 43,2607–2627.

Cramer, M. D., Hoffmann, V., & Verboom, G. A. (2008). Nutrient availability moderates transpiration in *Ehrharta calycina*. Oecologia, 179, 1048–1057.

D'Orangeville, L., Duchesne, L., Houle, D., Kneeshaw, D., Côté, B., & Pederson, N. (2016). Northeastern North America as a potential refugium for boreal forests in a warming climate. Science, 352, 1452–1455.

D'Orangeville, L., Houle, D., Duchesne, L., Phillips, R. P., Bergeron, Y., & Kneeshaw, D. (2018). Beneficial effects of climate warming on boreal tree growth may be transitory. J Nature Communications, 9, 3213.

D'Orangeville, L., St-Laurent, M.-H., Boisvert-Marsh, L., Zhang, X., Bastille-Rousseau, G., & Itter, M. (2023). Current Symptoms of Climate Change in Boreal Forest Trees and Wildlife. In M. M. Girona, H. Morin, S. Gauthier, & Y. Bergeron (Eds.), Boreal Forests in the Face of Climate Change. Springer International Publishing, Cham, 747–771.

Dai, A., Zhao, T., & Chen, J. (2018). Climate Change and Drought: a Precipitation and Evaporation Perspective. Current Climate Change Reports, 4, 301–312.

Davies, S. J., I. Abiem, K. Abu Salim, S. Aguilar, D. Allen, A. Alonso, K. Anderson-Teixeira, A. Andrade, G. Arellano, P. S. Ashton, P. J. Baker, M. E. Baker, J. L. Baltzer, Y. Basset, P. Bissiengou, S. Bohlman, N. A. Bourg, W. Y. Brockelman, S. Bunyavejchewin, D. F. R. P. Burslem, M. Cao, D. Cárdenas, L.-W. Chang, C.-H. Chang-Yang, K.-J. Chao, W.-C. Chao, H. Chapman, Y.-Y. Chen, R. A. Chisholm, C. Chu, G. Chuyong, K. Clay, L. S. Comita, R. Condit, S. Cordell, H. S. Dattaraja, A. A. de Oliveira, J. den Ouden, M. Detto, C. Dick, X. Du, Á. Duque, S. Ediriweera, E. C. Ellis, N. L. E. Obiang, S. Esufali, C. E. N. Ewango, E. S. Fernando, J. Filip, G. A. Fischer, R. Foster, T. Giambelluca, C. Giardina, G. S. Gilbert, E. Gonzalez-Akre, I. A. U. N. Gunatilleke, C. V. S. Gunatilleke, Z. Hao, B. C. H. Hau, F. He, H. Ni, R. W. Howe, S. P. Hubbell, A. Huth, F. Inman-Narahari, A. Itoh, D. Janík, P. A. Jansen, M. Jiang, D. J. Johnson, F. A. Jones, M. Kanzaki, D. Kenfack, S. Kiratiprayoon, K. Král, L. Krizel, S. Lao, A. J. Larson, Y. Li, X. Li, C. M. Litton, Y. Liu, S. Liu, S. K. Y. Lum, M. S. Luskin, J. A. Lutz, H. T. Luu, K. Ma, J.-R. Makana, Y. Malhi, A. Martin, C. McCarthy, S. M. McMahon, W. J. McShea, H. Memiaghe, X. Mi, D. Mitre, M. Mohamad, L. Monks, H. C. Muller-Landau, P. M. Musili, J. A. Myers, A. Nathalang, K. M. Ngo, N. Norden, V. Novotny, M. J. O'Brien, D. Orwig, R. Ostertag, K. Papathanassiou, G. G. Parker, R. Pérez, I. Perfecto, R. P. Phillips, N. Pongpattananurak, H. Pretzsch, H. Ren, G. Reynolds, L. J. Rodriguez, S. E. Russo, L. Sack, W. Sang, J. Shue, A. Singh, G.-Z. M. Song, R. Sukumar, I.-F. Sun, H. S. Suresh, N. G. Swenson, S. Tan, S. C. Thomas, D. Thomas, J. Thompson, B. L. Turner, A. Uowolo, M. Uriarte, R. Valencia, J. Vandermeer, A. Vicentini, M. Visser, T. Vrska, X. Wang, X. Wang, G. D. Weiblen, T. J. S. Whitfeld, A. Wolf, S. J. Wright, H. Xu, T. L. Yao, S. L. Yap, W. Ye, M. Yu, M. Zhang, D. Zhu, L. Zhu, J. K. Zimmerman, and D. Zuleta. (2021). ForestGEO: Understanding forest diversity and dynamics through a global observatory network. Biological Conservation 253:108907.

De Swaef, T., De Schepper, V., Vandegehuchte, M. W., & Steppe, K. (2015). Stem diameter variations as a versatile research tool in ecophysiology. Journal of Ecology, 35, 1047–1061.

Dearborn, K. D., and J. L. Baltzer. 2021. Unexpected greening in a boreal permafrost peatland undergoing forest loss is partially attributable to tree species turnover. Global Change Biology:gcb.15608.

Dearborn, K. D., C. A. Wallace, R. Patankar, and J. L. Baltzer. 2021. Permafrost thaw in boreal peatlands is rapidly altering forest community composition. Journal of Ecology 109:1452–1467.

Deslauriers, A., Beaulieu, M., Balducci, L., Giovannelli, A., Gagnon, M. J., & Rossi, S. (2014). Impact of warming and drought on carbon balance related to wood formation in black spruce. Annals of Botany, 114(2), 335–345. https://doi.org/10.1093/aob/mcu111

Detto, M., A. Molini, G. Katul, P. Stoy, S. Palmroth, and D. Baldocchi. (2012). Causality and Persistence in Ecological Systems: A Nonparametric Spectral Granger Causality Approach. The American Naturalist 179, 524–535.

Díaz, S., J. G. Hodgson, K. Thompson, M. Cabido, J. H. C. Cornelissen, A. Jalili, G. Montserrat-Martí, J. P. Grime, F. Zarrinkamar, Y. Asri, S. R. Band, S. Basconcelo, P. Castro-Díez, G. Funes, B. Hamzehee, M. Khoshnevi, N. Pérez-Harguindeguy, M. C. Pérez-Rontomé, F. A. Shirvany, F. Vendramini, S. Yazdani, R. Abbas-Azimi, A. Bogaard, S. Boustani, M. Charles, M. Dehghan, L. de Torres-Espuny, V. Falczuk, J. Guerrero-Campo, A. Hynd, G. Jones, E. Kowsary, F. Kazemi-Saeed, M. Maestro-Martínez, A. Romo-Díez, S. Shaw, B. Siavash, P. Villar-Salvador, and M. R. Zak. (2004). The plant traits that drive ecosystems: Evidence from three continents. Journal of Vegetation Science 15, 295–304.

Díaz, S., J. Kattge, J. H. C. Cornelissen, I. J. Wright, S. Lavorel, S. Dray, B. Reu, M. Kleyer, C. Wirth, I. Colin Prentice, E. Garnier, G. Bönisch, M. Westoby, H. Poorter, P. B. Reich, A. T. Moles, J. Dickie, A. N. Gillison, A. E. Zanne, J. Chave, S. Joseph Wright, S. N. Sheremet'ev, H. Jactel, C. Baraloto, B. Cerabolini, S. Pierce, B. Shipley, D. Kirkup, F. Casanoves, J. S. Joswig, A. Günther, V. Falczuk, N. Rüger, M. D. Mahecha, and L. D. Gorné. (2016). The global spectrum of plant form and function. Nature 529:167–171.

Dietrich, L., Zweifel, R., & Kahmen, A. (2018). Daily stem diameter variations can predict the canopy water status of mature temperate trees. Tree Physiology, 38, 941–952.

Dixon, H. H., & Joly, J. (1894). On the ascent of sap. Proceedings of the Royal Society of London, 57, 3–5.

Drew, D. M., and G. M. Downes. (2009). The use of precision dendrometers in research on daily stem size and wood property variation: A review. Dendrochronologia 27:159–172.

Drew, D. M., Richards, A. E., Downes, G. M., Cook, G. D., & Baker, P. (2011). The development of seasonal tree water deficit in *Callitris intratropica*. Tree Physiology, 31, 953–964.

Drew, M. C. (1997). Oxygen deficiency and root metabolism: Injury and Acclimation Under Hypoxia and Anoxia Annual Review of Plant Physiology and Plant Molecular Biology, 48, 223–250.

Dufour-Tremblay, G., E. Lévesque, and S. Boudreau. (2012). Dynamics at the treeline: differential responses of Picea mariana and Larix laricina to climate change in eastern subarctic Québec. Environmental Research Letters 7,044038.

Dufour-Tremblay, G., Lévesque, E., & Boudreau, S. (2012). Dynamics at the treeline: differential responses of *Picea mariana* and *Larix laricina* to climate change in eastern subarctic Québec. Environmental Research Letters, 7, 044038.

Dulamsuren, C., H. Coners, C. Leuschner, and M. Hauck. (2023). Climatic control of high-resolution stem radius changes in a drought-limited southern boreal forest. Trees.

Dusenge, M. E., S. Madhavji, and D. A. Way. (2020). Contrasting acclimation responses to elevated CO_2 and warming between an evergreen and a deciduous boreal conifer. Global Change Biology 26, 3639–3657.

Dusenge, M. E., Ward, E. J., Warren, J. M., Stinziano, J. R., Wullschleger, S. D., Hanson, P. J., & Way, D. A. (2021). Warming induces divergent stomatal dynamics in co-occurring boreal trees. Global Change Biology, 27, 3079–3094.

Ecosystem Classification Group. 2008. Ecological regions of the Northwest Territories, Taiga Shield. Page (Northwest Territories, Ed.). Dept. of Environment and Natural Resources, Government. of the Northwest Territories, Yellowknife, N.T.

Ecosystem Classification Group. 2009. Ecological regions of the Northwest Territories: Taiga Plains. Rev. Dept. of Environment and Natural Resources, Govt. of the Northwest Territories, Yellowknife, NWT.

Eliades, M., Bruggeman, A., Djuma, H., & Lubczynski, M. W. (2018). Tree Water Dynamics in a Semi-Arid, *Pinus brutia* Forest. Water, 10, 1039.

Elliott-Fisk, D. (2000). The taiga and boreal forest. In North American Terrestrial Vegetation, edited by M. G. Barbour and W. D. Billings. Cambridge University Press.

Evans, C., DeSotle, R., Mattilio, C., Yankowsky, E., Chenaille, A.-A., & Whiston, A. (2016). A Fine-scale Examination of *Larix laricina* and *Picea mariana Abundances* along Abiotic Gradients in an Adirondack Peatland. Northeastern Naturalist, 23, 420–433.

Evans, J. R. (1989). Photosynthesis and nitrogen relationships in leaves of C3 plants. Oecologia, 78, 9–19.

Ewers, B. E., and R. Oren. (2000). Analyses of assumptions and errors in the calculation of stomatal conductance from sap flux measurements. Tree Physiology 20, 579–589.

Ewers, B. E., Gower, S. T., Bond-Lamberty, B., & Wang, C. K. (2005). Effects of stand age and tree species on canopy transpiration and average stomatal conductance of boreal forests. Journal of Ecology, 28, 660–678.

Ewers, B. E., R. Oren, and J. S. Sperry. (2000). Influence of nutrient versus water supply on hydraulic architecture and water balance in *Pinus taeda*. Plant, Cell & Environment 23, 1055–1066.

Farnè, M., and A. Montanari. (2022). A Bootstrap Method to Test Granger-Causality in the Frequency Domain. Computational Economics 59, 935–966.

Farquhar, G. D., Hubick, K. T., Condon, A. G., & Richards, R. A. (1989). Carbon isotope fractionation and plant water-use efficiency. In Stable Isotopes in Ecological Research, edited by P. W. Rundel, J. R. Ehleringer, and K. A. Nagy. Springer New York, New York, NY, 21–40.

Fatichi, S., & Pappas, C. (2017). Constrained variability of modeled T: ET ratio across biomes. Geophysical Research Letters, 44, 6795–6803.

Fatichi, S., Pappas, C., & Ivanov, V. Y. (2016). Modeling plant-water interactions: an ecohydrological overview from the cell to the global scale. Wiley Interdisciplinary Reviews: Water, 3, 327–368.

Fiora, A., & Cescatti, A. (2006). Diurnal and seasonal variability in radial distribution of sap flux density: implications for estimating stand transpiration. Tree Physiology, 26, 1217–1225.

Fisher, J. B., Whittaker, R. J., & Malhi, Y. (2011). ET come home: potential evapotranspiration in geographical ecology. Global Ecology and Biogeography, 20, 1–18.

Ford, C. R., Goranson, C. E., Mitchell, R. J., Will, R. E., & Teskey, R. O. (2005). Modeling canopy transpiration using time series analysis: A case study illustrating the effect of soil moisture deficit on *Pinus taeda*. Journal of Ecology, 130, 163–175.

Ford, C. R., Hubbard, R. M., Kloeppel, B. D., & Vose, J. M. (2007). A comparison of sap flux-based evapotranspiration estimates with catchment-scale water balance. Agricultural and Forest Meteorology, 145, 176–185.

Forrester, D. I. (2015). Transpiration and water-use efficiency in mixed-species forests versus monocultures: effects of tree size, stand density and season. Tree Physiology, 35, 289–304.

Foster, A. C., J. A. Wang, G. V. Frost, S. J. Davidson, E. Hoy, K. W. Turner, O. Sonnentag, H. Epstein, L. T. Berner, A. H. Armstrong, M. Kang, B. M. Rogers, E. Campbell, K. R. Miner, K. M. Orndahl, L. L. Bourgeau-Chavez, D. A. Lutz, N. French, D. Chen, J. Du, T. A. Shestakova, J. K. Shuman, K. Tape, A.-M. Virkkala, C. Potter, and S. Goetz. (2022). Disturbances in North American boreal forest and Arctic tundra: impacts, interactions, and responses. Environmental Research Letters 17,113001.

Fowler D.P., Park, Y.S., and Loo-Dinkins, J. (1992). Larix Laricina—Silvics and Genetics. In McDonald, K. J., Schmidt, W. C., & Intermountain Research Station (Ogden, Utah). (1995). Ecology and management of larix forests : a look ahead : proceedings of an international symposium, Whitefish, Montana, U.S.A. October 5-9, 1992 /. Ogden, UT : U.S. Dept. of Agriculture, Forest Service, Intermountain Research Station,. https://doi.org/10.5962/bhl.title.109332

Garnier, E., & Berger, A. (1986). Effect of water stress on stem diameter changes of peach trees growing in the field. The Journal of Applied Ecology, 23, 193.

Garon-Labrecque, M.-È., Léveillé-Bourret, É., Higgins, K., & Sonnentag, O. (2016). Additions to the boreal flora of the Northwest Territories with a preliminary vascular flora of Scotty Creek. The Canadian Field-Naturalist, 129, 349.

Gauthier, S., Bernier, P., Kuuluvainen, T., Shvidenko, A. Z., & Schepaschenko, D. G. (2015). Boreal forest health and global change. Science, 349, 819–822.

Ghimire, C. P., H. J. (Ilja) Van Meerveld, B. W. Zwartendijk, L. A. Bruijnzeel, M. Ravelona, J. Lahitiana, and M. W. Lubczynski. (2022). Vapour pressure deficit and solar radiation are the major drivers of transpiration in montane tropical secondary forests in eastern Madagascar. Agricultural and Forest Meteorology 326,109159.

Giardina, F., P. Gentine, A. G. Konings, S. I. Seneviratne, and B. D. Stocker. (2023). Diagnosing evapotranspiration responses to water deficit across biomes using deep learning. New Phytologist. :nph.19197.

Gibert, A., Gray, E. F., Westoby, M., Wright, I. J., & Falster, D. S. (2016). On the link between functional traits and growth rate: meta-analysis shows effects change with plant size. Journal of Ecology, 104, 1488–1503.

Gibson, C., K. Cottenie, T. Gingras-Hill, S. V. Kokelj, J. L. Baltzer, L. Chasmer, and M. R. Turetsky. (2021). Mapping and understanding the vulnerability of northern peatlands to permafrost thaw at scales relevant to community adaptation planning. Environmental Research Letters 16, 055022.

Girardin, M. P., Hogg, E. H., Bernier, P. Y., Kurz, W. A., Guo, X. J., & Cyr, G. (2016b). Negative impacts of high temperatures on growth of black spruce forests intensify with the anticipated climate warming. Global Change Biology, 22, 627–643.

Girardin, M. P., O. Bouriaud, E. H. Hogg, W. Kurz, N. E. Zimmermann, J. M. Metsaranta, R. de Jong, D. C. Frank, J. Esper, U. Büntgen, X. J. Guo, and J. Bhatti. (2016). No growth stimulation of Canada's boreal forest under half-century of combined warming and CO_2 fertilization. Proceedings of the National Academy of Sciences 113:E8406–E8414.

Girardin, M. P., X. J. Guo, J. Metsaranta, D. Gervais, E. Campbell, A. Arsenault, M. Isaac-Renton, J. E. Harvey, J. Bhatti, and E. H. Hogg. (2021). A national tree-ring data repository for Canadian forests (CFS-TRenD): structure, synthesis, and applications. Environmental Reviews 29, 225–241.

Girden, E. R., and R. Kabacoff. (2011). Evaluating research articles from start to finish. 3rd ed. SAGE, London.

Göbel, L., Coners, H., Hertel, D., Willinghöfer, S., & Leuschner, C. (2019). The Role of Low Soil Temperature for Photosynthesis and Stomatal Conductance of Three Graminoids From Different Elevations. Frontiers in Plant Science, 10.

Gower, S. T., and J. H. Richards. (1990). Larches: Deciduous Conifers in an Evergreen World. BioScience 40, 818–826.

Gower, S. T., Kloeppel B. D., and Reich, P.B. (1992). Carbon, Nitrogen, and Water Use by Larches and Co-occurring Evergreen Conifers. In McDonald, K. J., Schmidt, W. C., & Intermountain Research Station (Ogden, Utah). (1995). Ecology and management of larix forests : a look ahead : proceedings of an international symposium, Whitefish, Montana, U.S.A. October 5-9, 1992 /. Ogden, UT : U.S. Dept. of Agriculture, Forest Service, Intermountain Research Station,. https://doi.org/10.5962/bhl.title.109332

Gower, S. T., Vogel, J. G., Norman, J. M., Kucharik, C. J., Steele, S. J., & Stow, T. K. (1997). Carbon distribution and aboveground net primary production in aspen, jack pine, and black spruce stands in Saskatchewan and Manitoba, Canada. Journal of Geophysical Research: Atmospheres, 102, 29029–29041.

Granger, C. W. J. (1969). Investigating Causal Relations by Econometric Models and Cross-spectral Methods. Econometrica 37, 424.

Granger, C. W. J. (1988). Some recent development in a concept of causality. Journal of Econometrics 39, 199–211.

Granier, A. (1987). Evaluation of transpiration in a Douglas-fir stand by means of sap flow measurements. Tree Physiology, 3, 309–320.

Granier, A., Biron, P., Breda, N., Pontailler, J. Y., & Saugier, B. (1996). Transpiration of trees and forest stands: short and long-term monitoring using sapflow methods. Global Change Biology, 2, 265–274.

Gričar, J., & Čufar, K. (2008). Seasonal dynamics of phloem and xylem formation in silver fir and Norway spruce as affected by drought. Russian Journal of Plant Physiology, 55(4), 538–543. https://doi.org/10.1134/S102144370804016X

Gullo, M. A., & Salleo, S. (1988). Different strategies of drought resistance in three Mediterranean sclerophyllous trees growing in the same environmental conditions. New Phytologist, 108, 267–276.

Güney, A., Zweifel, R., Türkan, S., Zimmermann, R., Wachendorf, M., & Güney, C. O. (2020). Drought responses and their effects on radial stem growth of two co-occurring conifer species in the Mediterranean mountain range. Annals of Forest Science, 77, 105.

Gutierrez Lopez, J., Tor-ngern, P., Oren, R., Kozii, N., Laudon, H., & Hasselquist, N. J. (2021). How tree species, tree size, and topographical location influenced tree transpiration in northern boreal forests during the historic 2018 drought. Global Change Biology, 27, 3066–3078.

Hadiwijaya, B., Pepin, S., Isabelle, P. E., & Nadeau, D. F. (2020). The Dynamics of Transpiration to Evapotranspiration Ratio under Wet and Dry Canopy Conditions in a Humid Boreal Forest. Forests, 11, 237.

Hagemeier, M., & Leuschner, C. (2019). Functional Crown Architecture of Five Temperate Broadleaf Tree Species: Vertical Gradients in Leaf Morphology, Leaf Angle, and Leaf Area Density. Forests, 10(3), 265. https://doi.org/10.3390/f10030265

Hämäläinen, A., Runnel, K., Mikusiński, G., Himelbrant, D., Fenton, N. J., & Lõhmus, P. (2023). Living Trees and Biodiversity Boreal Forests in the Face of Climate Change. Advances in Global Change Research, 74, 145–166.

Harmon, R. E., H. R. Barnard, F. D. Day-Lewis, D. Mao, and K. Singha. (2021). Exploring Environmental Factors That Drive Diel Variations in Tree Water Storage Using Wavelet Analysis. Frontiers in Water 3, 682285.

Harrison, J. L., A. B. Reinmann, A. S. Maloney, N. Phillips, S. M. Juice, A. J. Webster, and P. H. Templer. (2020). Transpiration of Dominant Tree Species Varies in Response to Projected Changes in Climate: Implications for Composition and Water Balance of Temperate Forest Ecosystems. Ecosystems 23, 1598–1613.

Hatala, J. A., M. Detto, and D. D. Baldocchi. (2012). Gross ecosystem photosynthesis causes a diurnal pattern in methane emission from rice: GEP CAUSES DIURNAL CH_4 FLUX IN RICE. Geophysical Research Letters 39.

Helbig, M., Chasmer, L. E., Kljun, N., Quinton, W. L., Treat, C. C., & Sonnentag, O. (2017). The positive net radiative greenhouse gas forcing of increasing methane emissions from a thawing boreal forest-wetland landscape. Global Change Biology, 23, 2413–2427.

Helbig, M., J. M. Waddington, P. Alekseychik, B. D. Amiro, M. Aurela, A. G. Barr, T. A. Black, P. D. Blanken, S. K. Carey, J. Chen, J. Chi, A. R. Desai, A. Dunn, E. S. Euskirchen, L. B. Flanagan, I. Forbrich, T. Friborg, A. Grelle, S. Harder, M. Heliasz, E. R. Humphreys, H. Ikawa, P.-E. Isabelle, H. Iwata, R. Jassal, M. Korkiakoski, J. Kurbatova, L. Kutzbach, A. Lindroth, M. O. Löfvenius, A. Lohila, I. Mammarella, P. Marsh, T. Maximov, J. R. Melton, P. A. Moore, D. F. Nadeau, E. M. Nicholls, M. B. Nilsson, T. Ohta, M. Peichl, R. M. Petrone, R. Petrov, A. Prokushkin, W. L. Quinton, D. E. Reed, N. T. Roulet, B. R. K. Runkle, O. Sonnentag, I. B. Strachan, P. Taillardat, E.-S. Tuittila, J.-P. Tuovinen, J. Turner, M. Ueyama, A. Varlagin, M. Wilmking, S. C. Wofsy, and V. Zyrianov. (2020). Increasing contribution of peatlands to boreal evapotranspiration in a warming climate. Nature Climate Change 10, 555–560.

Helbig, M., Sonnentag, O., & Pappas, C. (2016a). Permafrost thaw and wildfire: Equally important drivers of boreal tree cover changes in the Taiga Plains, Canada. Geophysical Research Letters, 43, 1598–1606.

Helbig, M., Wischnewski, K., Kljun, N., Chasmer, L. E., Quinton, W. L., Detto, M., & Sonnentag, O. (2016b). Regional atmospheric cooling and wetting effect of permafrost thaw-induced boreal forest loss. Global Change Biology, 22, 4048–4066.

Hermosilla, T., Bastyr, A., Coops, N. C., White, J. C., & Wulder, M. A. (2022). Mapping the presence and distribution of tree species in Canada's forested ecosystems. Remote Sensing of Environment, 282, 113276.

Herzog, K., R. Hasler, and R. Thum. (1995). Diurnal changes in the radius of a subalpine Norway spruce stem: their relation to the sap flow and their use to estimate transpiration. Trees 10.

Hinckley, T. M., & Bruckerhoff, D. N. (1975). The effects of drought on water relations and stem shrinkage of Quercus alba. Can J Bot, 53, 62–72.

Hinckley, T., & Lassoie, J. (1981). Radial growth in conifers and deciduous trees, a comparison. Mitteilungen der forstlichen Bundesversuchsanstalt Wien, 17–56.

Hirons, A. D., and P. A. Thomas. (2017). Applied Tree Biology. John Wiley & Sons, Ltd, Chichester, UK.

Hochberg, U., Rockwell, F. E., Holbrook, N. M., & Cochard, H. (2018). Iso/Anisohydry: A plant–environment interaction rather than a simple hydraulic trait. Trends in Plant Science, 23, 112–120.

Hogg, E. H. (Ted), J. P. Brandt, and M. Michaelian. (2008). Impacts of a regional drought on the productivity, dieback, and biomass of western Canadian aspen forests. Canadian Journal of Forest Research 38, 1373–1384.

Hubbell, S. P. (2005). Neutral theory in community ecology and the hypothesis of functional equivalence. Functional Ecology, 19, 166–172.

Iijima, Y., Ohta, T., Kotani, A., Fedorov, A. N., Kodama, Y., & Maximov, T. C. (2014). Sap flow changes in relation to permafrost degradation under increasing precipitation in an eastern Siberian larch forest. Ecohydrology, 7, 177–187.

Ireson, A. M., A. G. Barr, J. F. Johnstone, S. D. Mamet, G. van der Kamp, C. J. Whitfield, N. L. Michel, R. L. North, C. J. Westbrook, C. DeBeer, K. P. Chun, A. Nazemi, and J. Sagin. (2015).

The changing water cycle: the Boreal Plains ecozone of Western Canada. WIREs Water 2, 505–521.

Islam, M. A., & Macdonald, S. E. (2005). Effects of variable nitrogen fertilization on growth, gas exchange, and biomass partitioning in black spruce and tamarack seedlings. Can J Bot, 83, 1574–1580.

Islam, M. A., Macdonald, S. E., & Zwiazek, J. J. (2003). Responses of black spruce (*Picea mariana*) and tamarack (*Larix laricina*) to flooding and ethylene. Tree Physiology, 23, 545–552.

Jarvis, P. G., & McNaughton, K. G. (1986). Stomatal Control of Transpiration: Scaling Up from Leaf to Region. Advances in Ecological Research, 1–49.

Jarvis, P. G., Massheder, J. M., Hale, S. E., Moncrieff, J. B., Rayment, M., & Scott, S. L. (1997). Seasonal variation of carbon dioxide, water vapor, and energy exchanges of a boreal black spruce forest. Journal of Geophysical Research: Atmospheres, 102, 28953–28966.

Ježík, M., Blaženec, M., Letts, M. G., Ditmarová, Ľ., Sitková, Z., & Střelcová, K. (2015). Assessing seasonal drought stress response in Norway spruce (*Picea abies* (L.) Karst.) by monitoring stem circumference and sap flow. Ecohydrology, 8, 378–386.

Jorgenson, M. T., & Osterkamp, T. E. (2005). Response of boreal ecosystems to varying modes of permafrost degradation. Canadian Journal of Forest Research, 35, 2100–2111.

Kaiser, H. F. (1961). A note on Guttman's lower bound for the number of common factors. British Journal of Statistical Psychology, 14, 1–2.

Kannenberg, S. A., K. A. Novick, M. R. Alexander, J. T. Maxwell, D. J. P. Moore, R. P. Phillips, and W. R. L. Anderegg. (2019). Linking drought legacy effects across scales: From leaves to tree rings to ecosystems. Global Change Biology 25, 2978–2992.

Kassambara, A. (2023). ggpubr: 'ggplot2' Based Publication Ready Plots. R package. https://CRAN.R-project.org/package=ggpubr

Kichenin, E., D. A. Wardle, D. A. Peltzer, C. W. Morse, and G. T. Freschet. (2013). Contrasting effects of plant inter- and intraspecific variation on community-level trait measures along an environmental gradient. Functional Ecology 27, 1254–1261.

King, G., P. Fonti, D. Nievergelt, U. Büntgen, and D. Frank. (2013). Climatic drivers of hourly to yearly tree radius variations along a 6°C natural warming gradient. Agricultural and Forest Meteorology 168, 36–46.

Kloeppel, B. D., Gower, S. T., Vogel, J. G., & Reich, P. B. (2000). Leaf-level resource use for evergreen and deciduous conifers along a resource availability gradient. Functional Ecology, 14(3), 281–292. https://doi.org/10.1046/j.1365-2435.2000.00439.x

Köcher, P., Horna, V., & Leuschner, C. (2013). Stem water storage in five coexisting temperate broad-leaved tree species: significance, temporal dynamics and dependence on tree functional traits. Tree Physiology, 33, 817–832.

Köstner, B. (2001). Evaporation and transpiration from forests in Central Europe- relevance of patch-level studies for spatial scaling. Meteorology and Atmospheric Physics, 76, 69–82.

Kozii, N., K. Haahti, P. Tor-ngern, J. Chi, E. M. Hasselquist, H. Laudon, S. Launiainen, R. Oren, M. Peichl, J. Wallerman, and N. J. Hasselquist. (2020). Partitioning growing season water balance within a forested boreal catchment using sap flux, eddy covariance, and a process-based model. Hydrology and Earth System Sciences 24, 2999–3014.

Kozii, N., K. Haahti, P. Tor-ngern, J. Chi, E. M. Hasselquist, H. Laudon, S. Launiainen, R. Oren, M. Peichl, J. Wallerman, and N. J. Hasselquist. (2020). Partitioning growing season water balance within a forested boreal catchment using sap flux, eddy covariance, and a process-based model. Hydrology and Earth System Sciences 24, 2999–3014.

Krogh, S. A., J. W. Pomeroy, and P. Marsh. (2017). Diagnosis of the hydrology of a small Arctic basin at the tundra-taiga transition using a physically based hydrological model. Journal of Hydrology 550, 685–703.

Kropp, H., Loranty, M., Alexander, H. D., Berner, L. T., Natali, S. M., & Spawn, S. A. (2017). Environmental constraints on transpiration and stomatal conductance in a Siberian Arctic boreal forest. Journal of Geophysical Research: Biogeosciences, 122, 487–497.

Krůček, M., Král, K., Cushman, K., Missarov, A., & Kellner, J. R. (2020). Supervised Segmentation of Ultra-High-Density Drone Lidar for Large-Area Mapping of Individual Trees. Remote Sensing, 12, 3260.

Kume, T., Tsuruta, K., Komatsu, H., Kumagai, T., Higashi, N., Shinohara, Y., & Otsuki, K. (2010). Effects of sample size on sap flux-based stand-scale transpiration estimates. Tree Physiology, 30, 129–138.

Lambers, H., Chapin, F. S., & Pons, T. L. (2008). Plant physiological ecology, Second edition. Springer, New York, NY.

Landsberg, J., & Waring, R. (2016). Water relations in tree physiology: where to from here? Tree Physiology, Online: https://academic.oup.com/treephys/article-lookup/doi/10.1093/treephys/tpw102

Lê, S., Josse, J., & Husson, F. (2008). FactoMineR: An R Package for Multivariate Analysis. Journal of Statistical Software, 25. Retrieved from http://www.jstatsoft.org/v25/i01/ (Accessed on 9 February 2022).

Leštianska, A., P. Fleischer, K. Merganičová, P. Fleischer, and K. Střelcová. (2020). Influence of Warmer and Drier Environmental Conditions on Species-Specific Stem Circumference Dynamics and Water Status of Conifers in Submontane Zone of Central Slovakia. Water 12, 2945.

Lewis, R. G., & Morton, B. R. (1921). *Native trees of Canada / by B.R. Morton ; with notes on nomenclature and utilization by R.G. Lewis.* Ottawa : Dept. of the Interior, Forestry Branch,. https://doi.org/10.5962/bhl.title.17808

Li, H., F. Huang, X. Hong, and P. Wang. (2022). Evaluating Satellite-Observed Ecosystem Function Changes and the Interaction with Drought in Songnen Plain, Northeast China. Remote Sensing 14, 5887.

Lieffers, V. J., & Rothwell, R. L. (1987). Rooting of peatland black spruce and tamarack in relation to depth of the water table. Canadian Journal of Botany, 65, 817–821.

Liu, J., Cheng, F., Munger, W., Jiang, P., Whitby, T. G., Chen, S., Ji, W., & Man, X. (2020). Precipitation extremes influence patterns and partitioning of evapotranspiration and transpiration in a deciduous boreal larch forest. Agricultural and Forest Meteorology, 287, 107936.

Liu, Q., C. Peng, R. Schneider, D. Cyr, N. G. McDowell, and D. Kneeshaw. (2023). Drought-induced increase in tree mortality and corresponding decrease in the carbon sink capacity of Canada's boreal forests from 1970 to 2020. Global Change Biology 29, 2274–2285.

Lloyd, A. H., and A. G. Bunn. (2007). Responses of the circumpolar boreal forest to 20th century climate variability. Environmental Research Letters 2, 045013.

Lockhart, J. A. (1965). An analysis of irreversible plant cell elongation. Journal of Theoretical Biology, 8, 264–275.

Looker, N., Martin, J., Hoylman, Z., Jencso, K., & Hu, J. (2018). Diurnal and seasonal coupling of conifer sap flow and vapor pressure deficit across topoclimatic gradients in a subalpine catchment. Ecohydrology, 11, e1994.

Ma, S., Baldocchi, D. D., Mambelli, S., & Dawson, T. E. (2011). Are temporal variations of leaf traits responsible for seasonal and inter-annual variability in ecosystem CO 2 exchange? Functional Ecology, 25(1), 258–270. https://doi.org/10.1111/j.1365-2435.2010.01779.x

Macdonald, S. E., & Lieffers, V. J. (1990). Photosynthesis, water relations, and foliar nitrogen of *Picea mariana* and *Larix laricina* from drained and undrained peatlands. Canadian Journal of Forest Research, 20, 995–1000.

Mackay, D. S., Ewers, B. E., Loranty, M. M., & Kruger, E. L. (2010). On the representativeness of plot size and location for scaling transpiration from trees to a stand. Journal of Geophysical Research: Biogeosciences, 115.

Maillet, J., Nehemy, M. F., Mood, B., Pappas, C., Bonsal, B., & Laroque, C. P. (2022). A multi-scale dendroclimatological analysis of four common species in the southern Canadian boreal forest. Dendrochronologia, 72, 125936.

Maire, V., I. J. Wright, I. C. Prentice, N. H. Batjes, R. Bhaskar, P. M. van Bodegom, W. K. Cornwell, D. Ellsworth, Ü. Niinemets, A. Ordonez, P. B. Reich, and L. S. Santiago. (2015). Global effects of soil and climate on leaf photosynthetic traits and rates. Global Ecology and Biogeography 24, 706–717.

Mamet, S. D., Brown, C. D., Trant, A. J., & Laroque, C. P. (2019). Shifting global *Larix* distributions: Northern expansion and southern retraction as species respond to changing climate. Journal of Biogeography, 46, 30–44.

Marchand, W., M. P. Girardin, H. Hartmann, M. Lévesque, S. Gauthier, and Y. Bergeron. (2021). Contrasting life-history traits of black spruce and jack pine influence their physiological response to drought and growth recovery in northeastern boreal Canada. Science of The Total Environment 794, 148514.

Marshall, D. C. (1958). Measurement of sap flow in conifers by heat transport. Plant Physiology, 33, 385–396.

Martin, T. A., Brown, K. J., Kučera, J., Meinzer, F. C., Sprugel, D. G., & Hinckley, T. M. (2001). Control of transpiration in a 220-year-old *Abies amabilis* forest. Forest Ecology and Management, 152, 211–224.

Martínez-Sancho, E., Vásconez Navas, L. K., Seidel, H., Dorado-Liñán, I., & Menzel, A. (2017). Responses of Contrasting Tree Functional Types to Air Warming and Drought. Forests, 8, 450.

Martínez-Vilalta, J., Mencuccini, M., Vayreda, J., & Retana, J. (2010). Interspecific variation in functional traits, not climatic differences among species ranges, determines demographic rates across 44 temperate and Mediterranean tree species. Journal of Ecology, 98, 1462–1475.

Martínez-Vilalta, J., Sala, A., & Piñol, J. (2004). The hydraulic architecture of *Pinaceae* – a review. Plant Ecology, 171, 3–13.

Martínez-Vilalta, J., & Garcia-Forner, N. (2017). Water potential regulation, stomatal behaviour, and hydraulic transport under drought: deconstructing the iso/anisohydric concept. Plant, Cell & Environment, 40, 962–976.

Matheny, A. M., Bohrer, G., Vogel, C. S., Morin, T. H., He, L., Frasson, R. P. de M., ... Curtis, P. S. (2014). Species-specific transpiration responses to intermediate disturbance in a northern hardwood forest: Transpiration response to disturbance. Journal of Geophysical Research: Biogeosciences, 119, 2292–2311.

Matheny, A. M., R. P. Fiorella, G. Bohrer, C. J. Poulsen, T. H. Morin, A. Wunderlich, C. S. Vogel, and P. S. Curtis. (2017). Contrasting strategies of hydraulic control in two codominant temperate tree species. Ecohydrology 10.

Maynard, D. S., L. Bialic-Murphy, C. M. Zohner, C. Averill, J. van den Hoogen, H. Ma, L. Mo, G. R. Smith, A. T. R. Acosta, I. Aubin, E. Berenguer, C. C. F. Boonman, J. A. Catford, B. E. L. Cerabolini, A. S. Dias, A. González-Melo, P. Hietz, C. H. Lusk, A. S. Mori, Ü. Niinemets, V. D. Pillar, B. X. Pinho, J. A. Rosell, F. M. Schurr, S. N. Sheremetev, A. C. da Silva, Ê. Sosinski, P. M.

van Bodegom, E. Weiher, G. Bönisch, J. Kattge, and T. W. Crowther. (2022). Global relationships in tree functional traits. Nature Communications 13, 3185.

McCullough, D. G., Werner, R. A., & Neumann, D. (1998). Fire and insects in northern and boreal forest ecosystems of North America. Annual Review of Entomology, 43, 107–127.

McDowell, N., Barnard, H., Bond, B., Hinckley, T., Hubbard, R., Ishii, H., Köstner, B., Magnani, F., Marshall, J., Meinzer, F., Phillips, N., Ryan, M., & Whitehead, D. (2002). The relationship between tree height and leaf area: sapwood area ratio. Oecologia, 132, 12–20.

McDowell, N., W. T. Pockman, C. D. Allen, D. D. Breshears, N. Cobb, T. Kolb, J. Plaut, J. Sperry, A. West, D. G. Williams, and E. A. Yepez. (2008). Mechanisms of plant survival and mortality during drought: why do some plants survive while others succumb to drought? New Phytologist 178, 719–739.

Meinzer, F. C., Bond, B. J., Warren, J. M., & Woodruff, D. R. (2005). Does water transport scale universally with tree size? Functional Ecology, 19, 558–565.

Meinzer, F. C., James, S. A., & Goldstein, G. (2004). Dynamics of transpiration, sap flow, and use of stored water in tropical forest canopy trees. Tree Physiology, 24, 901–909.

Mészáros, I., P. Kanalas, A. Fenyvesi, J. Kis, B. Nyitrai, E. Sz, V. Oláh, Z. Demeter, Á. Lakatos, and I. Ander. (2011). Diurnal and Seasonal Changes in Stem Radius Increment and Sap Flow Density Indicate Different Responses of Two Co-existing Oak Species to Drought Stress:12.

Mirabel, A., Girardin, M. P., Metsaranta, J., Way, D., & Reich, P. B. (2023). Increasing atmospheric dryness reduces boreal forest tree growth. In Review. Retrieved from https://www.researchsquare.com/article/rs-2611306/v1 (Accessed on 28 March 2023).

Mirabel, A., M. P. Girardin, J. Metsaranta, E. M. Campbell, A. Arsenault, P. B. Reich, and D. Way. (2022). New tree-ring data from Canadian boreal and hemi-boreal forests provide insight for

improving the climate sensitivity of terrestrial biosphere models. Science of The Total Environment 851, 158062.

Monteith, J. L. (1981). Evaporation and surface temperature. Quarterly Journal of the Royal Meteorological Society, 107, 1–27.

Moore, G. W., Bond, B. J., Jones, J. A., Phillips, N., & Meinzer, F. C. (2004). Structural and compositional controls on transpiration in 40- and 450-year-old riparian forests in western Oregon, USA. Tree Physiology, 24, 481–491.

Morse, P. D., Wolfe, S. A., Kokelj, S. V., & Gaanderse, A. J. R. (2016). The occurrence and thermal disequilibrium state of permafrost in forest ecotopes of the Great Slave Region, Northwest Territories, Canada. Permafrost and Periglacial Processes, 27, 145–162.

Nehemy, M. F., Benettin, P., Asadollahi, M., Pratt, D., Rinaldo, A., & McDonnell, J. J. (2021). Tree water deficit and dynamic source water partitioning. Hydrological Processes, 35.

Nehemy, M. F., Maillet, J., Perron, N., Pappas, C., Sonnentag, O., Baltzer, J. L., Laroque, C. P., & McDonnell, J. J. (2022). Snowmelt Water Use at Transpiration Onset: Phenology, Isotope Tracing, and Tree Water Transit Time. Water Resources Research, 58.

Nehemy, M. F., Pierrat, Z., Maillet, J., Richardson, A. D., Stutz, J., Johnson, B., Helgason, W., Barr, A. G., Laroque, C. P., & McDonnell, J. J. (2023). Phenological assessment of transpiration: The stem-temp approach for determining start and end of season. Agricultural and Forest Meteorology, 331, 109319.

Niinemets, Ü. (2001). Global-scale climatic controls of leaf dry mass per area, density, and thickness in trees and shrubs. Ecology, 82, 453–469.

Niinemets, Ü. (2010). A review of light interception in plant stands from leaf to canopy in different plant functional types and in species with varying shade tolerance. Ecological Research, 25, 693–714.

Novák, V. (2012). Evapotranspiration in the Soil-Plant-Atmosphere System. Dordrecht: Springer Netherlands. Online: http://link.springer.com/10.1007/978-94-007-3840-9

Oberhuber, W., Hammerle, A., & Kofler, W. (2015a). Tree water status and growth of saplings and mature Norway spruce (*Picea abies*) at a dry distribution limit. Frontiers in Plant Science, 6.

Oberhuber, W., Kofler, W., Schuster, R., & Wieser, G. (2015b). Environmental effects on stem water deficit in co-occurring conifers exposed to soil dryness. International Journal of Biometeorology, 59, 417–426.

Obu, J., Westermann, S., Bartsch, A., Berdnikov, N., Christiansen, H. H., Dashtseren, A., Delaloye, R., Elberling, B., Etzelmüller, B., Kholodov, A., Khomutov, A., Kääb, A., Leibman, M. O., Lewkowicz, A. G., Panda, S. K., Romanovsky, V., Way, R. G., Westergaard-Nielsen, A., Wu, T., Yamkhin, J., & Zou, D. (2019). Northern Hemisphere permafrost map based on TTOP modelling for 2000–2016 at 1 km² scale. Earth-Science Reviews, 193, 299–316.

Oishi, A. C., Oren, R., & Stoy, P. C. (2008). Estimating components of forest evapotranspiration: A footprint approach for scaling sap flux measurements. Agricultural and Forest Meteorology, 148, 1719–1732.

Oishi, A. C., R. Oren, and P. C. Stoy. (2008). Estimating components of forest evapotranspiration: A footprint approach for scaling sap flux measurements. Agricultural and Forest Meteorology 148, 1719–1732.

Oksanen, J., Kindt, R., Legendre, P., O'Hara, B., Simpson, G. L., Solymos, P., Stevens, M. H. H. & Wagner, H. (2008). vegan: Community Ecology Package (R package version 1.15-1).

Oliver, T. H., M. S. Heard, N. J. B. Isaac, D. B. Roy, D. Procter, F. Eigenbrod, R. Freckleton, A. Hector, C. D. L. Orme, O. L. Petchey, V. Proença, D. Raffaelli, K. B. Suttle, G. M. Mace, B. Martín-López, B. A. Woodcock, and J. M. Bullock. (2015). Biodiversity and Resilience of Ecosystem Functions. Trends in Ecology & Evolution 30,673–684.

Onoda, Y., M. Westoby, P. B. Adler, A. M. F. Choong, F. J. Clissold, J. H. C. Cornelissen, S. Díaz, N. J. Dominy, A. Elgart, L. Enrico, P. V. A. Fine, J. J. Howard, A. Jalili, K. Kitajima, H. Kurokawa, C. McArthur, P. W. Lucas, L. Markesteijn, N. Pérez-Harguindeguy, L. Poorter, L. Richards, L. S. Santiago, E. E. Sosinski, S. A. Van Bael, D. I. Warton, I. J. Wright, S. Joseph Wright, and N. Yamashita. (2011). Global patterns of leaf mechanical properties: Global patterns of leaf mechanical properties. Ecology Letters 14, 301–312.

Oren, R., & Pataki, D. E. (2001). Transpiration in response to variation in microclimate and soil moisture in southeastern deciduous forests. Oecologia, 127, 549–559.

Oren, R., Phillips, N., Ewers, B. E., Pataki, D. E., & Megonigal, J. P. (1999). Sap-flux-scaled transpiration responses to light, vapor pressure deficit, and leaf area reduction in a flooded Taxodium distichum forest. Tree Physiology, 19, 337–347

Oren, R., Phillips, N., Katul, G., Ewers, B. E., & Pataki, D. E. (1998). Scaling xylem sap flux and soil water balance and calculating variance: a method for partitioning water flux in forests. Annales des Sciences Forestières, 55, 191–216.

Osnas, J. L. D., M. Katabuchi, K. Kitajima, S. J. Wright, P. B. Reich, S. A. V. Bael, N. J. B. Kraft, M. J. Samaniego, S. W. Pacala, and J. W. Lichstein. (2018). Divergent drivers of leaf trait variation within species, among species, and among functional groups. Proceedings of the National Academy of Sciences 115, 5480–5485.

Osterkamp, T. E., Viereck, L., Shur, Y., Jorgenson, M. T., Racine, C., Doyle, A., & Boone, R. D. (2000). Observations of thermokarst and its impact on Boreal Forests in Alaska, U.S.A. Arctic, Antarctic, and Alpine Research, 32, 303–315.

Pan, J., Sharif, R., Xu, X., & Chen, X. (2021). Mechanisms of Waterlogging Tolerance in Plants: Research Progress and Prospects. Frontiers in Plant Science, 11, 627331. https://doi.org/10.3389/fpls.2020.627331

Pappas, C., A. M. Matheny, J. L. Baltzer, A. G. Barr, T. A. Black, G. Bohrer, M. Detto, J. Maillet, A. Roy, O. Sonnentag, and J. Stephens. (2018). Boreal tree hydrodynamics: asynchronous, diverging, yet complementary. Tree Physiology.

Patankar, R., Quinton, W. L., Hayashi, M., & Baltzer, J. L. (2015). Sap flow responses to seasonal thaw and permafrost degradation in a subarctic boreal peatland. Trees, 29, 129–142.

Peguero-Pina, J. J., Vilagrosa, A., Alonso-Forn, D., Ferrio, J. P., Sancho-Knapik, D., & Gil-Pelegrín, E. (2020). Living in Drylands: Functional adaptations of trees and shrubs to cope with high temperatures and water scarcity. Forests, 11, 1028.

Peng, C., Z. Ma, X. Lei, Q. Zhu, H. Chen, W. Wang, S. Liu, W. Li, X. Fang, and X. Zhou. (2011). A drought-induced pervasive increase in tree mortality across Canada's boreal forests. Nature Climate Change 1, 467–471.

Pepin, S., Plamondon, A. P., & Britel, A. (2002). Water relations of black spruce trees on a peatland during wet and dry years. Wetlands, 22, 225–233.

Pérez-Harguindeguy, N., Díaz, S., Garnier, E., Lavorel, S., Poorter, H., Jaureguiberry, P., *et al*. (2013). New handbook for standardised measurement of plant functional traits worldwide. Australian Journal of Botany, 61(3), 167. https://doi.org/10.1071/BT12225

Perron, N., J. L. Baltzer, and O. Sonnentag. (2023). Spatial and temporal variation in forest transpiration across a forested boreal peatland complex. Hydrological Processes 37.

Pierrat, Z., M. F. Nehemy, A. Roy, T. Magney, N. C. Parazoo, C. P. Laroque, C. Pappas, O. Sonnentag, K. Grossmann, D. R. Bowling, U. Seibt, A. Ramirez, B. Johnson, W. Helgason, A. Barr, and J. Stutz. (2021). Tower-Based Remote Sensing Reveals Mechanisms Behind a Two-phased Spring Transition in a Mixed-Species Boreal Forest. Journal of Geophysical Research: Biogeosciences 126.

Plomion, C., Leprovost, G., & Stokes, A. (2001). Wood Formation in Trees. Plant Physiology, 127(4), 1513–1523. https://doi.org/10.1104/pp.010816

Poorter, L., S. J. Wright, H. Paz, D. D. Ackerly, R. Condit, G. Ibarra-Manríquez, K. E. Harms, J. C. Licona, M. Martínez-Ramos, S. J. Mazer, H. C. Muller-Landau, M. Peña-Claros, C. O. Webb, and I. J. Wright. (2008). Are functional traits good predictors of demographic rates? Evidence from five neotropical forests. Ecology, 89, 1908–1920.

Poyatos, R., V. Granda, R. Molowny-Horas, M. Mencuccini, K. Steppe, and J. Martínez-Vilalta. (2016). SAPFLUXNET: towards a global database of sap flow measurements. Tree Physiology 36, 1449–1455.

Poyatos, R., V. Granda, V. Flo, M. A. Adams, B. Adorján, D. Aguadé, M. P. M. Aidar, S. Allen, M. S. Alvarado-Barrientos, K. J. Anderson-Teixeira, L. M. Aparecido, M. A. Arain, I. Aranda, H. Asbjornsen, R. Baxter, E. Beamesderfer, Z. C. Berry, D. Berveiller, B. Blakely, J. Boggs, G. Bohrer, P. V. Bolstad, D. Bonal, R. Bracho, P. Brito, J. Brodeur, F. Casanoves, J. Chave, H. Chen, C. Cisneros, K. Clark, E. Cremonese, H. Dang, J. S. David, T. S. David, N. Delpierre, A. R. Desai, F. C. Do, M. Dohnal, J.-C. Domec, S. Dzikiti, C. Edgar, R. Eichstaedt, T. S. El-Madany, J. Elbers, C. B. Eller, E. S. Euskirchen, B. Ewers, P. Fonti, A. Forner, D. I. Forrester, H. C. Freitas, M. Galvagno, O. Garcia-Tejera, C. P. Ghimire, T. E. Gimeno, J. Grace, A. Granier, A. Griebel, Y. Guangyu, M. B. Gush, P. J. Hanson, N. J. Hasselquist, I. Heinrich, V. Hernandez-Santana, V. Herrmann, T. Hölttä, F. Holwerda, J. Irvine, S. Isarangkool Na Ayutthaya, P. G. Jarvis, H. Jochheim, C. A. Joly, J. Kaplick, H. S. Kim, L. Klemedtsson, H. Kropp, F. Lagergren, P. Lane, P. Lang, A. Lapenas, V. Lechuga, M. Lee, C. Leuschner, J.-M. Limousin, J. C. Linares, M.-L. Linderson, A. Lindroth, P. Llorens, Á. López-Bernal, M. M. Loranty, D. Lüttschwager, C. Macinnis-Ng, I. Maréchaux, T. A. Martin, A. Matheny, N. McDowell, S. McMahon, P. Meir, I. Mészáros, M. Migliavacca, P. Mitchell, M. Mölder, L. Montagnani, G. W. Moore, R. Nakada, F. Niu, R. H. Nolan, R. Norby, K. Novick, W. Oberhuber, N. Obojes, A. C. Oishi, R. S. Oliveira, R. Oren, J.-M. Ourcival, T. Paljakka, O. Perez-Priego, P. L. Peri, R. L. Peters, S. Pfautsch, W. T. Pockman, Y. Preisler, K. Rascher, G. Robinson, H. Rocha, A. Rocheteau, A. Röll, B. H. P. Rosado, L. Rowland, A. V. Rubtsov, S. Sabaté, Y. Salmon, R. L. Salomón, E. Sánchez-Costa, K. V. R.

Schäfer, B. Schuldt, A. Shashkin, C. Stahl, M. Stojanović, J. C. Suárez, G. Sun, J. Szatniewska, F. Tatarinov, M. Tesař, F. M. Thomas, P. Tor-ngern, J. Urban, F. Valladares, C. van der Tol, I. van Meerveld, A. Varlagin, H. Voigt, J. Warren, C. Werner, W. Werner, G. Wieser, L. Wingate, S. Wullschleger, K. Yi, R. Zweifel, K. Steppe, M. Mencuccini, and J. Martínez-Vilalta. (2020). Global transpiration data from sap flow measurements: the SAPFLUXNET database. Preprint, Biosphere – Biogeosciences.

Prentice, I. C., N. Dong, S. M. Gleason, V. Maire, and I. J. Wright. (2014). Balancing the costs of carbon gain and water transport: testing a new theoretical framework for plant functional ecology. Ecology Letters 17, 82–91.

Price, D. T., R. I. Alfaro, K. J. Brown, M. D. Flannigan, R. A. Fleming, E. H. Hogg, M. P. Girardin, T. Lakusta, M. Johnston, D. W. McKenney, J. H. Pedlar, T. Stratton, R. N. Sturrock, I. D. Thompson, J. A. Trofymow, and L. A. Venier. (2013). Anticipating the consequences of climate change for Canada's boreal forest ecosystems. Environmental Reviews, 21, 322–365.

Quiñonez-Piñón, M. R., & Valeo, C. (2017). Allometry of Sapwood Depth in Five Boreal Trees. Forests, 8, 457.

Quinton, W. L., & Baltzer, J. L. (2013). The active-layer hydrology of a peat plateau with thawing permafrost (Scotty Creek, Canada). Hydrogeology Journal, 21, 201–220.

Quinton, W. L., Hayashi, M., & Chasmer, L. E. (2009). Peatland Hydrology of Discontinuous Permafrost in the Northwest Territories: Overview and Synthesis. Canadian Water Resources Journal, 34, 311–328.

Quinton, W., A. Berg, M. Braverman, O. Carpino, L. Chasmer, R. Connon, J. Craig, É. Devoie, M. Hayashi, K. Haynes, D. Olefeldt, A. Pietroniro, F. Rezanezhad, R. Schincariol, and O. Sonnentag. (2019). A synthesis of three decades of hydrological research at Scotty Creek, NWT, Canada. Hydrology and Earth System Sciences 23, 2015–2039.

R Core Team. (2020). R: A Language and Environment for Statistical Computing. R Foundation for Statistical Computing, Vienna, Austria.

Rantanen, M., A. Yu. Karpechko, A. Lipponen, K. Nordling, O. Hyvärinen, K. Ruosteenoja, T. Vihma, and A. Laaksonen. (2022). The Arctic has warmed nearly four times faster than the globe since 1979. Communications Earth & Environment 3, 168.

Reich, P. B. (2014). The world-wide 'fast–slow' plant economics spectrum: a traits manifesto. Journal of Ecology, 102, 275–301.

Reich, P. B., K. M. Sendall, A. Stefanski, R. L. Rich, S. E. Hobbie, and R. A. Montgomery. (2018). Effects of climate warming on photosynthesis in boreal tree species depend on soil moisture. Nature 562, 263–267.

Reich, P. B., R. Bermudez, R. A. Montgomery, R. L. Rich, K. E. Rice, S. E. Hobbie, and A. Stefanski. (2022). Even modest climate change may lead to major transitions in boreal forests. Nature 608, 540–545.

Reich, P. B., Walters, M. B., & Ellsworth, D. S. (1992). Leaf Life-Span in Relation to Leaf, Plant, and Stand Characteristics among Diverse Ecosystems. Ecological Monographs, 62, 365–392.

Reich, P. B., Walters, M. B., Kloeppel, B. D., & Ellsworth, D. S. (1995). Different photosynthesis-nitrogen relations in deciduous hardwood and evergreen coniferous tree species. Oecologia, 104(1), 24–30. https://doi.org/10.1007/BF00365558

Robinson, A., Lehmann, J., Barriopedro, D., Rahmstorf, S., & Coumou, D. (2021). Increasing heat and rainfall extremes now far outside the historical climate. npj Climate and Atmospheric Science, 4, 45.

Rosas, T., M. Mencuccini, C. Batlles, Í. Regalado, S. Saura-Mas, F. Sterck, and J. Martínez-Vilalta. (2021). Are leaf, stem and hydraulic traits good predictors of individual tree growth? Functional Ecology 35, 2435–2447.

Rosas, T., Mencuccini, M., Barba, J., Cochard, H., Saura-Mas, S., & Martínez-Vilalta, J. (2019). Adjustments and coordination of hydraulic, leaf, and stem traits along a water availability gradient. New Phytologist, 223, 632–646.

Rosch, A., and H. Schmidbauer. (2018). WaveletComp 1.1: A guided tour through the R package.

Ruiz-Pérez, G., and G. Vico. (2020). Effects of Temperature and Water Availability on Northern European Boreal Forests. Frontiers in Forests and Global Change 3:34.

Sabater, A. M., H. C. Ward, T. C. Hill, J. L. Gornall, T. J. Wade, J. G. Evans, A. Prieto-Blanco, M. Disney, G. K. Phoenix, M. Williams, B. Huntley, R. Baxter, M. Mencuccini, and R. Poyatos. (2020). Transpiration from subarctic deciduous woodlands: Environmental controls and contribution to ecosystem evapotranspiration. Ecohydrology 13.

Sack, L., & Holbrook, N. M. (2006). Leaf Hydraulics. Annual Review of Plant Biology, 57, 361–381.

Salomón, R. L., R. L. Peters, R. Zweifel, U. G. W. Sass-Klaassen, A. I. Stegehuis, M. Smiljanic, R. Poyatos, F. Babst, E. Cienciala, P. Fonti, B. J. W. Lerink, M. Lindner, J. Martinez-Vilalta, M. Mencuccini, G.-J. Nabuurs, E. van der Maaten, G. von Arx, A. Bär, L. Akhmetzyanov, D. Balanzategui, M. Bellan, J. Bendix, D. Berveiller, M. Blaženec, V. Čada, V. Carraro, S. Cecchini, T. Chan, M. Conedera, N. Delpierre, S. Delzon, Ľ. Ditmarová, J. Dolezal, E. Dufrêne, J. Edvardsson, S. Ehekircher, A. Forner, J. Frouz, A. Ganthaler, V. Gryc, A. Güney, I. Heinrich, R. Hentschel, P. Janda, M. Ježík, H.-P. Kahle, S. Knüsel, J. Krejza, Ł. Kuberski, J. Kučera, F. Lebourgeois, M. Mikoláš, R. Matula, S. Mayr, W. Oberhuber, N. Obojes, B. Osborne, T. Paljakka, R. Plichta, I. Rabbel, C. B. K. Rathgeber, Y. Salmon, M. Saunders, T. Scharnweber, Z. Sitková, D. F. Stangler, K. Stereńczak, M. Stojanović, K. Střelcová, J. Světlík, M. Svoboda, B. Tobin, V. Trotsiuk, J. Urban, F. Valladares, H. Vavrčík, M. Vejpustková, L. Walthert, M. Wilmking, E. Zin, J. Zou, and K. Steppe. (2022). The 2018 European heatwave led to stem dehydration but not to consistent growth reductions in forests. Nature Communications 13, 28.

Salvucci, G. D., J. A. Saleem, and R. Kaufmann. (2002). Investigating soil moisture feedbacks on precipitation with tests of Granger causality. Advances in Water Resources 25, 1305–1312.

Sánchez-Costa, E., Poyatos, R., & Sabaté, S. (2015). Contrasting growth and water use strategies in four co-occurring Mediterranean tree species revealed by concurrent measurements of sap flow and stem diameter variations. Agricultural and Forest Meteorology, 207, 24–37.

Sánchez-Pinillos, M., D'Orangeville, L., Boulanger, Y., Comeau, P., Wang, J., Taylor, A. R., & Kneeshaw, D. (2022). Sequential droughts: A silent trigger of boreal forest mortality. Global Change Biology, 28, 542–556.

Saxe, H., Cannell, M. G. R., Johnsen, Ø., Ryan, M. G., & Vourlitis, G. (2001). Tree and forest functioning in response to global warming. New Phytologist, 149, 369–399.

Schäfer, C., Rötzer, T., Thurm, E. A., Biber, P., Kallenbach, C., & Pretzsch, H. (2019). Growth and tree water deficit of mixed Norway spruce and European beech at different heights in a tree and under heavy drought. Forests, 10, 577.

Schlesinger, W. H., & Jasechko, S. (2014). Transpiration in the global water cycle. Agricultural and Forest Meteorology, 189–190, 115–117.

Schneider, C. A., Rasband, W. S., & Eliceiri, K. W. (2012). NIH Image to ImageJ: 25 years of image analysis. Nature Methods, 9, 671–675.

Scholz, F. C., Bucci, S. J., Goldstein, G., Meinzer, F. C., Franco, A. C., & Miralles-Wilhelm, F. (2008). Temporal dynamics of stem expansion and contraction in savanna trees: withdrawal and recharge of stored water. Tree Physiology, 28, 469–480.

Schulze, E. D. (1986). Carbon Dioxide and Water Vapor Exchange in Response to Drought in the Atmosphere and in the Soil. Annual Review of Plant Physiology, 37, 247–274.

Seibt, U., Rajabi, A., Griffiths, H., & Berry, J. A. (2008). Carbon isotopes and water use efficiency: sense and sensitivity. Oecologia, 155, 441–454.

Seidl, R., D. Thom, M. Kautz, D. Martin-Benito, M. Peltoniemi, G. Vacchiano, J. Wild, D. Ascoli, M. Petr, J. Honkaniemi, M. J. Lexer, V. Trotsiuk, P. Mairota, M. Svoboda, M. Fabrika, T. A. Nagel, and C. P. O. Reyer. (2017). Forest disturbances under climate change. Nature Climate Change 7, 395–402.

Shook, K. (2015). WISKIr: acquires data from a WISKI web server.

Sniderhan, A. E., & Baltzer, J. L. (2016). Growth dynamics of black spruce (*Picea mariana*) in a rapidly thawing discontinuous permafrost peatland. Journal of Geophysical Research: Biogeosciences, 121, 2988–3000.

Sniderhan, A. E., Mamet, S. D., & Baltzer, J. L. (2021). Non-uniform growth dynamics of a dominant boreal tree species (*Picea mariana*) in the face of rapid climate change. Canadian Journal of Forest Research, 51, 565–572.

Spence, C., Hedstrom, N. (2018). Hydrometeorological data from Baker Creek Research Watershed, Northwest Territories, Canada. Earth System Science Data Discussions, 1–24.

Spence, C., N. Hedstrom, S. E. Tank, W. L. Quinton, D. Olefeldt, S. Goodman, and N. Dion. (2020). Hydrological resilience to forest fire in the subarctic Canadian shield. Hydrological Processes 34:4940–4958.

Spence, C., Woo, M. (2002). Hydrology of subarctic Canadian shield: bedrock upland. Journal of Hydrology, 262, 111–127.

Standen, K. M. (2022). Changes in plant community composition, structure, and function in response to permafrost thaw. Theses and Dissertations (Comprehensive), Wilfrid Laurier University.

Standen, K. M., & Baltzer, J. L. (2021). Permafrost condition determines plant community composition and community-level foliar functional traits in a boreal peatland. Ecology and Evolution, 11, 10133–10146.

Steppe, K., D. J. W. De Pauw, R. Lemeur, and P. A. Vanrolleghem. (2006). A mathematical model linking tree sap flow dynamics to daily stem diameter fluctuations and radial stem growth. Tree Physiology 26, 257–273.

Steppe, K., De Pauw, D. J. W., Doody, T. M., & Teskey, R. O. (2010). A comparison of sap flux density using thermal dissipation, heat pulse velocity, and heat field deformation methods. Agricultural and Forest Meteorology, 150, 1046–1056.

Stoy, P. C., T. El-Madany, J. B. Fisher, P. Gentine, T. Gerken, S. P. Good, S. Liu, D. G. Miralles, O. Perez-Priego, T. H. Skaggs, G. Wohlfahrt, R. G. Anderson, M. Jung, W. H. Maes, I. Mammarella, M. Mauder, M. Migliavacca, J. A. Nelson, R. Poyatos, M. Reichstein, R. L. Scott, and S. Wolf. (2019). Reviews and syntheses: Turning the challenges of partitioning ecosystem evaporation and transpiration into opportunities. Biogeosciences Discussions. 1–47.

Sulla-Menashe, D., Woodcock, C. E., & Friedl, M. A. (2018). Canadian boreal forest greening and browning trends: an analysis of biogeographic patterns and the relative roles of disturbance versus climate drivers. Environmental Research Letters, 13, 014007.

Sullivan, P. F., Pattison, R. R., Brownlee, A. H., Cahoon, S. M. P., & Hollingsworth, T. N. (2017). Limited evidence of declining growth among moisture-limited black and white spruce in interior Alaska. Scientific Reports, 7, 15344.

Taggart, R. E., & Cross, A. T. (2009). Global greenhouse to icehouse and back again: The origin and future of the Boreal Forest biome. Global and Planetary Change, 65, 115–121.

Taiz, L., & Zeiger, E. (2002). Plant physiology. 3rd ed. Sinauer Associates, Sunderland, Mass.

Tang, J., Bolstad, P. V., Ewers, B. E., Desai, A. R., Davis, K. J., & Carey, E. V. (2006). Sap flux–upscaled canopy transpiration, stomatal conductance, and water use efficiency in an old growth forest in the Great Lakes region of the United States. Journal of Geophysical Research: Biogeosciences, 111. [Online: https://agupubs.onlinelibrary.wiley.com/doi/abs/10.1029/2005JG000083]

Tardieu, F. (1993). Will increases in our understanding of soil-root relations and root signaling substantially alter water flux models? Philosophical Transactions of the Royal Society B, 341, 57–66.

Tardieu, F., & Simonneau, T. (1998). Variability among species of stomatal control under fluctuating soil water status and evaporative demand: modeling isohydric and anisohydric behaviors. Journal of Experimental Botany, 49, 419–432.

Torrence, C., and G. P. Compo. (1998). A Practical Guide to Wavelet Analysis. Bulletin of the American Meteorological Society 79, 61–78.

Traver, E., Ewers, B. E., Mackay, D. S., & Loranty, M. M. (2010). Tree transpiration varies spatially in response to atmospheric but not edaphic conditions: Spatial tree transpiration. Functional Ecology, 24, 273–282.

Triviño, M., M. Potterf, J. Tijerín, P. Ruiz-Benito, D. Burgas, K. Eyvindson, C. Blattert, M. Mönkkönen, and R. Duflot. (2023). Enhancing Resilience of Boreal Forests Through Management Under Global Change: a Review. Current Landscape Ecology Reports.

Tyree, M. T., and F. W. Ewers. (1991). The hydraulic architecture of trees and other woody plants. New Phytologist 119, 345–360.

Van Cleve, K., Barney, R., & Schlentner, R. (1981). Evidence of temperature control of production and nutrient cycling in two interior Alaska black spruce ecosystems. Canadian Journal of Forest Research, 11, 259–274.

Van Herk, I. G., Gower, S. T., Bronson, D. R., & Tanner, M. S. (2011). Effects of climate warming on canopy water dynamics of a boreal black spruce plantation. Canadian Journal of Forest Research, 41, 217–227.

Vandegehuchte, M. W., & Steppe, K. (2012). Improving sap flux density measurements by correctly determining thermal diffusivity, differentiating between bound and unbound water. Tree Physiology, 32, 930–942.

Vandegehuchte, M. W., Burgess, S. S. O., Downey, A., & Steppe, K. (2015). Influence of stem temperature changes on heat pulse sap flux density measurements. Tree Physiology, 35, 346–353.

Venturas, M. D., J. S. Sperry, and U. G. Hacke. (2017). Plant xylem hydraulics: What we understand, current research, and future challenges: Plant xylem hydraulics. Journal of Integrative Plant Biology 59, 356–389.

Volaire, F. (2018). A unified framework of plant adaptive strategies to drought: Crossing scales and disciplines. Global Change Biology, 24, 2929–2938.

Walker, X. J., M. C. Mack, and J. F. Johnstone. (2015). Stable carbon isotope analysis reveals widespread drought stress in boreal black spruce forests. Global Change Biology 21, 3102–3113.

Walker, X., & Johnstone, J. F. (2014). Widespread negative correlations between black spruce growth and temperature across topographic moisture gradients in the boreal forest. Environmental Research Letters, 9, 064016.

Wang, J. A., Sulla-Menashe, D., Woodcock, C. E., Sonnentag, O., Keeling, R. F., & Friedl, M. A. (2020). Extensive land cover change across Arctic–Boreal Northwestern North America from disturbance and climate forcing. Global Change Biology, 26, 807–822.

Wang, J., Taylor, A. R., & D'Orangeville, L. (2023). Warming-induced tree growth may help offset increasing disturbance across the Canadian boreal forest. Proceedings of the National Academy of Sciences of the USA, 120, e2212780120.

Wang, J., Wen, X., Lyu, S., & Guo, Q. (2021). Transition in multi-dimensional leaf traits and their controls on water use strategies of co-occurring species along a soil limiting-resource gradient. Ecological Indicators, 128, 107838.

Wang, K., & Dickinson, R. E. (2012). A review of global terrestrial evapotranspiration: Observation, modeling, climatology, and climatic variability. Reviews of Geophysics, 50. [Online: https://agupubs.onlinelibrary.wiley.com/doi/abs/10.1029/2011RG000373]

Wang, Y., Hogg, E. H., Price, D. T., Edwards, J., & Williamson, T. (2014). Past and projected future changes in moisture conditions in the Canadian boreal forest. The Forestry Chronicle, 90, 678–691.

Waring, R. H., & Running, S. W. (1998). Forest ecosystems: analysis at multiple scales. 2nd ed. Academic Press, San Diego.

Warren, C. R., McGrath, J. F., & Adams, M. A. (2001). Water Availability and Carbon Isotope Discrimination in Conifers. Oecologia, 127, 476–486.

Warren, J. M., Jensen, A. M., Ward, E. J., Guha, A., Childs, J., Wullschleger, S. D., & Hanson, P. J. (2021). Divergent species-specific impacts of whole ecosystem warming and elevated CO_2 on vegetation water relations in an ombrotrophic peatland. Global Change Biology, 27, 1820–1835.

Warren, R. K. (2015, August). Examining the spatial distribution of soil moisture and its relationship to vegetation and permafrost dynamics in a Subarctic permafrost peatland. M.Sc. Thesis, The University of Guelph, Guelph, Ontario, Canada.

Warren, R. K., Pappas, C., Helbig, M., Chasmer, L. E., Berg, A. A., Baltzer, J. L., Quinton, W. L., & Sonnentag, O. (2018). Minor contribution of overstorey transpiration to landscape evapotranspiration in boreal permafrost peatlands: Contribution of overstory transpiration in a boreal permafrost peatland. Ecohydrology, e1975.

Way, D. A., & Sage, R. F. (2008). Elevated growth temperatures reduce the carbon gain of black spruce [*Picea mariana* (Mill.) B.S.P.]: Temperature and carbon balance in black spruce. Global Change Biology, 14, 624–636.

Westerband, A. C., Funk, J. L., & Barton, K. E. (2021). Intraspecific trait variation in plants: a renewed focus on its role in ecological processes. Annals of Botany, 127, 397–410.

Westoby, M., D. S. Falster, A. T. Moles, P. A. Vesk, and I. J. Wright. (2002). Plant Ecological Strategies: Some Leading Dimensions of Variation Between Species. Annual Review of Ecology and Systematics 33, 125–159.

Whitman, E., Parisien, M.-A., Thompson, D. K., & Flannigan, M. D. (2019). Short-interval wildfire and drought overwhelm boreal forest resilience. Scientific Reports, 9, 18796.

Wickham, H. (2016). ggplot2: Elegant Graphics for Data Analysis. Springer-Verlag New York.

Wiken, E., Jiménez Nava, F., & Griffith, G. (2011). North American Terrestrial Ecoregions: Level III. Commission for Environmental Cooperation, Montreal, QC, Canada. 149 pp.

Wolfe, S. A., Landhäusser, S. M., Lieffers, V. J., & Silins, U. (2011). Seedling growth and water use of boreal conifers across different temperatures and near-flooded soil conditions. Canadian Journal of Forest Research, 41, 2292–2300.

Wolken, J. M., S. M. Landhäusser, V. J. Lieffers, and U. Silins. (2011). Seedling growth and water use of boreal conifers across different temperatures and near-flooded soil conditions. Canadian Journal of Forest Research 41, 2292–2300.

Wright, I. J. (2002). Plant Ecological Strategies: Some Leading Dimensions of Variation Between Species. Annual Review of Ecology and Systematics, 33, 125–59.

Wright, I. J., N. Dong, V. Maire, I. C. Prentice, M. Westoby, S. Díaz, R. V. Gallagher, B. F. Jacobs, R. Kooyman, E. A. Law, M. R. Leishman, Ü. Niinemets, P. B. Reich, L. Sack, R. Villar, H. Wang, and P. Wilf. (2017). Global climatic drivers of leaf size. Science 357, 917–921.

Wright, I. J., P. B. Reich, M. Westoby, D. D. Ackerly, Z. Baruch, F. Bongers, J. Cavender-Bares, T. Chapin, J. H. C. Cornelissen, M. Diemer, J. Flexas, E. Garnier, P. K. Groom, J. Gulias, K. Hikosaka, B. B. Lamont, T. Lee, W. Lee, C. Lusk, J. J. Midgley, M.-L. Navas, Ü. Niinemets, J. Oleksyn, N. Osada, H. Poorter, P. Poot, L. Prior, V. I. Pyankov, C. Roumet, S. C. Thomas, M. G. Tjoelker, E. J. Veneklaas, and R. Villar. (2004). The worldwide leaf economics spectrum. Nature 428, 821–827.

Wright, S. N., Thompson, L. M., Olefeldt, D., Connon, R. F., Carpino, O. A., Beel, C. R., & Quinton, W. L. (2022). Thaw-induced impacts on land and water in discontinuous permafrost: A review of the Taiga Plains and Taiga Shield, northwestern Canada. Earth-Science Reviews, 232, 104104.

Wu, Y., X. Zhang, Y. Fu, F. Hao, and G. Yin. (2020). Response of Vegetation to Changes in Temperature and Precipitation at a Semi-Arid Area of Northern China Based on Multi-Statistical Methods. Forests 11, 340.

Wullschleger, S. D., & King, A. W. (2000). Radial variation in sap velocity as a function of stem diameter and sapwood thickness in yellow-poplar trees. Tree Physiology, 20, 511–518.

Wullschleger, S. D., F. C. Meinzer, and R. A. Vertessy. (1998). A review of whole-plant water use studies in tree. Tree Physiology 18, 499–512.

Xue, F., Y. Jiang, M. Dong, M. Wang, X. Ding, X. Yang, M. Cui, H. Xu, and M. Kang. (2022). Different drought responses of stem water relations and radial increments in *Larix principis-rupprechtii* and *Picea meyeri* in a montane mixed forest. Agricultural and Forest Meteorology 315:108817.

Xue, F., Y. Jiang, M. Dong, M. Wang, X. Ding, X. Yang, M. Cui, H. Xu, and M. Kang. (2022). Seasonal and daily variations in stem water relations between co-occurring Larix principis-rupprechtii and Picea meyeri at different elevations. Forest Ecology and Management 504, 119821.

Yang, X., Tang, J., Mustard, J. F., Wu, J., Zhao, K., Serbin, S., & Lee, J.-E. (2016). Seasonal variability of multiple leaf traits captured by leaf spectroscopy at two temperate deciduous forests. Remote Sensing of Environment, 179, 1–12. https://doi.org/10.1016/j.rse.2016.03.026

Yang, J., Q. Zhang, W. Song, X. Zhang, and X. Wang. (2022). Radial Growth of Trees Rather Than Shrubs in Boreal Forests Is Inhibited by Drought. Frontiers in Plant Science 13, 912916.

Yi, C., and N. Jackson. (2021). A review of measuring ecosystem resilience to disturbance. Environmental Research Letters 16, 053008.

Zhang, J.-G., Guan, J.-H., Shi, W.-Y., Yamanaka, N., & Du, S. (2015). Interannual variation in stand transpiration estimated by sap flow measurement in a semi-arid black locust plantation, Loess Plateau, China. Ecohydrology, 8, 137–147.

Zhang, W., F. Wei, S. Horion, R. Fensholt, M. Forkel, and M. Brandt. (2022). Global quantification of the bidirectional dependency between soil moisture and vegetation productivity. Agricultural and Forest Meteorology 313, 108735.

Zhang, X., G. Flato, M. Kirchmeier-Young, L. Vincent, H. Wan, X. Wang, R. Rong, J. Fyfe, G. Li, and V. V. Kharin. (2019). Changes in temperature and precipitation across Canada. Canada's changing climate report. 112–193.

Zhao, M., G. A, Y. Liu, and A. G. Konings. (2022). Evapotranspiration frequently increases during droughts. Nature Climate Change 12, 1024–1030.

Zimmermann, R., Schulze, E.-D., Wirth, C., Schulze, E.-E., Mcdonald, K. C., Vygodskaya, N. N., & Ziegler, W. (2000). Canopy transpiration in a chronosequence of Central Siberian pine forests. Global Change Biology, 6, 25–37.

Zweifel, R. (2016). Radial stem variations – a source of tree physiological information not fully exploited yet. Plant, Cell & Environment, 39, 231–232.

Zweifel, R., F. Sterck, S. Braun, N. Buchmann, W. Eugster, A. Gessler, M. Häni, R. L. Peters, L. Walthert, M. Wilhelm, K. Ziemińska, and S. Etzold. (2021). Why trees grow at night. New Phytologist 231:2174–2185.

Zweifel, R., Item, H., & Hasler, R. (2000). Stem radius changes and their relation to stored water in stems of young Norway spruce trees. Trees, 15, 50–57.

Zweifel, R., Item, H., & Hasler, R. (2001). Link between diurnal stem radius changes and tree water relations. Tree Physiology, 21, 869–877.

Zweifel, R., W. Eugster, S. Etzold, M. Dobbertin, N. Buchmann, and R. Häsler. (2010). Link between continuous stem radius changes and net ecosystem productivity of a subalpine Norway spruce forest in the Swiss Alps. New Phytologist 187, 819–830.

Zweifel, R., Zimmermann, L., & Newbery, D. M. (2005). Modeling tree water deficit from microclimate: an approach to quantifying drought stress. Tree Physiology, 25, 147–156.

Appendices

Appendix I (Chapter 2)

Figure SI.1 : A dendrometer installed on the stem of a black spruce tree at Scotty Creek (SCC).

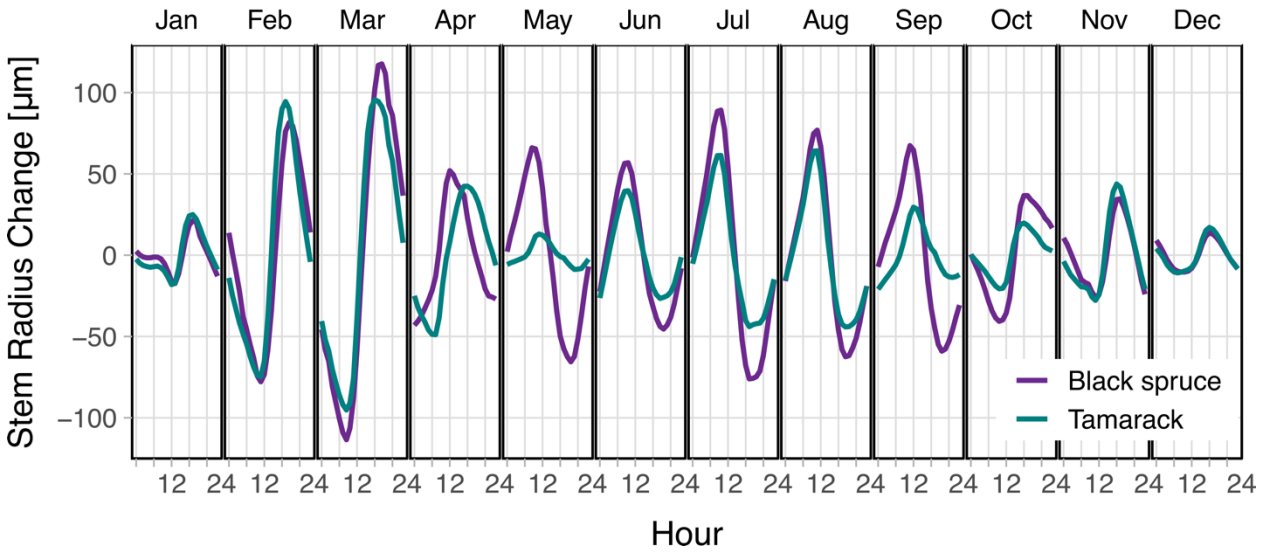

Figure SI.2 Half-hourly mean stem radius changes for tamarack and black spruce at Scotty Creek for each month in 2019. In this example, the sinusoidal pattern of stem radius changed from being temperature driven to transpiration driven in May for black spruce and June for tamarack.

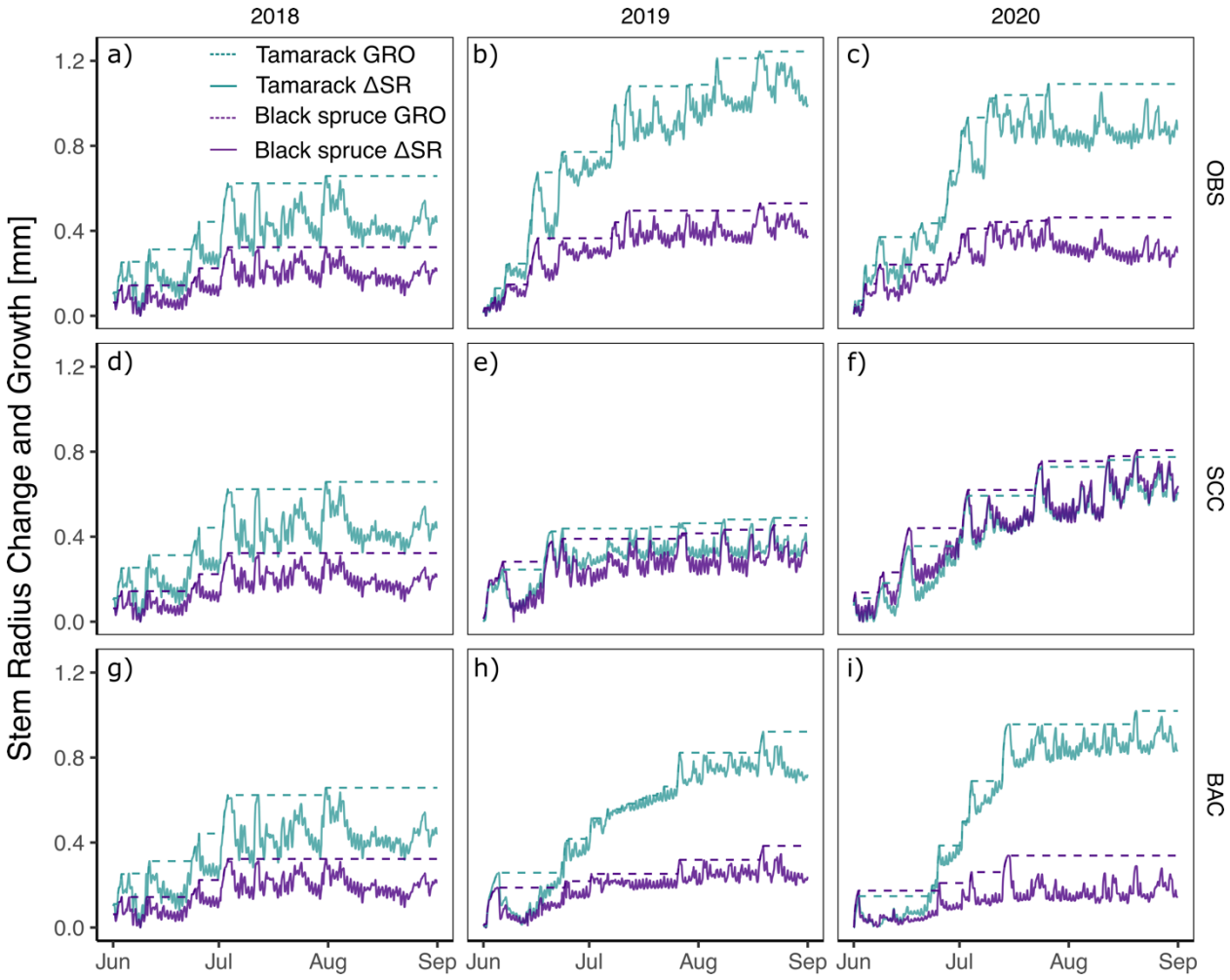

Figure SI.3 Average stem radius change (ΔSR) and cumulative annual growth (GRO) averaged across all individuals of black spruce and tamarack at Old Black Spruce (OBS; a, b, and c), Scotty Creek (SCC; d and e) Baker Creek (BAC; f and g) June to August 2018, 2019 and 2020. Growth period length was determined as the period between transpiration onset in the spring and end in the fall. Species-level growth for each site and year was partitioned from the stem radius change.

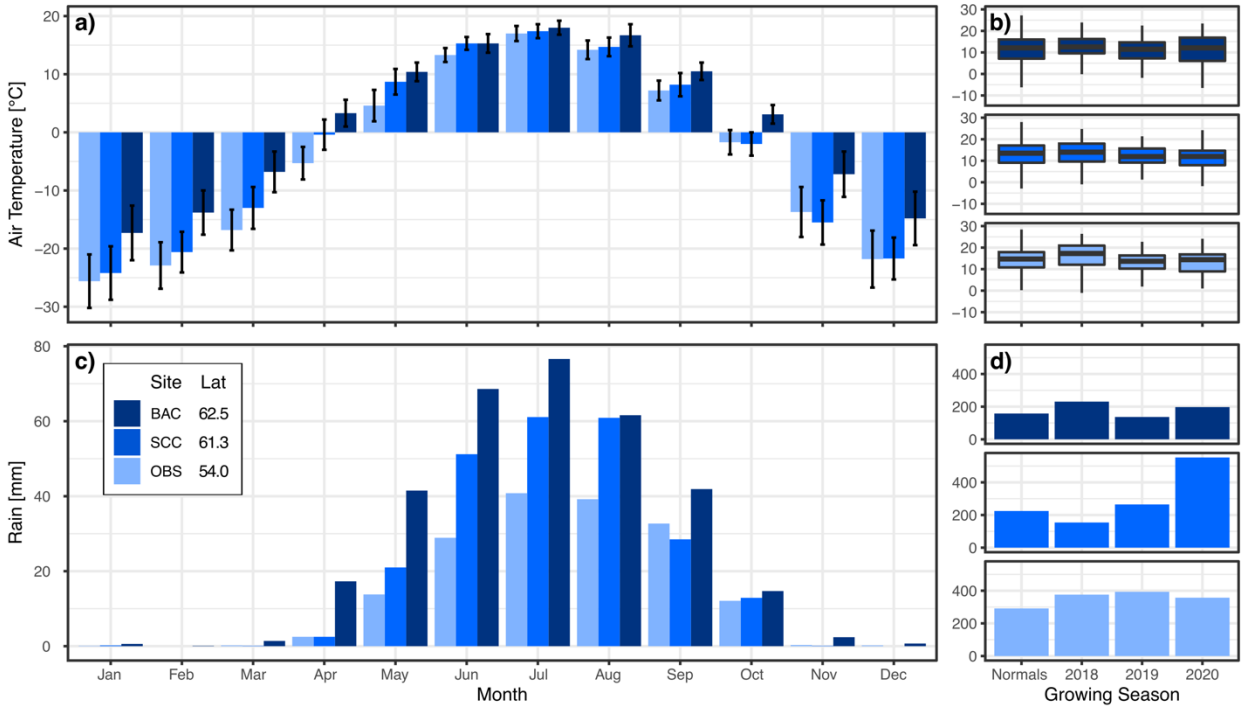

Figure SI.4 Meteorological conditions representing the monthly climate normals (a and c) between 1981 – 2010 for Old Black Spruce (OBS), Scotty Creek (SCC), and Backer Creek (BAC). Summer climate normals were compared to local air temperature (b) and rainfall (d) at OBS, SCC and BAC. Climate normals were collected from the nearest Environment and Climate Change Canada meteorological stations located in Prince Albert, SK (OBS), Fort Simpson (SCC) and Yellowknife (BAC). Local air temperature and rainfall were determined using micrometeorological stations located at each site.

Table SI.1 The mean daily tree water deficit (TWD; mm) and cumulative annual growth (growth; mm/yr.) for black spruce and tamarack individuals from Old Black Spruce (OBS), Scotty Creek (SCC) and Baker Creek (BAC) in 2019 and 2020 and OBS in 2018. The numbers in parentheses represent the standard deviation of values measured for individual trees at each site.

Site	Species	TWD (mm)	Growth (mm/yr.)
BAC	Tamarack	0.105 (0.07)	0.616 (0.56)
	Black spruce	0.115 (0.05)	0.120 (0.11)
SCC	Tamarack	0.121 (0.05)	0.394 (0.27)
	Black spruce	0.147 (0.06)	0.295 (0.25)
OBS	Tamarack	0.153 (0.08)	0.868 (0.50)
	Black spruce	0.112 (0.05)	0.481 (0.25)
MEAN	Tamarack	0.127 (0.07)	0.612 (0.46)
	Black spruce	0.125 (0.06)	0.313 (0.26)

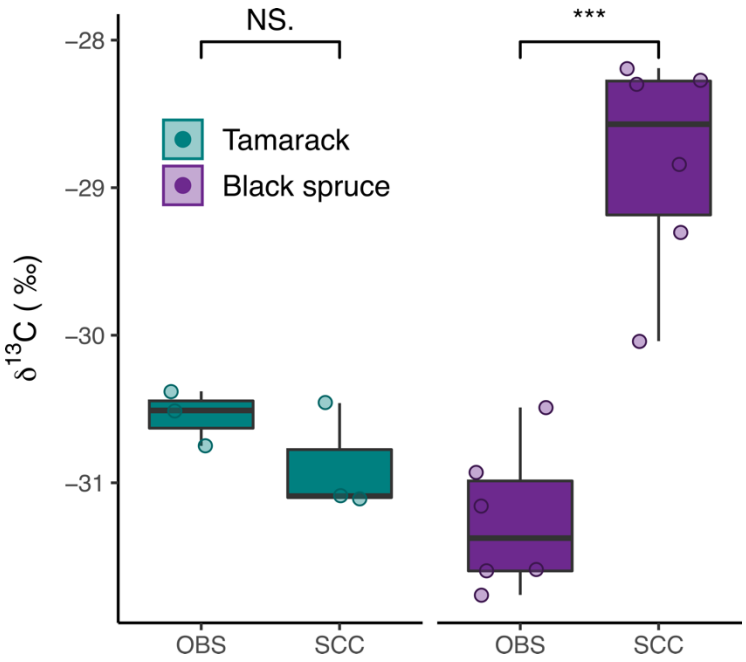

Figure SI.5 Comparisons between $\delta^{13}C$ of tamarack (teal) needles from Old Black Spruce (OBS) and Scotty Creek (SCC) and black spruce (purple) needles from OBS and SCC. The difference between species was compared using a Wilcoxon rank sum test (NS. = no significance,* p = 0.05, ** p =0.01, *** = p < 0.001).

Appendix II (Chapter 3)

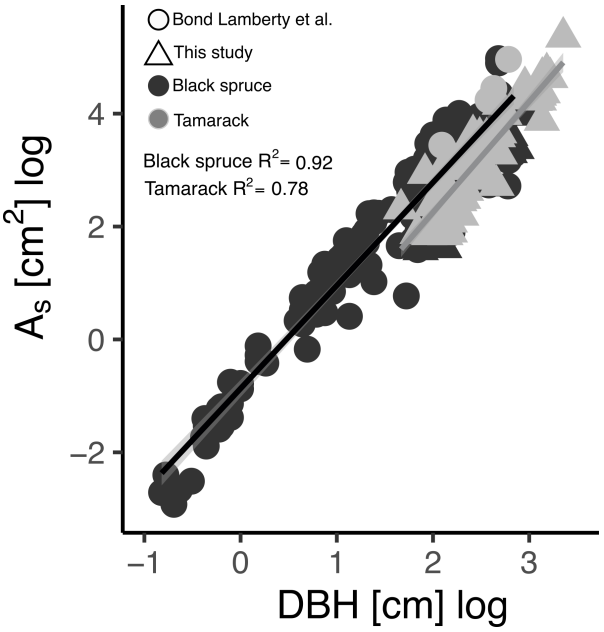

Figure SII.1 Allometric relationship between the log of tree diameter at breast height (DBH; cm, measured at 1.3m) and the log of sapwood area (As; cm2) for black spruce (n = 201) and tamarack (n = 64). Samples were taken from trees at Scotty Creek and other boreal forest stands in northwestern Canada (Bond-Lamberty 2002).

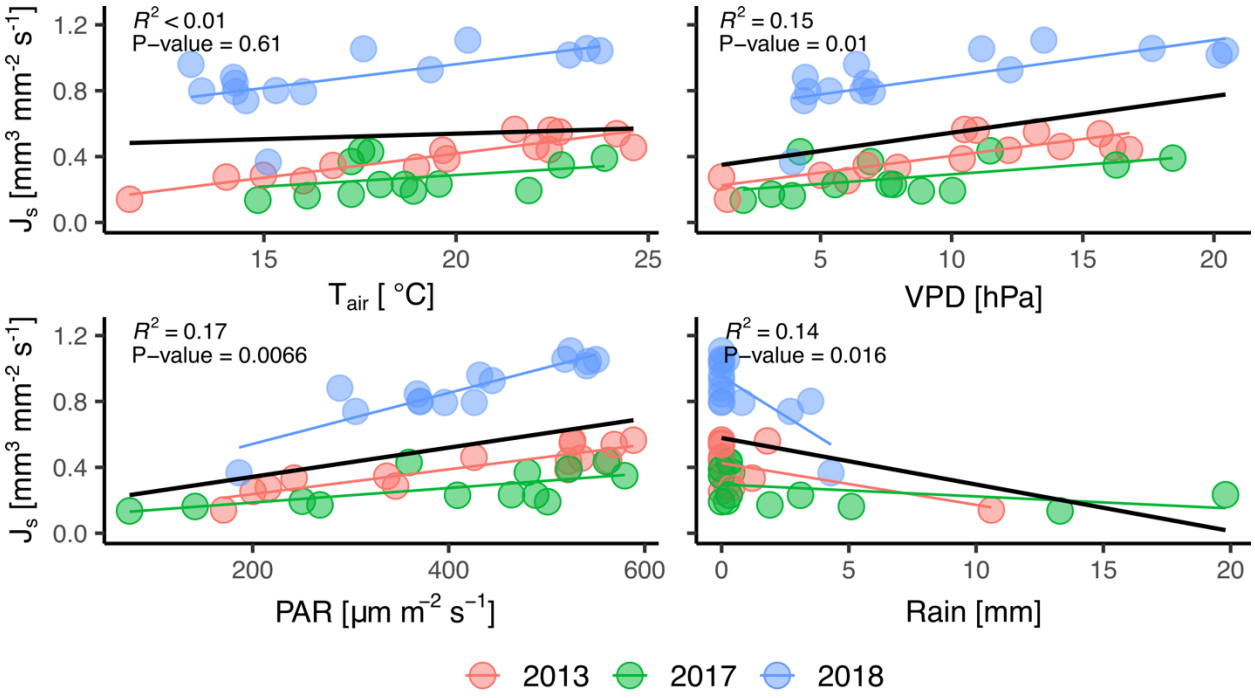

Figure SII.2 The relationship between daily (total) sap flux density (J_s; mm^3 cm^{-2} s^{-1}) and the meteorological conditions including daily mean air temperature (T_{air}; ºC), mean daily vapor pressure deficit (VPD; hPa), mean daily photosynthetically active radiation (PAR; µm m^{-2} s^{-1}) and total daily rainfall (Rain, mm). Linear relationships between the daily J_s and the meteorological conditions are plotted for each year individually (coloured lines) and for all three years combined (black line). The R^2 and p-values represent the relationship between the meteorological condition and the daily J_s for all three years combined. There was a positive linear relationship between daily J_s and both mean daily VPD (adj. $R^2 = 0.36$, $F_{(1, 41)} = 24.25$, $p < .001$,) and PAR (adj. $R^2 = 0.35$, $F_{(1, 41)} = 23.50$, $p < .001$), and a negative linear relationship with total daily rainfall (adj. $R^2 = 0.20$, $F_{(1, 41)} = 11.24$, $p = 0.002$). Daily J_s was weakly but significantly correlated with T_{air} (adj. $R^2 = 0.08$, $F_{(1, 41)} = 4.54$, $p = 0.039$).

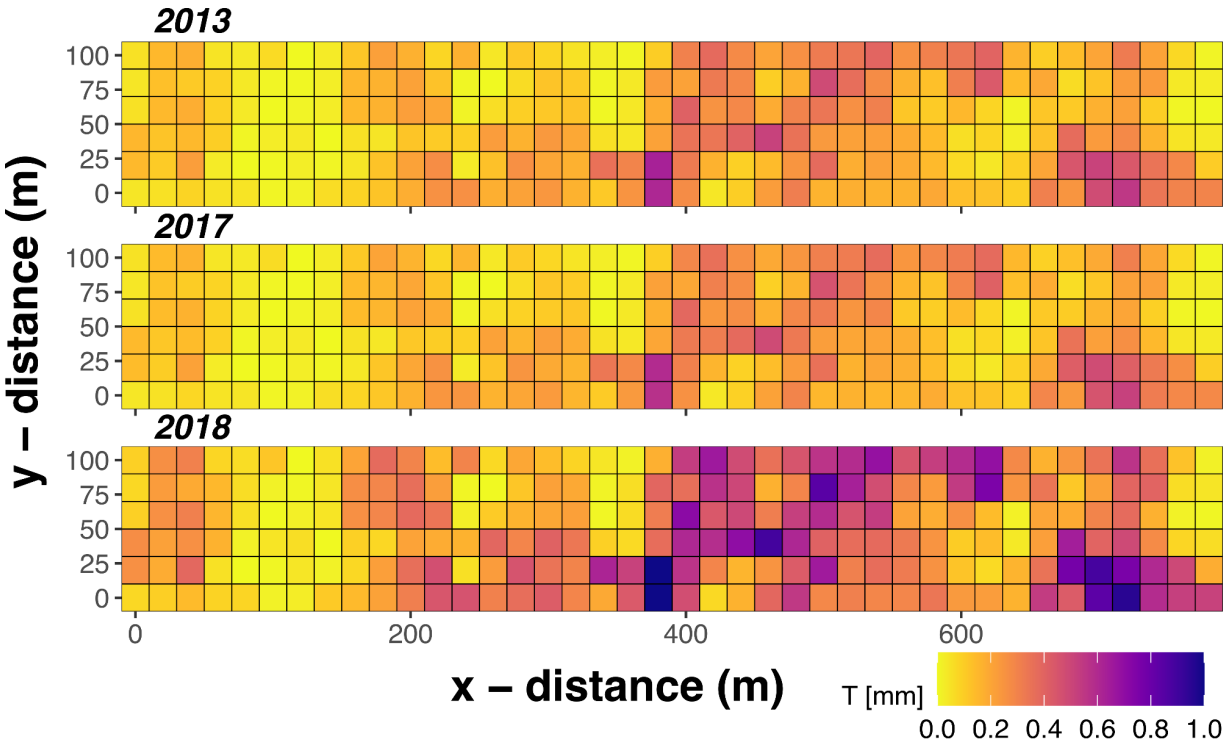

Figure SII.3 A comparison of the daily grid-cell transpiration (T; mm) averaged across the sampling period (27 June to 11 July) for each year (2013, 2017, and 2018). Transpiration was determined using the tree diameter of black spruce and tamarack stem larger than 1 cm that was measured in the plot between 2012 and 2014.

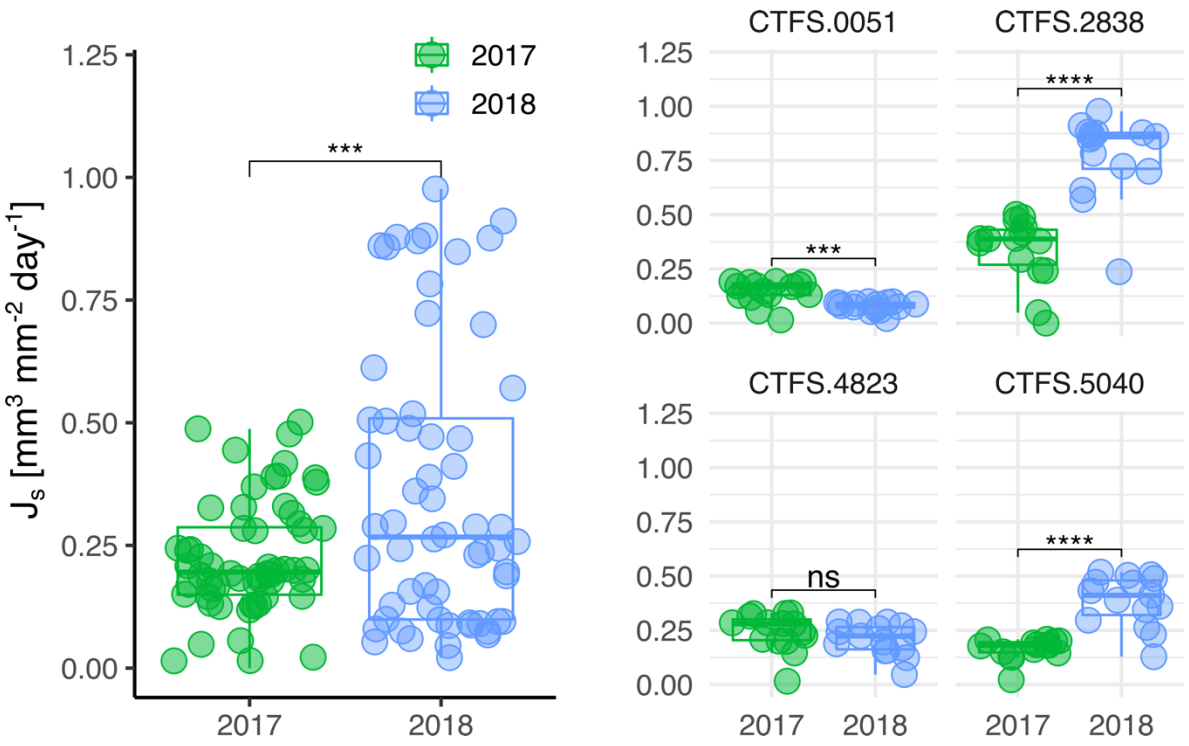

Figure SII.4 A comparison of the total daily J_s between 2017 and 2018 for trees that were instrumented in both years. The left side of the panel represents the daily J_s for all six trees, while the plots on the right represent the daily J_s for each tree individually. The numbers above each panel represent the tree identification number in the plot. Daily J_s was compared between years using a paired sample t-test (rstatix package in R). Significance values are denoted with an * representing p-values equal to 0 to 0.0001 (****), 0.0001 to 0.001 (***), from 0.001 to 0.01 (**), 0.01 to 0.05 (*) and greater than 0.05 (ns).

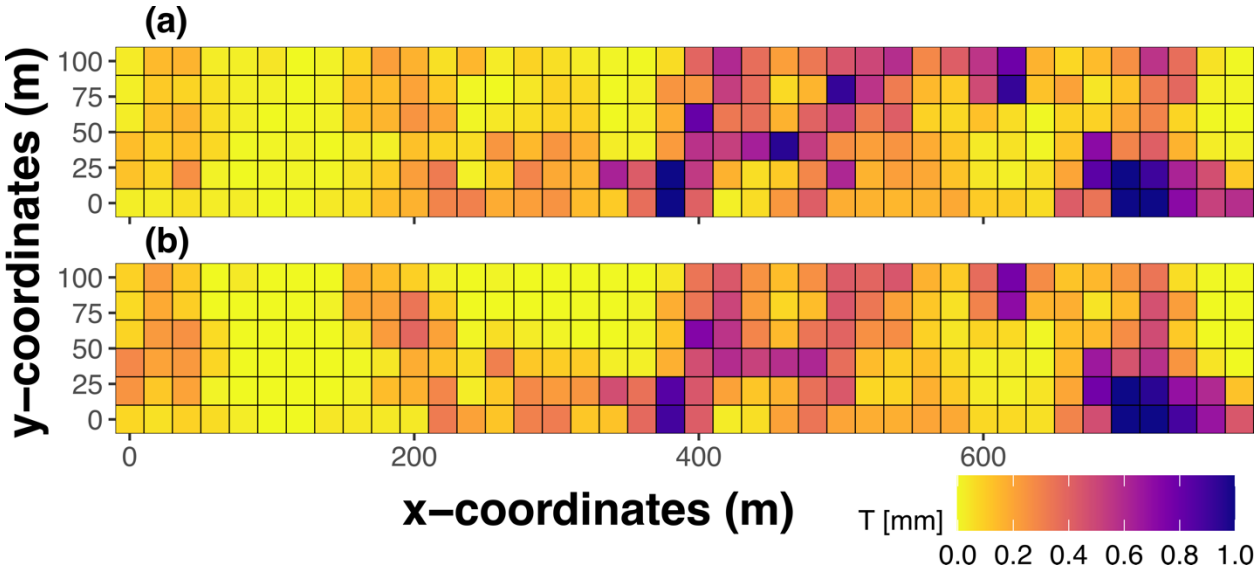

Figure SII.5 The daily transpiration (T; mm) for each grid-cell in the plot adjusted to account for grid-cell basal area (a) and PC1 (a gradient of soil moisture and permafrost presence, b).

Appendix III (Chapter 4)

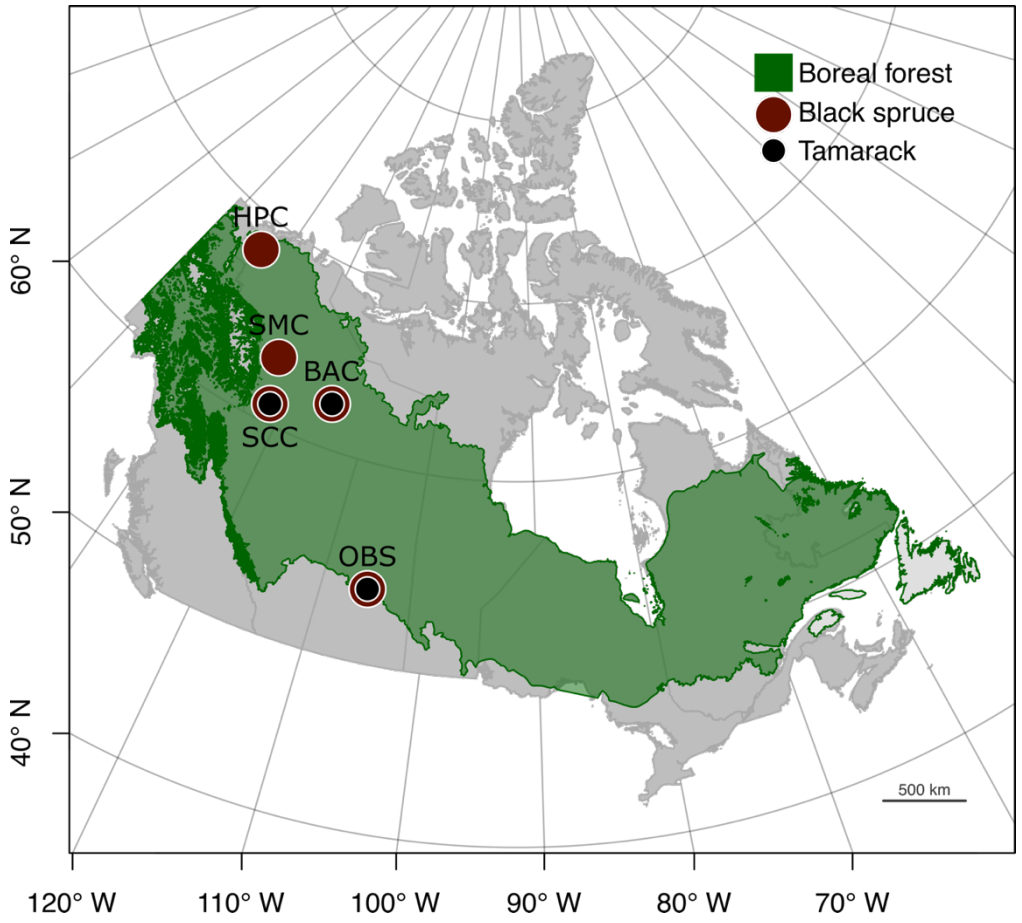

Figure SIII.1 Five sites in Canada's boreal forest biome (shaded green) where black spruce (*Picea mariana*) and tamarack (*Larix laricina*) were sampled for tree water deficit: Old Black Spruce (OBS), Scotty Creek (SCC), Baker Creek (BAC), Smith Creek (SMC) and Havikpak Creek (HPC).

Table SIII.1 Site information for the five sites. Site location is given as latitude and longitude (Lat, Long; °), the ecozone classification was based on the Terrestrial Ecozones of Canada (Wiken, 1986), mean annual precipitation (MAP; mm) and mean annual temperature (MAT; °C) (Environment Canada, Historical Data) and permafrost classification was based on the 2010 assessment of permafrost across Canada released in 2016 (National Resources Canada, 2010). Landcover classification was determined from the Landcover SPOT from 2005 to 2010 (Natural Resources Canada, 2018) and includes evergreen conifer forest, high density (ECF-HD), evergreen conifer forest, low density (ECF-LD), herb/shrub wetlands (HSW), low to sparse conifer forest/lichen understory (LSCF, and barren (B) landcover. Vegetation parameters include dominant overstory species, and overstory tree crown closure (OCC). Site edaphic characteristics are from the Soil Landscapes of Canada Version 3.2 (digital webmap) and include soil drainage class, with well drained (W), moderately well drained (MW), poorly drained (P), very poorly drained (VP) and imperfectly drained (I); and dominant parent material. Near surface soil organic layer thickness (SOL; cm) and active layer thickness (ALT, cm) were determined for each table from the main references listed in the table.

	OBS	SCC	BAC	SMC	HPC
Lat, Long (°)	53.987, -105.118	61.310, -121.287	62.546, -114.433	63.153, -123.252	68.320, -133.519
Ecozone	Boreal Plains	Taiga Plains	Taiga Shield	Taiga Plains	Taiga Plains
MAP (mm)	482	347	284	258	228
MAT (°C)	1.3	-2.6	-3.9	-4.7	-6.7
Permafrost	Permafrost-free	Sporadic Discontinuous	Extensive Discontinuous	Extensive Discontinuous	Continuous
Landcover	ECF-HD	ECF-HD /HSW	ECF-LD	B / LSCF	*ECF-LD*
Overstory	*Picea mariana, Larix laricina, Pinus banksiana*	*Picea mariana, Larix laricina*	*Picea mariana, Larix laricina, Pinus banksiana*	*Picea mariana, Picea glauca, Larix laricina*	*Picea mariana, Picea glauca*
OCC	Closed	*Open*	*Open*	Open	Open
Soil Drainage	P – VP	P - VP	MD - W	P - VP	I
Dominant soil material	Mineral	Organic	Mineral	Mineral	Mineral
SOL (cm)	20 - 30	50 - 800	~25 - 60 cm	100 – 200	30–60
ALT (cm)	NA	~50 – 90	~30 – 85	~62 - 85	40 - 80
Selected References	Gower *et al*. 1997, Jarvis *et al.* 1997	Quinton *et al*. 2009; Quinton *et al.* 2019	Gibson *et al.* 2018; Spence and Hedstrom 2018	Walmsley and Lavkulich 1975, Throop *et al.* 2012	Black and Bliss 1980

Table SIII.2 Micrometeorological instrumentation to measure evapotranspiration, photosynthetically active radiation (PAR measured as photosynthetic photon flux density), vapour pressure deficit (VPD), air temperature (T_{air}), rain and soil moisture (measured as volumetric water content) across the five sites. The reference is the primary resource that describes the instrumental set-up for each site.

Variable	OBS	SCC	BAC	SMC	HPC
ET	Closed-and enclosed-path CO_2/H_2O gas analysers (LI7000, and LI-7200, LI-COR Inc.) and a 3-D sonic anemometer (R3-50, Gill Instruments, Lymington, UK, and CSAT3, Campbell Scientific Inc.)	Open-path CO_2/H_2O gas analyser (EC150; Campbell Scientific Inc.) and a 3-D sonic anemometer (CSAT3A; Campbell Scientific Inc.)	Krypton Hygrometer (KH_20; Campbell Scientific Inc.) and a 3-D sonic anemometer (CSAT3A; Campbell Scientific Inc.)	Enclosed-path CO_2/H_2O gas analyser (LI-7200, LICOR Inc.) and a 3-D sonic anemometer (CSAT3; Campbell Scientific Inc.)	pen-path CO_2/H_2O gas analyser (EC150; Campbell Scientific Inc.) and a 3-D sonic anemometer (CSAT3A; Campbell Scientific Inc.)
PAR	Quantum Sensor (LI-190R; LI-COR Inc., Lincoln, NE, USA)	PAR Quantum Sensor (PQS1; Kipp & Zonen, B.V. Delft, Netherlands)	N/A	PAR Quantum Sensor (PQS1; Kipp & Zonen)	PAR Quantum Sensor (PQS1; Kipp & Zonen)
T_{air}, and Relative Humidity (VPD)	Temperature and Relative Humidity Probe (HMP45C; Vaisala Inc., Oy, Finland)	HygroClip 2 Humidity Temperature Probes (HC2-S3; Rotronic AG, Bassersdorf, Switzerland)	Temperature and Relative Humidity Probe (HMP45C; Vaisala Inc.)	Temperature and Relative Humidity Probe (HC2S3; Campbell Scientific Inc., Logan, UT, USA)	Temperature and Relative Humidity Probe (HC2S3; Campbell Scientific Inc.)
Rain	Model, 3000 with Alter shield, Belfort Instruments, Baltimore, MD, USA)	Tipping Bucket Raingauge (ARG100;, Campbell Scientific Inc.)	Tipping Bucket Rain Gage (TE525; Texas Electronics Inc., Dallas, TX, USA)	Metric Rain Gage (TE525MM-L; Texas Electronics Inc.)	All Weather Precipitation – Rain Gauge (T-200B, Geonor, Inc. Branchville, NJ, USA)
Soil Moisture	Water Content Reflectometer (CS615, Campbell Scientific,)	Water Content Reflectometer (CS616, Campbell Scientific Inc.)	HydraProbe (Stevens Water, Portland, OR, USA)	Water Content Reflectometer (CS616, Campbell Scientific Inc.)	Water Content Reflectometer (CS616, Campbell Scientific Inc.)
Height	25 m	15 m	15 m	15 m	15 m
Main References	(Barr *et al.* 2012, Nehemy *et al.* 2023)	Helbig *et al.* 2016b	(Spence *et al.* 2020)	Schulze *et al.* in prep	Helbig *et al.* 2016b

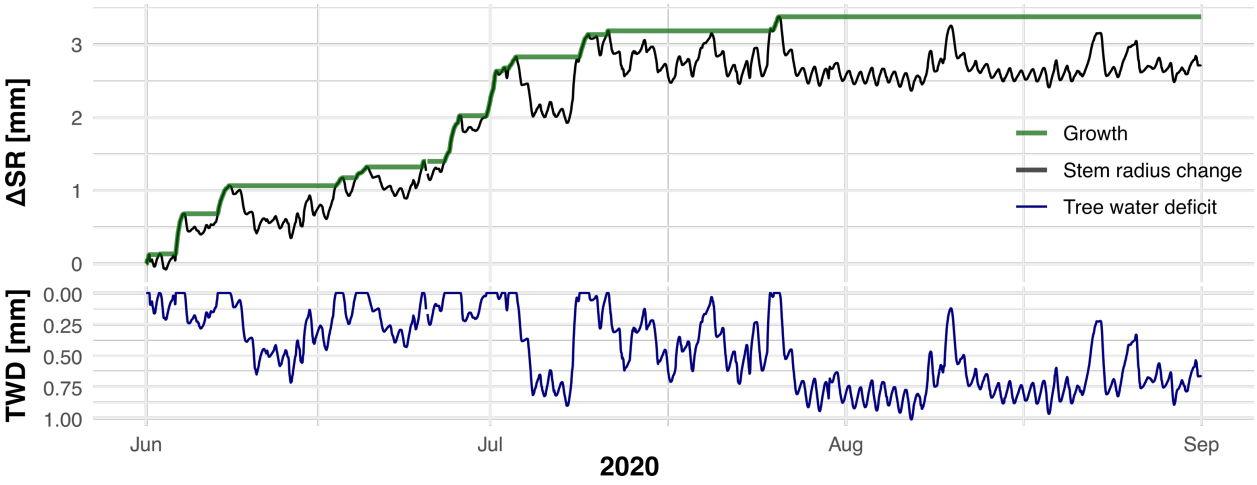

Figure SIII.2 Partitioning of stem radius change (ΔSR, mm, black line) into growth (mm, green line) and tree water deficit (TWD, mm, blue line). Growth was measured as the difference between the stem radius change at a given time (ΔSR_t) and the previous maximum measure (ΔSR_{max}). When $\Delta SR_t > \Delta SR_{max}$ then growth is occurring, but when $\Delta SR_t < \Delta SR_{max}$, growth is zero (Zweifel, 2016; Zweifel *et al*. 2021). This creates a stepwise increase in growth where ΔSR_{max} was reset to a new higher level when the current ΔSR_t exceeded the previous ΔSR_{max}. Growth was subtracted from the ΔSR time series to obtain TWD (blue line) (Zweifel *et al*. 2016). The value of TWD represents the volume of water required for a stem to fully re-hydrate. A TWD equal to zero represented fully hydrated stem tissue, and a positive TWD (> 0) represented dehydrated stem tissue. Note that the axis for TWD is presented here in reverse (zero on top and 1 at the bottom).

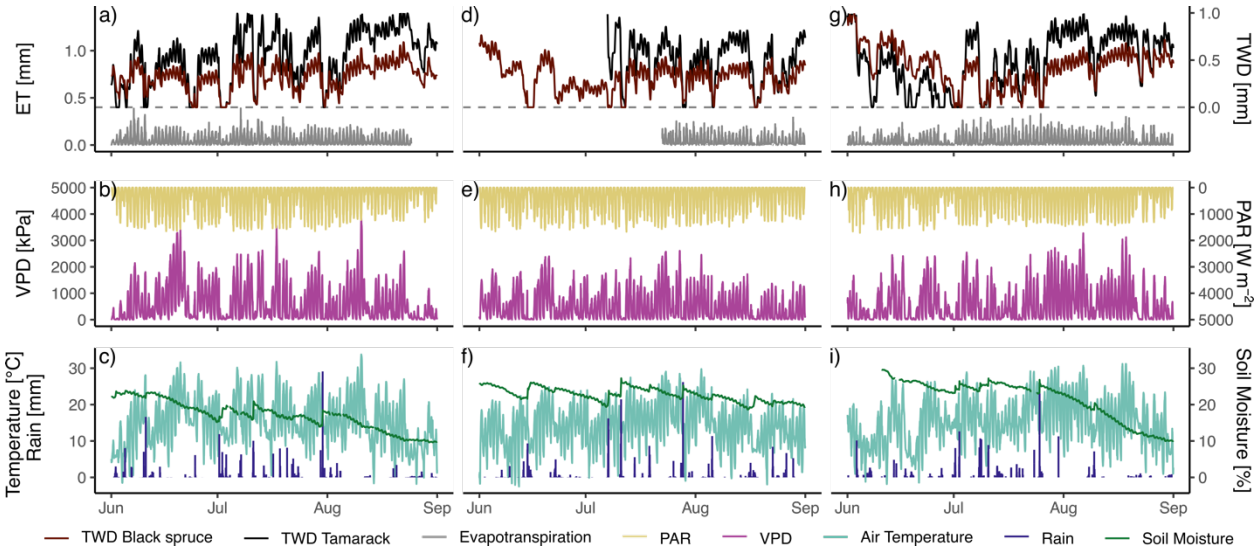

Figure SIII.3 The half-hourly measurements of tree water deficit (TWD) and potential environmental controls measured at Old Black Spruce in 2018, 2019 and 2020. Measurements of tree water deficit were for black spruce and tamarack. Environmental controls include evapotranspiration (ET), photosynthetically active radiation (PAR), vapour pressure deficit (VPD), air temperature, rain, and soil moisture.

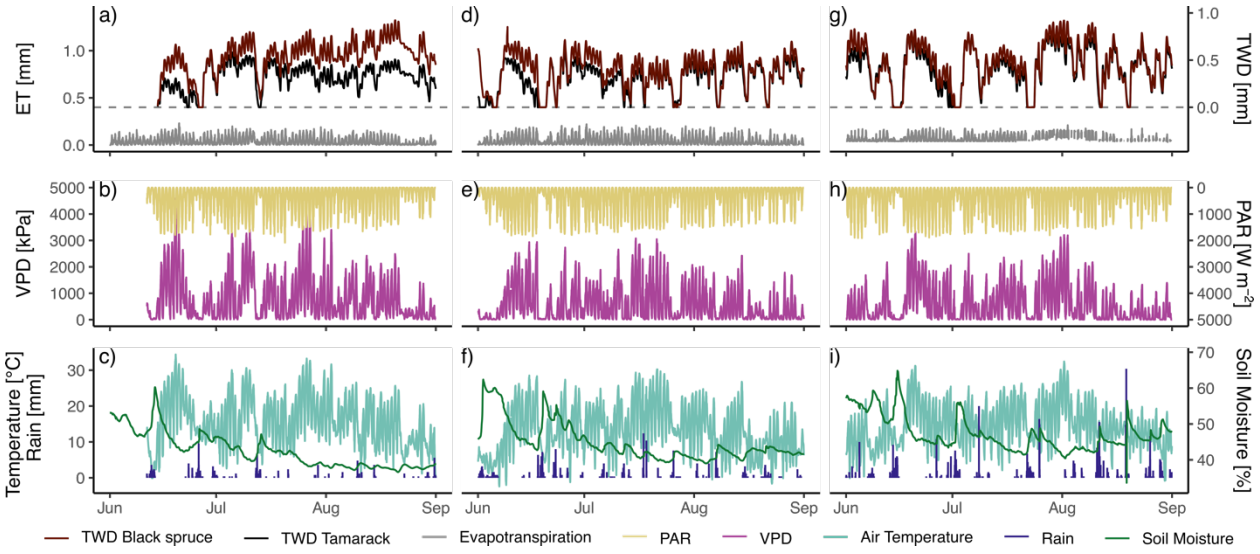

Figure SIII.4 The half-hourly measurements of tree water deficit (TWD) and potential environmental controls measured at Scotty Creek in 2018, 2019 and 2020. Measurements of tree water deficit were for black spruce and tamarack. Environmental controls include evapotranspiration (ET), photosynthetically active radiation (PAR), vapor pressure deficit (VPD), air temperature, rain, and soil moisture.

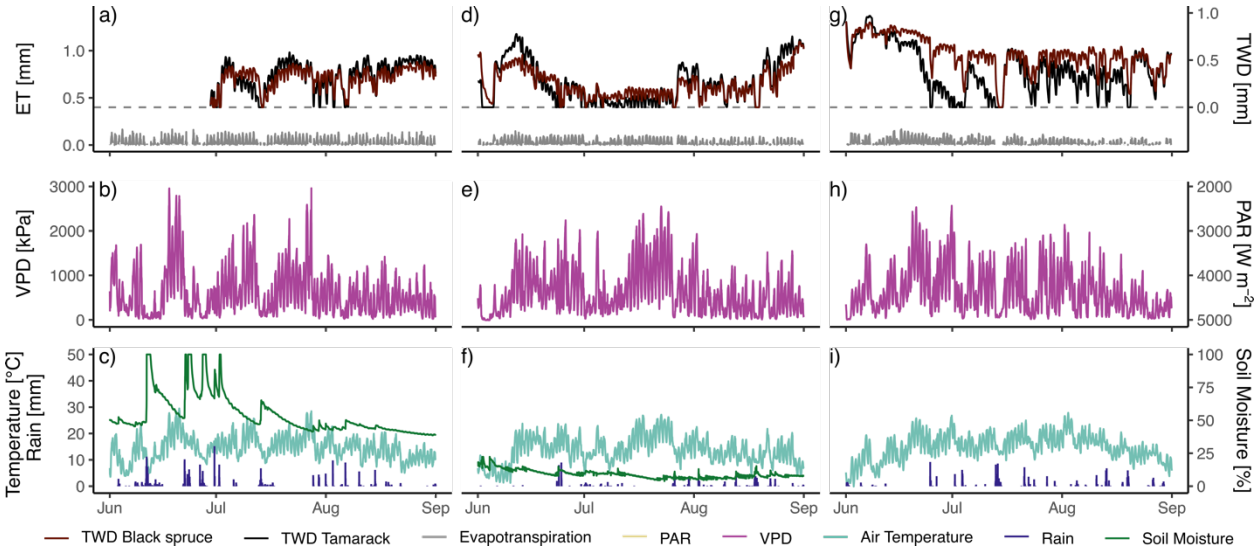

Figure SIII.5 The half-hourly measurements of tree water deficit (TWD) and potential environmental controls measured at Baker Creek in 2018, 2019 and 2020. Measurements of tree water deficit were for black spruce and tamarack. Environmental controls include evapotranspiration (ET), vapour pressure deficit (VPD), air temperature, rain, and soil moisture.

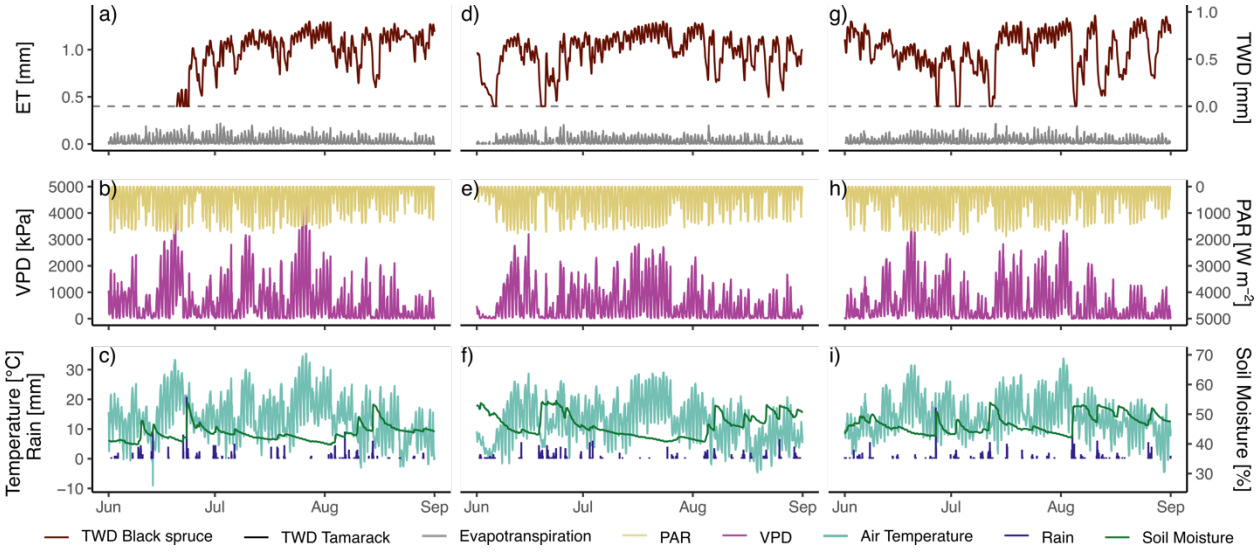

Figure SIII.6 The half-hourly measurements of tree water deficit (TWD) and potential environmental controls measured at Smith Creek in 2018, 2019 and 2020. Measurements of tree water deficit were for black spruce. Environmental controls include evapotranspiration (ET), photosynthetically active radiation (PAR), vapour pressure deficit (VPD), air temperature, rain, and soil moisture.

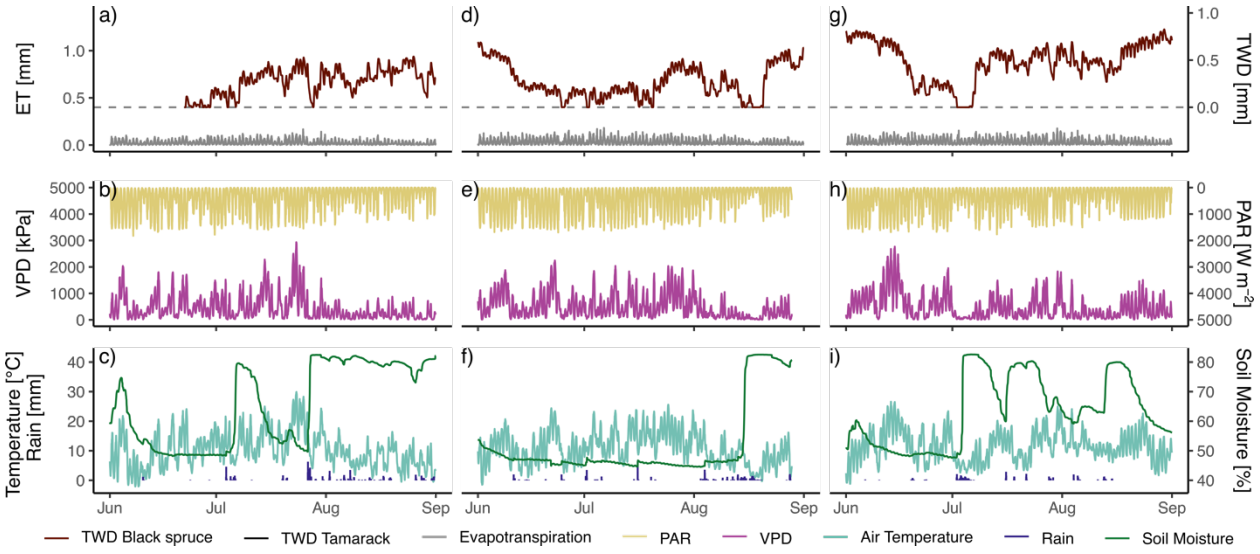

Figure SIII.7 The half-hourly measurements of tree water deficit (TWD) and potential environmental controls measured at Havikpak Creek in 2018, 2019 and 2020. Measurements of tree water deficit were for black spruce. Environmental controls include evapotranspiration (ET), photosynthetically active radiation (PAR), vapour pressure deficit (VPD), air temperature, rain, and soil moisture.

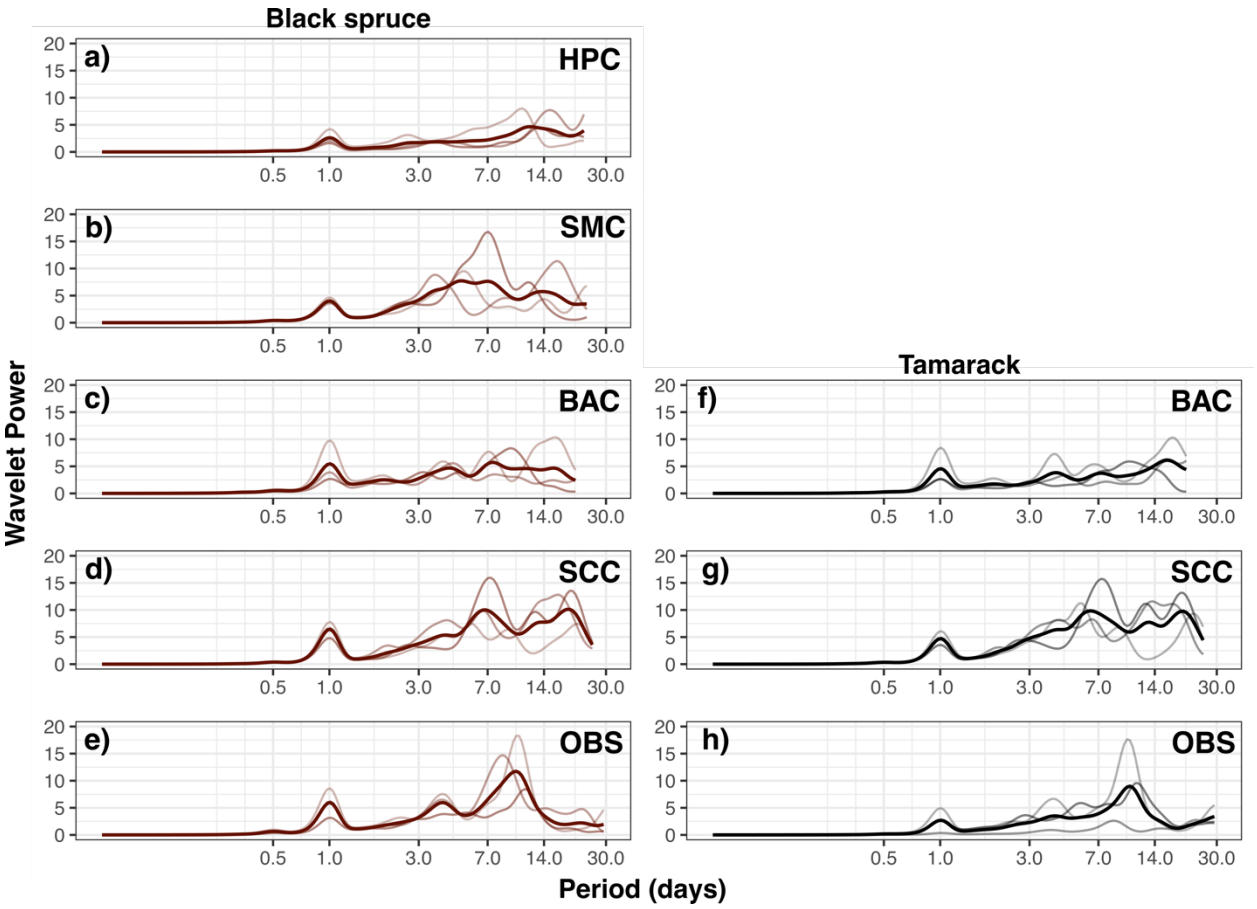

Figure SIII.8 Plotting the average wavelet power of species-averaged black spruce and tamarack tree water deficit at Old Black Spruce (OBS), Scotty Creek (SCC), Baker Creek (BAC), Smith Creek (SMC) and Havikpak Creek (HPC, from south to north) in June, July and August 2018, 2019, and 2020. The period along the y-axis indicates the frequencies (in days) while the date on the x-axis indicates the wavelet power (%). Thick lines represent the average wavelet power for tree water deficit in 2018, 2019 and 2020, and fine lines represent the wavelet power for each year.

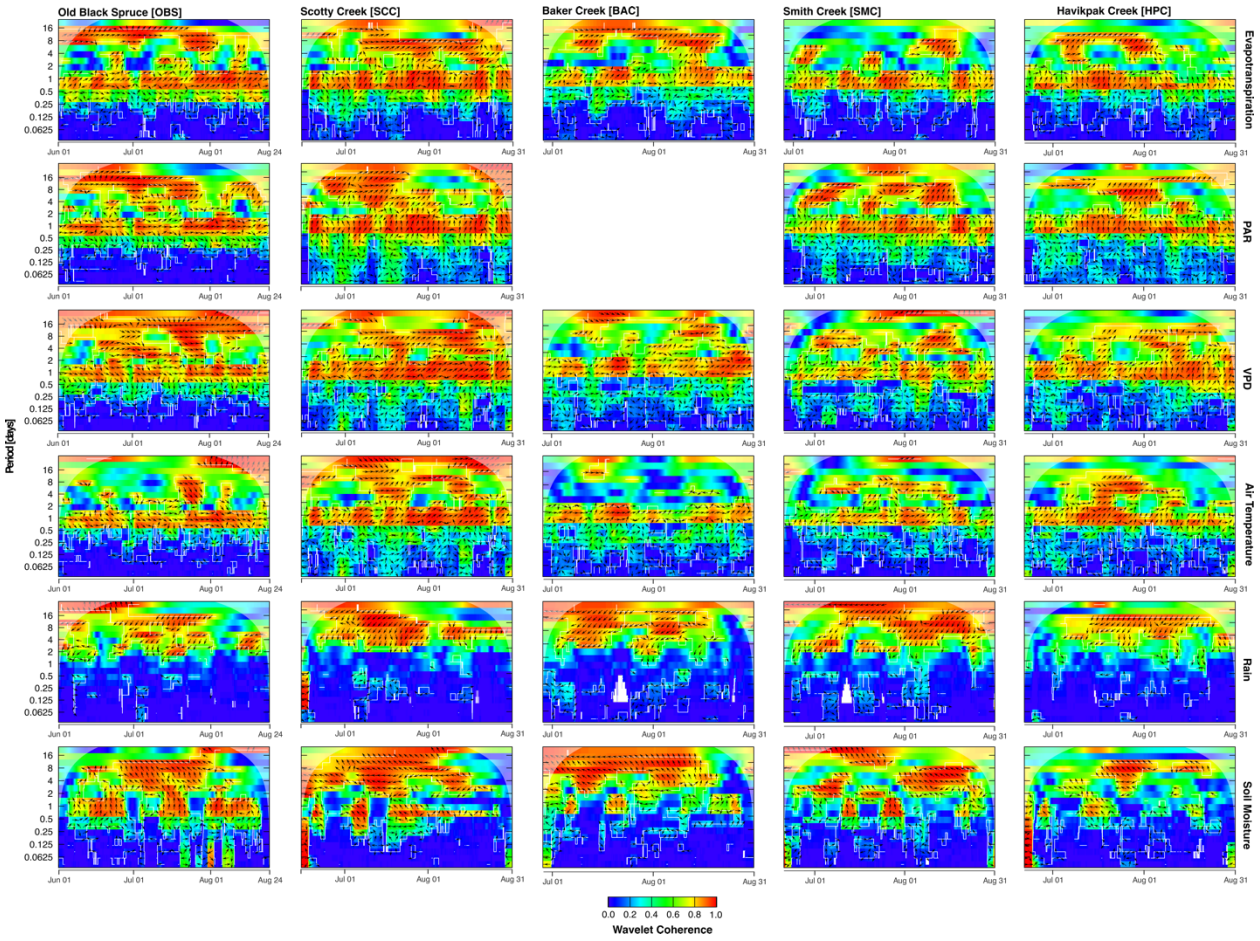

Figure SIII.9 The wavelet coherence between tree water deficit of black spruce and evapotranspiration, and environmental controls at Old Black Spruce, Scotty Creek, Baker Creek, Smith Creek and Havikpak Creek in 2018. Environmental controls include photosynthetically active radiation (PAR), vapour pressure deficit (VPD), air temperature, rain and soil moisture between June – August 2018 (when data was available). The period represents the frequency (in days) at which we observe a coherence between variables at a given time during the study period (June to August). The colour represents the level of coherence between variables, warmer red colours indicating higher coherence, and cooler blue colours indicating lower coherence. The highest wavelet coherence is observed from the ~ daily to sixteen day time periods for most variables. As the series becomes longer, there are increasing border effects at a given period; indicated by the cone of influence that becomes relatively larger at longer periods. Only coherence and arrows within the cone of influence (the non-shaded portion of the plots) was considered. Arrows indicate the direction of the relationship between tree water deficit and the environmental condition. Horizontal arrows pointing to the right indicate that the two series are in phase at the respective period with little phase differences. Horizontal arrows pointing to the left indicate that the two series are out of phase. Arrows pointed to the right and down, or left and up indicate tree water deficit is leading (in and out of phase, respectively). Arrows pointed to the right and up or left and down, indicate that environmental controls are leading (in and out of phase, respectively).

Arrows are only plotted within white contour lines indicating significance (with respect to the null hypothesis of white noise processes) at the 10% level.

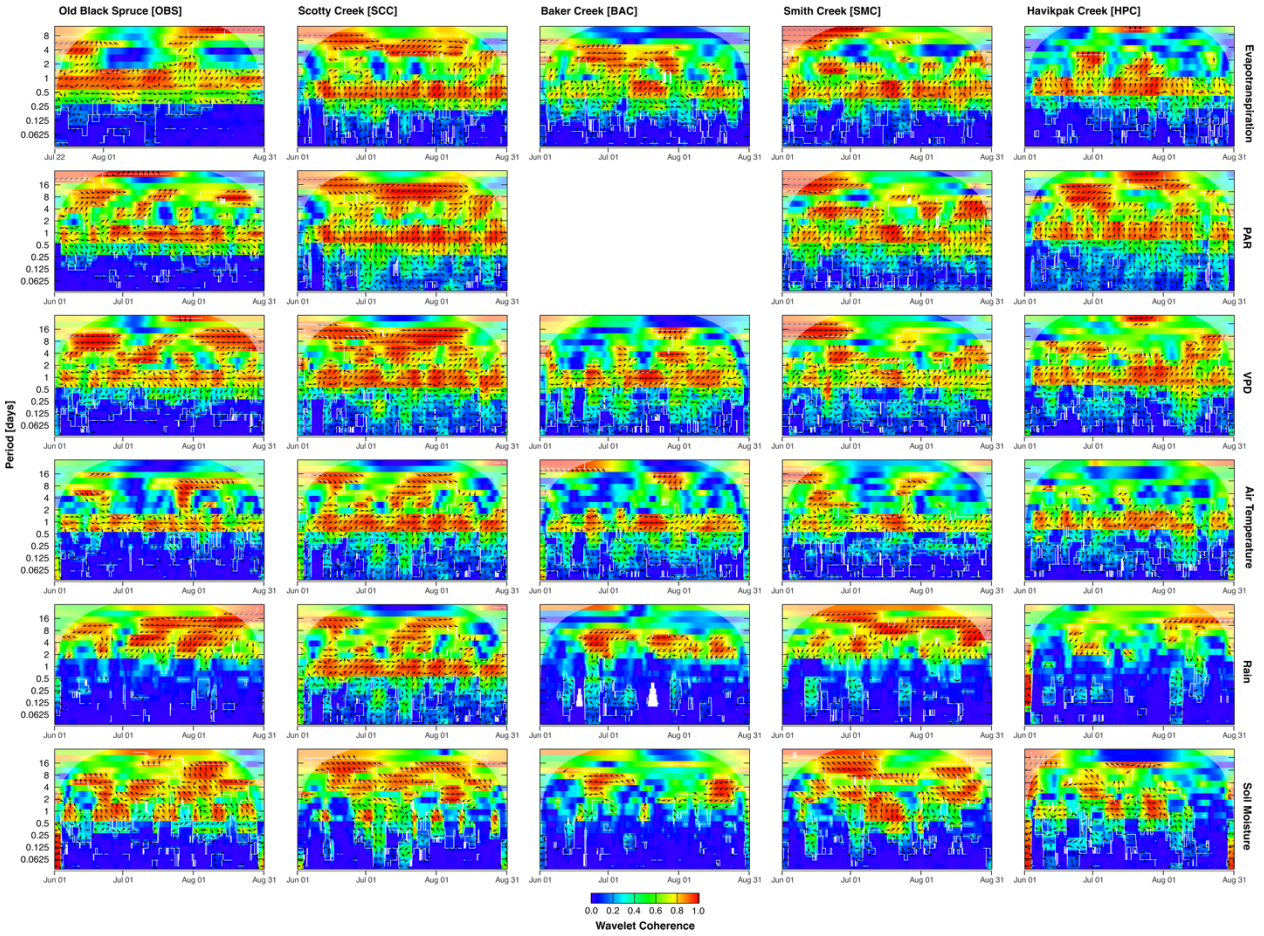

Figure SIII.10 The wavelet coherence between tree water deficit of black spruce and evapotranspiration, and environmental controls at Old Black Spruce, Scotty Creek, Baker Creek, Smith Creek and Havikpak Creek in 2019. Environmental controls include photosynthetically active radiation (PAR), vapour pressure deficit (VPD), air temperature, rain and soil moisture between June – August 2020 (when data was available).

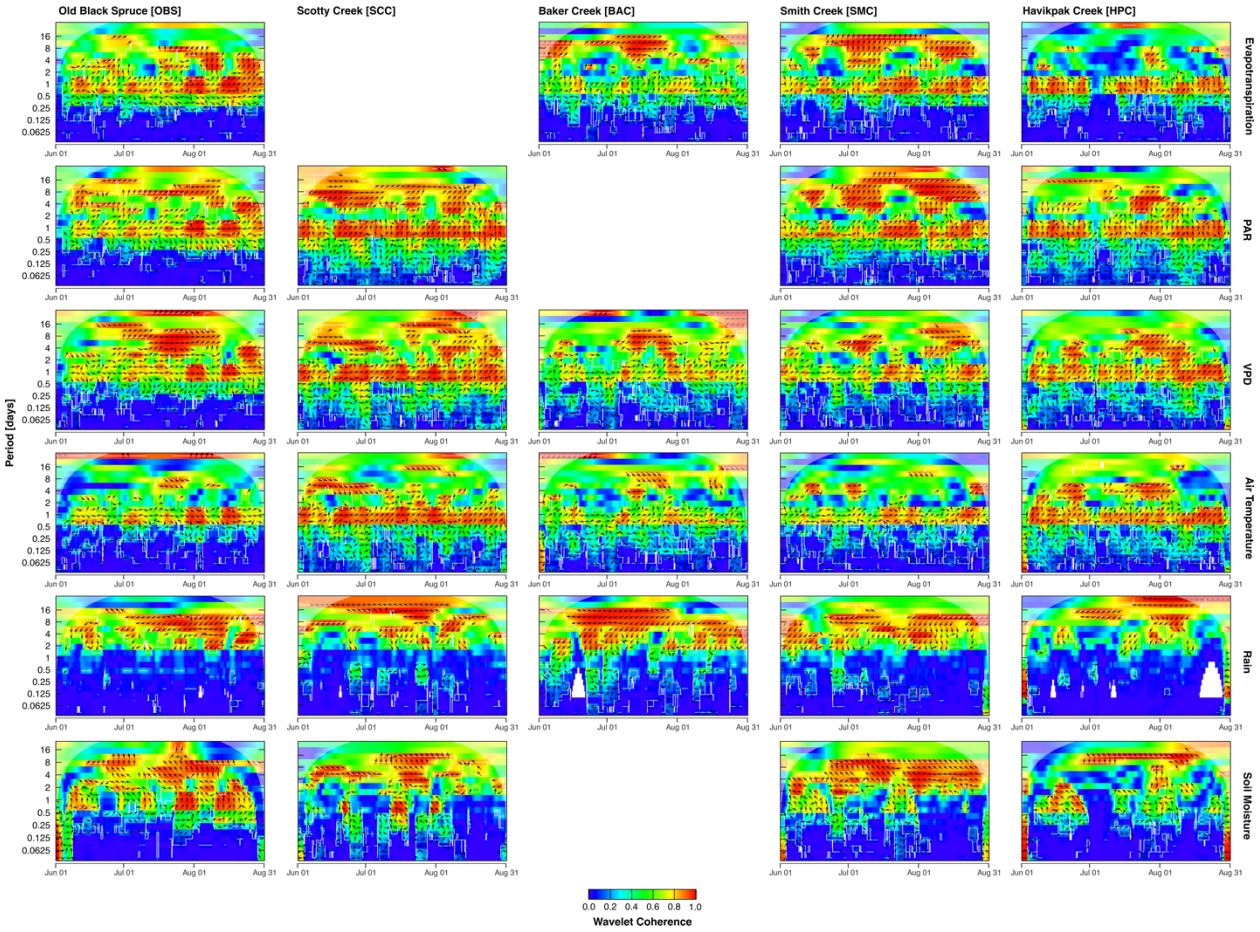

Figure SIII.11 The wavelet coherence between tree water deficit of black spruce and evapotranspiration, and environmental controls at Old Black Spruce, Scotty Creek, Baker Creek, Smith Creek and Havikpak Creek in 2020. Environmental controls include photosynthetically active radiation (PAR), vapour pressure deficit (VPD), air temperature, rain and soil moisture between June – August 2020 (when data was available).

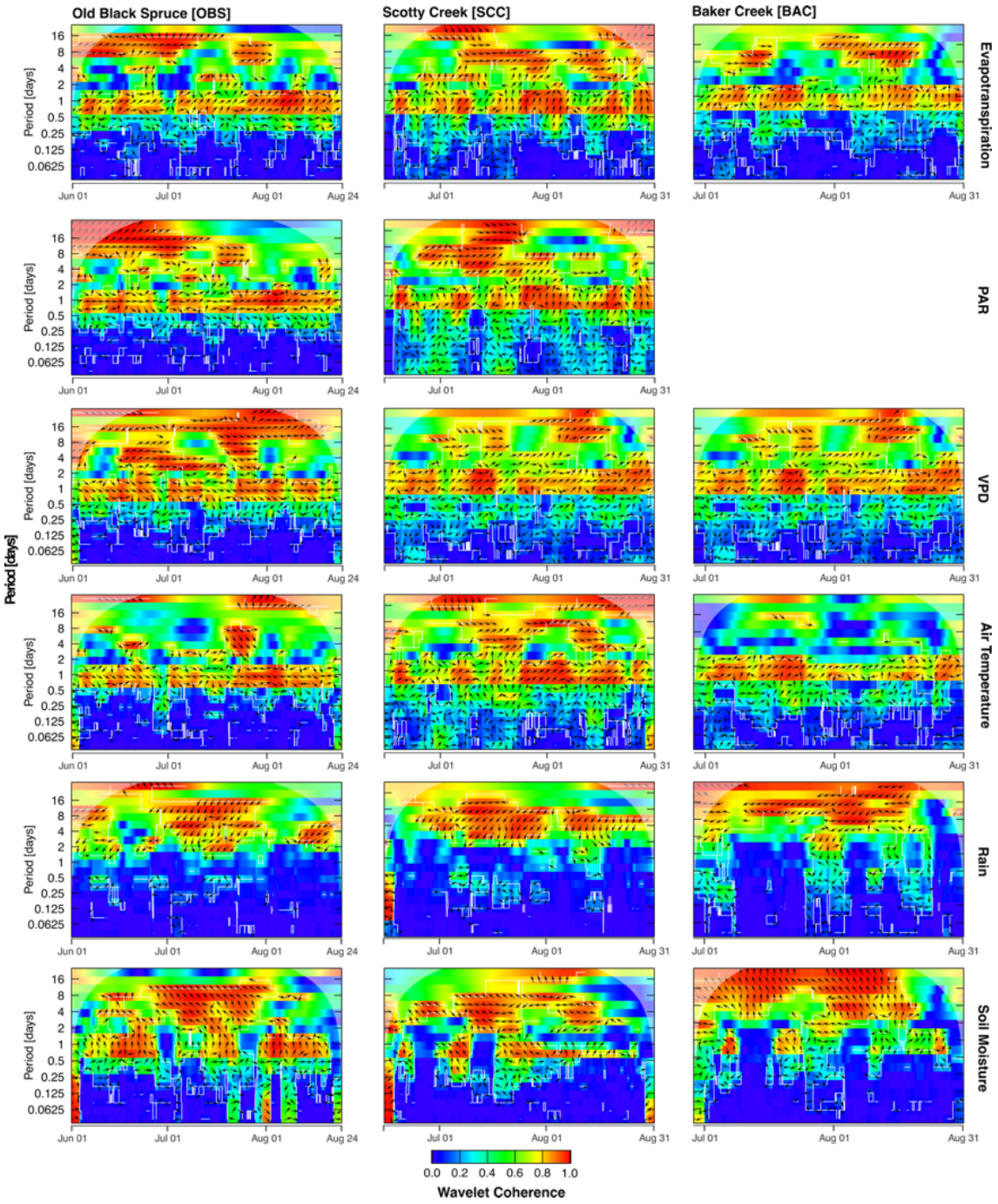

Figure SIII.12 The wavelet coherence between tree water deficit of tamarack and evapotranspiration, and environmental controls at Old Black Spruce, Scotty Creek, and Baker Creek, Smith Creek in 2018. Environmental controls include photosynthetically active radiation (PAR), vapour pressure deficit (VPD), air temperature, rain and soil moisture between June – August 2018 (when data was available).

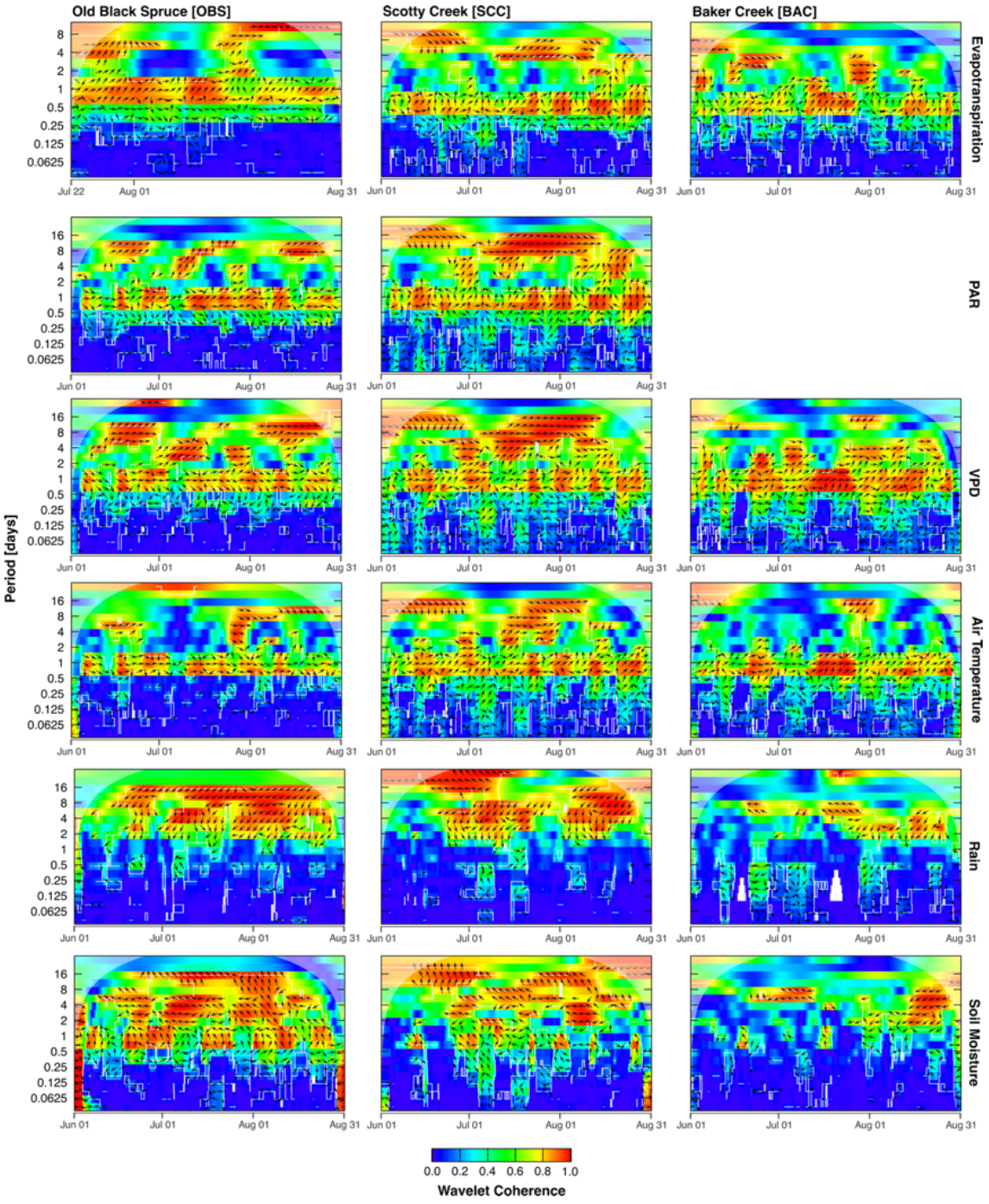

Figure SIII.13 The wavelet coherence between tree water deficit of tamarack and evapotranspiration, and environmental controls at Old Black Spruce, Scotty Creek, and Baker Creek, Smith Creek in 2019. Environmental controls include photosynthetically active radiation (PAR), vapour pressure deficit (VPD), air temperature, rain and soil moisture between June – August 2019 (when data was available).

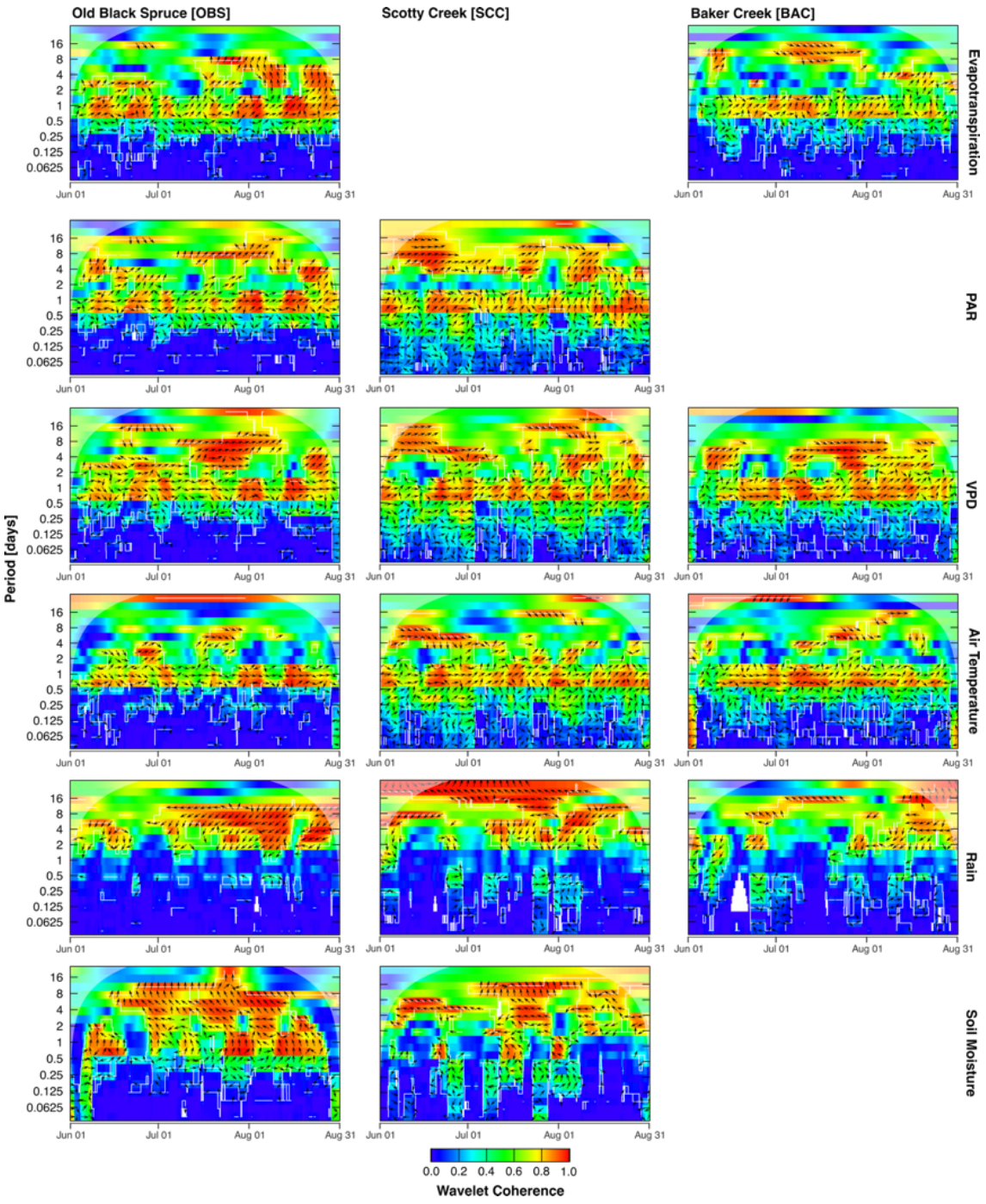

Figure SIII.14 The wavelet coherence between tree water deficit of tamarack and evapotranspiration, and environmental controls at Old Black Spruce, Scotty Creek, and Baker Creek, Smith Creek in 2020. Environmental controls include photosynthetically active radiation (PAR), vapour pressure deficit (VPD), air temperature, rain and soil moisture between June – August 2020 (when data was available).

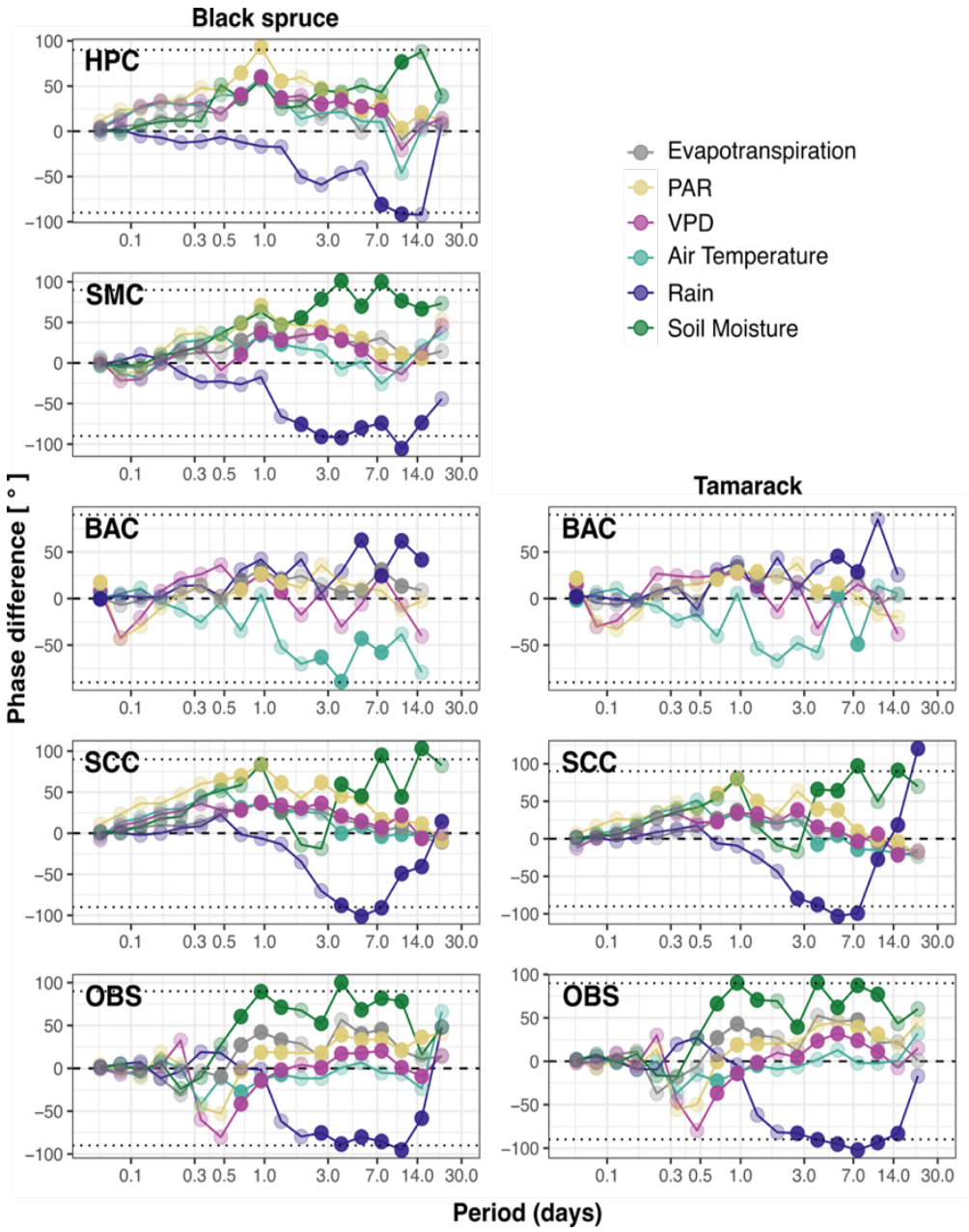

Figure SIII.15 Phase difference angle distributions between the tree water deficit (Y) and environmental controls (X) for black spruce at Old Black Spruce (OBS), Scotty Creek (SCC), Baker Creek (BAC) Smith Creek (SMC) and Havikpak Creek (HPC) and tamarack at OBS, SCC and BAC. Environmental controls include evapotranspiration, photosynthetically active radiation (PAR), vapour pressure deficit (VPD), air temperature, rain and soil moisture. Circles with dark shading represent periods with significant ($p < 0.05$) coherence between tree water deficit and environmental controls. Series with phase difference intervals between [-90; 90] are in phase, indicating that an increase in series X (environmental controls) is coherent with an increase in series Y (tree water deficit). Series with phase difference intervals between [-180; -90 and 90; 180]

are out of phase, indicating that an increase in series X (environmental controls) is coherent with a decrease in series Y (tree water deficit).

Table SIII.3 Average coherence, on a scale of zero to one, (2018 – 2020) between tree water deficit and environmental variables at each site, including Old Black Spruce (OBS), Scotty Creek (SCC), Baker Creek (BAC), Smith Creek (SMC) and Havikpak Creek (HPC). Environmental variables include evapotranspiration (ET), photosynthetically active radiation (PAR), vapour pressure deficit (VPD), air temperature, rain and soil moisture (θ). Asterix symbolises values with significant average coherence ($p < 0.05$). Longer periods (>Day) represent 1.3 to 10 days.

	Day					**>Day**				
Black Spruce	**OBS**	**SCC**	**BAC**	**SMC**	**HPC**	**OBS**	**SCC**	**BAC**	**SMC**	**HPC**
ET	0.76*	0.75*	0.60*	0.69*	0.65*	0.61*	0.62*	0.62*	0.60*	0.44
PAR	0.70*	0.80*	NA	0.73*	0.71*	0.67*	0.71*	NA	0.64*	0.64*
VPD	0.64*	0.77*	0.64*	0.62*	0.69*	0.71*	0.73*	0.51*	0.61*	0.65*
T_{air}	0.60*	0.73*	0.62*	0.58*	0.67*	0.50	0.64*	0.39	0.49	0.53
Rain	0.11	0.12	0.14	0.14	0.15*	0.63*	0.58	0.56	0.66*	0.51*
θ	0.54*	0.39*	0.27*	0.35*	0.37*	0.64*	0.61*	0.58*	0.66*	0.50
Tamarack	**OBS**	**SCC**	**BAC**			**OBS**	**SCC**	**BAC**		
ET	0.69*	0.67*	0.57*			0.57*	0.56*	0.55		
PAR	0.63*	0.70*	NA			0.60*	0.65*	NA		
VPD	0.61*	0.68*	0.69*			0.65*	0.68*	0.61*		
T_{air}	0.57*	0.69*	0.66*			0.48	0.60*	0.38		
Rain	0.14	0.14	0.18			0.64*	0.59*	0.53		
θ	0.58*	0.37*	0.29*			0.65*	0.59*	0.55*		

Measuring sap flux density

Sap flux density (J_s) can be determined using various methods. At OBS, SMC and HPS, we measured sap flux density of black spruce using thermal dissipation sap flow sensors and at SCC we measured J_s using heat ratio method sap flow sensors. Due to technical challenges related to power supply from solar powered systems in remote areas, we were unable to obtain consistent measurements of J_s throughout the measurements period. Thus species-level J_s could not be analysed alongside TWD, ET and environmental controls using wavelet analysis.

We installed Granier-type thermal dissipation sensors to measure sap flow density (Granier, 1987) of black spruce at OBS (n = 24), HPC (n = 27) and SMC (n = 12) in May 2016, June 2016, and June 2018, respectively. The Granier-type thermal dissipation (TD) sensors were self-manufactured following Pappas *et al*. (2018) and previously described in detail elsewhere (Matheny *et al*. 2014). The TD sensors (Figure SIII.6) use two hollow needles 20 mm in length and 0.9 mm in diameter inserted radially into the north-facing side of the stem at ~1.3 m from the ground before being wrapped in an aluminium insulation to prevent heating from solar radiation. The upper needle of the TD sensor is wrapped in constantan wire which is constantly heated with a power supply of 0.2 W (Lu *et al.* 2004). The reference needle is located 10 cm below the heated needle and contains no heated element (Lu *et al.* 2004). The heated and reference needles both contain type-T thermocouples which provide an integrated measure of temperature along the 20 mm length of the needle. The temperature difference (ΔT, recorded in mV) between the heated and the reference needles is used to measure the heat transfer caused by the movement of sap within the xylem (sapwood tissue) of the stem (Granier 1987, Lu *et al.* 2004, Hölttä *et al.* 2015, Pappas *et al.* 2018). The temperature difference is recorded every minute using an AM16/32 multiplexer and either a CR1000 or CR3000 datalogger (Campbell Scientific, Logan, UT, USA). The data was then aggregated into hourly averages.

We measured sapwood depth of trees of different diameters at each site to identify individuals where the probe (=20 mm) is inserted in non-conducting wood, which can underestimate sap flux measurements if not corrected (Clearwater *et al*. 1999; Peters *et al*. 2018). The TD data was processed using the TREX R package (Tree sap flow Extractor; R Core Team, 2019) (Peters *et*

al. 2021). Raw measurements were converted to sap flux density ($cm^3\ cm^{-2}$ sapwood h^{-1}) following the workflow implemented in TREX (Granier, 1987; Peters *et al*. 2021). Briefly, the sap flux density is calculated using the temperature difference between a heated and an unheated probe relative to the maximum temperature difference during zero flow conditions (ΔT_{max}). Because of the lack of species- and site-specific calibration, we used calibration coefficients from the literature as implemented in TREX, in combination with a best-fit assessment (Peters *et al*. 2021). We used the 'genus' level calibration coefficients for black spruce ('Picea') when calculating sap flux densities (using function: tdm_cal.sfd).

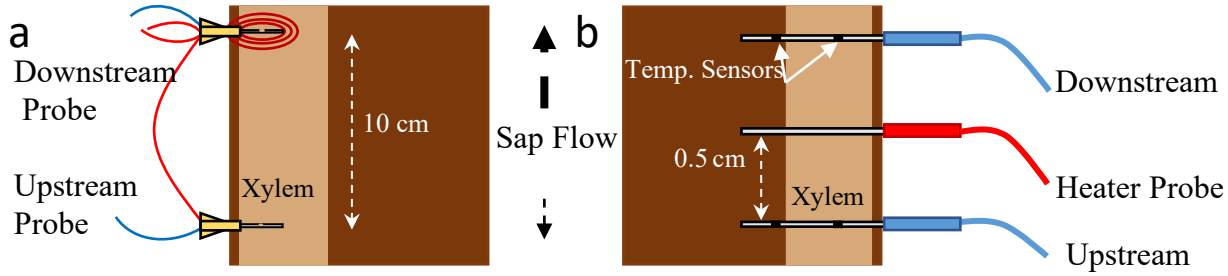

Figure SIII.16 Schematic of the thermal dissipation probes (a) and the heat ratio probes (b) inserted into the stem of a tree. The arrow indicated the direction of primary sap flow within the stem. The dark brown on the light brown represents the sapwood (i.e., xylem) of the stem. Diagram of the heat ratio method adapted from the HRM Installation & Operation Manual, ICT International Pty Ltd., Australia. Diagram is not to scale.

At SCC, heat-ratio method (HRM) sensors were used to measure J_s of black spruce in 2017 (n = 6) and 2018 (n = 12). The HRM sensors use a central heater probe in the conducting xylem (sapwood) of a black spruce stem, positioned equidistant between an upstream and downstream temperature probe (Burgess *et al.* 2001). Each temperature probe has two thermistors, the first located at 12.5 mm and second at 27.5 mm into the stem. For our analysis, only the first thermistor (12.5 mm) was used as the second thermistor (27.5 mm) was located in the non-conducting wood tissues (heartwood) of the sampled trees. The central heater probe releases a heat pulse of 10 Joules every 10 minutes, warming the surrounding sap and transferring heat towards the downstream and upstream temperature probes. Before each pulse, an initial (baseline) temperature is recorded, followed by a measurement of the temperature increase in the downstream and upstream probes

following the heat pulse. The downstream and upstream temperature differences are used to derive the magnitude and direction of sap velocity (V_h, $cm^3\ cm^{-2}\ h^{-1}$; Equation 4) (Burgess *et al.* 2001). The V_h is then used to determine the J_s based on sapwood density, water content, and sapwood area using the Sap Flow Tool software (ICT International Armidale, New South Wales, Australia; Burgess *et al.* 2001). The J_s time-series were averaged to hourly measurements and manually adjusted using a linear transformation to coordinate zero-flow conditions with periods of no biophysical drivers of sap movement (i.e., night-time periods when vapour pressure deficit was near zero, or during or immediately following a precipitation event; Eliades *et al.* 2018). Small gaps in the data set (<3 h) were filled using linear interpolation.

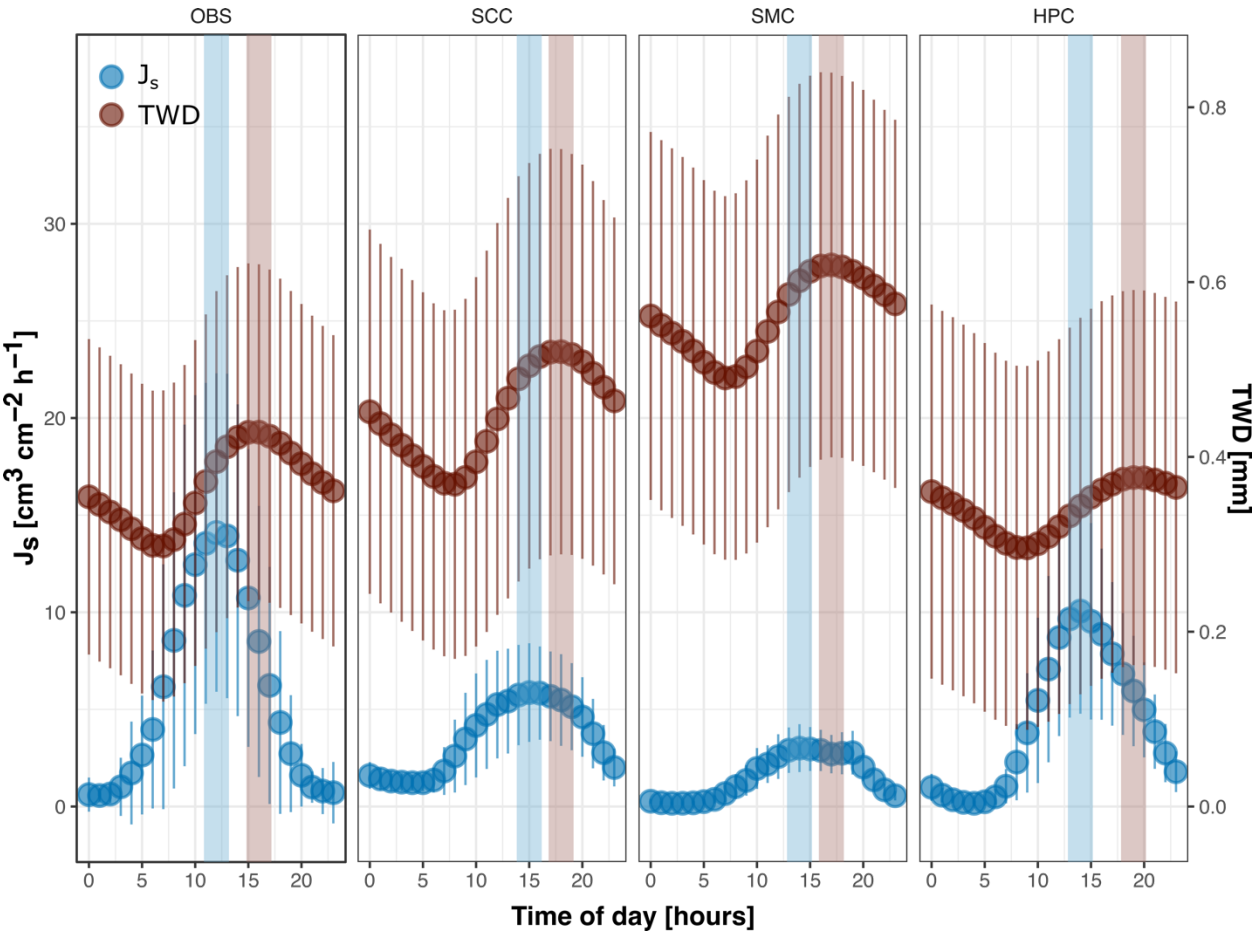

Figure SIII.17 Average hourly tree water deficit (TWD; red) and sap flux density (J_s; blue) in June, July and August for black spruce at Old Black Spruce (OBS; 2018 – 2020), Scotty Creek (SCC; 2017 – 2018), Smith Creek (SMC; 2021) and Havikpak Creek (HPC; 2021). Error bars indicate standard deviation for each hourly mean measurements and shaded vertical lines in blue represent the timing of peak J_s, and in red represent the timing of peak TWD. At all sites, black spruce reached peak daily J_s, a proxy for transpiration, 3 – 6 hours before peak TWD.

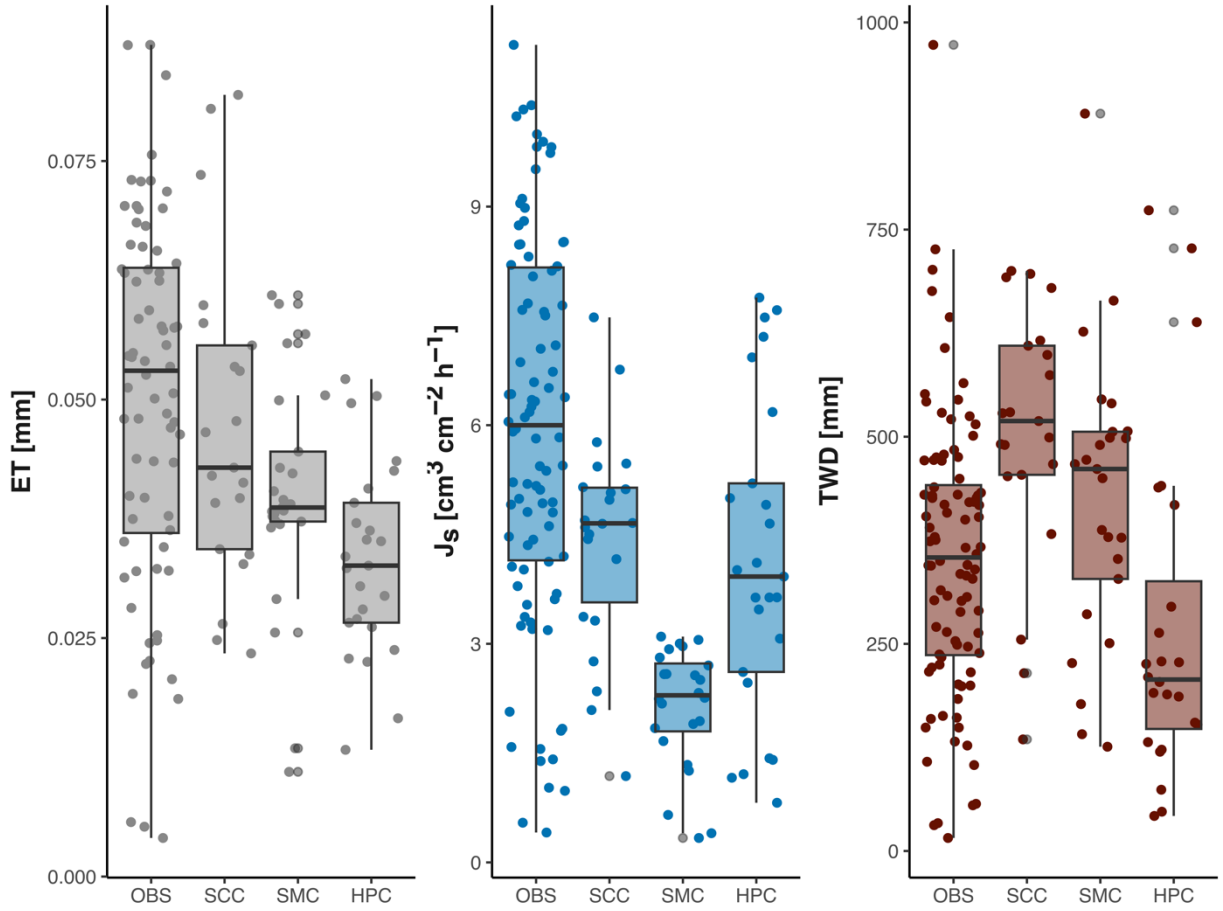

Figure SIII.18 Mean daily evapotranspiration (ET), sap flux density (J_s) and tree water deficit (TWD). Mean daily ET was measured from Old Black Spruce (OBS), Smith Creek (SMC), and Havikpak Creek (HPC) in June - August 2018 – 2020, and from Scotty Creek in June - August, 2018 and 2019. Mean daily J_s was measured from OBS in June - August, 2018 – 2020, from SCC in June - August 2017 and 2018, from SMC in June – August 2021, and from HPC in June – August 2021. The mean daily TWD was determined for black spruce across all sites for June – August in 2018 – 2020. The individual points represent daily values during the sampling period outlined above. The centre line of each boxplot represents the median, while whiskers correspond to the first and third quartiles (the 25th and 75th percentiles).

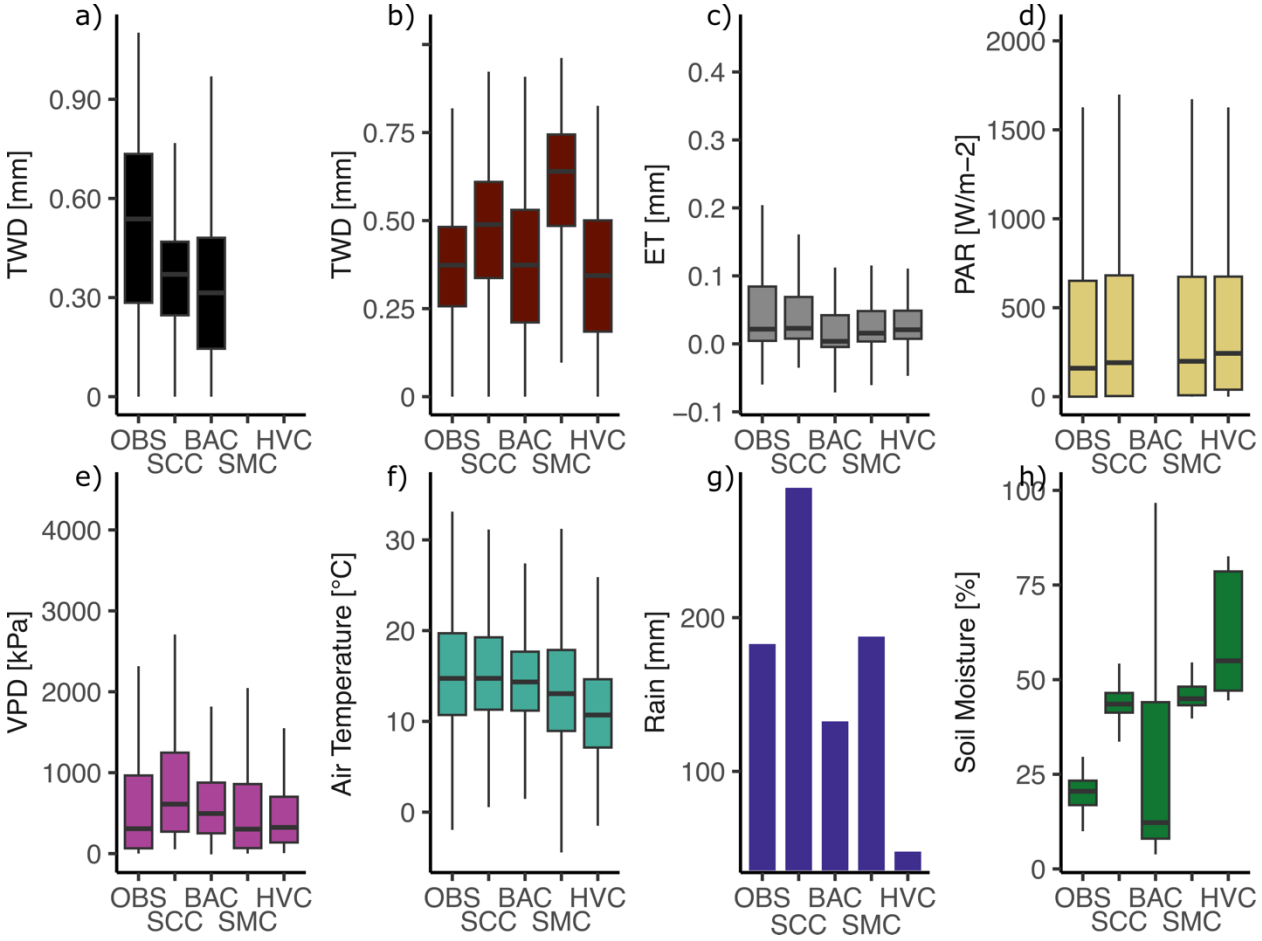

Figure SIII.19 Average half-hourly tree water deficit (TWD) for tamarack at Old Black Spruce (OBS), Scotty creek (SCC), and Baker Creek (BAC; a), tree water deficit for black spruce at OBS, SCC, BAC, Smith Creek (SMC) and Havikpak Creek (HPC; b), evapotranspiration (ET; c); photosynthetically active radiation (PAR; d), vapour pressure deficit (VPD; e), air temperature (f), total rain (g) and average half-hourly soil moisture (h) between June – August 2018, 2019 and 2020 (when data was available). The centre line of each boxplot represents the median, while whiskers correspond to the first and third quartiles (the 25th and 75th percentiles).